

732  
2019

# Berichte

zur Polar- und Meeresforschung

Reports on Polar and Marine Research

## **The Expedition PS117 of the Research Vessel POLARSTERN to the Weddell Sea in 2018/2019**

Edited by

Olaf Boebel

with contributions of the participants

Die Berichte zur Polar- und Meeresforschung werden vom Alfred-Wegener-Institut, Helmholtz-Zentrum für Polar- und Meeresforschung (AWI) in Bremerhaven, Deutschland, in Fortsetzung der vormaligen Berichte zur Polarforschung herausgegeben. Sie erscheinen in unregelmäßiger Abfolge.

Die Berichte zur Polar- und Meeresforschung enthalten Darstellungen und Ergebnisse der vom AWI selbst oder mit seiner Unterstützung durchgeführten Forschungsarbeiten in den Polargebieten und in den Meeren.

Die Publikationen umfassen Expeditionsberichte der vom AWI betriebenen Schiffe, Flugzeuge und Stationen, Forschungsergebnisse (inkl. Dissertationen) des Instituts und des Archivs für deutsche Polarforschung, sowie Abstracts und Proceedings von nationalen und internationalen Tagungen und Workshops des AWI.

Die Beiträge geben nicht notwendigerweise die Auffassung des AWI wider.

Herausgeber

Dr. Horst Bornemann

Redaktionelle Bearbeitung und Layout

Birgit Reimann

Alfred-Wegener-Institut  
Helmholtz-Zentrum für Polar- und Meeresforschung  
Am Handelshafen 12  
27570 Bremerhaven  
Germany

[www.awi.de](http://www.awi.de)

[www.reports.awi.de](http://www.reports.awi.de)

Der Erstautor bzw. herausgebende Autor eines Bandes der Berichte zur Polar- und Meeresforschung versichert, dass er über alle Rechte am Werk verfügt und überträgt sämtliche Rechte auch im Namen seiner Koautoren an das AWI. Ein einfaches Nutzungsrecht verbleibt, wenn nicht anders angegeben, beim Autor (bei den Autoren). Das AWI beansprucht die Publikation der eingereichten Manuskripte über sein Repositorium ePIC (electronic Publication Information Center, s. Innenseite am Rückdeckel) mit optionalem print-on-demand.

The Reports on Polar and Marine Research are issued by the Alfred Wegener Institute, Helmholtz Centre for Polar and Marine Research (AWI) in Bremerhaven, Germany, succeeding the former Reports on Polar Research. They are published at irregular intervals.

The Reports on Polar and Marine Research contain presentations and results of research activities in polar regions and in the seas either carried out by the AWI or with its support.

Publications comprise expedition reports of the ships, aircrafts, and stations operated by the AWI, research results (incl. dissertations) of the Institute and the Archiv für deutsche Polarforschung, as well as abstracts and proceedings of national and international conferences and workshops of the AWI.

The papers contained in the Reports do not necessarily reflect the opinion of the AWI.

Editor

Dr. Horst Bornemann

Editorial editing and layout

Birgit Reimann

Alfred-Wegener-Institut  
Helmholtz-Zentrum für Polar- und Meeresforschung  
Am Handelshafen 12  
27570 Bremerhaven  
Germany

[www.awi.de](http://www.awi.de)

[www.reports.awi.de](http://www.reports.awi.de)

The first or editing author of an issue of Reports on Polar and Marine Research ensures that he possesses all rights of the opus, and transfers all rights to the AWI, including those associated with the co-authors. The non-exclusive right of use (einfaches Nutzungsrecht) remains with the author unless stated otherwise. The AWI reserves the right to publish the submitted articles in its repository ePIC (electronic Publication Information Center, see inside page of verso) with the option to "print-on-demand".

*Titel: Die Schelfeiskante der kleinen, quasi-permanenten Polynja westlich der Atka-Bucht am 11 Januar 2019, wo wir ein Gezeitenexperiment durchführten während wir auf einen Personalwechsel warteten  
(Foto: Hung-An Tian, NIOZ).*

*Cover: The ice shelf edge on 11 January 2019 at the small, quasi-permanent polynya to the west of Atka Bay where we conducted the tidal experiment while on standby for personal exchange  
(Photo: Hung-An Tian, NIOZ).*

# **The Expedition PS117 of the Research Vessel POLARSTERN to the Weddell Sea in 2018/2019**

---

**Edited by  
Olaf Boebel  
with contributions of the participants**

**Please cite or link this publication using the identifiers**

**<http://hdl.handle.net/10013/epic.e314ca93-36d1-4454-afa8-8e2802029acd> and**

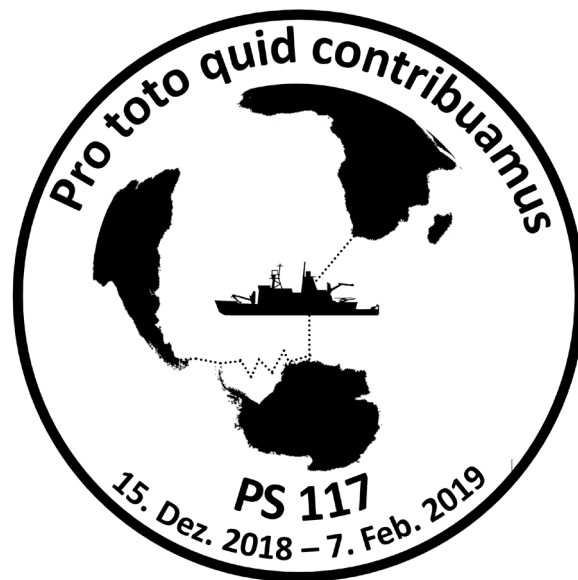
**[https://doi.org/10.2312/BzPM\\_0732\\_2019](https://doi.org/10.2312/BzPM_0732_2019)**

**ISSN 1866-3192**

**PS117**

**15 December 2018 - 7 February 2019**

**Cape Town – Punta Arenas**



**Chief Scientist  
Olaf Boebel**

**Coordinator  
Rainer Knust**

## Contents

<b>1.</b>	<b>Zusammenfassung und Fahrtverlauf</b>	<b>3</b>
<b>2.</b>	<b>Weather Conditions</b>	<b>10</b>
<b>3.</b>	<b>HAFOS: Maintaining the AWI's Long Term Ocean Observatory in the Weddell Sea</b>	<b>15</b>
<b>3.1</b>	<b>Physical oceanography</b>	<b>15</b>
3.1.1	Hydrographic moorings	16
3.1.2	<i>In-situ</i> calibration of moored instruments	25
3.1.3	CTD observations	27
3.1.4	Lowered ADCP	33
3.1.5	Vessel mounted ADCP	38
3.1.6	HAFOS Sound source array	40
3.1.7	RAFOS source tuning	44
3.1.8	Salinometer measurements	47
3.1.9	Argo float deployments (on behalf of BSH)	49
3.1.10	Use of MiniROV vLBV300 (Fiona) for mooring recovery	53
<b>3.2</b>	<b>Ocean acoustics</b>	<b>63</b>
<b>3.3</b>	<b>Transport variations of the Antarctic Circumpolar Current</b>	<b>78</b>
<b>4.</b>	<b>Iron (Fe) Limitation and Viruses, Phytoplankton Caught between a Rock and a Hard Place; Fephyrus</b>	<b>81</b>
<b>4.1</b>	<b>Titan, CTD sampling system for trace metals</b>	<b>83</b>
<b>4.2</b>	<b>Nutrients</b>	<b>87</b>
<b>4.3</b>	<b>Trace metal sampling and analysis</b>	<b>94</b>
<b>4.4</b>	<b>Trace metal biogeochemistry and proteomics</b>	<b>99</b>
<b>4.5</b>	<b>Viral and microbial ecology</b>	<b>102</b>
<b>5.</b>	<b>PICCOLO and SOCCOM Floats</b>	<b>110</b>
<b>5.1</b>	<b>PICCOLO and SOCCOM floats</b>	<b>111</b>
<b>5.2</b>	<b>Sampling and float deployment locations</b>	<b>112</b>
5.2.1	DIC/TA samples	112
5.2.2	pH/TA samples	113
5.2.3	HPLC/POC	113
5.2.4	Salinity	114
5.2.5	Dissolved oxygen Samples	114

5.3	Preliminary data for dissolved oxygen	115
5.4	Preliminary data of PICCOLO floats	116
5.5	Preliminary data of SOCCOM floats	117
6.	Occurrence of Microplastics in the Antarctic Seas	120
7.	Sea Ice Production and Ecology Study (SIPES 2)	132
8.	<b>ALGENOM-2: Molecular Ecology and Evolution of Primary Producers</b>	<b>147</b>
8.1	Microevolutionary genomics of <i>Fragilariopsis kerguelensis</i>	147
8.2	Taxonomic and gene expressional trends in protistan plankton communities along temperature gradients	149
9.	<b>Combined Effects of Temperature and Organic Matter Availability on Degradation Activity By Antarctic Bacterioplankton</b>	<b>154</b>
9.1	WP 1: Field studies	154
9.2	WP 2: On-board experiments on temperature effects and organic matter availability on bacterial communities	158
10.	<b>Molecular Ecology, Physiology and Life History Tools to Monitor Antarctic Toothfish (<i>Dissostichus mawsoni</i>) populations in the Weddell Sea</b>	<b>162</b>
11.	<b>Yopp AWIMET-PS: The “Year of Polar Prediction” (Yopp): Additional Radiosoundings during the Special Observing Period</b>	<b>167</b>
	<b>Abbildungsverzeichnis / Index of Figures</b>	<b>169</b>
	<b>Tabellenverzeichnis / Index of Tables</b>	<b>174</b>
	<b>APPENDIX</b>	<b>179</b>
A.1	Teilnehmende Institute / Participating Institutions	178
A.2	Fahrtteilnehmer / Cruise Participants	182
A.3	Schiffsbesatzung / Ship’s Crew	185
A.4	Stationsliste / Station List	186

# 1. ZUSAMMENFASSUNG UND FAHRTVERLAUF

Olaf Boebel

AWI

Die Antarktisexpedition PS117 führte von Kapstadt, Südafrika, über die *Neumayer-Station III*, Antarktis, in das Weddellmeer und weiter nach Punta Arenas, Chile (Abb. 1.1). Die Expedition beinhaltete logistische und wissenschaftliche Vorhaben. Die logistischen Aufgaben (Versorgung *Neumayer III* mit Treibstoff und Vorräten) wurden vollständig umgesetzt. Ein großer Teil der Ziele der wissenschaftlichen Vorhaben wurden in bewährter Zusammenarbeit zwischen Schiff und Wissenschaft erreicht. Insbesondere konnten die durch den Abbruch der früheren Expedition PS89 ausgefallenen Untersuchungen der Biologie des Meereises zumindest in Teilen nachgeholt werden. Aufgrund eines medizinischen Notfalls musste die Expedition in der ersten Woche unterbrochen werden, um die russische Station Novolasarewskaja anzulaufen. Eine weiterer medizinische Indikation erforderte einen Personalwechsel an der *Neumayer-Station III*, der aufgrund der flugtechnischen Planung erst zum 17. Januar erfolgen konnte. Diese Umplanung erforderte es, Stationen, die für den Zeitraum nach Neumayer geplant waren, vorzuziehen, was wiederum Umwege und damit weitere Zeitverluste bedingte. Aufgrund der außergewöhnlichen geringen Meereisbedeckung und geringen Sturmhäufigkeit konnten diese jedoch in Teilen durch ein schnelleres Vorankommen des Schiffes kompensiert werden, so dass mit Ausnahme eines stark ausgedünnten CTD Schnittes entlang des Greenwich Meridians und weniger als erhofften Netzfängen die gesteckten Ziele erreicht werden konnten.

Auf der *Polarstern* Expedition PS117 wurden Beiträge zu wissenschaftlichen Projekten aus den Bereichen physikalische Ozeanographie, Meeresbiologie und Meteorologie gewonnen, die gemeinsam darauf abzielen, die Entwicklung der Wassermassen des Weddellmeers und seiner ökologischen und chemischen Kreisläufe zu verstehen. Die Projekte und die damit verbundenen Aktivitäten (Tab. 1.1) an Bord waren im Einzelnen:

**HAFOS** (Hybrid Antarctic Float Observing System) untersuchte mittels ozeanographischer Tiefseeverankerungen, hydrographischen Schnitten und autonomen Floats die Zirkulation und Entwicklung des Warmen Tiefenwassers und Bodenwassers des Weddellmeeres. Biologische Aspekte von HAFOS betreffen die akustische Ökologie des Weddellmeeres und seiner Fauna, wofür Verankerungen mit autonomen Unterwasserrekordern ausgestattet wurden.

- Aufnahme von 5 Tiefseepegel (PIES) entlang des GoodHope Schnittes (zzgl. 1 PIES Aufnahmeversuch) (für das CNRS, Frankreich);
- Fahren von 49 CTD Stationen mit Rosette und I-ADCP;
- Aufnahme von 19 ozeanographischen Verankerungen sowie Auslage von 12 ozeanographischen Verankerungen;
- 3 ROV Einsätze zur Verankerungsbergung;
- Auslegung von 10 Argo Floats (für das BSH, Deutschland);
- Kalibrierung von 5 RAFOS Schallquellen;
- Kontinuierliche Erfassung von Temperatur, Salzgehalt und Strömungsprofilen.

**FePhyrus** untersuchte die Quellen und Senken von Spurenmetallen und Isotopen im Weddellmeer und der Lazarev See sowie die Wechselwirkung zwischen Eisen und dem mikrobiellen Nahrungsnetz;

- Fahren von 32 Ultra Clean CTD Stationen;
- Durchführung von 4 Bioassay Experimenten.

**SOCOM** (Southern Ocean Carbon and Climate Observations and Modelling) beobachtete und modellierte biogeochemische Kreisläufe des Südpolarmeeres mit dem Zweck, Klimamodelle zu verbessern; die Beobachtungen werden mittels biogeochemischer, profilierender Treibbojen durchgeführt, die über das gesamte Südpolarmeer hinweg verteilt, ausgelegt wurden.

- Auslegung von 12 geochemischen Argo Floats.

Im Projekt **Microplastics** wurde das Vorkommen und die Verteilung von Mikroplastik im Wasser und den Lebewesen des Südlichen Ozeans untersucht.

- 24 Manta Netzfänge (jeweils: 200 m<sup>-3</sup>);
- 85 Seepasserproben (ü. Seewasserpumpe) (jeweils: 3.7 m<sup>-3</sup>).

**SIPES 2 (Sea Ice Production and Ecology Study)** untersuchte die Bedeutung des Meereises für pelagische Nahrungsnetze und für den Kohlenstofffluss zu Toppredatoren (Seevögel und –Säugetiere).

- 22 Netzfänge mit dem MultiRMT (davon 2 disfunktional);
- 15 Netzfänge mit dem SUIT Netz (davon 1 Erprobung);
- 10 ROV Einsätze zur Unter-Eis Beprobung;
- 8 Beprobungen des Meereises (Eisstationen);
- 10 Flüge zur Tierbeobachtung (18:59);
- Einsatz von 2 Hand-CTDs zur Kalibrierung;
- 387 h zur Tierbeobachtung vom Peildeck aus.

**ALGENOM-2** untersuchte ökologische und evolutionäre Differenzierung entlang meridionalen Umweltgradienten im Südozean auf molekularer Ebene, in Gemeinschaften von einzelligen Eukaryoten sowie in ausgewählten Mikroalgentaxathe.

- Netzfänge auf 21 Stationen mit dem Handnetz bei gleichzeitiger Beprobung der Rosette auf je 2 Tiefen.

Das Projekt **CombiBac** soll zu einem besseren Verständnis von Remineralisierungsprozessen unter besonderer Berücksichtigung von Temperatureinflüssen und Substratverfügbarkeit im Weddell Meer beitragen. Zu diesem Zweck wurden Parameter der bakteriellen Aktivität, die Zusammensetzung der Bakterioplankton Gemeinschaft und Konzentrationen des organischen Materials in Feldproben und Experimenten an Bord bestimmt.

- Bei allen AWI CTD Stationen wurden die Rosette mit 8l in allen verfügbaren Tiefen sowie die SIPES Eisstationsproben beprobt.

Das Projekt "**Molecular ecology, physiology and life history tools to monitor Antarctic toothfish (*Dissostichus mawsoni*) populations in the Weddell Sea**" zielte darauf ab, lebenden schwarzen Seehecht und weitere endemische Fischarten der Antarktis

(Notothenioidei) mittels beköderter Reusenfallen zu fangen, um deren Physiologie, Genetik, Populationsstruktur und –dynamik näher zu untersuchen (Grant.-No: AWI\_PS117\_08). Ein neuartiger, gezielter Ansatz zur Gewinnung einer begrenzten Menge (max. 5 Tonnen) dieser Art (*D. mawsoni*) für biologische, genomische und ökophysiologische Forschungsarbeit wurde mit Hilfe des Einsatzes von Langleinen-Verankerungen im Rahmen des Übereinkommens über die Erhaltung der lebenden Meeresschätze der Antarktis (Convention on the Conservation of the Antarctic Marine Living Resources (CCAMLR)) untersucht (Grant.-No: AWI\_PS117\_09).

- 2 Auslagen und Aufnahmen Fischfallen (davon jedoch nur 1 Aufnahme erfolgreich);
- Auslage und Aufnahme von 4 Langleinen Verankerungen zum Fischfang.

**YoPP AWImet-PS** wird, als Beitrag zum „Year of Polar Prediction“ (YOPP) die Häufigkeit von Radiosondenaufstiegen von Bord *Polarstern* von 1 auf 2 bis 4 pro Tag erhöhen.

- Durchführung von 163 Radiosondenaufstiegen.

Letztendlich dienten die Helikopter als Transportmittel um vom Schiff abgesetzte Arbeiten, logistische Aufgaben und Beobachtungsflüge durchzuführen. Insgesamt ergaben sich 53 Flüge von 36:21 h kumulativer Dauer:

- 1 Flug zur Eiserkundung (0:09 h);
- 16 wissenschaftliche Flüge (05:18) zum Ausbringen der Eisstationen;
- 3 Trainingsflüge (02:24);
- 3 logistische Flüge (Transporte, 0:58);
- 21 Personentransporte bei Neumayer (8:33);
- 9 Flüge zur Tierbeobachtung (18:59).

**Tab. 1.1:** Verteilung der Stationszeiten nach Gerät

Instrument	Anzahl	Gesamtzeit [dd hh:mm]
CTD Ozeanographie	49	5 08:12
Hand Netz	25	0 02:14
'PIES'	6	0 15:18
'Ultra Clean CTD'	32	2 10:36
'Manta Netz	24	0 16:42
'SUIT'	15	1 02:10
'Test'	1	0 00:33
'Float' Auslage	22	0 01:32
Verankerung	48	3 20:32
'Multi-RMT'	22	1 14:42
Eisstation	6	0 16:55
ROV Einsatz	10	0 16:57
Schallquellenkalibration	5	0 07:45
Fischfalle	4	0 04:40
Hand CTD	2	0 00:13

Summe Stationszeiten: 17d 19h 01min.

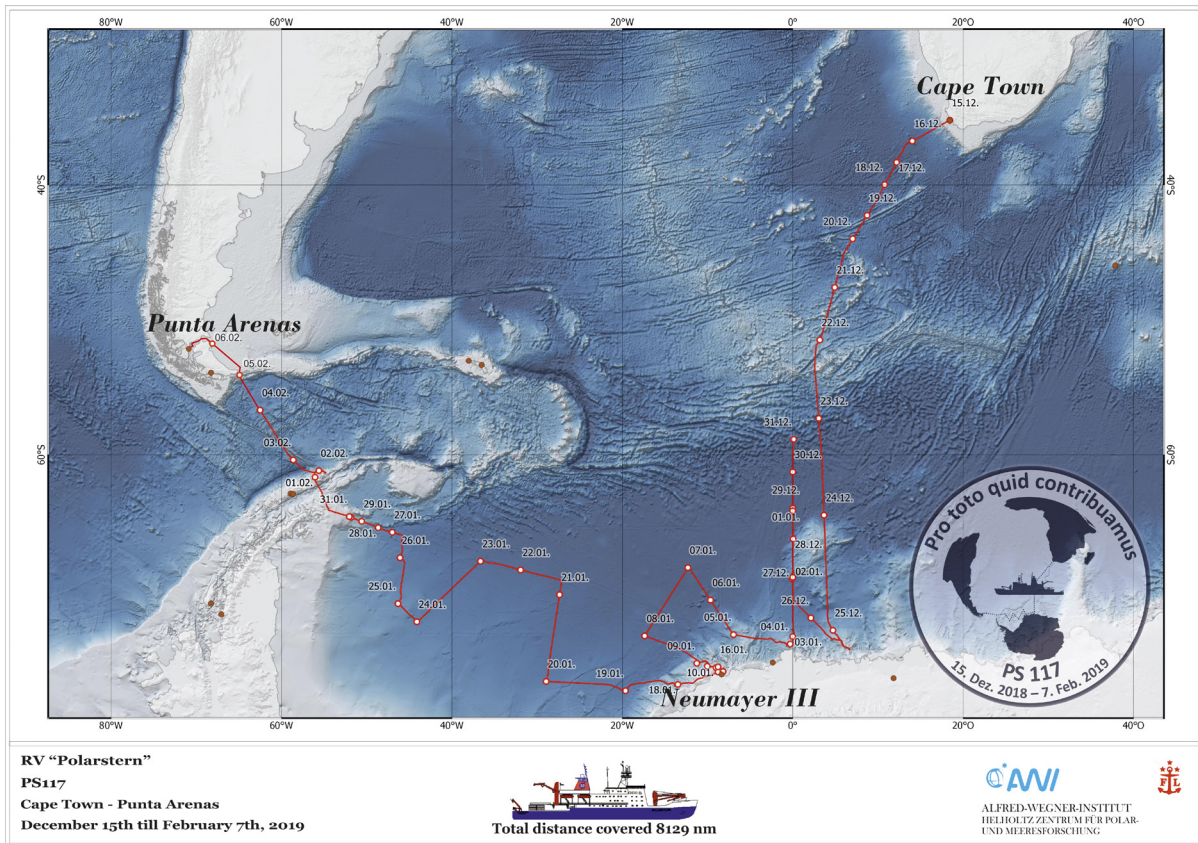


Abb. 1.1: Fahrtverlauf der Antarktis Expedition PS117. Beginn der Reise war am 15 Dezember 2018 in Kapstadt, Südafrika, Ende am 7 Februar 2019 in Punta Arenas, Chile. Siehe auch <https://doi.pangaea.de/10.1594/PANGAEA.899721>.

Fig. 1.1: Track of expedition PS117 to the Antarctic, starting in Cape Town on 15 December 2018, ending in Punta Arenas, Chile, on 7 February 2019. See also <https://doi.pangaea.de/10.1594/PANGAEA.899721>.

## SUMMARY AND ITINERARY

The expedition PS117 to the Antarctic took *Polarstern* from Cape Town, South Africa, via the German *Neumayer Station III*, Antarctica, to the Weddell Sea and on to Punta Arenas, Chile (Fig. 1.1). The expedition comprised logistic and scientific undertakings. The logistic tasks (provision of *Neumayer Station III* with fuel and supplies) were fully achieved. Due to the well-proven collaboration between the crew and the scientific party the scientific goals could be completed to a large extent. In particular, biological studies originally planned for expedition PS89, which had to be cut short for technical reasons, could be executed this time, at least in parts. Due to a medical evacuation, the expedition had to be interrupted in the first week to steam to the Russian Station Novolazarevskaya as quickly as possible. Another medical case required the exchange of personnel which - for logistic reasons - could only be performed on 16 January. The replanning required to serve stations which originally had been scheduled after our call to *Neumayer Station*, which implied extensive detours and consequently a loss of time. However, the extremely low ice cover and low storm activity this year allowed the ship to proceed faster than usually, compensating in parts for our losses in time. Ultimately, with the exception of a highly thinned-out section along the Greenwich meridian and lesser net trawls as hoped for, most of the scientific goals were achieved.

*Polarstern* expedition PS117 sought to provide contributions to scientific projects encompassing physical oceanography, marine biology and meteorology, with the general aim to improve our understanding of the evolution of the Weddell Sea water masses and the ecological and chemical cycles of the Weddell Sea. In addition to the immediate scientific programme, this expedition also served to resupply the German *Neumayer Station III*, Antarctica to support the multifaceted scientific activities originating from there. Specific scientific projects conducted throughout the expedition and related activities aboard (Tab. 1.1) were:

**HAFOS** (Hybrid Antarctic Float Observing System), investigated the circulation and evolution of Warm Deep Water and Weddell Sea Bottom Water by means of oceanographic deep-sea moorings, hydrographic sections and autonomous floats, the latter of which also extend the international Argo Project to the polar seas. Biological aspects of HAFOS concern the acoustic ecology of the Weddell Sea and its fauna, for which moorings were equipped with autonomous recorders.

- Recovery of 5 Pressure Sensor Equipped Inverted Echosounders (PIES) along the GoodHope section (plus 1 PIES failed recovery attempt) (for CNRS, France);
- Casting 49 CTD stations with rosette and I-ADCP;
- Recovery of 19 oceanographic moorings as well as deployment of 12 oceanographic moorings;
- 3 ROV deployments for mooring recoveries;
- Deployment of 10 Argo floats (for BSH, Germany);
- Calibration of 5 RAFOS sound sources;
- Continuous acquisition of temperature, salinity and current profiles (sADCP).

**FePhyrus** investigated the sources and sinks of trace metals and isotopes in the Weddell Sea and Lazarev Sea and the interaction between iron and the microbial food web.

- Casting of 32 Ultra Clean CTD stations;
- Conducting 4 Bioassay experiments.

**SOCOM** (Southern Ocean Carbon and Climate Observations and Modelling) observing and modelling the biogeochemical cycles of the Southern Ocean as a means of improving climate modelling; observations are made by having deployed biogeochemical profiling floats (BGC-Argo) that are being distributed throughout the Southern Ocean. UK **PICCOLO** (Processes Influencing Carbon Cycling: Observations of the Lower Limb of the Antarctic Overturning) scientists study the key processes controlling the rate of Southern Ocean carbon uptake, via the release of Argo floats and carbonate chemistry data collection on the Greenwich Meridian section in the Weddell Sea.

- Deployment of 12 geochemical Argo floats.

The project **Microplastics** explored the occurrence and distribution of microplastics in water and biota in the Southern Ocean.

- 24 Manta trawls (200 m<sup>3</sup> each);
- 85 seawater samples via sea water pump (3.7 m<sup>3</sup> each).

**SIPES 2 (Sea Ice Production and Ecology Study)** investigated the ecological importance of sea ice for the pelagic food web and carbon supply to top predators (birds and mammals).

- 22 trawls with the MultiRMT (thereof 2 dysfunctional);
- 15 trawls with the SUIT net (thereof 1 trial);
- 10 ROV deployment for under-ice sampling;
- 8 ice stations (retrieving sea ice cores);
- 10 endotherm observation flights (18:59);
- deployment of 2 hand-CTDs for calibration;
- 387 h for endotherm observations from the observation deck.

**ALGENOM-2** investigated the molecular evolutionary and ecological dynamics of unicellular eukaryotic assemblages and of selected taxa thereof.

- Hand net catches at 21 stations with simultaneous sampling of the rosette on 2 depths.

**CombiBac** aimed for a better understanding of bacterial remineralization processes in the Weddell Sea with emphasis on their dependence on water temperature and substrate concentration. For this purpose, parameters of bacterial activity, the composition of bacterioplankton communities and concentrations of organic matter were determined in field samples and during on-board experiments.

- The rosette was sampled for 8l on all available depths, as well as samples of the SIPES ice stations.

The project “**Molecular ecology, physiology and life history tools to monitor Antarctic toothfish (*Dissostichus mawsoni*) populations in the Weddell Sea**” aimed at catching alive Antarctic toothfish and other endemic Notothenioids by means of baited traps to investigate their physiology, genetics, population structure and dynamics (Grant.-No: AWI\_PS117\_08). A novel, targeted approach to catch a limited amount (max. 5 tonnes) of toothfish for biological, genomic and ecophysiological research was explored by deployment of long-line moorings in support of the conservation and sustainable management of Antarctic toothfish (*D. mawsoni*) in the Weddell Sea, which was carried out under the Convention on the Conservation of the Antarctic Marine Living Resources (CCAMLR) (Grant.-No: AWI\_PS117\_09).

- 2 deployments and recoveries of fish traps ( only 1 recovery successful);
- Deployment and recovery of 4 long-line moorings to catch fish.

**YoPP AWImet-PS**, as contribution to the „Year of Polar Prediction“ (YOPP) increased the rate of radiosoundings on board *Polarstern* from 1 or 2 to 4 launches per day.

- 163 meteorologic radiosonde launches.

Finally, the helicopters served as means of transport for studies set apart from the ship. In total, 19 flights of 9:14 h cumulative duration were flown:

- 1 flight for sea ice reconnaissance; (0:09 h);
- 16 scientific flights (05:18) to deploy the sea ice stations;
- 3 training flights (02:24);
- 3 logistic flights (transports, 0:58);
- 21 transports of personnel at *Neumayer Station III* (8:33);
- 9 flight for animal observations (18:59).

## 2. WEATHER CONDITIONS

Max Miller, Thomas Bruns, Juliane Hempelt

DWD

### **Passage from Cape Town to Novolazarevskaya**

The subtropical high spread its centre in east-west-direction hardly south of the African Continent and moved southward a bit. Together with a low over South Africa the “Cape-Doctor” (stormy and gusty south-easterly winds) was temporarily forced at Cape Town. On Saturday afternoon, December 15, 2018, 16:30 pm, *Polarstern* left Cape Town for the campaign PS117. Light north-westerly winds, 21°C and sunny skies were observed. But when passing the harbour’s exit, the “Cape-Doctor” hit us: winds veered rapidly southeast and freshened up to 8 Bft. Leaving the coastal region behind us winds abated. On Sunday morning (Dec. 16) we measured only light winds while approaching the ridge. We were cruising under the influence of the subtropical high until Wednesday (19.12.). While the wind increased up to 5 Bft and swell reached 2 to 2.5 m, the first moorings were recovered without any problems. On our way south, we arrived in the west wind zone in the night before Thursday (20.12). Until Sunday (23.12) we encountered three depressions with wind force never dropping below 6 Bft, however, at times reaching Bft 9 on Thursday and Saturday (22.12.). Significant wave height varied between 4 and 5 m. Due to the serious illness of a crew member it was decided on Saturday to directly head to the Russian Antarctic Station *Novolazarevskaya*, where we arrived on the second Christmas day (25.12.). During this expedition, the weather situation was characterized by a large low pressure system southeast of Bouvet Island that slowly travelled southeastward. On its southern edge, *Polarstern* passed through a strong southeasterly wind field reaching force 7 Bft right from the beginning. Approaching the edge of the shelf ice, wind had decreased to 5 Bft, whereas flight weather conditions were suitable for evacuating the patient.

### **Research between *Novolazarevskaya* and *Neumayer Station III***

On the second Christmas day (26.12.), a heavy gale developed south of the Falkland Islands, rapidly moving northeastward. The lowest pressure 955 hPa was reached near 58°S 003°W. Therefore, the research area of *Polarstern* experienced a lively advection of humid air from Southeast. Wind force 6 Bft dominated and convectively enhanced snow fall occurred repeatedly. In the course of time, the low moved eastward and filled up off the coast of the eastern parts of Dronning Maud Land. For a few of days, intermediate high pressure influence provided gentle westerly winds 4 to 5 Bft, however, light snowfall was always on the agenda. Finally, on New Year’s Day 2019 the phase came to an end with the approach of a new gale that passed *Polarstern* in the North und caused a lot of heavy snowfall. Thereafter, several less intense depressions with short intermediate highs characterized the following 10 days with variable but relatively calm weather. On Sunday (13.01.) *Polarstern* berthed for 5 days at the shelf ice edge near *Neumayer III*. During this week, intense cyclones travelled from the Drake Passage eastward on a northerly track. The shelf ice edge was not affected by these developments, here small pressure gradients were associated with light winds and low cloud levels. However, an extreme cyclogenesis took place on Thursday (17.01.) near 60°S 043°W in lee of the Antarctic Peninsula. In the afternoon of this day, *Polarstern* was about to take over new passengers by helicopter.

### Research in the Weddell Sea

The storm achieved its mature stage on Sunday (20.01.) with a central pressure of 945 hPa at 65°S 46°W, when *Neumayer III* reported easterly wind gust of force 12 Bft. At that time, *Polarstern* was operating on the southern edge of the low where easterly winds did not exceed 7 Bft. However, a high wind sea had been generated on the eastern flank of the low, which arrived as swell of 5 m significant wave height in the area of the ship on Sunday afternoon (20.01.) Therefore, some research activities were hindered or restricted. Light snowfall, as well as freezing rain, accompanied with poor visibility and low clouds dominated until Monday (21.01.). While *Polarstern* steamed on a northerly course, the gale started weakening and the centre moved slowly southwestward into the Weddell Sea. Consequently, the ship arrived at the northern flank of the low where westerly winds of force 6 to 7 Bft and significant wave heights up to 5m prevailed. Finally, on Wednesday (23.01.) weak high pressure influence became effective. On its way to the northern end of the Antarctic Peninsula, *Polarstern* followed a zigzag course according to the scientific schedule, stopping at stations for a several hours or even up to half a day. High pressure influence persisted also on Thursday (24.01) along with improved visibility and rising cloud ceiling. Thus, for the first time since leaving *Neumayer III*, an extended helicopter operation took place to count birds and mammals over an area of sea ice. On Friday and Saturday (25./26.01.), a low slowly propagated eastward along 64°S. Its frontal system brought snowfall into the northern edge of the Weddell Sea, however, research activities were not affected, despite a few light snow showers. Rather conversely, the sun showed up for a while. Therefore, further helicopter flights took place, despite a few isolated snow showers. On Sunday afternoon (27.01.), the conditions even improved as pressure rose over the Weddell Sea.

In the night before Monday (28.01.), a frontal system approaching from the West brought some snowfall that was followed by rain. While the corresponding low deepened and moved eastward north of 60°S, a secondary low moved into the Weddell Sea causing further precipitation on Tuesday (29.01.). Under high pressure influence, the following days were characterized by a gentle southerly breeze, low clouds in the morning and sometimes brightness in the afternoon. On Friday (01.02.), after several days of research in the sea area between 63.5°S 51.5°W and 63.0°S 54.5°W, *Polarstern* steamed towards Elephant Island to stay for one day of station work.

### Passage from Elephant Island to Punta Arenas

On Saturday (02.02.), a large low pressure system north of Western Antarctica released a secondary low which crossed the Antarctic Peninsula on Sunday (03.01.). Simultaneously, a strong and stationary high formed over Argentina. Therefore, the meridional pressure gradient increased over the Drake Passage. Due to further lows following on a similar track, near gale westerly winds and high waves persisted for five days. While *Polarstern* was steaming towards Le Marie-Strait, wind force reached 8 Bft on Sunday (03.02.) and Monday (04.02.) accompanied by significant wave heights of about 5 m. Die originally scheduled „Last CTD“ was cancelled. In the night before Tuesday (05.02.) wind ceased and waves calmed. The further expedition along the southern flank of the Argentine high was first characterized by clear sky at times, a light to moderate westerly breeze and wave heights up to 1.5 m. In the night before Wednesday (06.02.), however, the cold front of a gale near the western entrance of the Drake Passage crossed Patagonia, and the vessels track, as well, reaching 8 Bft for three hours. Moderate to fresh south-westerly winds were blowing, when *Polarstern* arrived at Punta Arenas in the morning of Thursday, February 07th 2019.

Weather statistics of this expedition are provided in Fig. 2.1 through Fig. 2.6.

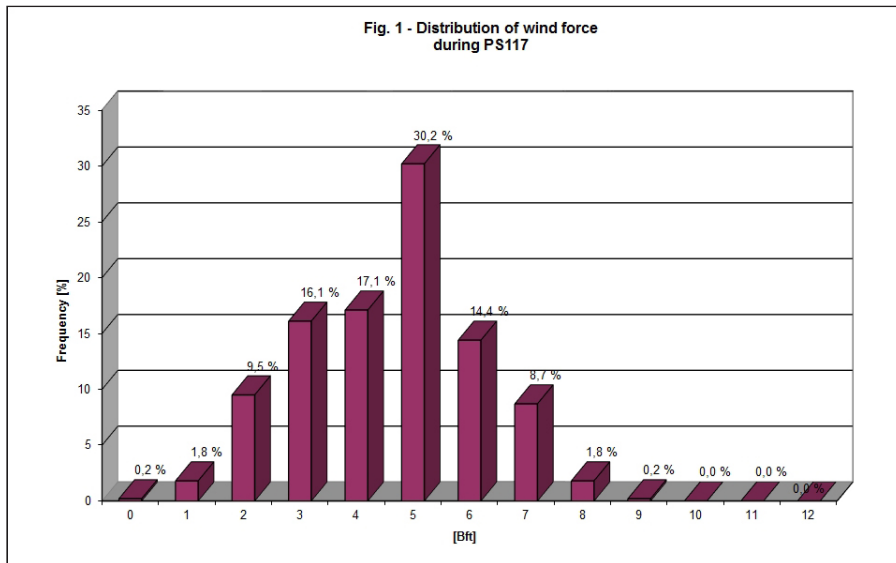


*Fig. 2.1: Distribution of wind force during PS117*

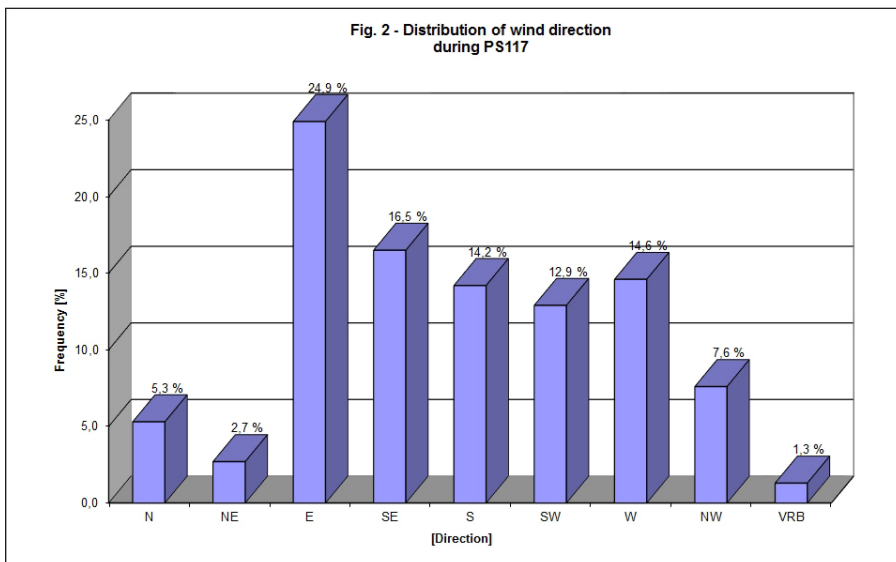


*Fig. 2.2: Distribution of wind directions during PS117*

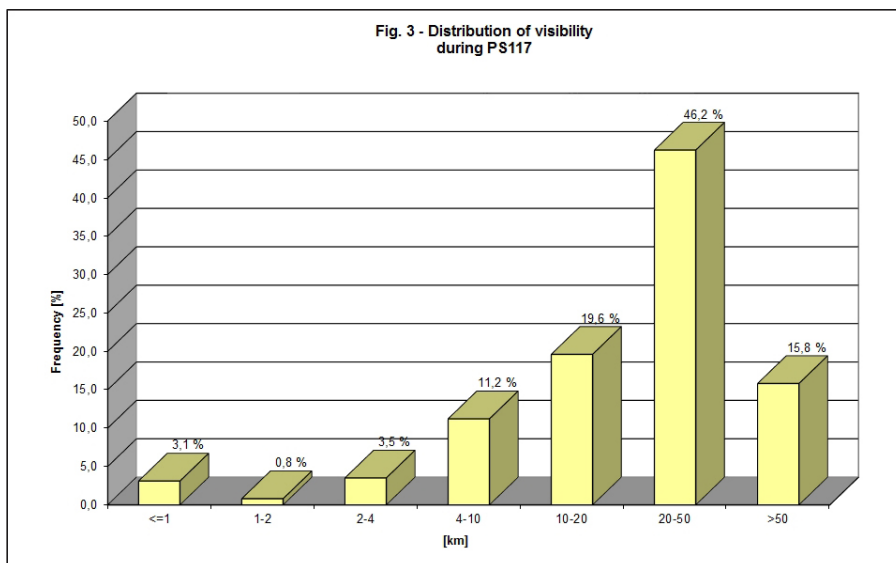


*Fig. 2.3: Distribution of wave heights during PS117*

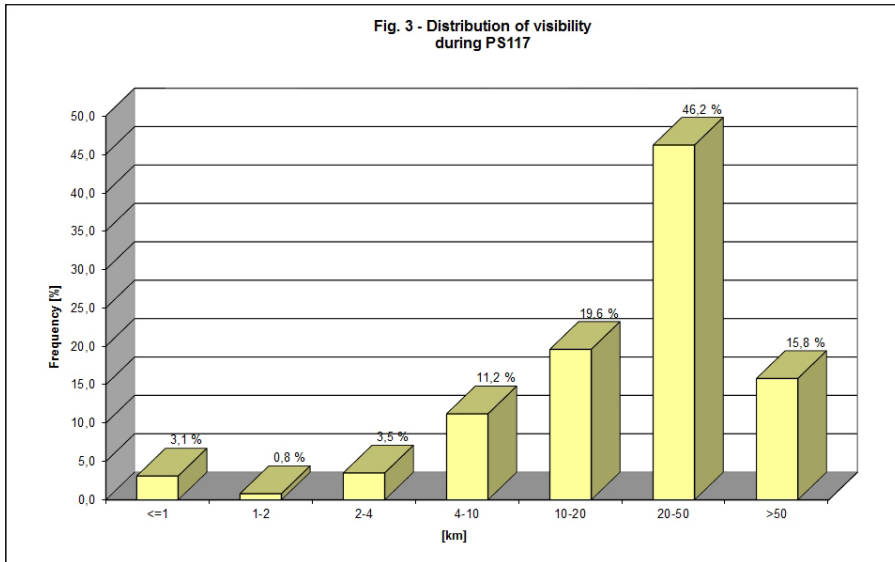


Fig. 2.4: Distribution of cloud coverage during PS117.

**Weather enroute PS117  
from 15.12.2018 00 UTC to 06.02.2019 08 UTC**

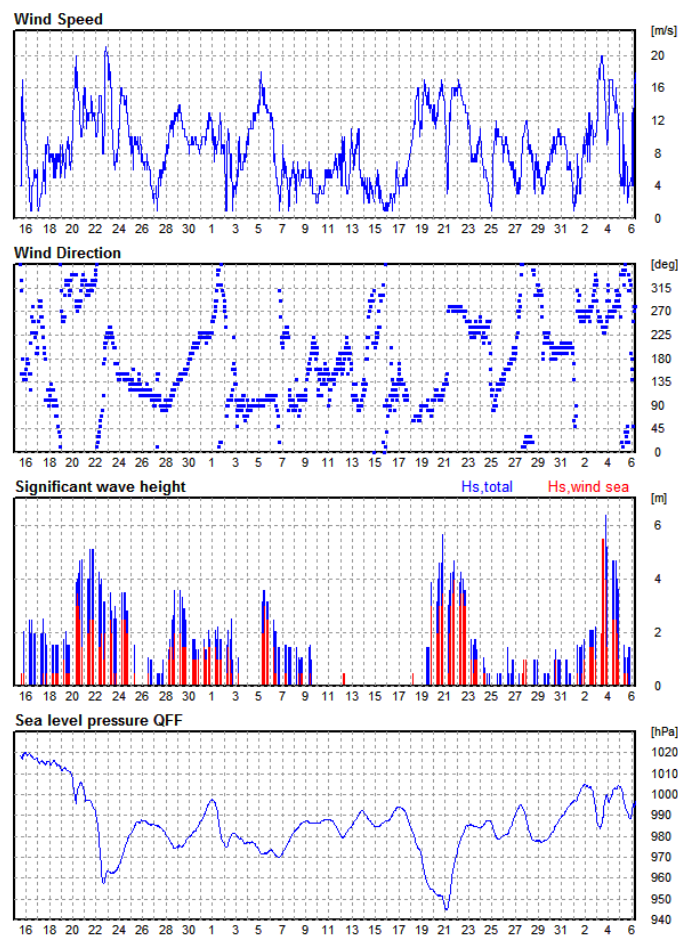


Fig. 2.5: Weather en route PS117

**Weather enroute PS117**  
 from 15.12.2018 00 UTC to 06.02.2019 08 UTC

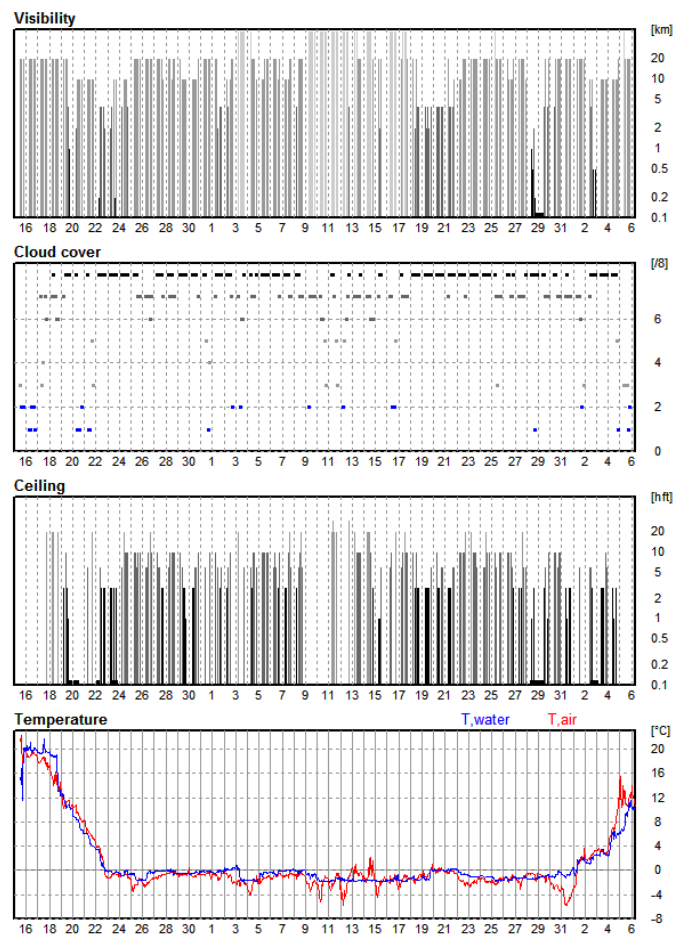


Fig. 2.6: Distribution of wave heights during PS117

### **3. HAFOS: MAINTAINING THE AWI'S LONG TERM OCEAN OBSERVATORY IN THE WEDDELL SEA**

#### **3.1 Physical oceanography**

Olaf Boebel<sup>1</sup>, Jakob Allersholt<sup>1,2</sup>, Paul Chamberlain<sup>1,3</sup>, Carina Engicht<sup>1</sup>, Diego Filun<sup>1</sup>, Rainer Graupner<sup>1</sup>, Moritz Krusenbaum<sup>1,4</sup>, Marlene Meister<sup>1,6</sup>, Nicolas le Pailh<sup>1</sup>, Lewin Probst<sup>1</sup>, Gerd Rohardt<sup>1</sup>, Janin Schaffer<sup>1</sup>, Margarita Smolentseva<sup>1</sup>, Stefanie Spiesecke<sup>1</sup>, Sarah Zwicker<sup>1,7</sup>

<sup>1</sup>AWI  
<sup>2</sup>HS Brhvn  
<sup>3</sup>Scripps  
<sup>4</sup>CAU / GEOMAR  
<sup>5</sup>HUB  
<sup>6</sup>U Bremen  
<sup>7</sup>UOL

**Grant No: AWI\_PS117\_01**

#### **Outline and objectives**

Due to its ability to internally store and transport vast amounts of heat and CO<sub>2</sub>, the ocean is a key element of the global climate system. Its response to changes in the forcing is expressed and controlled by its stratification, which is governed by the vertical distribution of temperature and salinity. Until the turn of the century, shipborne observations were the only means of obtaining sufficiently accurate vertical profiles of water mass properties, but progress in sensor technology now allows using automated systems. The current backbone of the Global Ocean Observing System (GOOS) is the Argo system, which consists of an array of more than 3,000 profiling floats, distributed throughout the world oceans. Provided by an international group of oceanographic institution, it aims at establishing a real-time data stream of mid- and upper (< 2,000 m) ocean temperature and salinity profiles augmented by a mid-depth oceanic circulation pattern due to the floats' intrinsic drift between profiles.

However, Argo in its current form is restricted to oceanic regions that are ice free year-round, as the floats need to surface to be localized and to transmit their profile data via satellite link. HAFOS (Hybrid Antarctic Float Observing System) constitutes an extension of this system into seasonally ice covered waters of the Weddell Gyre, overcoming these limitations through a combination of well tested technologies to close the observational gaps in the Antarctic Ocean. To this end, the AWI pushed technological developments to extend the operational range of Argo floats into seasonally ice-covered regions by initiating the development of the NEMO float (Navigating European Marine Observer) which features an ice sensing algorithm (ISA, Klatt et al., 2007), triggering the abort of a floats' ascent to the sea surface when the presence of sea ice is likely, as determined from the existence of a layer of near surface winter water. To be able to (retrospectively) track the floats that continued their mission under sea ice, RAFOS (Rossby et al., 1986) (Ranging And Fixing Of Sound) technology is used, based on an array of currently 14 moored (with 11 redeployed during this expedition) RAFOS sound sources.

To determine trends and fluctuations in the characteristics of the main Antarctic water masses (Warm Deep Water, WDW and Antarctic Bottom Water, ABW), a set of more than a dozen hydrographic moorings has been maintained and expanded throughout the past 30 years by

AWI. HAFOS builds on this backbone by having added RAFOS sound sources for under-ice tracking of Argo floats since 2002. Near bottom recorders continue truly climatological time series as sentinels for climate change in the formation areas of bottom waters whereas the profiling floats record the water mass properties in the upper ocean layers. Passive acoustic monitoring allows linking marine mammal distribution in the open ocean to ongoing ecosystem changes, thereby complementing the physical measurements with biosphere observations at its highest trophic level. The effort focuses on a region where year-round marine mammal observations are notoriously sparse and difficult to obtain.

HAFOS complements international efforts to establish an ocean observing systems in the Antarctic as a legacy of the International Polar Year 2007/2008 (IPY) and as a contribution to the Southern Ocean Observing System (SOOS), which is under development under the auspices of the Scientific Committee of Antarctic Research (SCAR) and the Scientific Committee on Oceanic Research (SCOR).

Additionally, in support of the international Argo programme, 10 floats were deployed *en route* on behalf of the German BSH (Bundesamt für Seeschifffahrt und Hydrographie). To foster our involvement in the GoodHope section and in support of our French colleagues early in the expedition we successfully retrieved 5 PIES while the attempted recovery of one additional PIES was unsuccessful.

Most oceanographic instruments are, by and large, designed for deployment periods of maximal 3 years before they need to be recovered for maintenance and battery replacement. Hence, one major goal of *Polarstern* expedition PS117 was to recover and redeploy moorings deployed during PS103 in 2016/17, to be able to continue these observations for another 2-3 years.

#### 3.1.1 Hydrographic moorings

##### Work at sea

The oceanographic studies during *Polarstern* expedition PS117 focussed on two major areas, the Greenwich Meridian and the Weddell Sea, continuing more than 30 years of *in-situ* observations in the Atlantic sector of the Southern Ocean (Fig. 3.1). Moorings were exchanged to obtain time series of water mass properties throughout the deep and the surface layers, but also information on habitat usage by marine mammals. For this purpose, the moorings host current meters, temperature and salinity sensors and passive acoustic recorders. During the previous expedition (PS103) it was not possible to retrieve one of the moorings due to a failure of its release. For this reason, a ROV (remotely operated vehicle) was taken aboard PS117 to recover this moorings by attaching a recovery rope to it, see section “Mooring recovery with a ROV” for more details on this effort.

To enhance the vertical resolution and to calibrate moored sensors, CTD stations were occupied at the mooring locations. The CTD/water sampler consists of a SBE911plus CTD system in combination with a carousel water sampler SBE32 with 24 12-l bottles. To determine the distance to the bottom, an altimeter from Benthos was mounted. A transmissometer CSTAR and a fluorometer EcoFLR from Wetlabs, and a SBE43 oxygen sensor from Seabird Electronics were incorporated in the sensor package. Additionally, a lowered ADCP system was attached to the rosette sampler to measure the current velocity profile, see Chapter “Lowered ADCP”.

All mooring were recovered successfully, albeit AWI250-1 required the use ROV Fiona to attach a recovery rope to the top floatation, as the mooring had been deployed six years prior to this recovery attempt and the acoustic release did not respond to the release command. and Tab. 3.2 provide summaries of mooring recoveries and deployments.

### 3. HAFOS: Maintaining the AWI's Long Term Ocean Observatory in the Weddell Sea

**Tab. 3.1:** Mooring recoveries during PS117. <sup>1)</sup> indicates PIES landers, <sup>2)</sup> indicates the PIES landers that did not surface, <sup>3)</sup> indicates recovery of a mooring deployed during ANT-XXIX/2 (PS81 2012/13); all other moorings were deployed during PS103 (2016/17). "CTD Stat.Nr." is the station number of the CTD cast carried out at the mooring location.

Mooring	Latitude	Longitude	Depth [m]	Deployment		Recovery		CTD Stat. Nr.
PIES-2 <sup>1</sup>	36° 13.21' S	13° 18.10' E	4832	06.12.2014	10:17	16.12.2018	18:14	1-1
PIES-3 <sup>1</sup>	37° 24.46' S	12° 31.12' E	5070	25.07.2015	20:17	17.12.2018	06:24	2-1
PIES-4 <sup>2</sup>	38° 36.10' S	11° 45.77' E	5120	07.12.2014	07:54	17.12.2018	19:05	3-1
PIES-5 <sup>1</sup>	39° 58.57' S	10° 47.67' E	4775	07.12.2014	19:56	18.12.2018	11:27	4-1
PIES-6 <sup>1</sup>	41° 20.90' S	09° 53.28' E	4680	27.07.2015	11:22	19.12.2018	00:01	5-1
PIES-7 <sup>1</sup>	42° 41.65' S	08° 44.24' E	4970	28.07.2015	18:19	19.12.2018	11:15	6-3
AWI227-14	59° 03.03' S	00° 06.43' E	4641	24.12.2016	16:15	31.12.2018	00:38	22-2
AWI229-13	64° 00.49' S	00° 00.84' W	5165	26.12.2016	19:25	01.01.2019	16:12	18-2
AWI231-12	66° 31.03' S	00° 04.49' W	4577	28.12.2016	15:24	27.12.2018	10:32	15-1
AWI244-5	69° 00.32' S	06° 59.56' W	2946	01.01.2017	16:09	05.01.2019	12:30	33-1
AWI248-2	65° 58.12' S	12° 13.87' W	5047	02.01.2017	16:56	06.01.2019	21:08	34-2
AWI245-4	69° 03.64' S	17° 23.45' W	4736	11.01.2017	18:20	08.01.2019	07:23	35-6
AWI249-2	70° 53.54' S	28° 53.47' W	4401	13.01.2017	16:32	20.01.2019	06:00	53-4
AWI209-8	66° 36.45' S	27° 07.29' W	4872	18.01.2017	15:24	21.01.2019	15:00	54-2
AWI208-8	65° 41.79' S	36° 41.01' W	4766	19.01.2017	22:15	23.01.2019	09:42	56-2
AWI250-1 <sup>3</sup>	68° 28.95' S	44° 06.67' W	4100	15.01.2013	14:53	24.01.2019	11:30	58-1
AWI250-2	68° 27.84' S	44° 08.71' W	4137	21.01.2017	19:09	24.01.2019	16:15	58-1
AWI257-1	64° 12.94' S	47° 29.42' W	4293	23.01.2017	17:23	27.01.2019	12:35	64-4
AWI258-1	64° 03.99' S	48° 22.83' W	3933	24.01.2017	08:36	28.01.2019	08:41	66-1
AWI259-1	63° 55.02' S	49° 16.09' W	3449	24.01.2017	15:35	28.01.2019	17:03	68-2
AWI260-1	63° 46.70' S	50° 05.38' W	2819	25.01.2017	08:39	29.01.2019	08:55	71-1
AWI207-10	63° 39.36' S	50° 48.68' W	2555	26.01.2017	10:27	29.01.2019	12:44	72-3
AWI261-1	63° 30.87' S	51° 38.14' W	1700	26.01.2017	18:55	30.01.2019	09:09	76-1
AWI262-1	63° 24.20' S	52° 17.22' W	672	28.01.2017	09:44	30.01.2019	17:05	81-2
AWI251-2	61° 01.26' S	55° 58.84' W	331	29.01.2017	15:36	01.02.2019	17:16	99-2

**Tab. 3.2:** Mooring deployments during PS117. <sup>1)</sup> denotes a mooring not deployed due to bad weather conditions.

Mooring	Latitude	Longitude	Depth [m]	Deployment (Time in UTC)	
AWI227-15	59° 03.02' S	00° 06.44' E	4605	31.12.2018	10:10
AWI229-14	64° 01.26' S	00° 00.83' W	5060	01.01.2019	22:38
AWI231-13	66° 31.03' S	00° 04.48' W	4580	27.12.2018	18:34
AWI244-6	69° 00.08' S	07° 01.65' W	2900	05.01.2019	20:01
AWI248-3	65° 58.12' S	12° 13.84' W	4950	07.01.2019	10:37
AWI245-5	69° 03.64' S	17° 23.49' W	4734	08.01.2019	14:20

### 3.1 Physical oceanography

Mooring	Latitude	Longitude	Depth [m]	Deployment (Time in UTC)	
AWI249-3	70° 53,22' S	28° 56,97' W	4407	20.01.2019	12:00
AWI209-9 <sup>1</sup>	-	-	-	21.01.2019	-
AWI208-9	65° 41.78' S	36° 41.01' W	4766	23.01.2019	16:01
AWI250-3	68° 28.85' S	44° 05.94' W	4141	24.01.2019	20:28
AWI257-2	64° 12.94' S	47° 29.38' W	4215	27.01.2019	17:50
AWI207-11	63° 39.36' S	50° 48.66' W	2555	29.01.2019	17:08
AWI251-3	61° 01.38' S	55° 58.68' W	334.8	01.02.2019	18:31

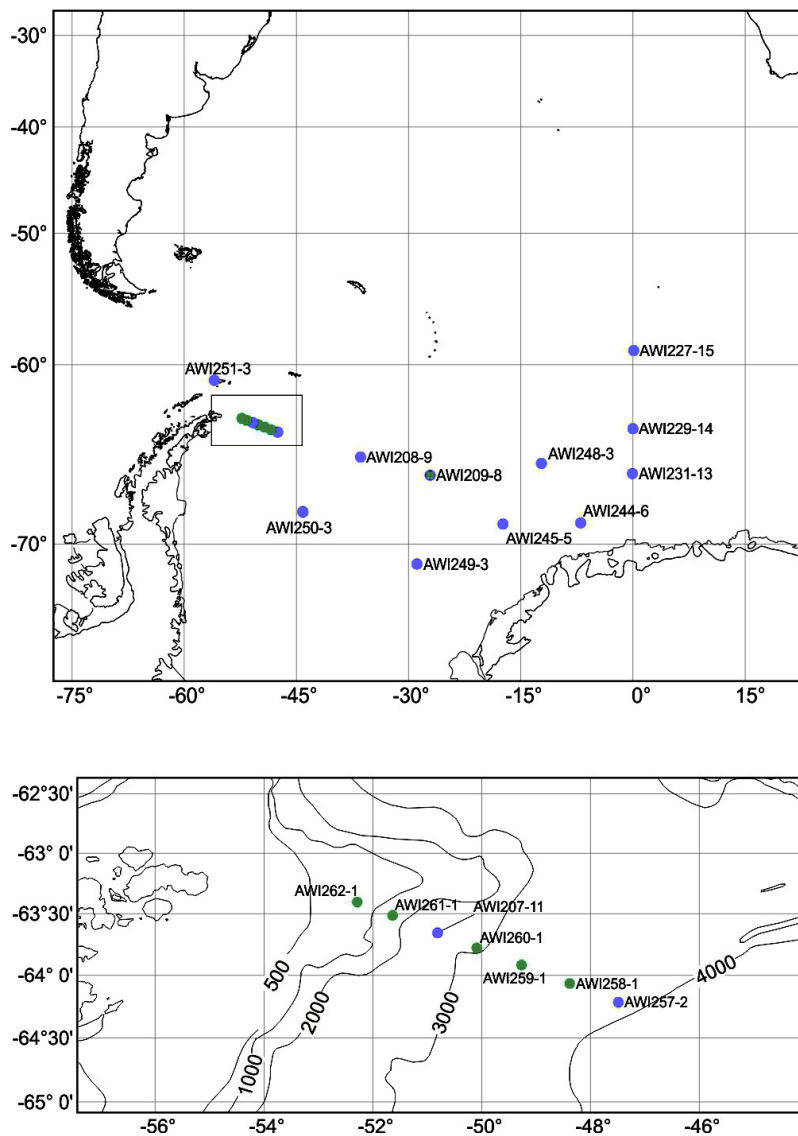


Fig. 3.1: Map of mooring locations occupied since 2016/17 or earlier. The lower panel is an enlargement of the black box in the top panel. Green dots indicate moorings recovered and blue dots moorings exchanged during this expedition PS117. The current number “n” of the mooring ID “AWIxxx-n” is the number of the deployed mooring. If the mooring was not exchanged, “n” represents the number of the recovered mooring.

### 3. HAFOS: Maintaining the AWI's Long Term Ocean Observatory in the Weddell Sea

Details regarding the instrumentation of the deployed moorings are listed in Tab. 3.3.

**Tab. 3.3:** Instrumentation of deployed oceanographic moorings

Mooring	Latitude Longitude	Water Depth [m]	Date Time	Instrument Type	Instrument Serial Number	Instrument Depth [m]
AWI227-15	59° 03.02' S	4605	31.12.2018	PAM	1006	300
	00° 06.44' E		10:10	SBE37	12479	4597
AWI229-14	64° 01.26' S	5060	01.01.2019	SBE37	9494	50
	00° 00.83' W		22:38	SBE37	9495	100
				SBE37	9496	150
				SBE37	9497	200
				AquaD	12654	230
				SBE37	9492	231
				PAM	1060	300
				SBE37	2098	330
				SBE37	2385	430
				SBE37	2382	530
				SBE37	2396	630
				SBE37	3811	734
				AquaD	12658	735
				SBE37	12481	5152
AWI231-13	66° 31.03' S	4580	27.12.2018	PAM	1056	300
	00° 04.48' W		18:34	SBE37	10944	4534
AWI244-6	69° 00.08' S	2900	05.01.2019	PAM	1049	300
	07° 01.65' W		20:01	SBE37	8122	2903
AWI248-3	65° 58.12' S	4950	07.01.2019	PAM	1012	300
	12° 13.84' W		10:37	SBE37	8123	5003
AWI245-5	69° 03.64' S	4734	08.01.2019	PAM	1014	300
	17° 23.49' W		14:20	SBE37	8124	4693
AWI249-3	70° 53.22' S	4407	20.01.2019	PAM	1010	300
	28° 56.97' W		12:00	SBE37	8126	4357
AWI208-9	65° 41.78' S	4766	23.01.2019	PAM	1020	300
	36° 41.01' W		16:01	AquaD	12685	806
				SBE37	3812	807
				SBE37	9841	4758
AWI250-3	68° 28.85' S	4141	24.01.2019	PAM	1048	300
	44° 05.94' W		20:28	AquaD	12718	819
				SBE37	3813	820
				SBE37	9839	4094
AWI257-2	64° 12.94' S	4215	27.01.2019	PAM	1033	300
	47° 29.38' W		17:50	RCM	11888	813
				SBE37	10944	814
				SBE37	9493	4285
AWI207-11	63° 39.36' S	2555	29.01.2019	SBE37	10934	250
	50° 48.66' W			QM150	23548	291

### 3.1 Physical oceanography

Mooring	Latitude Longitude	Water Depth [m]	Date Time	Instrument Type	Instrument Serial Number	Instrument Depth [m]
				PAM	1032	300
				AquaD	12745	802
				SBE37	6928	803
				SBE37	10937	2200
				AVT	3517	2248
				SBE39	8641	2259
				SBE39	8642	2305
				SBE39	8643	2355
				SBE37	10943	2406
				QM150	24053	2545
				SBE37	9847	2545
AWI251-3	61° 01.378' S 55° 58.676' W	335	01.02.2019	PAM	AU0085	179
				PAM	1002	181
				AZFP	55037	288
				QM150	5373	322
				SBE37	2096	322

#### Abbreviations

AVT	Aanderaa Current Meter with Temperature Sensor
AZFP	Acoustic Zooplankton and Fish Profiler (acoust.)
PAM	Passive Acoustic Monitor (Type: AURAL or SONOVAULT)
PIES	Pressure Inverted Echo Sounder
RCM11	Aanderaa Doppler Current Meter (acoust.)
SBE37	SeaBird Electronics, Type: MicroCat, to measure Temperature and Conductivity
SBE39	SeaBird Electronics Temperature Logger
SBE56	SeaBird Electronics Temperature Logger
SOSO	RAFOS Sound Source
AquaD	Nortek Aquadopp Acoustic Current Meter
QM150	RD Instruments Doppler Current Profiler, Typ Quarter Master 150 kHz
mab	Depth of instruments given in meters above bottom

A noteworthy addition to our standard instrumentation concerns mooring AWI251-03, close to Elephant Island. There an AZFP (Acoustic Zooplankton and Fish Profiler, ASL) is using the backscatter of acoustic pings at four different frequencies (38 kHz, 125 kHz, 455 kHz, 769 kHz) to detect zooplankton. AZFP55037 was deployed at 280 m water depth and is set to ping four times every 10 minutes. Data of every ping will be stored without averaging. The pulse length for every frequency is set to the maximum to bring the maximum power into the water column. The range for the measurement is set to 309 m, with bin sizes of 0.25 m. A deployment period of 1,100 days was assumed for the calculation of storage space.

### 3. HAFOS: Maintaining the AWI's Long Term Ocean Observatory in the Weddell Sea

Additionally a 75 kHz ADCP (Acoustic Doppler Current Profiler, SN 5373) was deployed in that mooring at 320 m water depth. The ADCP pings every 10 minutes, 5 minutes apart from the AZFP pings. Apart from information on the oceanic currents at the mooring position, its data is also intended to be used for analysis of presence of zooplankton.

#### Preliminary operational results

Details of the recovered moorings, their instrumentation and the length of each retrieved data record are listed in Tab. 3.4. In general, the instruments performed well, providing, with few exceptions, data for the full deployment period. One instrument had recorded data for prolonged deployment period of up to 6 years.

**Tab. 3.4:** Moorings recovered during PS117. Date and time of the recovery represent date and time of the first release command.

Mooring PIES	Latitude Longitude	Water Depth [m]	Date Time		Instrument Type	Serial Number	Instrument Depth [m]	Record Length (days) [Remarks]
			a. deployed	b. recovered				
AWI227-14	59° 03.03' S	4641	24.12.2016		PAM	1004	1070	[1]
	00° 06.43' E		16:37	31.12.20186	SBE37	218	4597	736
			00:38					
AWI229-13	64° 00.49' S	5165	26.12.2016		RCM11	296	202	571
	00° 00.84' W		10:03		SBE37	1228	300	736
			01.01.2019		SBE37	2089	400	736
			16:12		SBE37	2388	500	736
					SBE37	2389	600	736
					SBE37	8127	650	736
					SBE37	8128	700	736
					RCM11	461	709	599
					PAM	1053	993	[1]
					SBE37	233	5152	736
AWI231-12	66° 31.03' S	4477	28.12.2016		PAM	1021	223	[1]
	00° 04.49' W		09:28		PAM	1022	570	[1]
			27.12.2018		PAM	1023	859	[1]
			10:32		PAM	1024	1064	[1]
					PAM	1026	2074	[1]
					SBE37	235	4535	729
AWI244-5	69° 00.32' S	2946	01.01.2017		SOSO	D0049	842	[2]
	06° 59.56' W		08:55		PAM	1057	1044	[1]
			05.01.2019		SBE37	1232	2903	734
			12:30					
AWI248-2	65° 58.12' S	5047	02.01.2017		SOSO	D0024	833	[2]
	12° 13.87' W		10:00		PAM	1058	1035	[1]
			06.01.2019		SBE37	1233	5003	735
			21:08					
AWI245-4	69° 03.47' S	4736	11.01.2017		SOSO	D0048	802	[2]

### 3.1 Physical oceanography

Mooring PIES	Latitude Longitude	Water Depth [m]	Date Time a. deployed b. recovered	Instrument Type	Serial Number	Instrument Depth [m]	Record Length (days) [Remarks]
	17° 23.45' W		08:00	PAM	1005	1004	[1]
			08.01.2019	SBE37	8130	4693	727
			07:23				
AWI249-2	70° 53.55' S	4364	13.01.2017	SOSO	D0028	837	[2]
	28° 53.47' W		06:00	PAM	1061	1041	[1]
				SBE37	8131	4357	737
AWI209-8	66° 36.45' S	4872	15.01.2017	SOSO	D0047	854	[2]
	27° 07.29' W		06:00	PAM	1008	1053	[1]
			21.01.2019	SBE37	9487	4864	733
			15:11				
AWI208-8	65° 41.79' S	4766	19.01.2017	SOSO	D0030	830	[2]
	36° 41.01' W		14:00	PAM	1009	1032	[1]
			23.01.2019	SBE37	9488	4758	743
			09:42				
AWI250-1	68° 28.95' S	4100	15.01.2013	SOSO	Web 23	798	[2]
	44° 06.67' W		14:53	PAM	1031	1041	[1]
			24.01.2019	SBE37	9848	4057	2210
			16:08				
AWI250-2	68° 27.84' S	4137	21.01.2017	SOSO	D0045	834	[2]
	44° 08.71' W		19:09	PAM	1003	1036	[1]
			24.01.2019	SBE37	10931	4094	732
			11:30				
AWI257-1	64° 12.94' S	4293	23.01.2017	SOSO	D0026	803	[2]
	47° 29.42' W		17:23	SBE37	2234	200mab	733
			27.01.2019	AVT	9768	150mab	733
			12:35	SBE39	7862	130mab	733
				SBE37	10948	100mab	733
				SBE39	7861	70mab	733
				AVT	9390	50mab	733
				SBE39	7860	40mab	733
				SBE37	10928	10mab	733
				AVT	9782	8mab	733
AWI258-1	64° 03.99' S	3933	24.01.2017	SBE37	9491	200mab	733
	48° 22.83' W		08:36	AVT	9187	150mab	733
			28.01.2019	SBE39	7865	130mab	733

### 3. HAFOS: Maintaining the AWI's Long Term Ocean Observatory in the Weddell Sea

Mooring PIES	Latitude Longitude	Water Depth [m]	Date Time a. deployed b. recovered	Instrument Type	Serial Number	Instrument Depth [m]	Record Length (days) [Remarks]
			08:41	SBE37	10939	100mab	733
				SBE39	7864	70mab	733
				AVT	9770	50mab	733
				SBE39	7863	40mab	733
				SBE37	10946	10mab	[6]
				AVT	9998	8mab	733
AWI259-1	63° 55.02' S	3449	24.01.2017	RCM11	506	350mab	<u>584</u>
	49° 16.09' W		15:35	SBE37	2090	300mab	733
			28.01.2019	SBE39	7868	250mab	733
			17:03	SBE39	7867	200mab	733
				SBE39	7866	150mab	733
				RCM11	568	100mab	<u>421</u>
				SBE37	10929	99mab	733
				RCM11	500	40mab	<u>533</u>
				SBE37	2093	8mab	733
AWI260-1	63° 46.70' S	2819	25.01.2017	RCM11	462	350mab	<u>579</u>
	50° 05.38' W		08:39	SBE37	9832	300mab	733
			29.01.2019	SBE39	7871	250mab	733
			08:55	SBE39	7870	200mab	733
				SBE39	7869	150mab	733
				RCM11	486	100mab	<u>641</u>
				SBE37	2092	99mab	733
				RCM11	504	40mab	<u>609</u>
				SBE37	2101	8mab	733
AWI207-10	63° 39.36' S	2555	26.01.2017	AVT	11613	305	733
	50° 48.68' W		10:27	SBE37	10930	318	733
			29.01.2019	RCM11	569	808	<u>549</u>
			12:44	SOSO	D0048	959	[2]
				PAM	1029	1061	[1]
				RCM11	619	356mab	<u>439</u>
				SBE37	10947	355mab	733
				SBE39	7877	300mab	733
				SBE39	7876	250mab	733
				SBE39	7872	200mab	733
				AVT	10503	150mab	733
				SBE37	2395	149mab	733
				AVT	8037	40mab	733
				SBE37	10941	10mab	733

### 3.1 Physical oceanography

Mooring PIES	Latitude Longitude	Water Depth [m]	Date Time a. deployed b. recovered	Instrument Type	Serial Number	Instrument Depth [m]	Record Length (days) [Remarks]
AWI261-1	63° 30.87' S	1700	26.01.2017	PAM	1011	842	[1]
	51° 38.14' W		18:55	AVT	9783	352mab	733
			30.01.2019	SBE37	1234	350mab	732
			09:09	SBE56	6988	300mab	732
				SBE56	6987	250mab	[3]
				SBE56	6986	200mab	732
				AVT	9786	150mab	733
				SBE37	9490	149mab	732
				AVT	9997	40mab	733
				SBE37	10938	8mab	732
AWI262-1	63° 24.20' S	672	28.01.2017	AVT	8048	350mab	732
	52° 17.22' W		09:44	SBE37	10933	300mab	732
			30.01.2019	SBE56	6991	250mab	732
			17:05	SBE56	6990	175mab	732
				AVT	8402	150mab	732
				SBE56	6989	100mab	732
				SBE37	10935	50mab	732
				AVT	8403	40mab	732
				SBE37	10936	8mab	732
AWI251-2	61° 01.26' S	331	29.01.2017	PAM	1031	215	[1]
	55° 58.84' W		15:36	PAM	AU0231	220	[1]
			01.02.2019	SBE37	3814	319	733
			17:16				

#### Remarks

The underlined number of days of record length indicated shorter records due to battery or memory failures.

mab      Depth of instruments given in meters above bottom

[1]      to be processed

[2]      passive instrument

[3]      instrument lost

[4]      recovery failed

[5]      mooring lost

[6]      no data recorded

3.1.2 *In-situ* calibration of moored instruments

Work at sea

All Seabird® instruments (SBE37, SBE39plus, and SBE56) were compared *in-situ* with the 911plus CTD system prior to mooring deployment (Tab. 3.5) or after (Tab. 3.6) recovery. Up to 15 units can be attached at a time to the frame of the water sampler. For the *in-situ* calibration the sampling interval was set to 10 seconds and programmed to begin sampling prior to the CTD reaching its maximum depth. The CTD/RO was stopped at the maximum depth for 5 minutes to obtain approximately 30 records for comparison with the CTD reading. If the temperature- and conductivity differences in SeasaveV7 display indicated an inhomogeneous water layer, the CTD/RO was lifted by 50 or 100 m prior to beginning the *in-situ* calibration.

**Tab. 3.5:** Comparison for Seabird sensors SBE37 moored during PS117. Columns CTD and PRES indicate the corresponding station number and the CTD pressure during the 5 minute stop.  $X_{corr} = X_{reading} + dX$ , with X = temperature (t), conductivity(c) or pressure (p).

SN	Typ	dp	dt	dc	CTD	PRES
8122	SBE37	0,7	0,0010	0,0019	004-01	4859
8123	SBE37	0,6	0,0014	0,0029		
8124	SBE37	-1,6	0,0011	0,0048		
8126	SBE37	1,7	0,0009	0,0031		
9492	SBE37	-3,4	-0,0001	0,0017		
9494	SBE37	-3,3	0,0006	0,0010		
9495	SBE37	-1,0	0,0009	0,0038		
9496	SBE37	-3,7	0,0008	0,0038		
9497	SBE37	-4,4	0,0008	0,0044		
9847	SBE37	-1,3	0,0017	0,0041		
10934	SBE37	-4,3	0,0007	0,0054		
10950	SBE37	-4,9	0,0006	0,0045		
2382	SBE37		0,0022	0,0220	006-03	4987
2385	SBE37		0,0003	0,0208		
2396	SBE37		0,0016	0,0109		
9493	SBE37	-4,7	0,0011	0,0026		
9831	SBE37	-3,9	0,0003	0,0021		
9839	SBE37	-5,3	0,0006	0,0010		
9841	SBE37	-4,7	0,0014	0,0010		
10937	SBE37	-2,6	0,0012	0,0096		
10943	SBE37	-6,1	0,0018	0,0035		
10944	SBE37	-5,7	0,0003	0,0009		
12479	SBE37	-4,5	0,0012	0,0079		
12481	SBE37	-3,4	0,0012	0,0044		
2096	SBE37	-4,3	0,0008	0,0057	014-01	3053
2098	SBE37	-4,4	0,0011	0,0034		
3811	SBE37	2,7	0,0015	0,0056		
3812	SBE37	3,3	0,0013	0,0060		
3813	SBE37	1,8	0,0036	0,0050		
8641	SBE39	-5,4	0,0016			

### 3.1 Physical oceanography

SN	Typ	dp	dt	dc	CTD	PRES
8642	SBE39	-7,4	0,0012			
8643	SBE39	-7,2	0,0008			
6928	SBE37		0,0011	0,0110		
7690	SBE37	1,2	0,0024	0,0028		

**Tab. 3.6:** Offsets for Seabird sensors SBE37 and SBE39 recovered during PS117. Their temperature and conductivity data was adjusted based on a linear interpolation between prior (dt1, dc1) and post recovery (dt2, dc2 dp2) offsets. For pressure the post recovery offset was applied as a constant offset.  $X_{corr} = X_{reading} + dX$ , with X = temperature (t), conductivity(c) or pressure (p).

MOORING	SN	dt1	dc1	dt2	dc2	dp2
227-14	218	-0,0012	0,0180	-0,0007	0,0213	0,0000
229-13	233	-0,0030	0,0168	-0,0021	0,0105	0,0000
229-13	1228	0,0003	0,0070	0,0006	0,0069	0,0000
229-13	2089	0,0002	0,0092	0,0008	0,0027	4,0833
229-13	2388	0,0007	0,0210	0,0014	0,0190	0,0000
229-13	2389	0,0015	0,0227	0,0024	0,0214	0,0000
229-13	8127	-0,0006	0,0034	0,0003	0,0040	-3,9754
229-13	8128	-0,0005	0,0053	0,0005	0,0057	-5,7335
231-12	235	-0,0035	0,0215	0,0015	0,0191	0,0000
244-5	1232	0,0027	0,0124	0,0018	0,0082	-2,2000
248-2	1233	0,0016	0,0117	-0,0028	0,0024	-1,8000
245-4	8130	0,0023	0,0062	0,0021	0,0036	-6,7000
249-2	8131	0,0015	-0,0010	-0,0031	-0,0067	-5,0000
208-8	9487	0,0018	0,0053	-0,0027	0,0000	-6,3000
209-8	9488	0,0020	0,0057	-0,0026	0,0004	-6,3000
250-1	9848	0,0000	0,0000	-0,0028	-0,0046	-8,7000
250-2	10931	0,0030	0,0123	-0,0023	0,0002	-7,5000
257-1	2234	0,0034	0,0135	-0,0017	0,0016	-5,7000
257-1	7862	0,0001	0,0000	-0,0027	0,0000	-9,0000
257-1	10948	0,0028	0,0047	-0,0023	-0,0018	-11,3000
257-1	7861	0,0003	0,0000	-0,0026	0,0000	-0,7000
257-1	7860	0,0000	0,0000	-0,0028	0,0000	-7,6000
257-1	10928	0,0019	0,0075	-0,0024	-0,0038	-10,7000
258-1	9491	0,0018	0,0036	0,0014	0,0014	-6,9000
258-1	7865	0,0000	0,0000	0,0003	0,0000	-9,6000
258-1	10939	0,0018	0,0093	0,0015	0,0053	-6,6000
258-1	7864	-0,0005	0,0000	-0,0033	0,0000	-8,2000
258-1	7863	-0,0003	0,0000	0,0004	0,0000	-9,8000
259-1	2090	0,0036	0,0088	0,0017	0,0033	-6,0000
259-1	7868	0,0000	0,0000	0,0010	0,0000	-7,9000
259-1	7867	0,0021	0,0000	0,0005	0,0000	-7,4000

### 3. HAFOS: Maintaining the AWI's Long Term Ocean Observatory in the Weddell Sea

MOORING	SN	dt1	dc1	dt2	dc2	dp2
259-1	7866	-0,0003	0,0000	0,0002	0,0000	-9,1000
259-1	10929	0,0019	0,0063	0,0016	0,0000	-8,4000
259-1	2093	0,0036	0,0105	0,0024	0,0052	-5,6000
260-1	9832	0,0020	0,0036	0,0012	0,0001	-6,3000
260-1	7871	0,0003	0,0000	-0,0003	0,0000	-6,8000
260-1	7870	0,0023	0,0000	-0,0011	0,0000	-5,3000
260-1	7869	0,0023	0,0000	-0,0007	0,0000	-4,1000
260-1	2092	0,0037	0,0133	0,0013	0,0023	-5,2000
260-1	2101	0,0034	0,0094	0,0014	0,0015	-3,9000
207-10	10930	0,0021	0,0061	0,0005	0,0021	-4,7000
207-10	10947	0,0013	0,0044	-0,0002	0,0018	-6,3000
207-10	7877	-0,0002	0,0000	-0,0008	0,0000	-7,7000
207-10	7876	-0,0004	0,0000	-0,0006	0,0000	-7,1000
207-10	7872	0,0023	0,0000	-0,0006	0,0000	-2,4000
207-10	2395	0,0029	0,0091	0,0009	0,0041	0,7000
207-10	10941	0,0023	0,0066	0,0016	0,0040	-6,6000
261-1	1234	0,0026	0,0100	0,0026	0,0100	0,0000
261-1	6988	0,0000	0,0000	0,0000	0,0000	0,0000
261-1	6987	0,0000	0,0000	0,0000	0,0000	0,0000
261-1	6986	0,0000	0,0000	0,0000	0,0000	0,0000
261-1	9490	0,0000	0,0000	0,0000	0,0000	0,0000
261-1	10938	0,0018	0,0027	0,0018	0,0027	0,0000
262-1	10933	0,0024	0,0024	0,0024	0,0024	0,0000
262-1	6991	0,0000	0,0000	0,0000	0,0000	0,0000
262-1	6990	0,0000	0,0000	0,0000	0,0000	0,0000
262-1	6989	0,0000	0,0000	0,0000	0,0000	0,0000
262-1	10935	0,0022	0,0045	0,0022	0,0045	0,0000
262-1	10936	0,0029	0,0033	0,0029	0,0033	0,0000
251-2	3814	0,0036	0,0081	0,0036	0,0081	0,0000

#### 3.1.3 CTD observations

##### Work at sea

- CTD casts were conducted pursuing three independent objectives:
- To revisit the spatially highly resolved repeat CTD section along the Greenwich meridian, across its entire length after six years;
- To collect temperature and salinity data at PIES and mooring positions for the estimation of the drifts of the moored sensors;
- To revisit the spatially highly resolved repeat CTD section at the tip of the Antarctic Peninsula, after two years.

### 3.1 Physical oceanography

The medical emergency and weather conditions required a rather impromptu planning for the the Greenwich section south of 50°S, resulting, once again, in a highly thinned out hydrographic section.

The rosette assembly comprised a SBE 911plus CTD system, combined with a carousel type SBE32 with 24 Niskin water samplers of 12 litre volume. Additionally, the assembly was equipped with an oxygen sensor SBE43, a Wetlabs C-Star transmissometer (wave length 650 nm; path length 25 cm), a Wetlabs Eco-FLR fluorometer, and a Benthos/DataSonics altimeter type PSA 916D.

CTD data was logged with Seabird's SeaSaveV7 data acquisition software to a local PC in raw format. ManageCTD, a Matlab™ based script developed at AWI, was employed to execute Seabird's SBEDataProcessing software, producing CTD profiles adjusted to 1-dbar intervals. ManageCTD additionally embedded metadata (header) information extracted from the DShip-ActionLog before conducting a preliminary de-spiking and data validation of the profile data.

Pre-processed data were saved in OceanDataView compatible format, to provide near real-time visualization of e.g. potential temperature and salinity, particularly to provide enroute (i.e. during the expedition) visualization of the unfolding hydrographic section.

The CTD was equipped with double sensors (Tab. 3.7) for temperature (SBE3plus) and conductivity (SBE4C). These sensors were calibrated prior to the expedition. Enroute comparison of the calibrated sensors nevertheless revealed differences of about of 2 mK in temperature and 1  $\mu\text{S}\cdot\text{cm}^{-1}$  in conductivity for *in-situ* measurements between the sensors. During cast 56-2 something intruded into the secondary sensor pair, including the oxygen sensor which did not flush out completely. Therefore sensors and pump were replaced after this station.

**Tab. 3.7:** CTD-Sensor configuration and the related station numbers

	#1 (primary); calibrated	#2 (secondary); calibrated	Stations
Temperature (SBE3plus)	2929; 23-Nov-2017	1198; 15-Nov-2017	1 to 56
Conductivity (SBE4c)	1373; 23-Nov-2017	1199; 15-Nov-2017	
Oxygen (SBE43)	-/-	2007; 08-Jun-2018	
Temperature (SBE3plus)	2929; 23-Nov-2017	5112; 29-Jun-2018	57 to 99
Conductivity (SBE4c)	1373; 23-Nov-2017	3570; 03-Jul-2018	
Oxygen (SBE43)	-/-	1597; 06-Jul-2018	

During this expedition, data from 46 full ocean depth CTD profiles were collected (Tab. 3.8). In addition, 3 shallow CTDs were cast to take water samples for other groups. A map of the locations of the CTD stations is provided by Fig. 3.2.

### 3. HAFOS: Maintaining the AWI's Long Term Ocean Observatory in the Weddell Sea

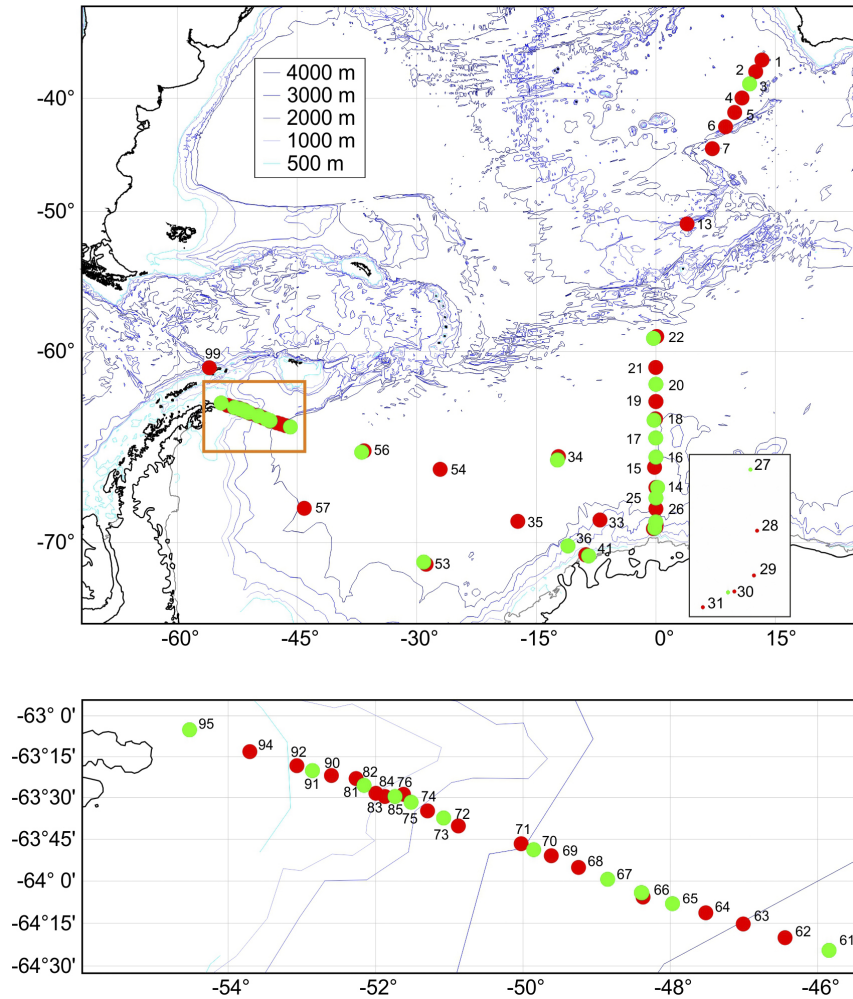


Fig. 3.2: Top: Map of locations of CTD stations. Labels indicate station and cast numbers as given in the station list. Bottom: Enlarged map of the CTD section at the tip of the Antarctic Peninsula; see box in map above.

Tab. 3.8: List of CTD profiles taken during PS117

Station	Cast	Date/Time	Latitude	Longitude	Echo Sounder [m]	Alti-meter [m]	CTD max. Pressure [dbar]
1	1	16-Dec-2018 17:40:13	36 13.356 S	13 18.294 E	4824	19	4915
2	1	17-Dec-2018 05:40:55	37 24.474 S	12 31.344 E	5054	14	5152
4	1	18-Dec-2018 10:32:00	39 58.518 S	10 47.808 E	4765	9	4859
5	1	18-Dec-2018 23:33:55	41 20.814 S	9 53.370 E	4678	9	4758
6	3	19-Dec-2018 15:14:42	42 41.628 S	8 44.268 E	4904	15	4987
7	1	20-Dec-2018 08:48:11	44 39.882 S	7 5.118 E	4592	12	4656
13	2	22-Dec-2018 02:26:20	50 59.994 S	3 55.602 E	3447	99	2030
14	1	26-Dec-2018 20:32:25	67 29.964 S	0 0.042 W	4634	10	4681
15	1	27-Dec-2018 07:41:08	66 30.870 S	0 10.176 W	4517		4555

### 3.1 Physical oceanography

Station	Cast	Date/Time	Latitude	Longitude	Echo Sounder [m]	Alti-meter [m]	CTD max. Pressure [dbar]
18	2	28-Dec-2018 19:43:29	63 57.876 S	0 1.746 W	5204	7	5279
19	1	29-Dec-2018 10:59:38	63 0.006 S	0 0.006 E	5307	8	5391
19	4	29-Dec-2018 15:11:19	63 0.018 S	0 0.084 W	5307		63
21	1	30-Dec-2018 13:53:10	60 59.760 S	0 0.648 W	5395	9	5468
22	2	31-Dec-2018 04:53:06	59 3.054 S	0 6.432 E	4645	20	4674
26	1	03-Jan-2019 03:49:46	68 30.000 S	0 0.024 W	4265	9	4298
28	1	04-Jan-2019 00:20:01	69 13.680 S	0 1.878 E	2782	10	2784
29	1	04-Jan-2019 04:05:41	69 19.656 S	0 0.684 E	2426	9	2413
30	1	04-Jan-2019 06:42:31	69 21.786 S	0 6.696 W	2105	9	2087
31	1	04-Jan-2019 12:07:21	69 23.880 S	0 18.582 W	1885	6	1857
33	1	05-Jan-2019 10:06:12	69 0.654 S	6 59.886 W	2938		102
33	6	06-Jan-2019 01:17:04	69 1.596 S	6 57.828 W	2892	9	2880
34	2	07-Jan-2019 01:47:53	65 58.236 S	12 13.176 W	5048	9	5115
35	6	08-Jan-2019 18:04:46	69 4.326 S	17 18.516 W	4772	10	4825
41	1	11-Jan-2019 14:27:56	70 31.344 S	8 46.056 W	192	5	184
41	6	11-Jan-2019 21:19:41	70 31.344 S	8 46.086 W	194	5	187
41	9	12-Jan-2019 04:19:22	70 31.218 S	8 46.230 W	193	9	181
41	12	12-Jan-2019 09:16:21	70 31.338 S	8 46.116 W	195	3	201
53	4	20-Jan-2019 14:58:07	70 54.426 S	28 50.928 W	4400	9	4436
54	2	21-Jan-2019 20:15:18	66 36.732 S	27 3.564 W	4872	14	4924
56	2	23-Jan-2019 07:50:39	65 40.464 S	36 35.892 W	4771		3565
57	3	24-Jan-2019 18:12:00	68 28.878 S	44 5.760 W	4141		134
58	1	24-Jan-2019 23:13:49	68 27.948 S	44 1.008 W	4151		3566
62	1	27-Jan-2019 04:45:40	64 20.052 S	46 26.538 W	4425	8	4459
63	1	27-Jan-2019 10:08:18	64 15.210 S	47 0.678 W	4320	10	4349
64	4	27-Jan-2019 20:25:49	64 11.274 S	47 31.080 W	4208	10	4231
66	1	28-Jan-2019 06:04:21	64 5.712 S	48 22.278 W	3926	10	3938
68	2	28-Jan-2019 20:00:42	63 55.134 S	49 14.718 W	3464	8	3462
69	1	29-Jan-2019 00:46:12	63 50.958 S	49 36.900 W	3237	9	3232
71	1	29-Jan-2019 07:21:09	63 46.644 S	50 1.458 W	2857	9	2842
72	3	29-Jan-2019 18:33:29	63 40.224 S	50 52.620 W	2530	10	2506
74	1	30-Jan-2019 01:38:57	63 34.740 S	51 17.646 W	2241	5	2217
76	1	30-Jan-2019 06:48:57	63 28.746 S	51 37.254 W	1814	10	1788
81	2	30-Jan-2019 19:16:24	63 22.980 S	52 15.870 W	670	9	647
83	2	31-Jan-2019 02:18:11	63 28.356 S	51 59.670 W	1058	7	1032
84	1	31-Jan-2019 04:10:22	63 29.544 S	51 52.374 W	1206	6	1180
90	1	31-Jan-2019 17:55:16	63 21.882 S	52 35.904 W	498	9	476
92	1	31-Jan-2019 20:57:22	63 18.336 S	53 4.104 W	453	7	435
94	1	01-Feb-2019 00:05:47	63 13.188 S	53 42.426 W	306	5	293
99	3	01-Feb-2019 19:10:37	61 0.840 S	56 0.726 W	412	9	396

### Preliminary operational results

While the CTD section along the Greenwich Meridian could not be repeated completely (Fig. 3.2 and Fig. 3.3) due to time constraints, the temperature profile at 61°S shows the near-linear continuation of the warming in the aged Weddell Sea Bottom Water (WSBW, Fig. 3.4). Within the 50 m thick bottom layer of the WSBW, the temperature increased from  $-0.8435^{\circ}\text{C}$  (1992) to  $-0.7759^{\circ}\text{C}$  during PS117, which corresponds an increase of  $0.024^{\circ}\text{C}$  per decade. The measure from PS103 two years before amounted  $-0.7827^{\circ}\text{C}$ .

Towards the tip of the Antarctic Peninsula, 16 deep CTD casts were taken at high horizontal resolution between  $46^{\circ}\text{W}$  to  $54^{\circ}\text{W}$ , repeating a section regularly revisited since 1989. The thin cold bottom layer at the continental slope indicates newly formed Weddell Sea Bottom Water flowing northward along the slope (Fig. 3.5).

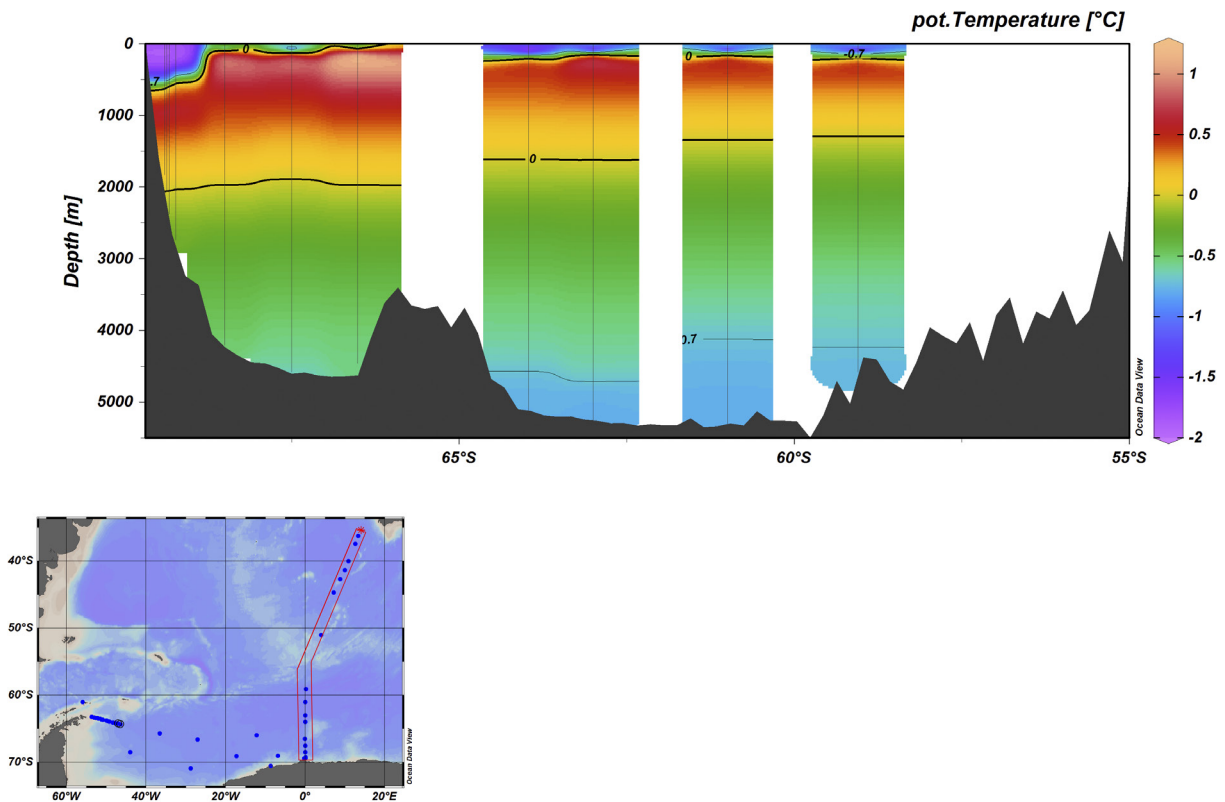


Fig. 3.3: Greenwich Meridian CTD section during PS117. Nominal station spacing is 60 nm, though some stations had to be skipped due to operational circumstances.

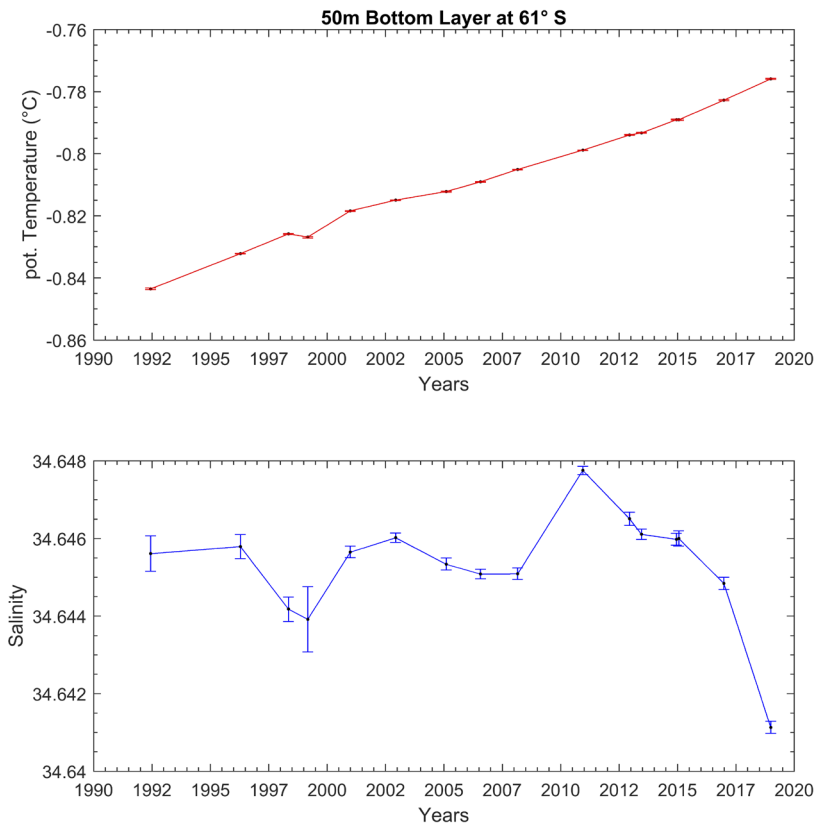


Fig. 3.4: Temperature (top) and salinity (bottom) records from past and current CTD casts at 61°S, 0°E.

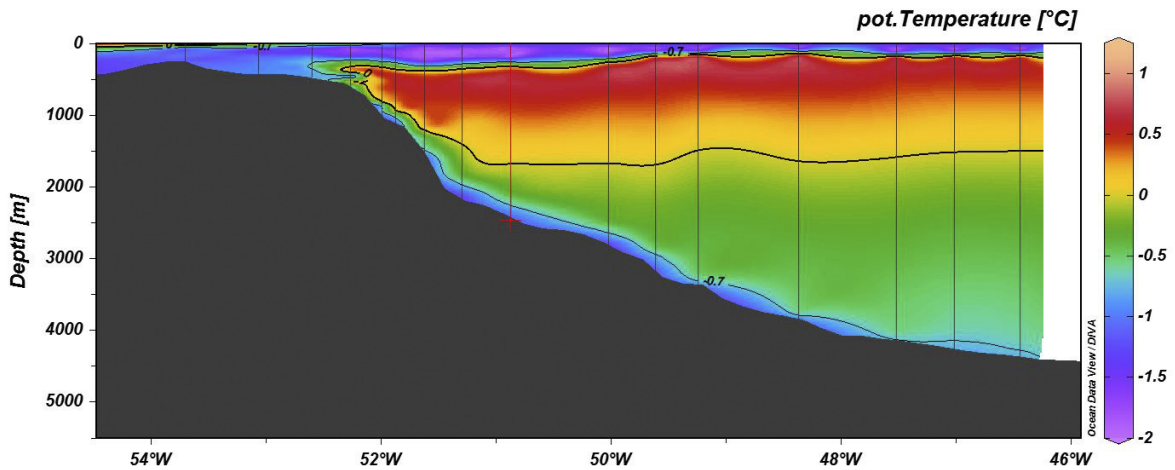


Fig. 3.5: Section of potential temperature at the tip of the Antarctic Peninsula

### 3.1.4 Lowered ADCP

#### Work at sea

##### *Set-up*

Two 300kHz RDI Workhorse ADCPs were mounted on the CTD rosette to act as lowered ADCPs (LADCP). The LADCP assembly consists of the two 300 kHz ADCPs (SN 23292 - Slave, SN23293 - Master) and a battery container. Communication was established to a computer in the winch control room via two cables (for master and slave) which were attached before and after each cast to the ADCPs. The ADCPs were operated using the GUI of the LADCP tool V1.7 from GEOMAR.

##### *Data collection*

LADCP measurements were conducted at all CTD stations. The data was downloaded after each cast. The Master (downward looking device) and slave (upward looking device) data file names consist of the station number (three digits), an abbreviation indicating the viewing direction (UP for upward and DN for downward) and a running number with three digits beginning with 000, representing the file number, in case there are multiple files. For example at station 4, data is saved in the files "004DN000.000" and "004UP000.000". These files are stored in a folder named alike the station number. In these folders log files documenting all actions conducted as starting (with configurations), stopping and downloading are kept as well.

When starting a new cast, the ADCP software automatically counts upwards to define the new station number. If the next station number differs from that, it is possible to set the counter of the software to any other number.

At station numbers 35, 56, and 99 the casts were originally recorded with a different station number (36, 55, and 100 respectively). To facilitate processing together with the CTD data and to avoid confusion, the names of the files were changed afterwards to the station names of the corresponding CTD stations. Furthermore, four CTD-LADCP casts were carried out at station 41 to capture a tidal cycle. Thus, in the following the folders were renamed to capture both station numbers and cast numbers. All processing routines were adjusted accordingly.

After cast 57 it was impossible to reconnect to the LADCP, neither via the LADCP tool nor BBtalk. A low battery voltage of 34 V was measured (instead of regular 46 V). After exchanging the batteries, the LADCP worked again without any problems.

##### *Configuration*

The settings documented in Tab. 3.9 and Tab. 3.10 were used during the entire expedition. Specifically, we used 25 bins with a bin size of 10 m (i.e., a maximum range of 250 m), beam coordinates, no blanking after transmission, narrow band processing, and a timing of the master and slave such that the acoustic energy of the master is separated by 0.55 seconds from the acoustic energy of the slave. These configurations were tested on PS100 and found to produce satisfying results.

##### *Data processing*

On board, data processing was carried out with the GEOMAR LADCP software Version 10 which is executed in Matlab. The software combines, if available, data from the LADCP, CTD, navigational data, and a vessel mounted ADCP to conduct the velocity inversion method.

The CTD data was prepared using a data conversion program called `prladcp` that opens seabird and initiates the steps `datcnv`, `celltm`, `binavg`, and `trans`. The resulting file has 1-second

### 3.1 Physical oceanography

resolution. Furthermore a CTD data file is needed which has a resolution of 1 dbar that was provided through the programme Manage CTD ran on the CTD computer. Navigational information was obtained from the VMADCP data based on NMEA navigational data strings during the cast. For post-processing navigational data from the CTD data may be used instead.

The software package executed in Matlab produces significant amounts of diagnostic output stored in a log file in the log folder and displayed in 16 figures saved in the folder plots. The output not only displays the calculated velocities in zonal (u) and meridional (v) directions, but also additional figures that help to identify error sources and problems of the acquisition process.

#### Preliminary operational results

Overall, the obtained information resembled the scientific assumptions and agreed well with vessel mounted ADCP data. Most of the time, the error of the velocities was on the order of 5 to 10  $\text{cms}^{-1}$ . Thus, data should be handled with care and post-processing is required.

Table 3.11 summarizes which casts suffered from one or more of the most common warnings. Common warnings were:

- Large compass differences ( $> 15^\circ$ ) occur due to the high latitude of the study area.
- The routine does not only the velocity inversion, but calculates a solution based on the shear method as well. If both disagree substantially, the error estimate is larger.

Reprocessing the data with a different setting may remedy these problems.

**Tab. 3.9:** Configuration file of the Master LADCP

CR1	Set to factory defaults
WM15	LADCP water ping mode 15
CB411	Baud rate 9600
RN MASTE	File name
CF11111	Allow serial output
EA0	No heading alignment
EB0	No heading bias
ES35	Salinity
EZ0111101	Fixed speed of sound
EX00111	Beam coordinates, use pitch-roll, 3 beam solution, bin mapping
WV250	Ambiguity velocity
WN25	25 bins
WS1000	10m bins
WF0	No blank after transmit
WB1	Narrow band
WP1	Single ping data
TE00:00:01.50	Ensemble length of 1.5 seconds
TP00:00.90	Ping length of 0.9 seconds
SM1	Master, SM2 for Slave
SI0	Sync pulse on every ping, n-a for Slave, but needs ST0300
SA011	Sync pulse before every ensemble
SB0	Ignore RS-422 break
CK	Keep parameters as user default
CS	Start pinging

**Tab. 3.10:** Configuration file of the Slave LADCP

CR1	Set to factory defaults
WM15	LADCP water ping mode 15
CB411	Baud rate 9600
RN SLAVE	File name
CF11111	Allow serial output
EA0	No heading alignment
EB0	No heading bias
ES35	Salinity
EZ0111101	Fixed speed of sound
EX00111	Beam coordinates, use pitch-roll, 3 beam solution, bin mapping
WV250	Ambiguity velocity
WN25	25 bins
WS1000	10m bins
WF0	No blank after transmit
WB1	Narrow band
WP1	Single ping data
TE00:00:01.50	Ensemble length of 1.5 seconds
TP00:00.90	Ping length of 0.9 seconds
SM2	Slave, SM1 for Master
ST0300	Slave timeout 300 seconds, n-a for Master, but needs SIO
SA011	Sync pulse before every ensemble
SB0	Ignore RS-422 break
CK	Keep parameters as user default
CS	Start pinging

**Tab. 3.11:** List of common problems with corresponding station numbers

Station-Cast PS117_	Large up- down compass difference (>15°)	Increased error because of shear- inverse difference	Found no SADCP data in time window	Found LARGE timing difference between ADCPs
004-01				
005-01	x			
006-03				
007-01		x		
013-02				
014-01				
015-01		x		
018-02		x		
021-01				
022-02				x
026-01				
028-01				
029-01				
030-01	x			
031-01				
033-06				
034-02		x		
035-06		x	x	
041-01				
041-06				
041-09				

Station-Cast PS117_	Large up- down compass difference (>15°)	Increased error because of shear- inverse difference	Found no SADCP data in time window	Found LARGE timing difference between ADCPs
041-12				
053-04		x		
054-03		x		
056-02				
057-06		x		
062-01				
063-01		x		
064-04		x		
066-01		x		
068-02		x		
069-01				
071-01				
072-03				
074-01				
076-01				
081-02				
083-02				
084-01				
090-01				
092-01				
094-01				
099-01				

#### Preliminary scientific results

CTD and LADCP measurements were preliminarily analysed during the expedition. Both CTD sections across the continental slope along the Prime Meridian (PM, Fig. 3.2) and east of the Antarctic Peninsula (AP, Fig. 3.2) confirmed the expected distribution of water masses (Fig. 3.6 and Fig. 3.7). At both locations, there exists a gradient of temperature at the surface between the Antarctic Surface Water offshore and the Shelf Water onshore (Fig. 3.6.a and Fig. 3.7.a). Below this two water masses, the Warm Deep Water (WDW, temperature > 0.5°C) resides, which is fed from the ACC into the Weddell Sea upstream of the PM.

The Weddell Sea Deep Water and the Weddell Sea Bottom Water (which is found at the AP only; WSBW, potential temperature < -0.7 °C), rest at depths below the WDW layer. At the PM, strong eastward velocities were observed by both the VADCP and the LADCP south of 68.5°S, where the temperature gradient is large. At the AP, the high resolution array reveals a V-shape distribution of temperature around the 1,400 m isobath which marks the boundary between properties of the water masses on the continental shelf downstream of the bottom water formation regions and the water masses within the gyre. A patch of potential temperatures below -0.7°C is observed at the bottom. It illustrates the downslope cascade of WSBW which was observed by the LADCP at several locations (Fig. 3.7.c, station 76 and 84). The VADCP section shows surface velocities alternating between northward and southward (Fig. 3.7b). The LADCP measurements reveal that the velocity fronts are barotropic (ig. 3.14c). These features have previously been described by Thomson et al. (2008) but further data analysis is needed to properly interpolate the velocities between the stations and compare the position of the fronts.

### 3. HAFOS: Maintaining the AWI's Long Term Ocean Observatory in the Weddell Sea

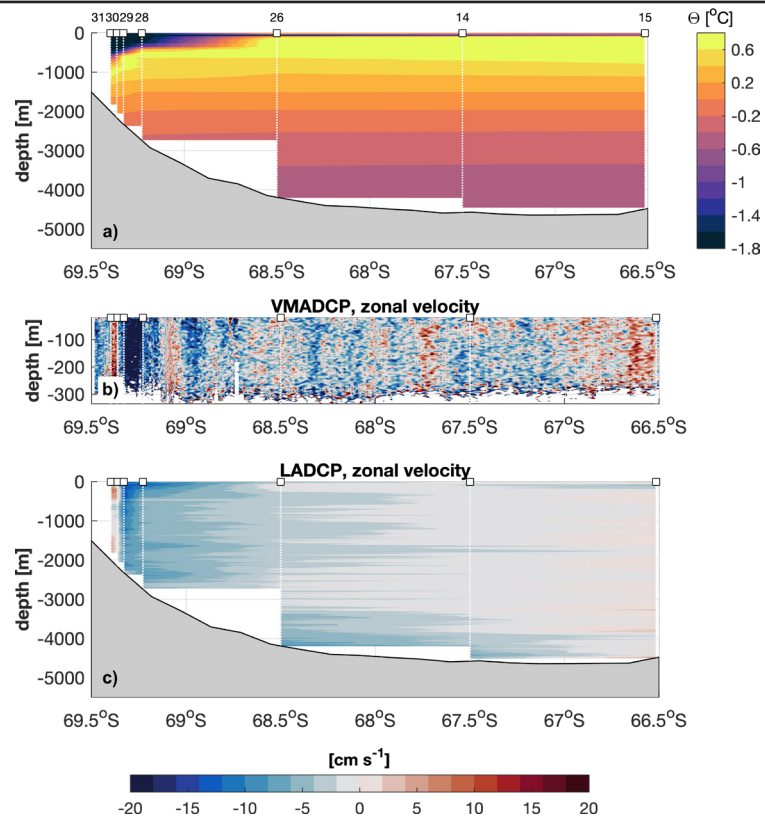


Fig. 3.6: Sections of a) potential temperature, b) zonal velocities measured by the VMADCP, and c) zonal velocities measured by the LADCP at the Antarctic shelf near the Greenwich meridian. The local ice conditions prohibited occupying stations further up the shelf. Note that all stations are located on the upstream (eastern) side of the local shelf tongue.

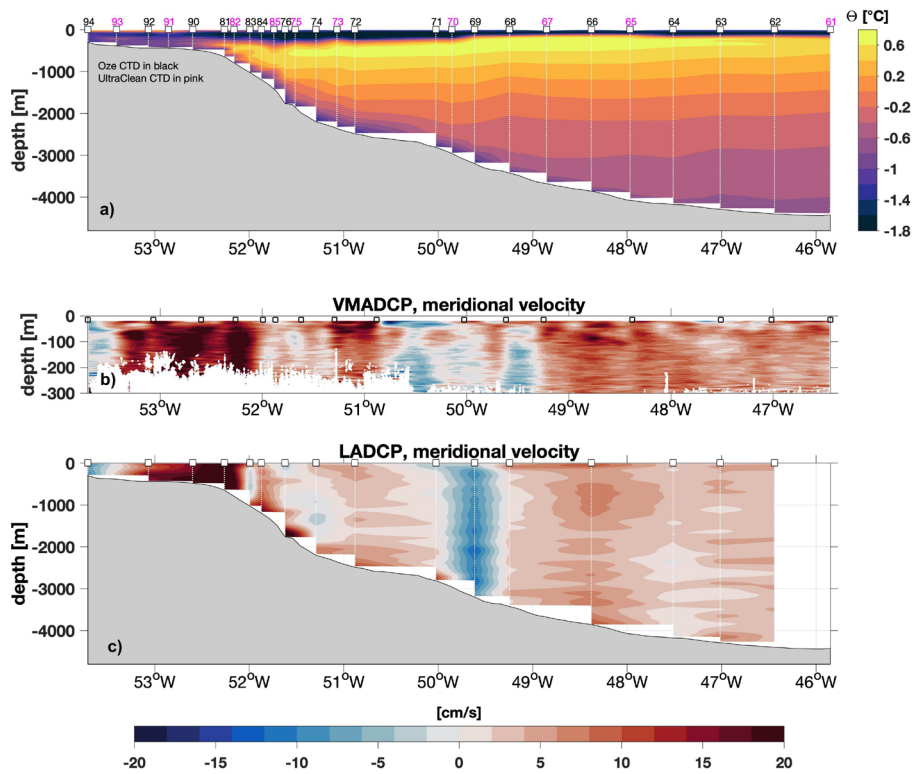


Fig. 3.7: Sections of a) potential temperature (top), b) meridional velocities measured by the VMADCP (middle), and c) meridional velocities measured by the LADCP at the Antarctic Peninsula (bottom).

#### 3.1.5 Vessel mounted ADCP

##### Work at sea

We measured profiles of ocean current velocity in the upper 300 m underway with a vessel mounted Acoustic Doppler Current Profiler (VMADCP). The RDI Ocean Surveyor instrument (150 kHz) is mounted at an angle of 45 degree in the 'Kastenkiel' of *Polarstern*. The instrument was configured in narrowband mode and set up to 80 bins with 4 m bin size (standard *Polarstern* configuration file: cmd\_OS150NB\_trigger\_off.txt) covering a range from 15 m (11 m transducer depth and 4 m blanking distance below the transducer) to about 200 - 300 m depending on sea state, ice conditions, ship's speed and backscatter signals. The ADCP was configured to send one ping per ensemble with an ensemble interval of two seconds.

The setup of navigational input was used from the vessel's GPS system. It worked almost flawlessly, except for some short events, when the communication from the GPS was lost. Problems to resolve velocities occurred due to low backscattering strength, low water depths and - or sea ice in front of the beams. Furthermore interferences with other acoustic signals from the vessel's Doppler log (79 kHz) and acoustic signals to release moorings degraded the velocity data.

For unknown reasons the ADCP stopped recording data for several hours 2 times throughout the expedition:

- 28 December, 01:50 UTC until 8:10 UTC
- 31 December, 18:10 UTC until 01 January, 17:50 UTC

The software VmDas (Teledyne RD Instruments) was used to set the ADCP's operating parameters and to record the data. Finally the Ocean Surveyor data was converted using Matlab routines last changed by Gerd Krahnmann in January 2015 (osheader.m, osdatasip.m, osrefine.m, osbottom.m). Hereby the VMADCP data was corrected by using a misalignment angle of  $1.12^\circ$  and an amplitude factor of 1.0171.

##### Preliminary scientific results

During a 24-hours stay within the coastal polynja regularly present behind a blockade formed by ice-bergs grounded about 30 nm west of Atka Seaport, repeated CTD casts, LADCP casts and VADCP measurement were collected spanning a full day at 3 hourly intervals (Fig. 3.8, Fig. 3.9 and Fig. 3.10). Data revealed the to and fro of the flow of water from below the ice cavity and the polynja. The meridional component of flow is asymmetric with a bias towards westward flows due to the coastal current.

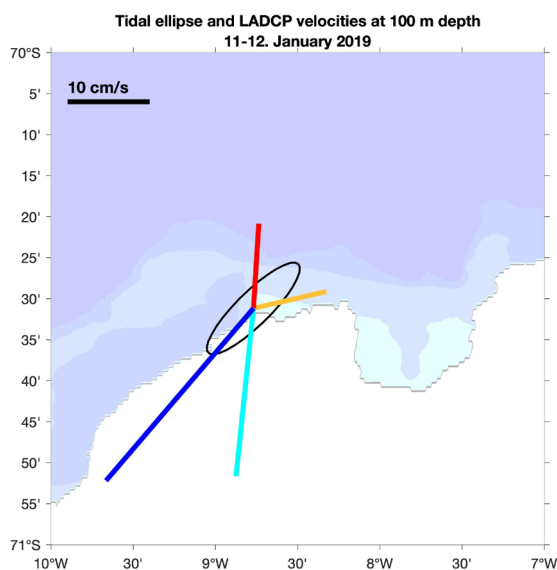


Fig. 3.8: Tidal ellipses and scaled vectors showing modelled flow directions during AWI-CTD station 1 (just before low tide), 6 (just before high tide), 9 (just after low tide) and 12 (as high tide) as obtained from the Padman et al. (2002) tidal modell.

### 3. HAFOS: Maintaining the AWI's Long Term Ocean Observatory in the Weddell Sea

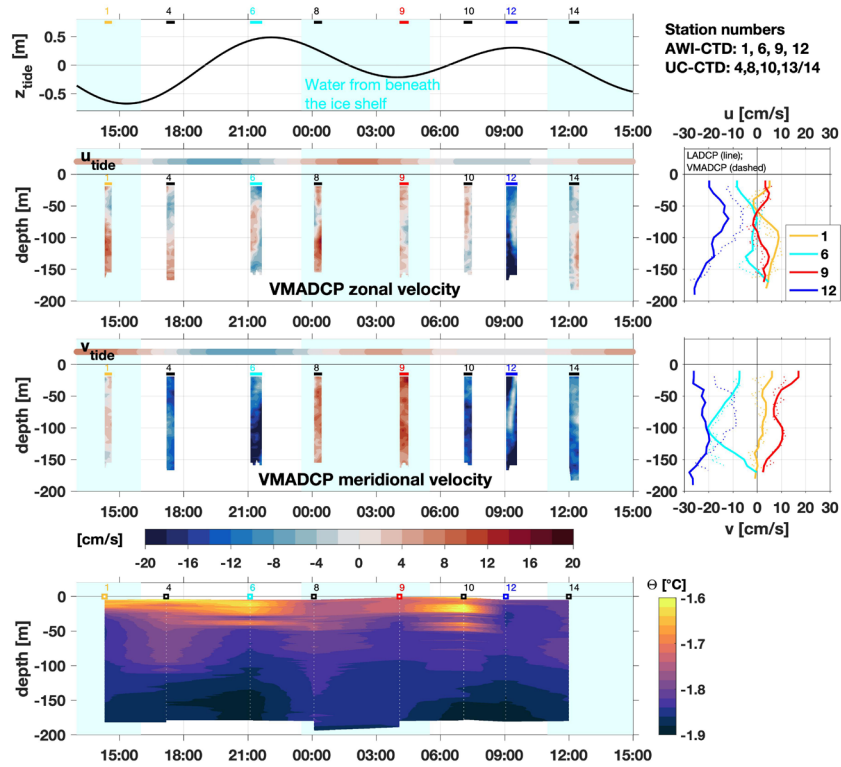


Fig. 3.9: Top to bottom: Modelled tidal height (black curve) and phases of rising tide (white) and ebbing tide (cyan); Vessel mounted ADCP zonal velocity profiles during periods while on station; ditto for meridional velocity; Potential temperature profiles, interpolated.

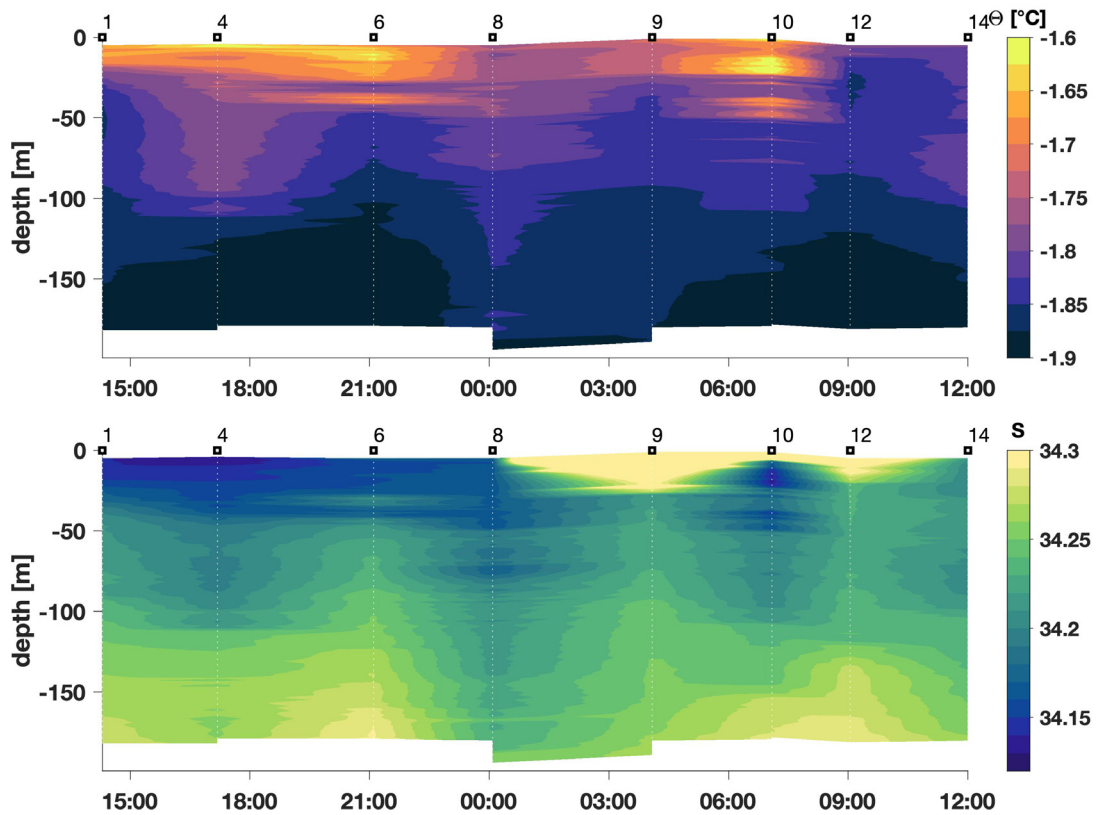


Fig. 3.10: Top: Potential temperature profiles while on station during tidal experiment, interpolated in time; bottom: salinity while on station during tidal experiment, interpolated in time

#### 3.1.6 HAFOS Sound source array

##### Work at sea

Due to the current unavailability of new RAFOS enhanced Argo floats, all NEMO floats previously deployed having drifted out of the range of the HAFOS sound source array, and the difficulties in tuning the new sources, RAFOS sources were only recovered and not redeployed during this expedition.

A total of 10 sound sources were recovered (Tab. 3.12). 9 of these sound sources were of the type NTSS (non tunable sound source, Develogic GmbH, Hamburg, Germany). One sound source, hosted by mooring AWI250-01 and having been deployed on ANT-XXIX/2 (PS81) in January 2013, was of type WEBB. A summary of sound source mooring activities is given in Tab. 3.12, Tab. 3.13, their locations are shown in Fig. 3.11.

After recovery, a communication cable was attached to the sound source and connected to a laptop through a serial connection and accessed to determine their operational state. The only sound source still reacting to the commands and starting a sweep at the scheduled time was the WEBB sound source, resulting in of over 2,000 days of operation! The WEBB sound source was set to an 'Idle' state for shipment back home. Communication attempts with all other sound sources were unsuccessful.

The unopened housings of these NTSS were left drying over night. The next day, the housings were opened to disconnect the batteries and retrieve the SD-card with the logfile. On this occasion, the battery packs of 2 sources were found burnt. The corresponding lithium-metal battery packs were securely packed into a special container for shipping.

Logfiles on the retrieved SD-cards suggests that problems with the amplifier might have caused the early operational end. This issue will be examined post expedition in detail.

**Tab. 3.12:** Recovery of sound sources during PS117

Mooring/ SoSo site	SN	Position  LAT LON	Deployment date	Water depth [m]	Pong time [GPS]	Mission duration [days]	resulting drift	post recovery communi- cation
			Recovery date	Instrument depth [m]			[sec/annum]	
245-04 W9	D0048 EI0045 BP2116	69° 03.64' S 017° 23.45' W	11.01.2017 08.01.2019	4736 802	13:10	0	--	NO
248-02 W12	D0024 EI0049 BP2122	65° 58.12' S 012° 13.87' W	02.01.2017 06.01.2019	5047 833	14:00	206 *)	--	NO
244-05 W11	D0049 EI0046 BP2050	69° 00.32' S 006° 59.56' W	01.01.2017 05.01.2019	2946 842	12:40	nn	--	NO
249-02 W13	D0028 EI0028	70°53.54' S 028°53.47' W	13.01.2017 20.01.2019	4401 837	13:50	737 *)	--	NO
209-08 W04	D0047 EI0067 BP2053	66°36.45' S 027°07.29' W	18.01.2017 21.01.2019	4872 854	13:30	733 *)	--	NO
208-08 W05	D0030 EI0030	65°41.79' S 036°41.79' W	19.01.2017 23.01.2019	4766 830	12:40	734 *)	--	NO
250-01 W14	W0024	68°28.95' S 044°06.67' W	05.01.2013 24.01.2019	4100 798	13:10	2210	2.5	YES

### 3. HAFOS: Maintaining the AWI's Long Term Ocean Observatory in the Weddell Sea

Mooring/ SoSo site	SN	Position  LAT LON	Deployment date	Water depth [m]  Instrument depth [m]	Pong time [GPS]	Mission duration [days]	resulting drift	post recovery communi- cation
			Recovery date				[sec/annum]	
250-02 W14	D0045 EI0060 BP2052	68°27.84' S 044°08.71' W	21.01.2017 24.01.2019	4137 834	13:30	nn	--	NO
257-01 W10	D0026 EI0055 BP2056	64°12.94' S 047°29.42' W	23.01.2017 27.01.2019	4170 923	13:50	169 *)	--	NO
207-09 W06	D0046 EI0044 BP2120	63°39.36' S 050°48.68' W	26.01.2017 29.01.2019	2490 808	14:10	7 *)	--	NO

\*) with uncertainties regarding the quality of the performance 1) During deployment: GPS=UTC+16s. 2) During deployment: GPS=UTC+18s

Sign of offsets: positive (+): unit is late, negative (-): unit is early

Prior to this expedition several sound sources were refurbished by the manufacturer, Develogic, with the aim to improve the signal amplitude, and as such, the range of the sound sources. Returned sound sources were scheduled for testing during PS117 and, if not yet finally tuned, to be tuned for the center frequency of the RAFOS signal at 260 Hz. At-sea tuning had been conducted successfully during earlier expeditions directly under hydrographic conditions similar to the deployment site (see Expedition Reports PS89, Boebel 2015 and PS103, Boebel, 2017). A redeployment of the sound sources was planned for the western part of the Weddell Sea.

However, due to the erratic performance during the testing/calibration procedure, it was decided not to deploy sound sources during PS117. For details on the performance issues see section RAFOS source tuning.

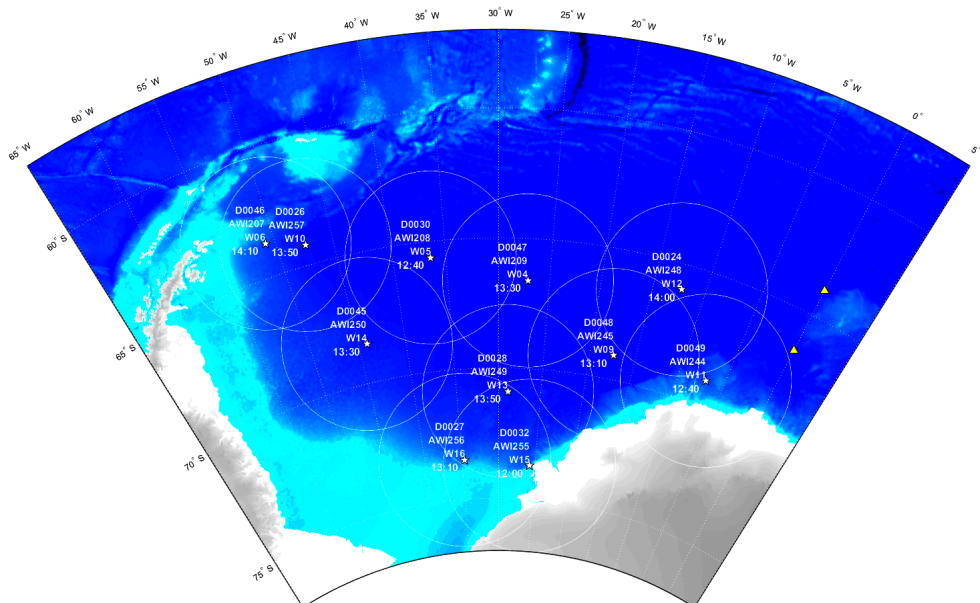


Fig. 3.11: HAFOS sound source array as installed up to Polarstern expedition PS117. White stars with concentric circles: Sources (re)deployed on PS103 with 200 nm range. All sound sources, but the 2 southernmost ones, were recovered during PS117. Top-left to the marked position: Serial number of sound source, mooring number, sound source position number and sweep time (GPS).

Tab. 3.13: Recovery of sound sources during PS117

Mooring /SoSo site	SN	Deployment Recovery	Type	Last sweep triggered <sup>*)</sup>	Last sweep completed * high voltage logged [V]	battery [V] internal / external	Issues
245-04 W9	D0048 EI0045 BP2116	11.01.2017 08.01.2019	1)	30.12.2018	not available	22.5 46.9	<u>EI</u> : no communication possible, high voltage fault on 12.01.2017, signal high voltage thereafter: <20V ; <u>BP</u> : moist silica gel pack, slight saltcrust inside housing near pressure port
248-02 W12	D0024 EI0049 BP2122	02.01.2017 06.01.2019	1)	07.01.2019	27.07.2017 434	23.7 47	<u>EI</u> : no communication possible, high voltage fault at 22.01.2017, amplifier shutdown at 27.07.2017, signal high voltage thereafter: <20V; <u>BP</u> : water in housing
244-05 W11	D0049 EI0046 BP2050	01.01.2017 05.01.2019	1)	not available	not available	burned 6	<u>EI</u> : burned out, endcaps destroyed; <u>BP</u> : no power on pins
249-02 W13	D0028 EI0028	13.01.2017 20.01.2019	2)	22.01.2019	22.01.2019 408	25.3 no ext. bat.	<u>EI</u> : no communication possible
209-08 W04	D0047 EI0067 BP2053	18.01.2017 21.01.2019	1)	23.01.2019	22.01.2019 432	46.23 47	<u>EI</u> : no communication possible
208-08 W05	D0030 EI0030	19.01.2017 23.01.2019	2)	23.01.2019	23.01.2019 420	25.3 no ext. bat.	<u>EI</u> : no communication possible
250-01 W14	W0024	05.01.2013 24.01.2019	3)	25.01.2019	25.01.2019 not applicable	not available	still working, sweep on deck OK (25.01.2019)
250-02 W14	D0045 EI0060 BP2052	21.01.2017 24.01.2019	1)	not available	not available	25.4 47.3	<u>EI</u> : no communication possible, signs of corrosion on electronics, SD-card corroded - not readable

3. HAFOS: Maintaining the AWI's Long Term Ocean Observatory in the Weddell Sea

Mooring /SoSo site	SN	Deployment Recovery	Type	Last sweep triggered <sup>1)</sup>	Last sweep completed * high voltage logged [V]	battery [V] internal / external	Issues
257-01 W10	D0026 EI0055 BP2056	23.01.2017 27.01.2019	1)	21.07.2017	11.07.2017 435	burned 47.3	<u>EI</u> : burned out, high voltage fault at 11.07.2017, thereafter: only sporadically successful sweeps, high voltage needed to be retrigged repeatedly
207-09 W06	D0046 EI0044 BP2120	26.01.2017 29.01.2019	1)	30.01.2019	02.02.2017 247	0-19 47	<u>EI</u> : no communication possible, amplifier shutdown on 03.02.2017, signal high voltage thereafter: <20V; <u>BP</u> : moist silica gel pack, saltcrust inside housing near pressure port
1) Develogic NTSS: additional external Battery Pack BP, Titanium housings with pressure valve (EI, BP); 2) Develogic NTSS: single composite housing;							
3) WEBB sound source							
*) information from instrument logfiles 'SYSTEM.LOG', if available							

#### 3.1.7 RAFOS source tuning

##### Work at sea

A detailed description of the objectives and approach of tuning RAFOS sources *in-situ* is given in the expedition report of *Polarstern* expedition ANT-XXIX/2 (PS81, Boebel, 2015). During PS117, the frequency response of 3 sound sources (D0043+EL0043, D0018+EL0061, D0017+EL0047) was gauged. All 3 systems had already been gauged on a previous expedition, but as

1. the tuning had not been finished during PS103 (D0017 gauged once only, D0018 gauged and cut once) and D0043 (final gauging pending)
2. the sources had been refurbished with a new resonator stack by the manufactures and the sources reassembled mixing up resonator parts (Resonator tubes, stacks, mechanical middle part).

a complete retuning of these sources was necessary. This was attempted by means of 5 gauging runs and cutting of source D0018 after its first gauging run.

Tuning (i.e. gauging and respective shortening the length of a resonator tube until it resonates at the RAFOS centre frequency of 260.14 Hz) of the systems was performed in 3 steps. Prior to shortening the frequency response of resonators was gauged by recording the acoustic emissions during seven consecutive 5Hz wide, 80s sweeps, separated by cool-down phases of 100s, preceded and followed by a standard RAFOS sweep.

- RAFOS sweep (259.38 Hz – 260.9 Hz)
- 247 Hz – 252 Hz
- 252 Hz – 257 Hz
- 257 Hz – 262 Hz
- 262 Hz – 267 Hz
- 267 Hz – 272 Hz
- RAFOS sweep (239.38 Hz – 260.9 Hz)

Sound sources were gauged in waters of at least 2,000 m depth by lowering the sound sources horizontally to 800 m with the CTD winch. To avoid entangling of the winch's cable, extra weights of 70 kg were attached to (below) the source by a rope shackle. 2 icListen acoustic recorders were attached 40 m above the sound source directly to the winch cable. One of the recorders was exchanged after every run. Local sound speeds were obtained from CTD data.

After completion of the gauging procedures, recordings from the acoustic recorder(s) were saved from the icListen's internal storage to a harddisk. Using Adobe Audition, sweeps belonging to a given sound source were manually cut at their start and end from the displayed spectrogram and saved as single files. Later these single sweeps were merged and saved as a single file containing the complete sweep from 247 Hz to 272 Hz.

A custom MATLAB™ script was used to determine the (current) resonance frequency of the highest root-mean-square amplitude. A second MATLAB™ script used this current resonance frequency, current tube length and environmental parameters (e.g. sound velocity at tuning depth, water density) to derive the target resonance length and the excess length to be cut.

Only source D0018 was cut once during this expedition for reasons explained below.

### Operational results

On 10 January 3 Develogic sound sources (D0018, D0029 and D0043) were scheduled for gauging.

- D0029 failed to start the on-deck test sweep at 30% power and was hence excluded from further activities.
- D0043 was lowered to 800 m depth for gauging. However, it aborted 2 of the 7 scheduled sweeps due to high voltage errors.
- D0018 performed well and a resonance frequency at 251 Hz was determined from the acoustic recordings (Fig. 3.12). A cut of 70 mm per side was calculated to reach the center resonance frequency around 260 Hz. The system was cut by 45 mm per side to allow for further cutting in case of any errors in the calculation.
- On 22 January another tuning session was held. Results for both sound sources, however, were rather disappointing.
- The previously gauged and cut sound source D0018 was tuned for the second time. We expecting the resonance frequency to be closer to 260 Hz but not exceeding this value. However, the calculated resonance frequency was now at 269 Hz (previously 251 Hz) and the maximum source level had dropped from 175 dB to 168 dB re 1  $\mu$ Pa (Fig. 3.13).
- D0043 was again tested in 800 m depth and this time all sweeps were completed as scheduled. However D0043 exhibited fluctuating source pressure levels rather than the expected bell-curve like behaviour. Source levels did not exceed 173 dB re 1  $\mu$ Pa (assuming a 20 log(r) drop between the source and the recorder (Fig. 3.14).
- As there are currently no active floats in the vicinity of the sound sources, and because of the inconclusive results from the tuning and the unreliability of the electronics it was decided that no sound sources would be deployed during this expedition.

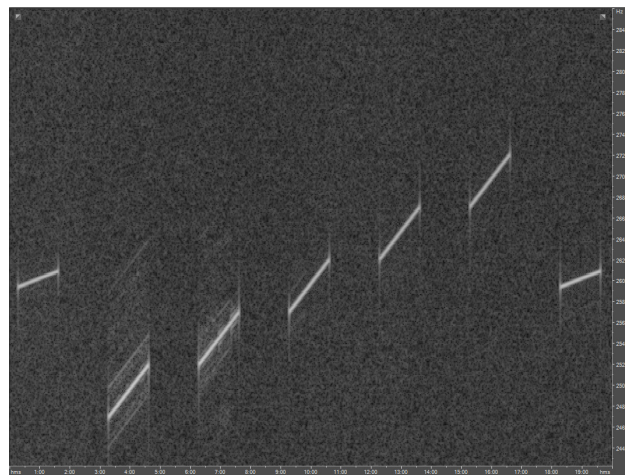


Fig. 3.12: Spectrogram as recorded by iCListen 1414 during first gauging of Develogic sound source D0018. Recognizable is the initial RAFOS sweep, the 5 frequency up-sweeps and the final RAFOS sweep.

### 3.1 Physical oceanography

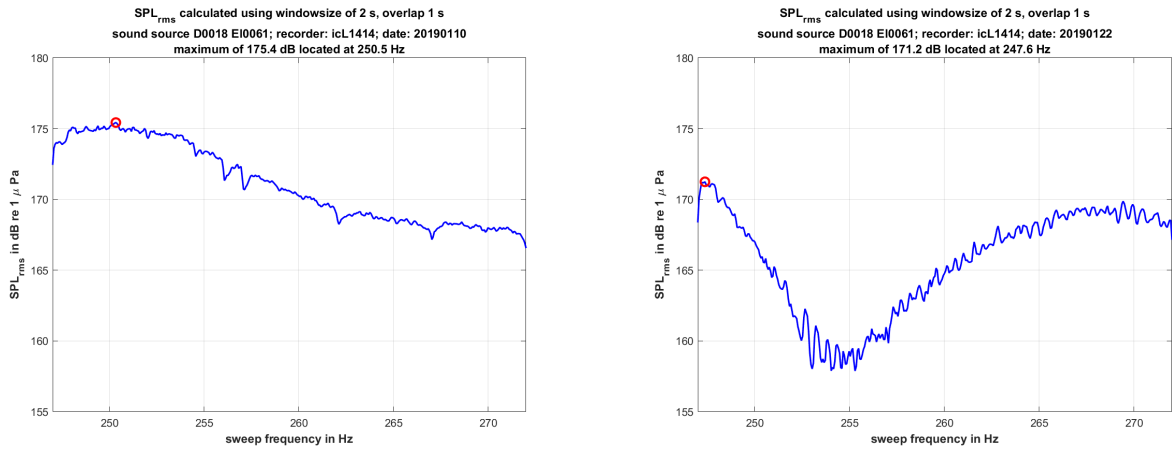


Fig. 3.13: Resonance curves of develgic RAFOS source D0018 before (left) and after (right) cutting.

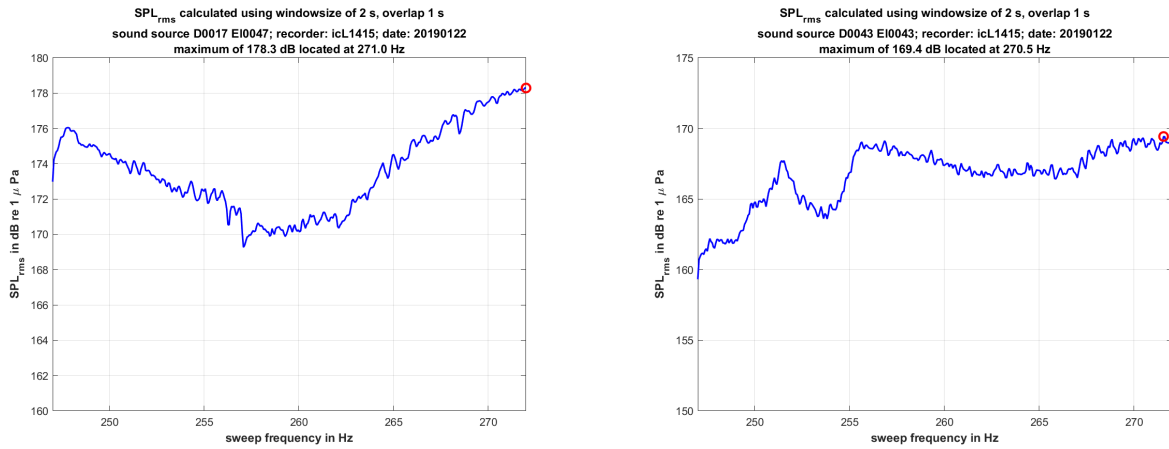


Fig. 3.14: Left: Resonance curve of develgic RAFOS source D0017 as recorded by icListen 1415 during 1st gauging. Right: Resonance curve of develgic RAFOS source D0043 as recorded by icListen 1415 (during 2nd gauging).

### 3.1.8 Salinometer measurements

#### Work at sea

To monitor the accuracy and precision of the CTD's conductivity sensors, water samples were taken on 17 deep CTD casts for salinity/conductivity measurements. Each time, double samples were drawn from the water sampler. To investigate the influence of pressure on conductivity, samples were taken at 2,000 m and >4,000 m depth. The sample location has to be within a homogeneous water layer, which are identified by little scattering of temperature and conductivity differences between sensor pairs. Salinities of the water samples were determined on board using an Optimare Precision Salinometer (OPS, Tab. 3.14). All samples were measured in five sessions. Every session started with standardization using Standard Sea Water batch no. P161;  $K_{15} = 0.99987$ , with expiry date 2020-05-03.

#### Preliminary results

*En route* comparisons between *in-situ* CTD data and salinometer based salinity measurements of water samples indicated that the conductivity sensor (SBE4c #1373) used in the primary sensor pair featured better accuracies (Fig. 3.15, red dots). For this sensor pair, the salinity correction is constant  $-0.0027$  for the entire expedition.

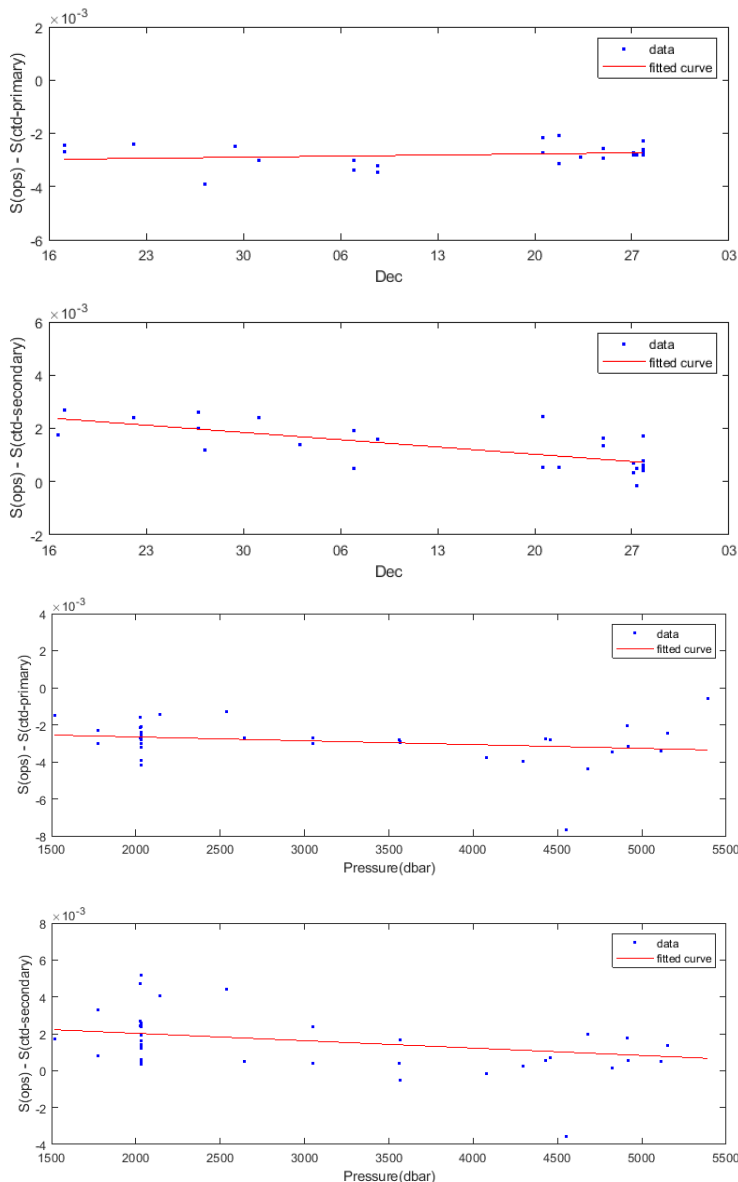


Fig. 3.15: Deviation in salinity between OPS measurements and *in-situ* CTD measurements versus time (top) and versus pressure (bottom) for the primary and secondary sensor. The pressure effect is slightly more pronounced for the secondary sensor and in addition the drift is notable while the drift is almost zero for the primary sensor.

**Tab. 3.14:** Salinity samples from the water sampler and measured with the OPS

Station	Date Time	Press	s0	s1	OPS	OPS-s0	OPS-s1
001-01	16.12.2018 15:47	4914	34.7308	34.7270	34.7288	-0.0020	0.0018
001-01	16.12.2018 15:47	4914	34.7308	34.7270	34.7287	-0.0021	0.0017
001-01	16.12.2018 15:47	2142	34.8155	34.8100	34.8142	-0.0013	0.0042
001-01	16.12.2018 15:47	2142	34.8155	34.8100	34.8139	-0.0016	0.0039
002-01	17.12.2018 03:46	5151	34.7224	34.7186	34.7201	-0.0023	0.0015
002-01	17.12.2018 03:46	5151	34.7224	34.7186	34.7198	-0.0026	0.0012
002-01	17.12.2018 03:46	2025	34.8164	34.8110	34.8138	-0.0026	0.0028
002-01	17.12.2018 03:46	2025	34.8164	34.8110	34.8136	-0.0028	0.0026
013-02	22.12.2018 01:38	2029	34.7308	34.7260	34.7284	-0.0024	0.0024
014-01	26.12.2018 18:52	4680	34.6521	34.6457	34.6481	-0.0040	0.0024
014-01	26.12.2018 18:52	4680	34.6521	34.6457	34.6473	-0.0048	0.0016
014-01	26.12.2018 18:52	2030	34.6728	34.6660	34.6687	-0.0041	0.0027
014-01	26.12.2018 18:52	2030	34.6728	34.6660	34.6685	-0.0043	0.0025
015-01	27.12.2018 05:57	4554	34.6563	34.6522	34.6489	-0.0074	-0.0033
015-01	27.12.2018 05:57	4554	34.6563	34.6522	34.6484	-0.0079	-0.0038
015-01	27.12.2018 05:57	2029	34.6744	34.6693	34.6704	-0.0040	0.0011
015-01	27.12.2018 05:57	2029	34.6744	34.6693	34.6706	-0.0038	0.0013
019-01	29.12.2018 09:05	5389	34.6489	34.6422	34.6485	-0.0004	0.0063
019-01	29.12.2018 09:05	5389	34.6489	34.6422	34.6481	-0.0008	0.0059
019-01	29.12.2018 09:05	2031	34.6696	34.6619	34.6657	-0.0039	0.0038
019-01	29.12.2018 09:05	2031	34.6696	34.6619	34.6685	-0.0011	0.0066
022-02	31.12.2018 03:09	3050	34.6573	34.6519	34.6543	-0.0030	0.0024
022-02	31.12.2018 03:09	2539	34.6610	34.6553	34.6597	-0.0013	0.0044
022-02	31.12.2018 03:09	2028	34.6653	34.6590	34.6637	-0.0016	0.0047
022-02	31.12.2018 03:09	1774	34.6680	34.6617	34.6650	-0.0030	0.0033
026-01	03.01.2019 02:16	4296	34.6567	34.6525	34.6531	-0.0036	0.0006
026-01	03.01.2019 02:16	4296	34.6567	34.6525	34.6524	-0.0043	-0.0001
026-01	03.01.2019 02:16	2030	34.6741	34.6688	34.6704	-0.0037	0.0016
026-01	03.01.2019 02:16	2030	34.6741	34.6688	34.6700	-0.0041	0.0012
034-02	07.01.2019 00:04	5112	34.6486	34.6447	34.6453	-0.0033	0.0006
034-02	07.01.2019 00:04	5112	34.6486	34.6447	34.6451	-0.0035	0.0004
034-02	07.01.2019 00:04	2031	34.6683	34.6634	34.6652	-0.0031	0.0018
034-02	07.01.2019 00:04	2031	34.6683	34.6634	34.6654	-0.0029	0.0020
035-06	08.01.2019 16:18	4825	34.6490	34.6454	34.6454	-0.0036	0.0000
035-06	08.01.2019 16:18	4825	34.6490	34.6454	34.6457	-0.0033	0.0003
035-06	08.01.2019 16:18	2030	34.6699	34.6651	34.6667	-0.0032	0.0016
035-06	08.01.2019 16:18	2030	34.6699	34.6651	34.6667	-0.0032	0.0016
053-04	20.01.2019 13:20	4431	34.6524	34.6491	34.6500	-0.0024	0.0009
053-04	20.01.2019 13:20	4431	34.6524	34.6491	34.6493	-0.0031	0.0002
053-04	20.01.2019 13:20	2028	34.6704	34.6658	34.6682	-0.0022	0.0024
053-04	20.01.2019 13:20	2028	34.6704	34.6658	34.6683	-0.0021	0.0025
054-02	21.01.2019 18:28	4921	34.6478	34.6441	34.6447	-0.0031	0.0006
054-02	21.01.2019 18:28	4921	34.6478	34.6441	34.6446	-0.0032	0.0005

Station	Date Time	Press	s0	s1	OPS	OPS-s0	OPS-s1
054-02	21.01.2019 18:28	2030	34.6664	34.6618	34.6642	-0.0022	0.0024
054-02	21.01.2019 18:28	2030	34.6664	34.6618	34.6644	-0.0020	0.0026
056-02	23.01.2019 06:28	3564	34.6568	34.6544	34.6539	-0.0029	-0.0005
056-02	23.01.2019 06:28	3564	34.6568	34.6544	34.6539	-0.0029	-0.0005
058-01	24.01.2019 21:59	3565	34.6584	34.6538	34.6555	-0.0029	0.0017
058-01	24.01.2019 21:59	3565	34.6584	34.6538	34.6554	-0.0030	0.0016
058-01	24.01.2019 21:59	2030	34.6695	34.6656	34.6668	-0.0027	0.0012
058-01	24.01.2019 21:59	2030	34.6695	34.6656	34.6671	-0.0024	0.0015
062-01	27.01.2019 03:15	4458	34.6475	34.6440	34.6448	-0.0027	0.0008
062-01	27.01.2019 03:15	4458	34.6475	34.6440	34.6446	-0.0029	0.0006
062-01	27.01.2019 03:15	2030	34.6675	34.6644	34.6646	-0.0029	0.0002
062-01	27.01.2019 03:15	2030	34.6675	34.6644	34.6649	-0.0026	0.0005
063-01	27.01.2019 08:37	4079	34.6544	34.6508	34.6507	-0.0037	-0.0001
063-01	27.01.2019 08:37	4079	34.6544	34.6508	34.6506	-0.0038	-0.0002
063-01	27.01.2019 08:37	2029	34.6672	34.6639	34.6643	-0.0029	0.0004
063-01	27.01.2019 08:37	2029	34.6672	34.6639	34.6645	-0.0027	0.0006
064-04	27.01.2019 18:57	3564	34.6578	34.6546	34.6550	-0.0028	0.0004
064-04	27.01.2019 18:57	3051	34.6606	34.6575	34.6579	-0.0027	0.0004
064-04	27.01.2019 18:57	2642	34.6628	34.6596	34.6601	-0.0027	0.0005
064-04	27.01.2019 18:57	2029	34.6685	34.6653	34.6659	-0.0026	0.0006
064-04	27.01.2019 18:57	2029	34.6685	34.6653	34.6659	-0.0026	0.0006
064-04	27.01.2019 18:57	1775	34.6712	34.6681	34.6689	-0.0023	0.0008
064-04	27.01.2019 18:57	1520	34.6747	34.6715	34.6732	-0.0015	0.0017

### 3.1.9 Argo float deployments (on behalf of BSH)

#### Work at sea

During PS117 a total of 10 ARVOR-I floats developed jointly by IFREMER and MARTEC Group were deployed for Argo Germany. Four of them are equipped with an adjustable Ice Sensing Algorithm (ISA), set to  $-1.79^{\circ}\text{C}$  between 50 and 20 dbar, with a surfacing response retarded by 1 profile. Profiles that could not be transmitted in real-time due to ISA-triggered aborts of surfacing attempts are stored into the float internal memory and transmitted next time the float surfaces. For data transmission Iridium SBD is used. The floats were ballasted to drift at a depth of 1,000 m and acquire profiles from 2,000 m depth upwards 1 day after deployment for the first profile and every 10 days for the next profiles. The first profile is taken 2 hours after activation and after having sagged to 2,000 m. The deployment positions are plotted in Fig. 3.16. Float identification information is given in Tab. 3.15, sorted by time of deployment.

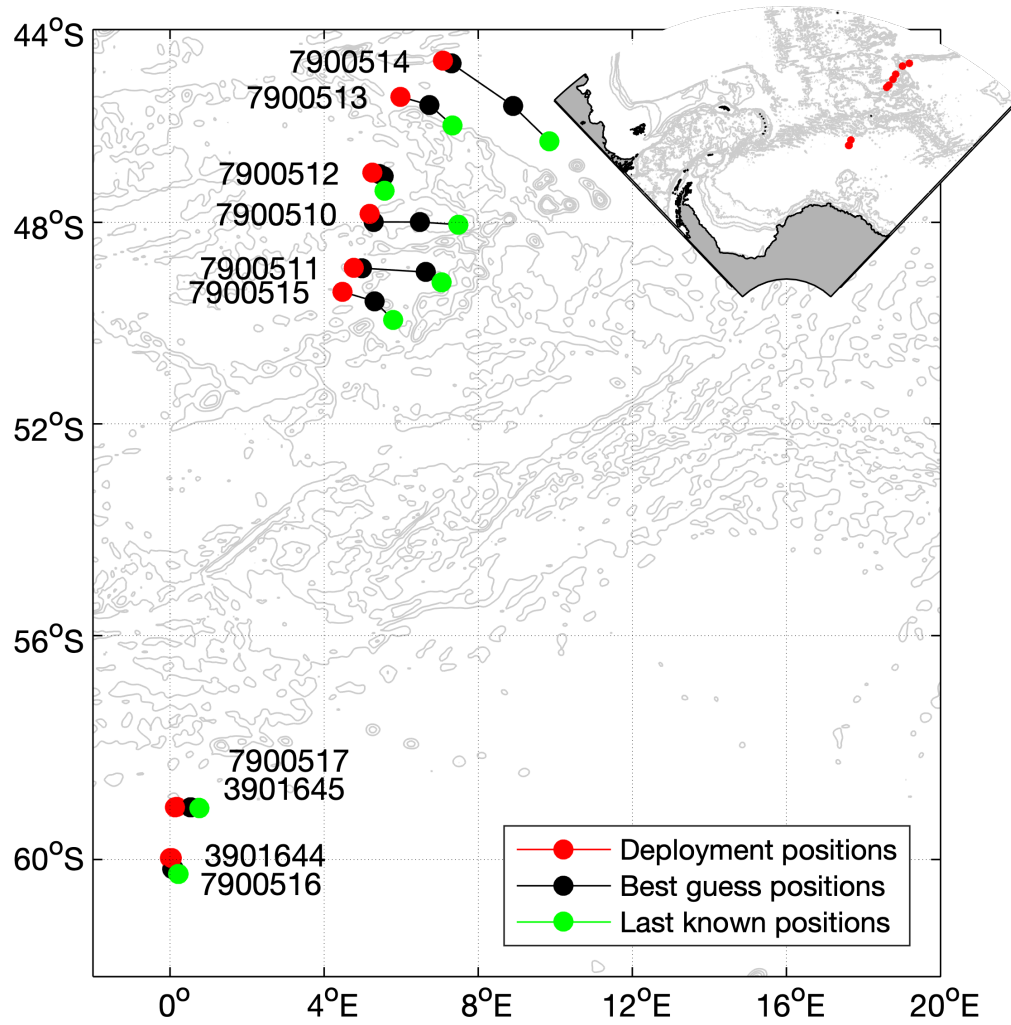


Fig. 3.16: Positions of ARVOR float deployments. The WMO number of the floats is indicated at each deployment position. Grey solid lines represent the isobaths -4000, -3000, -2000, and -1000. The map on the top right corner indicates the area of deployment.

**Tab. 3.15:** ARVOR float deployments. Float profiles can be downloaded on <https://www.jcommops.org/board/wa/Platform?ref=xxxxxxx> with xxxxxx standing for the wmo number. \*featuring Ice Sensing Algorithm (ISA).

S/N	WMO ID	ISA*	Test ok	Magnet sweep@	Deployed @	Lat	Lon	temp water [°C]	Sea ice [%]	Ship Speed/dir [kn]/[°]	Wind Speed/dir [kn]/[°]	Station No	Water Depth [m]	Station No of CTD
AI2600-18DE010	7900514		1	2018 12 20, 09:29	2018 12 30, 11:30	44°39.410'S	07°04.892'E	8.42	0	1.7/285	26.0/278	007	4592	007_01
AI2600-18DE011	7900513		1	2018 12 20, 21:18	2018 12 20, 21:24	46°02.719'S	05°56.533'E	6.34	0	5.2/200	28.6/339	008	3115	
AI2600-18DE012	7900512		1	2018 12 21, 02:51	2018 12 21, 02:57	47°01.247'S	5°34.059'E	6.09	0	4.7/201	29.2/334	009	4472	
AI2600-18DE008	7900510		1	2018 12 21, 08h21	2018 12 21, 08:31	47°59.641'S	05°10.758'E	5.63	0	4.9/200	22.7/306	010	4147	
AI2600-18DE013	7900511		1	2018 12 21, 13:58	2018 12 21, 14:09	49°00.300'S	04°45.870'E	4.29	0	5.2/213	28.4/322	011	3574	
AI2600-18DE009	7900515		1	2018 12 21, 19:28	2018 12 21, 19:38	50°00.544'S	04°20.909'E	3.90	0	5.8/207	26.6/329	012	2507	
AI2600-17DE001	3901645	X	1	2018 12 31, 14:30	2018 12 31, 14:45	59°03.030'S	0°06.430'E	-0.20	0	3.3/299	19.8/236	022	4681	022_02

### 3.1 Physical oceanography

S/N	WMO ID	ISA*	Test ok	Magnet sweep @	Deployed @	Lat	Lon	temp water [°C]	Sea ice [%]	Ship Speed/dir [kn]/[°]	Wind Speed/dir [kn]/[°]	Station No	Water Depth [m]	Station No of CTD
A12600-18DE001	7900517	X	1	2018 12 31, 14:40	2018 12 31, 14:50	59°03.030'S	0°06.430'E	-0.20	0	3.3/299	19.8/236	022	4681	022_02
A12600-17DE003	3901644	X	1	2018 12 31, 19:32	2018 12 31, 19:40	59°59.000'	0°00.000'E	-0.25	0	3.0/236	23.3/232	023	5368	
A12600-18DE002	7900516	X	1	2018 12 31, 19:26	2018 12 31, 19:40	59°59.000'	0°00.000'E	-0.25	0	3.0/236	23.3/232	023	5368	

### 3.1.10 Use of MiniROV vLBV300 (Fiona) for mooring recovery

#### Work at sea

Experience has shown, that, on occasion, acoustic releases fail to open the clutch to the anchor chain when acoustically commanded to do so. The reasons for this are manifold, including, e.g. electronic failure of the releases's electronic, low batteries or a mechanical jamming of the clutch by biofouling or anode residues. The risk of such failures increases with time. Nevertheless, to be able to recover such moorings, the Seabotix vLBV300 (vectorised Little Benthic Vehicle) ROV "Fiona" had been acquired and successfully deployed three years ago on *Polarstern* expedition PS103. However, as with any new technologies, the learning curve was steep then, and many issues remained unresolved during Fiona's first use. Particularly, the parallel feeding of both the ROV's tether and the recovery rope resulted in a tangling of the two in 2 out of 3 occasions, risking the ROV to become stuck at mid-depth when retrieving it, with the risk of damaging the tether or even losing the ROV when applying tension to the recovery rope. Secondly, the carabiner used to hook the recovery rope to the mooring rope appeared susceptible to breaking when subjected to shear forces. Thirdly, several software/ interface issues remained unresolved (see Expedition Report PS103, Boebel, 2017).

To overcome the first issue, a spool holding the recovery rope had meanwhile been constructed and was attached underneath the ROV, providing 400 m of high strength Dyneema rope. Once the ROV attached the carabiner to the mooring rope, it retracts or is being pulled back aboard, while unspooling the recovery rope. Hence, only either the tether or the recovery rope is present at a given distance from the ship, avoiding the risk of entanglement. While the latter aspect worked well, the ROV became quite difficult to maneuver due to this extra payload and a redesign appears warranted to overcome the difficulties we experienced.

Secondly, the original shackle type by which the recovery rope was attached to the mooring rope appeared to be susceptible to break when the carabiner was subjected to shear forces during recovery and its auto-trigger used to kick the mooring rope out of the carabiner. A more massive carabiner was used this time, without an out auto-trigger. To guide the mooring rope to the carabiner, a feeder was constructed, which guided the mooring rope into the carabiner during the final approach (Fig. 3.17). This modification worked remarkably well.



*Fig. 3.17: Feeder attached to front of Fiona (two black "antlers") with recovery rope (red) attached to shackle (not visible) in center of feeder. In the background the mobile GAPS antenna suspended over the side of the ship.*

Thirdly, handling of data protocols has been improved, such that the navigational display is now capable of displaying the ship (including an outline of the hull with correct heading), the ROV (as a dot, no heading), and the mooring's Posidonia transponder (multiple if available, one telegram per transponder ID).

The following section describes the set-up used to recover moorings with Fiona during PS117. Two set-up scenarios are considered: vessel based and mobile (i.e. from the sea ice) deployment, as implied by the location of the power supply and navigational beacons. However, the mobile set-up was not implemented or tested on this expedition.

Note that a set of “cook books” were developed during PS117, which are provided with Fionas documentation:

- ROV\_NavigationChecklist.pdf
- ROV\_PreFlightCheck.pdf
- ROV\_PreparationChecklist.pdf
- ROV\_Station\_protocol.pdf

#### *Vessel-based set-up*

##### **General requirements:**

- ROV equipment (as described in the checklists)
- GAPS (provided and operated by Lab-Electronician)
- Network access (Ethernet + telegrams, operated by Sysman)
- Power (provided by the electrician, organized through Lab Elo or Sysman. Power was supplied from outlets on helideck close to fire canon (sufficient fusing).

**Fiona's** location is continuously being tracked with the GAPS short baseline navigational system. Fiona bears a Applied Acoustic BAPS compatible Mini-beacon (transponder) which responds by sending ..... upon reception of an interrogation ping, while shipside the GAPS antenna is being deployed through the moonpool. However, the blocking of the moonpool by an unremovable “Verschlusskorb” during PS117 required deploying the mobile GAPS unit over the starboard side from the “großer Schiebebalken”.

**GAPS.** The mobile GAPS antenna was deployed to 15 m depth, i.e. below the ship's hull, via the 20-t boom (“Großer Schiebebalken”) from the working deck (Fig. 3.17). It was stabilized against rotation by two ropes attached GAPS-side to a horizontal bar attached to the top of the GAPS antenna and ship-side to mount points on the reeling farther to the front and back.

**ROV:** The ROV was deployed by its tether which was fed through the CTD's sheave mounted on the 5-to boom (“Kleiner Schiebebalken”). The ROV's position was received by GAPS as soon as the ROV was completely submerged, providing proof that the GAPS navigation is fully operational before the ROV descends. (This is possible as, with the GAPS antenna deployed over the side, as the line of sight between the GAPS antenna and the ROV is not blocked by the ship's hull (as it, contrastingly, would be for a “Brunnenschacht” set-up) even when the ROV is shallow. However, stable positions are only available once the ROV is below the GAPS' antenna depth.

The positioning set-up of the equipment is shown in Fig. 3.18.

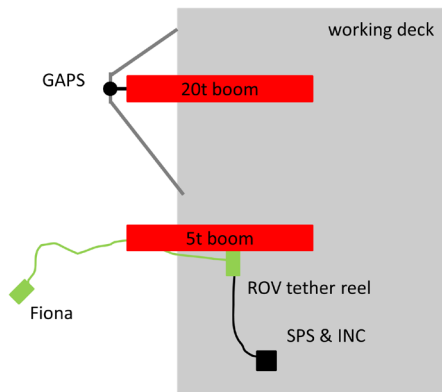


Fig. 3.18: Sketch of ship-side (deck-side) setup of mobile GAPS antenna and ROV Fiona deployment. Red: 20-t boom (Großer Schiebebalken) and 5-to boom (Kleiner Schiebebalken). Green: ROV Fiona with tether and tether reel. Black: ROV surface power supply (SPS) and integrated navigation console (INC).

**INC (Integrated Navigational Console) & SPS (Surface Power Supply):** An external keyboard and mouse was connected to the INC PC for ease of use when i.e., changing range and gain of the Gemini Sonar. In addition, a toughbook was used as independent navigation display. Initially, a separate navigation PC was intended to provide backup in case the INC would fail.

Use of the separate nav-PC has proven helpful by providing a good viewing angle for the second pilot (who's role is not to controlling the ROV but to provide navigation information to the active pilot), which is particularly important during high ambient light conditions.

It was suspected, yet remains unconfirmed, that the Nav-display on the INC has an excessive demand of computational power, causing the ROV's video to jerk, which might hamper steering the ROV. This should be assessed in detail on the next possible occasion.

#### *Mobile setup*

The mobile setup was not used on this expedition, hence there is no experience to report. For the power supply, at least one generator is required which has a minimum of three outlets and at least 6kW. The sockets are required for the following devices:

- Fiona
- INC, navigational PC (Toughbook)
- GAPS

#### *Issues and solutions*

**Problem description:** SeaNet Pro (running on the INC) requires navigation information to be provided as serial input. While 3 inputs are required to properly navigate Fiona, i.e.

- the ship's position,
- Fiona's position via GAPS,
- the mooring position via Posidonia,

the vLBV300 only features 2 USB ports for navigation or other input (like mouse and keyboard via USB hub).



serial port. The source code as well as the compiled version (compiled with .NET 3.5 client) can be found below. For every port pair given above, a new process of the udp2serial.exe program has to be started (e.g. "udp2serial.exe 7778 COMZ"). There are two ways how this program can be started. First, the input parameters can be set in a batch file that is calling the program. Second, the batch file can be started by double clicking the program. The program will respond by providing further instructions.

The UDP set-up was as follows:

- Ships UDP port 7778 (navigation PC)
- GAPS UDP port 4003
- Posidonia UDP port 8010

The UDP broadcast for ship position and heading was a custom telegram set up by the sysman, containing the datagrams GPHDT and GPGGA.

It is recommended to request the sysman to reset the network buffer on your IP for GAPS and Posidonia. This is to make sure that there is no delay in the datagrams received to the current state.

#### *Source code of udp2serial*

```
using System;
using System.IO.Ports;
using System.Net.Sockets;
using System.Net;
using System.Text;

namespace tcp2serial
{
    public static class Router
    {
        public static SerialPort ComPort;
        public static int UdpPortInt;
        public static UdpClient Client;
        public static IPEndPoint RemoteEndPoint;

        public static void Initialize(string ComPortName, int UdpPort)
        {
            Router.UdpPortInt = UdpPort;
            Router.ConnectComPort(ComPortName);
            Router.RemoteEndPoint = new IPEndPoint(IPAddress.Any, UdpPort);
            Router.BindUdpPortAndStartReceive(UdpPort);
        }

        public static void ConnectComPort(string PortName)
        {
            Router.ComPort = new SerialPort(PortName);
            Router.ComPort.PortName = PortName;
            Console.WriteLine("Connecting to com port...");
        }
    }
}
```

```
Router.ComPort.Open();
while (!ComPort.IsOpen)
{
    Console.WriteLine("...failed! Trying again...");
    Router.ComPort.Open();
}
Console.WriteLine("...done!");

return;
}

public static void BindUdpPortAndStartReceive(int UdpPort)
{
    Console.WriteLine("Connecting to local udp port...");
    Router.Client = new UdpClient(UdpPort);
    Console.WriteLine("...done!");
    Console.WriteLine("Waiting for incoming data to route through...");
    try
    {
        while (true)
        {
            byte[] received = Router.Client.Receive(ref Router.
RemoteEndPoint);
            string StringReceived = Encoding.ASCII.GetString(received, 0,
received.Length);

            ComPort.Write(StringReceived);
            Console.Write(StringReceived);

        }
    }
    catch (Exception e)
    {
        Console.WriteLine(e.ToString());
    }
}

}

class MainClass
{
    public static void Main(string[] args)
    {
        string ComPortName = "";
        string UDPPortName = "";
        int UDPPortInt = 0;

        if (args.Length == 2)
        {
            // get configuration
            ComPortName = args[0];
```

```
        UDPPortName = args[1];
    }
    else
    {
        Console.WriteLine("Please input serial port to use:");
        ComPortName = Console.ReadLine();
        Console.WriteLine("Please input udp port to use:");
        UDPPortName = Console.ReadLine();
    }
    UDPPortInt = Convert.ToInt32(UDPPortName);

    // Print configuration
    Console.WriteLine("Using ports:");
    Console.WriteLine(ComPortName);
    Console.WriteLine(UDPPortName);

    Router.Initialize(ComPortName, UDPPortInt);
    Console.WriteLine("Enter 'y' to exit!");
    while (Console.ReadLine() != "y")
    {
    }
}
}
```

## Operational results

### *Problems and diagnostics*

**Network problems:** There have been datagram problems in using the ships position and heading broadcast to UDP ports 7777 to two different PC's (INC and navigation PC). The reason why the datagram is not received when two PC's are listed was not resolved. The problem has however been overcome by using port 7777 on the INC and port 7778 on the navigation PC. A possible cause of the problem might be, that the software of the Sysman might not be capable of broadcasting to two different PC's to the same port.

To check if anything is received on the INC or navigational PC, the software NetCat can be used. In case of the ships position and heading in our setup the following call has been used from a console window: `ncat.exe -ul 7778`. The program `ncat.exe` is provided with Fiona's documentation.

Now all UDP packets that are received on this port are being printed to the terminal.

**Navigation beacon testing:** In order to test the navigation beacon before deployment, it was helpful to have a Frequency Generator App on a smartphone. Holding the smartphones telephone speaker to the transponder while emitting a frequency of 19.5kHz causes the beacon to respond with an audible beep of the same frequency.

### 3.1 Physical oceanography

#### Station logs

Station 00			
Dive number	01	Date/Time	
Objective	Checking the moonpool cap		
Summary	<ul style="list-style-type: none"> <li>The grabber was mounted.</li> <li>Therefore, Fiona was sinking down when no thruster was running.</li> <li>The system worked fine.</li> </ul>		
Files	fiona/stations/moonpool/inc/Thu_27_Dec_11_02*.avi fiona/stations/moonpool/inc/Thu_27_Dec_11_02*.V4LOG		

Station 047-01			
Dive number	02	Date/Time	16.01.2019 10:00
Objective	Recovering fish-mooring near Atka bay		
Summary	<ul style="list-style-type: none"> <li>Removed 50g of weight to make Fiona float.</li> <li>GAPS did not work because of defect beacon battery (marked accordingly).</li> <li>Went down to 60m without positioning.</li> <li>Fish-mooring has not been found with the sonar although it was in the expected range. The dive was aborted.</li> </ul>		
Files			

Station 048-02			
Dive number	03	Date/Time	16.01.2019 16:00
Objective	Recovering fishtrap near to Atka bay		
Summary	<ul style="list-style-type: none"> <li>During the flight it was almost impossible to drive the ROV with the required heading toward the target. There are two potential explanations:               <ul style="list-style-type: none"> <li>A current from ahead required to increase the horizontal thrust of the ROV resulting in problems steering it.</li> <li>Second, the video was lagging and thus we couldn't adjust the heading as quickly as needed.</li> </ul> </li> <li>Due to the problems moving into the desired direction, Fiona drifted below the ship.</li> <li>The dive was aborted and Fiona was recovered by pulling in the tether.</li> <li>SeaNet Pro crashed when using the mouse to change the range or gain of Gemini sonar.</li> </ul>		
Files	fiona/stations/048-02/inc/Wed_16_Jan_19_33*.avi fiona/stations/048-02/inc/Wed_16_Jan_19_33*.V4LOG		

### 3. HAFOS: Maintaining the AWI's Long Term Ocean Observatory in the Weddell Sea

Station 057-02			
Dive number	04	Date/Time	24.01.2019 14:00
Objective	Recovering of mooring AWI 250-1		
Summary	<ul style="list-style-type: none"> <li>• Removed another 50g of weight to make Fiona float.</li> <li>• The upper right front light (seen in direction of flying) was replaced, because it was damaged.</li> <li>• The tether was mounted on Fiona's back (instead of the top as for previous dives).</li> <li>• SeaNet Pro crashed several times when changing the gemini range and gain.</li> <li>• Recording was not restarted afterwards.</li> <li>• The mooring was not found at the expected position (based on Posidonia transponder at xx m depth) but xx m apart.</li> <li>• After hooking the mooring line, we drove the ROV approx. xx m backward toward the ship.</li> <li>• When the ROV got on deck, about 1/4 of the recovery line was left on the reel.</li> <li>• The mooring was recovered successfully.</li> <li>• The GoPro stopped recording after xx minutes because the battery was empty.</li> </ul>		
Files	fiona/stations/057-02/inc/Thu_24_Jan_14_22.avi fiona/stations/057-02/inc/Thu_24_Jan_14_22.V4LOG fiona/stations/057-02/gopro/ fiona/stations/057-02/toughbook/Do_24_Jan_14_21.V4LOG		

#### Summary

Three aspects stand out in comparison with the PS103 deployments:

During PS117, it was much harder to find the mooring in the sonar than previously. While on PS103 the sonar echo generally was found in the vicinity of the mooring transponder's position, during PS117 we once found the mooring at an entirely different location, and once did not find it at all

During PS117, the ROV was much harder to steer, not allowing to go beyond power setting 5 for the horizontal thrusters, while on PS103, power was even set to 10 without difficulties. On high power uses during PS117, Fiona dipped strongly forward or even to the side, causing the thrust to be directed in in undesired directions. This behaviour is probably due to the off-center torque caused by the additional recovery rope spool mounted now below the ROV.

The processing of navigational data was improved and now works as expected. Nevertheless, flaws in positions from acoustic SBNS occur and need to be taken in consideration when interpreting the ROVs track or location of the mooring.

#### Data management

The final records from moored instruments (CTD-recorders and current meters) have been post calibrated and are accessible through the PANGAEA data base via <https://doi.pangaea.de/10.1594/PANGAEA.875123> through \*.875139. The final processing of CTD-data will be conducted after post-expedition calibrations are available. All data will be stored and available through PANGAEA. P.I.: Olaf Boebel and Gerd Rohardt.

#### References

- Boebel O (2013) The expedition of the research vessel "Polarstern" to the Antarctic in 2012/2013 (ANT-XXIX/2) , Berichte zur Polar- und Meeresforschung = Reports on polar and marine research, Bremerhaven, Alfred Wegener Institute for Polar and Marine Research, 671 , 99 p. hdl:[10013/epic.42735](https://nbn-resolving.org/urn:nbn:de:epic:42735).
- Boebel O (2015) The Expedition PS89 of the Research Vessel Polarstern to the Weddell Sea in 2014/2015, Berichte zur Polar- und Meeresforschung = Reports on polar and marine research, Bremerhaven, Alfred Wegener Institute for Polar and Marine Research, 689 , 151 p. hdl:[10013/epic.45857](https://nbn-resolving.org/urn:nbn:de:epic:45857).
- Boebel O (2017) The Expedition PS103 of the Research Vessel POLARSTERN to the Weddell Sea in 2016/2017, Berichte zur Polar- und Meeresforschung = Reports on polar and marine research, Bremerhaven, Alfred Wegener Institute for Polar and Marine Research, 710 , 160 p. doi:[https://doi.org/10.2312/BzPM\\_0710\\_2017](https://doi.org/10.2312/BzPM_0710_2017), hdl:[10013/epic.51699](https://nbn-resolving.org/urn:nbn:de:epic:51699).
- Klatt O, Boebel O & Fahrbach E (2007) A profiling float's sense of ice. Journal of Atmospheric and Oceanic Technology, 24(7), 1301-1308.
- Padman L, Fricker H, Coleman R, Howard S & Erofeeva L (2002) A new tide model for the Antarctic ice shelves and seas. Annals of Glaciology, 34, 247-254 <https://doi.org/10.3189/172756402781817752>.
- Thompson Andrew & Heywood Karen (2008) Frontal structure and transport in the northwestern Weddell Sea. Deep-sea Research Part I: Oceanographic Research Papers, 55(10), 1229-1251 <https://doi.org/10.1016/j.dsr.2008.06.001>.

## 3.2 Ocean acoustics

Stefanie Spiesecke<sup>1</sup>, Diego Filun<sup>1</sup>, Marlene Meister<sup>1,2</sup>, Sarah Zwicker<sup>1,3</sup>, Olaf Boebel<sup>1</sup>;  
not on board: Elke Burkhardt<sup>1</sup>, Karolin Thomisch<sup>1</sup>, Ilse van Opzeeland<sup>1</sup>,  
<sup>1</sup>AWI  
<sup>2</sup>HUB  
<sup>3</sup>UOL

**Grant No: AWI\_PS89\_02**

### Objectives

The restricted accessibility of the Southern Ocean throughout most of the year confines our knowledge of the distribution patterns, habitat use and behavior of marine mammals in this area. Most of the Antarctic marine mammals produce species-specific vocalizations during a variety of behavioral contexts. Hence, passive acoustic monitoring (PAM) offers a valuable tool for research on these species, capable of covering large temporal and spatial scales. Particularly, in remote areas such as the Southern Ocean, moored PAM recorders are the tool of choice, as data can be collected year-round, under poor weather conditions, during darkness and in areas with dense ice cover.

The HAFOS observing system, a large scale oceanographic mooring array distributed throughout the Weddell Sea, is the host to numerous passive acoustic recorders which were recovered, refurbished and redeployed during PS117 to continue the long-term collection of passive acoustic data. The basin-wide design of the HAFOS observatory and the multi-year scale of data collection enables an unprecedented investigation of the spatio-temporal patterns in marine mammal biodiversity at the different mooring locations. The HAFOS array set-up and design also allow collecting information on the detection range of the various marine mammal sounds. Information on the distance over which marine mammal sounds can be detected by passive acoustic sensors is of vital importance when acoustic presence data are linked to information on environmental parameters in the context of studies of species-specific habitat usage. Detailed knowledge on detection ranges is key to ascertaining that the spatial scale of environmental variables, such as depth or sea ice coverage, matches with the range over which calling marine mammals can be detected by the recorders.

### Work at sea

#### Recovery of moored acoustic recorders

In total, 19 passive acoustic recorders, moored at 14 different positions, were recovered during PS117. These comprised 18 SonoVaults (manufactured by Develogic GmbH, Hamburg) and 1 AURAL (manufactured by MultiElectronique). 18 of these recorders had been deployed during *Polarstern* expedition PS103, while 1 recorder (SV1031) had been deployed 6 years ago in mooring AWI 250-01 during *Polarstern* expedition ANT-XXIX/2 (PS81). An overview of the recovery information of all recovered acoustic recorders is provided in Tab. 3.16 while deployment positions of the recorders are marked in Fig. 3.20.

After recovery, the acoustic recorders were rinsed with freshwater and cleaned from biological fouling. States of recovered recorders were accessed (if possible) by connecting a laptop through a serial connection and using a custom-made software for the SonoVaults and a software provided by Multi-Electronique for the AURAL (see Tab. 3.19 for a technical evaluation results). The recorders were then left to dry overnight to prevent damage to the electronics from water that retained in the threading of the recorder housing. After opening the recorder housing, the internal power supply was disconnected and its remaining voltage measured. In

### 3.2 Ocean Acoustics

case of the SonoVaults, all SD-cards, which had been labeled prior to deployment with the recorder's serial number, the recording module number and the SD card-slot, were removed and backed up (see below).

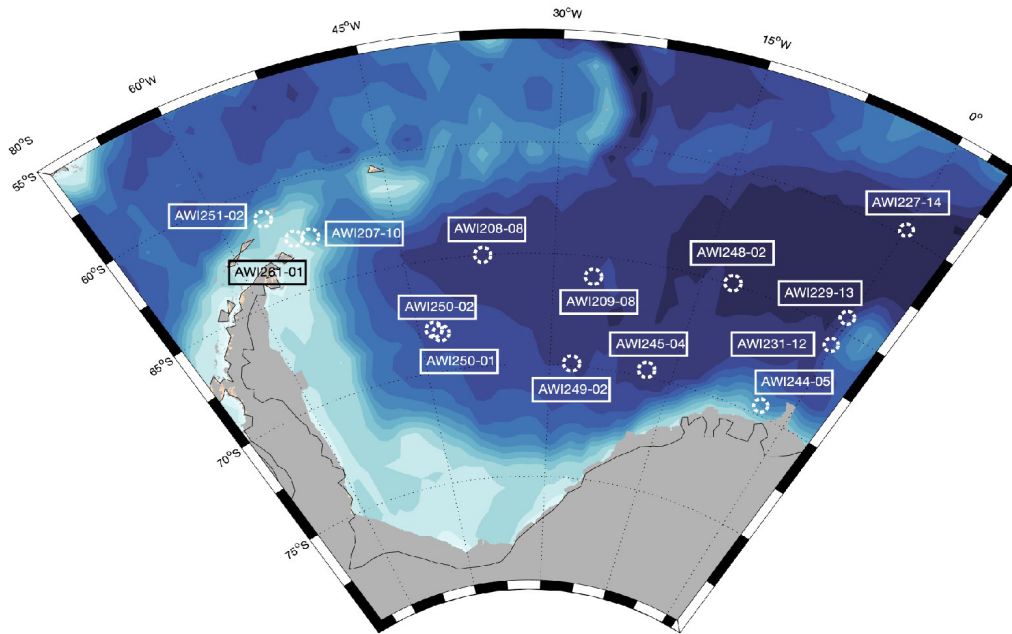


Fig. 3.20: Map showing the 14 locations of acoustic recorders recovered during PS117.

Each recovered recorder was calibrated post-recovery to allow calculations of received sound/signal levels. For the calibration, a Brüel & Kjaer calibrator (Type 4229) with the custom made adapter (SV.PA manufactured by Develogic) for the TC 4037 hydrophones was used. The calibration frequency is  $251.2 \text{ Hz} \pm 0.1\%$  (ISO 266) and the amplitude (at 1013 hPa) is 153.95 dB SPL. For the calibration measurement the recorder was set to the deployment sampling rate and a file size of 1 minute. Every minute the gain setting was changed successively from 0 – 7 (system gain settings representing 6 dB to 48 dB amplification). All recordings were stored and signal levels were calculated. Calibration of SV1013, recovered at the end of the expedition is still pending and will be concluded after the return of the instrument to Bremerhaven.

The hard disk with the acoustic data from the AURAL was also removed from the instrument. A calibration of this instrument was not performed, as no appropriate adapter is available for the HTI 96-min hydrophone.

Tab. 3.16: Overview of SonoVault and AURAL recorders recovered during PS117.

Mooring	Device SN	Position LAT LON	Deployment depth /m	Deployment date /time (UTC)	Recovery date	Gain /dB *)	Setup	Condition
AWI 227-14	SV1004	59° 03.03' S 000° 06.43' E	1070	24.12.2016 13:39	31.12.2018	41.4/ --	6857 Hz; 24bit; LowPower mode	a), d)
AWI 229-13	SV1053	64°00,49' S 000°00,84' E	1025	26.12.2016 16:02	01.01.2019	41.3/ --	6857 Hz; 24bit; LowPower mode	b), c)
AWI 231-12	SV1021	66°31,03' S 000°04,49' W	223	28.12.2016 12:34	27.12.2018	41.9/41.3	6857 Hz; 24bit; LowPower mode	a)
ditto	SV1022	66°31,03' S 000°04,49' W	570	28.12.2016 12:45	27.12.2018	42.5/41.8	6857 Hz; 24bit; LowPower mode	a)
ditto	SV1023	66°31,03' S 000°04,49' W	859	18.12.2016 13:05	27.12.2018	42.5/41.0	6857 Hz; 24bit; LowPower mode	a)
ditto	SV1024	66°31,03' S 000°04,49' W	1064	18.12.2016 13:12	27.12.2018	42.3 / 3)	6857 Hz; 24bit; LowPower mode	e)
ditto	SV1026	66°31,03' S 000°04,49' W	2074	18.12.2016 13:41	27.12.2018	41.6/ 3)	6857 Hz; 24bit; LowPower mode	f)
AWI 244-05	SV1057	69°00,32' S 006°59,56' W	1044	01.01.2017 14:33	05.01.2019	41.7/41.3	6857 Hz; 24bit; LowPower mode	b), f)
AWI 248-02	SV1058	65°58,12' S 012°13,87' W	1035	02.01.2017 14:35	07.01.2019	41.6 / 3)	6857 Hz; 24bit; LowPower mode	b), d), water in housing, Pressure Port open
AWI 245-04	SV1005	69°03.64' S 17°23.45' W	1004	11.01.2017 16:32	08.01.2019	41.6/38.6	6857 Hz; 24bit; LowPower mode	d)
AWI 249-02	SV1061	70°53.54' S 28°53.47' W	1040	13.01.2017 15:55	20.01.2019	29.9/ 3)	6857 Hz; 24bit; LowPower mode	e), d)

Mooring	Device SN	Position LAT LON	Deployment depth /m	Deployment date /time (UTC)	Recovery date	Gain /dB *)	Setup	Condition
AWI 209-08	SV1008	66°36.45' S 27°07.29' W	1053	18.01.2017 14:42	21.01.2019	41.2/ --	6857 Hz; 24bit; LowPower mode	b), e)
AWI 208-08	SV1009	65°41.79' S 36°41.012' W	1032	19.01.2017 20:15	23.01.2019	41.3/41	6857 Hz; 24bit; LowPower mode	b), a)
AWI 250-01	SV1031	68° 28.95' S 044° 06.67' W	1041	05.01.2013 14:21	24.01.2019	481)/44.9	5333 Hz; 24bit	b), f)
AWI 250-02	SV1003	68°27.84' S 44°08.71' W	1036	21.01.2017 18:26	24.01.2019	41.5/41	6857 Hz; 24bit; LowPower mode	a)
AWI 207-10	SV1029	63°39.36' S 50° 48.68 'W	1061	26.01.2017 09:28	29.01.2019	45.6/41.7	6857 Hz; 24bit; LowPower mode	a)
AWI 261-01	SV1011	63°30.87' S 51°38.14' W	842	26.01.2017 18:35	30.01.2019	41.6/41.2	6857 Hz; 24bit; LowPower mode	e)
AWI 251-02	SV1013	61°01.26' S 55°58.84' W	216	29.01.2017 15:30	01.02.2019	41.2/2)	6857 Hz; 24bit; LowPower mode	a), b)
AWI 251-02	AU0231	61°01.26' S 55°58.84' W	212	29.01.2017 15:30	01.02.2019	221)	32 kHz; 16bit; subsampling: 7 min every hour	a), b)
<p>a) system in good condition;  b) no communication established directly after recovery;  c) electronics damaged, batteries burned out, SD cards readable;  d) Hydrophone defect;  e) stopped early due to electronics failure (watchdog)  f) problems with electronics during test and calibration after recovery</p> <p>*) Calibration before/after recovery, using a B&amp;K Pistonphone at 251.2 Hz ± 0.1% (ISO 266) and the amplitude (at 1013 hPa) is 153.95 dB SPL</p> <p>1) Not calibrated; 2) calibration pending; 3) calibration not possible</p>								

**Data retrieval and backup**

12 of the 19 recovered passive acoustic devices recorded for a major part of their deployment period with recording periods ranging between 156 days and 671 days (Fig. 3.21). A total of approximately 15 TB and > 7100 days of passive acoustic data were obtained. In 5 recorders (SV1024, SV1058, SV1061, SV1008 and SV1011) recordings stopped early due to a firmware or electronics error (Tab. 3.17). Further details are discussed in section “Preliminary technical results”.

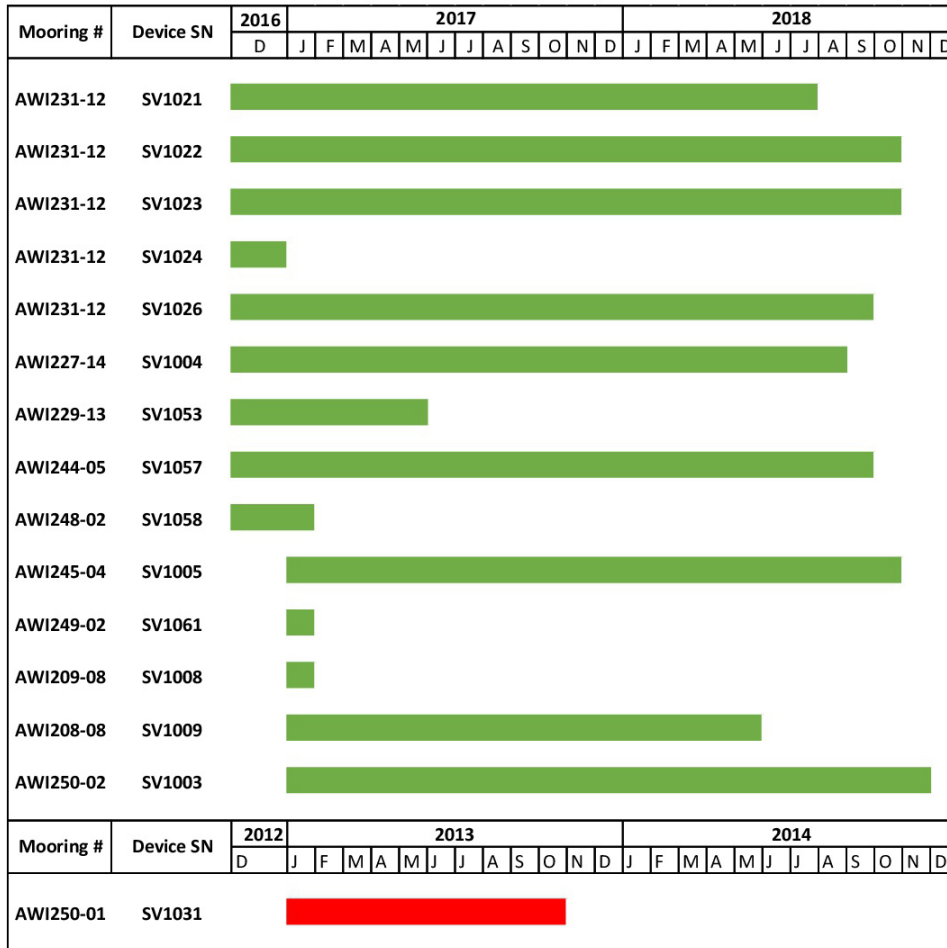


Fig. 3.21: Recording days of passive acoustic recorders retrieved during PS117. Note that AWI250-01 stems from a different deployment period (2012-2014) than all other recorders (2016-2018).

The SonoVault recorders store data on 35 SD cards (allowing a maximum of 2.2 TB of data storage per recorder for recorders deployed during PS103). After recovery, the SD cards were removed from the recorders and the acoustic data were copied using a custom-written shell script. Up to eight SD cards were copied simultaneously, with data initially saved with original filenames sorted into monthly and daily folders to one HDD (8 TB) drive. The backup process included the renaming of files based on each files’ internal time stamp (WAV-header) to the file name format ‘YYYYMMDD-HHMMSS\_AWIXXX-ZZ\_SVXXXX.wav’ (with X representing the IDs of mooring and SonoVault recorder, respectively and Z indicating the consecutive numbering of this mooring (i.e., the number of the current servicing cycle at a respective mooring)). After copying was completed, the data were synchronized with a second HDD (8 TB) used for the preliminary analysis on board.

### 3.2 Ocean Acoustics

3 SD cards (M0S0, M0S2, M2S2) recovered from SV1057 were initially inaccessible for the standard backup process. It was necessary to copy the data on a windows system to a second storage device (SD card) to be able to run the backup/renaming script on the data. SD cards from the burnt out (SV1053) instrument were attempted to be saved from further corrosion. They first were rinsed from residues with Milli-Q water, wiped dry and left drying over night. In a second step, contacts were cleaned using contact spray for electronics. In a last step the contacts were cleaned using a fibre pen. As a result, data from three SD-cards could be saved. Another three SD cards will have to be sent to a laboratory specializing on data recovery from the embedded microchips.

**Tab. 3.17:** Overview of the recording periods and SD-card status of all recorders that were recovered during PS117.

Mooring #	Device SN	Position	Deployment period	Recording period	Deployment Expedition	Recording error	Missing recorded period
AWI231-12	SV1021	66° 31.03' S	28.12.2016	26.12.2016	PS103	none	none
		000° 04.49' W	27.12.2018	23.07.2018			
	SV1022	66° 31.03' S	28.12.2016	27.12.2016	PS103	none	none
		000° 04.49' W	27.12.2018	23.10.2018			
	SV1023	66° 31.03' S	28.12.2016	26.12.2016	PS103	none	none
		000° 04.49' W	27.12.2018	28.10.2018			
	SV1024	66° 31.03' S	28.12.2016	26.12.2016	PS103	stopped early: watchdog	none
		000° 04.49' W	27.12.2018	28.12.2016			
	SV1026	66° 31.03' S	28.12.2016	26.12.2016	PS103	none	none
		000° 04.49' W	27.12.2018	03.10.2018			
AWI227-14	SV1004	59° 03.03' S	24.12.2016	22.12.2016	PS103	none	none
		000° 06.49' E	31.12.2018	18.09.2018			
AWI229-13	SV1053	64° 00.42' S	26.12.2016	25.12.2016	PS103	M0S1,M0S2, M0S3 not readable	31.01.2017 - 17.05.2017
		000° 00.84' W	01.01.2019	31.05.2017			
AWI244-05	SV1057	69° 00.32' S	01.01.2017	31.12.2016	PS103	none	none
		006° 59.56' W	05.01.2019	14.09.2018			
AWI248-02	SV1058	65°58,12' S	02.01.2017	31.12.2016	PS103	stopped early: watchdog	none
		012°13,87' W	07.01.2019	02.01.2017			
AWI245-04	SV1005	69°03.64' S	11.01.2017	09.01.2017	PS103	none	none
		017°23.45' W	08.01.2019	20.10.2018			
AWI249-02	SV1061	70°53.54' S	13.01.2017	06.01.2017	PS103	stopped early: watchdog	none
		028°53.47' W	20.01.2019	13.01.2017			
AWI209-08	SV1008	66°36.45' S	18.01.2017	14.01.2017	PS103	stopped early: watchdog	none
		027°07.29' W	21.01.2019	18.01.2017			
AWI208-08	SV1009	65°41.79' S	19.01.2017	17.01.2017	PS103	none	none
		036°41.012' W	23.01.2019	02.05.2018			
AWI250-01	SV1031	68° 28.95' S	05.01.2013	04.01.2013	ANTXXIX/2	none	none
		044° 06.67' W	24.01.2019	12.10.2013			

### 3. HAFOS: Maintaining the AWI's Long Term Ocean Observatory in the Weddell Sea

Mooring #	Device SN	Position	Deployment period	Recording period	Deployment Expedition	Recording error	Missing recorded period
AWI250-02	SV1003	68°27.84' S	21.01.2017	17.01.2017	PS103	none	none
		044°08.71' W	24.01.2019	11.11.2018			
AWI 207-10	SV1029	63°39.36' S	26.01.2017	18.01.2017	PS103	none	none
		050° 48.68 'W	29.01.2019	09.11.2018			
AWI 261-01	SV1011	63°30.87'S	26.01.2017	26.01.2017	PS103	stopped early: watchdog	none
		051°38.14' W	30.01.2019	26.01.2017			
AWI 251-02	SV1013	61°01.26' S	29.01.2013	26.01.2017	PS103	unknown	none
		55°58.84' W	02.02.2019	29.04.2017			
	AU0231	61°01.26' S	29.01.2013	27.01.2017	PS103	none	none
		55°58.84' W	02.02.2019	04.02.2018			

\*) Recorder burnt out

#### Deployment of moored acoustic recorders

A total of 12 SonoVault recorders were deployed in 12 moorings during PS117 (Fig. 3.22 and Tab. 3.18). These recorders are equipped with electronics version V4.1. All new recorders use the firmware version V4.13a. Additionally one AURAL recorder (Multi-Electronique, Canada) was deployed in one mooring alongside the SonoVault recorder in mooring AWI251-03.

Recorders were pre-deployment calibrated in the same manner as post-recovery calibrations described above, using the Brüel & Kjaer calibrator (Type 4229, c.f. 'Recovery of moored acoustic recorders').

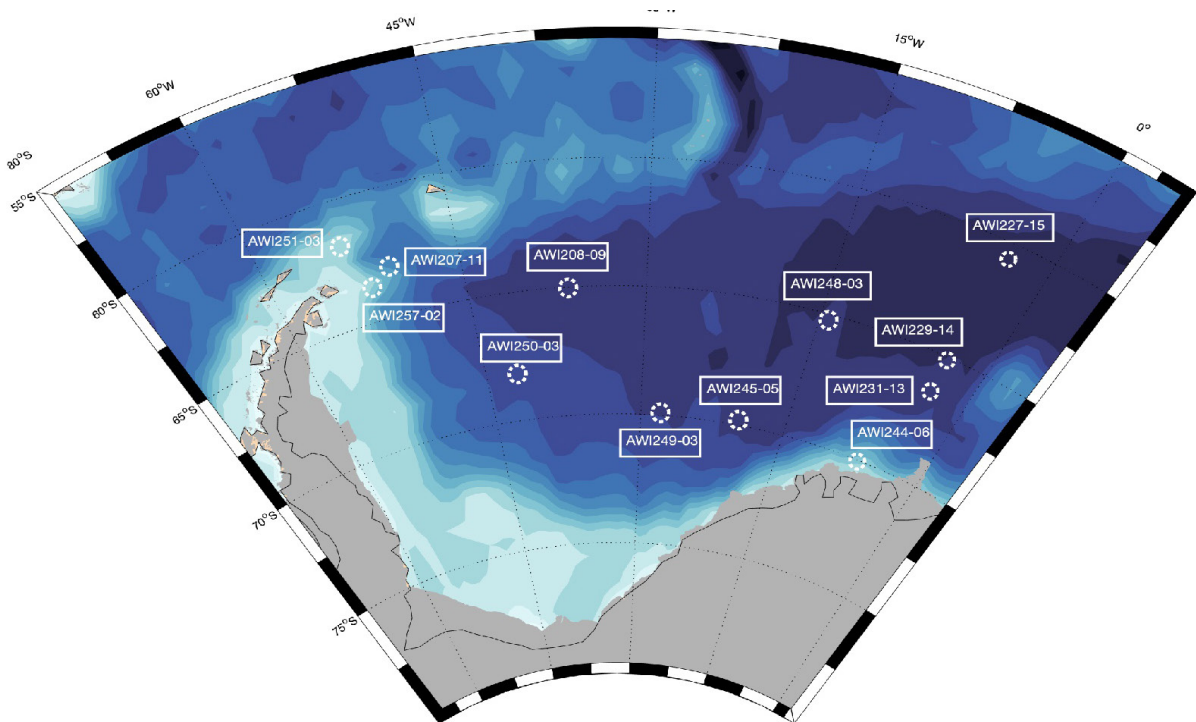


Fig. 3.22: Deployment positions of acoustic recorders moored during PS117

### 3.2 Ocean Acoustics

Prior to the deployment, newly formatted SD cards were placed into the SD card slots on each recording module. 12 recorders now contain 35 SD cards with a capacity of 128 GB each (acon Industrial Grade SD Cards), resulting in a total storage capacity of 4.4 TB per recorder. All SD cards were formatted to FAT32 using the freeware tool 'SDXCformatterFAT32'. On each first SD card (S0) of the first of five recording modules (M0-M4), the recording configuration (e.g., gain setting, sample rate) was stored. Additionally, the module number was copied onto S0 of every recording module to make the set of seven SD cards of this module available for storage.

The recorders were equipped with batteries (SAFT LS33600 or Tadiran SL-2780) and the O-rings were carefully checked, cleaned and greased before closing the housing. All SonoVaults were programmed to record at a sampling rate of 24 kHz with 24 bit and to store data in files of 600 s duration (Tab. 3.18). Internal data storage was structured to store data in daily folders. Gain was set to level 7 which in this hardware/firmware release corresponds to about 41 – 45 dB in all deployed recorders (Tab. 3.18). Every instrument was first tested for at least 2 days on their operational settings and then restarted at least 2 days prior to the deployment. SonoVaults were deployed with new mounts, consisting of two plastic clamps mounted at two positions around the housing. The clamps were then attached to the Dyneema mooring rope. All metal parts are titanium grade 5. From mooring AWI250-03 onward, recovered mounts were used to attach the recorders to the mooring line.

**Tab. 3.18:** Overview of acoustic recorders deployed during PS117

Mooring	Acoustic Recorder SN	Position LAT LON	Corr. water depth /m EK60	Deployment depth /m	Deployment date /time (UTC)	Gain /dB <sup>*)</sup>	Set-up
AWI 227-15	SV1006	59°03.02' S 000°06.44' W	4605	285	31.12.2018 09:58	44.2	24 kHz; 24bit; LowPower mode
AWI 229-14	SV1060	64°00.98' S 000°00.34' E	5060	329	01.01.2019 20:45	44.3	24 kHz; 24bit; LowPower mode
AWI 231-13	SV1056	66°31.03' S 000°04.48' W	4580	303	27.12.2018 18:14	44.5	24 kHz; 24bit; LowPower mode
AWI 244-06	SV1049	69°00.08' S 007°01.66' W	2900	300	05.01.2018 18:53	45.4	24 kHz; 24bit; LowPower mode
AWI 248-03	SV1012	65°58.13' S 012°13.84' W	4950	350	07.01.2019 10:27	44.4	24 kHz; 24bit; LowPower mode
AWI 245-05	SV1014	69°03.64' S 17°23.48' W	4734	300	08.01.2019 14:12	44.3	24 kHz; 24bit; LowPower mode
AWI 249-03	SV1010	70°53.22' S 28°56.97' W	4362	307	20.01.2019 09:52	40.1	24 kHz; 24bit; LowPower mode
AWI 208-09	SV1020	65°41.78' S 36°41.01' W	4714	294	23.01.2019 15:47	44.5	24 kHz; 24bit; LowPower mode

### 3. HAFOS: Maintaining the AWI's Long Term Ocean Observatory in the Weddell Sea

Mooring	Acoustic Recorder SN	Position LAT LON	Corr. water depth /m EK60	Deployment depth /m	Deployment date /time (UTC)	Gain /dB <sup>*)</sup>	Set-up
AWI 250-03	SV1048	68°28.85' S 44°05.94' W	4100	294	24.01.2019 20:28	41.8	24 kHz; 24bit; LowPower mode
AWI 257-02	SV1033	64°12.94' S 047°29.38' W	4292	311	27.01.2019 17:38	44.7	24 kHz; 24bit; LowPower mode
AWI 207-11	SV1032	63°39.36' S 050°48.66' W	2510	300	29.01.2019 17:00	45.1	24 kHz; 24bit; LowPower mode
AWI 251-03	SV1002	61°01.38' S 055°58.68' W	335	181	01.02.2019 18:21	41.3	25 kHz; 24bit; LowPower mode
	AU0085	61°01.38' S 055°58.68' W	335	179	01.02.2019 18:25	<sup>1)</sup>	32 kHz; 16bit; subsampling: 6 min every hour

\*) Calibration before deployment, using a B&K Pistonphone at 251.2 Hz  $\pm$  0.1% (ISO 266) and the amplitude (at 1013 hPa) is 153.95 dB SPL;

1) Not calibrated

In AWI251-03, additional instruments, i.e. an AZFP (Acoustic Zooplankton and Fish Profiler, ASL) and an ADCP (Acoustic Doppler Current Profiler) were deployed alongside the acoustic recorders for the detection of the presence of prey. The AZFP is using the backscatter of acoustic pings at four different frequencies (38 kHz, 125 kHz, 455 kHz, 769 kHz) to detect zooplankton. AZFP55037 is deployed at 280 m water depth and is set to ping four times every 10 minutes. Data of every ping will be stored without averaging. The pulse length for every frequency is set to the maximum to bring the maximum power into the water column. The range for the measurement is set to 309 m, with bin sizes of 0.25 m. A deployment period of 1,100 days was assumed for the calculation of storage space.

Additionally a 75 kHz ADCP (Acoustic Doppler Current Profiler, SN 5373) was deployed in 320m water depth. The ADCP pings every 10 minutes, 5 minutes apart from the AZFP pings. Apart from information on the currents at the mooring position, its data is also intended to be used for analysis of presence of zooplankton.

#### Maintenance of the PALAOA observatory

PALAOA ('Perennial Acoustic Observatory in the Antarctic Ocean) located on the Ekström Ice Shelf since 2005, collects continuous underwater recordings from a coastal Antarctic environment using a hydrophone deployed at ca. 160 m depths. With the ice shelf advancing by about 150 per year, the position is constantly changing. On 13 January 2019 the following positions were recorded:

- Hydrophone 70°30.258'S 008°12.717'W
- PALAOA station (recording unit) 70°30.402'S 008°12,703'W

During the supply of the *Neumayer Station III* from 28 Dec 2014 until 31 Dec 2014, an aluminum box, containing modified Sonovault electronics, was installed at the position of the former PALAOA container. It was recessed into the snow and is covered with a wooden board and some snow. The box (80cm x 60cm x 60cm) includes a Reson input module EC6073 for the active hydrophone (Reson TC4032) and a SonoVault electronics module, similar to those used in the moored recorders. For the power supply, four 90 Ah, 12V batteries were included, two connected in row for each, the active hydrophone and the recording electronics. The battery setup was changed later in 2015 to batteries two in a row and those rows in parallel, supplying both, the hydrophone and the recording electronics. Storage capacity is 4.4 TB (35 x 128 GB SDXC). With a sampling rate of 80 kHz at 24bit and a file size of 600s the PALAOA system was expected to run up to 6 months. Servicing is provided by the overwintering team of *Neumayer III*. However, based on the experience from the Neumayer staff, a servicing interval of approx. 3 months proved to be necessary. On January 13th 2019 the box was maintained and the recording quality was checked.

#### **Preliminary technical results**

##### *Mechanical status*

Recovered SonoVaults had been deployed with mounts, consisting of two plastic clamps, grabbing at two positions around the housing, with all metal parts being titanium grade 2. Screws were secured using punch-marks and thread locker. The clamps are attached to a 5 m Dyneema rope which is attached in-line to the main mooring line by rope shackles.

None of the recovered recorders exhibited signs of corrosion on neither the device nor the mounts. One clamp was broken, when the mounts were detached on deck. It is not clear if this happened on deck or in the water.

The recorders recovered from AWI250-01 and AWI251-02 were mounted in steel mooring frames. The sacrificial anodes were eroded by and large, but the frame showed no sign of corrosion. The AURAL recorder in mooring AWI251-02 was also moored in a metal frame, attached to a 3 m mooring rope. The frame was in good condition upon recovery. Both recorders, SonoVault SV1013 and AURAL AU0231, recovered from AWI251-02, showed significant biological fouling. Their hydrophones, however, were not affected.

Housings of the SonoVaults recorders are either metal/plastics composite or, in newer versions titanium with an embedded pressure valve in the lid of the titanium housings. The titanium housings showed signs of leakage at the pressure valve. One of these housings was burned out, though the cause could not be determined (SV1053). On a second device the pressure valve was open after recovery, inside the housing were approx. 200 ml of water (SV1058). As there were no signs of corrosion on parts inside the housing, and the batteries being seemingly intact, it is assumed that the water intake had occurred only recently. Another recorder of the same type had water inside the housing (SV1061), however not as much as in SV1058. In contrast to the titanium housings, none of the composite housing showed signs of leakage. Battery packs of the three housings with water intake were safely stored in a special container for lithium-metal batteries.

##### *Communication with recovered instruments*

Communication efforts after recovery were successful with 11 out of 18 SonoVault + 1 Aural recorders. The instruments were connected via RS232 to a computer. With a custom built software a connection was attempted and status information on the system was queried. Success of communication efforts and information retrieved from the recorders are listed in Tab. 3.19.

#### *Operation period and failures*

All SonoVaults had ceased recording prior to recovery. All devices were equipped with sufficient power supply and storage capacity to bridge the entire deployment period with recordings. Most of the recovered SonoVaults used the hardware version 4.1, with firmware version 4.12a, and were set to use the Low Power Mode for sampling. This led to longer recording times than during previous deployment periods, as the sampling mode in earlier deployments was set by default to a High Resolution Mode with significantly higher power consumption. (see Expedition Report PS103, Boebel, 2017).

Recorders SV1024, SV1053, SV1061, SV1008 only recorded for some days before a software error occurred. The reason for the software error is unknown. They ran for several days prior to the deployment without fault and were checked only hours before the deployment. The recorder SV1013 recovered from mooring AWI251-02 stopped recording after 3 months. The cause needs yet to be determined. The AURAL recorder from the same mooring position delivered one year of subsampled acoustic data (7 minutes every hour). In contrast to earlier deployment the operational period was shorter due to the increased number of measurements per day and the alkaline battery pack, used now instead of the custom made (but now unavailable) lithium battery packs.

#### *Clock drift and post calibration*

Where possible, the status of the system, the clock drift of the precision clock (SV1053 featured the alternative optional CSAC clock, but was burned out), voltage and SD-card status were checked using the communication software. To post-calibrate the hardware in combination with the hydrophone, a laboratory power supply was connected to the hardware. When communication was not possible, the time drift of the real-time-clock, which is powered independently by a lithium cell embedded on the electronics module, was determined (Sonovaults 1009 and 1057). This clock, however has a different drift than the precision clock which is used during the mission. However, throughout the recording period the difference between the real-time-clock and the precision clock is logged to the respective log-file. Tab. 3.19 gives the clock offsets.

A post calibration of each recovered recorder was performed to ensure the correct calculation of signal levels after recovery. The post calibration for the last recorder is still pending and will be completed in Bremerhaven.

#### *Preliminary data quality evaluation*

Some of the SonoVault recordings contained either pulsed or tonal (monofrequent) noise within the frequency range up to 1 kHz, which is likely caused by the electronics. The frequency range and intensity of the noise varies between recorders. The cause of this noise could not yet be determined. Tab. 3.19 summarizes the occurrence and type of noise found during the preliminary analysis of the recovered data.

**Tab. 3.19:** Overview of results of preliminary technical and data quality evaluation of recorders recovered during PS117

Mooring	Device SN	Communication established	remaining Volt initial Volt [V]	Instrument time vs UTC time clock drift [sec a-1]	Recording days	Recording status	Electronic noise present in recordings (preliminary results)
AWI231-12	SV1021	Yes 27.12.2018	13.3 (25)	SV: 13:58:16 UTC: 13:55:39 +78.7	574	end: battery low	Monotonous and pulsed noise <500 Hz, increasing to <1 kHz from June 2017
ditto	SV1022	Yes 27.12.2018	13.4 (25)	SV: 14:02:40 UTC: 14:01:45 +27.6	665	end: battery low	Monotonous and pulsed noise of varying intensity and frequency range (<1 kHz) from July 2017
ditto	SV1023	Yes 27.12.2018	11.1 (25)	SV: 14:17:37 UTC: 14:06:10 +344.2	671	end: battery low	No
ditto	SV1024	Yes 27.12.2018	24.9 (25)	SV: 14:09:42 UTC: 14:09:54 -3.5	1	stopped early: watchdog	--
ditto	SV1026	Yes 27.12.2018	12.2 (25)	SV: 14:22:03 UTC: 14:15:23 +199.9	646	end: battery low	Monotonous and pulsed noise <500 Hz, increasing to <1 kHz, recording is dominated by noise from February 2018
AWI227-14	SV1004	Yes 31.12.2018	12.5 (25)	SV: 08:35:47 UTC: 08:23:35 +362.8	633	end: battery low	No
AWI229-13	SV1053	No 01.01.2018	nn	burned out CSAC clock	156	burned out	Monotonous lines, 0-10 Hz, limited to some days
AWI244-05	SV1057	No 05.01.2019	nn	SV: 17:59:06 UTC: 17:53:58 <b>+153 1)</b>	622	end: battery low	No
AWI248-02	SV1058	No 06.01.2019	nn	not available	2	stopped early: watchdog	--

### 3. HAFOS: Maintaining the AWI's Long Term Ocean Observatory in the Weddell Sea

Mooring	Device SN	Communication established	remaining Volt initial Volt [V]	Instrument time vs UTC time clock drift [sec a-1]	Recording days	Recording status	Electronic noise present in recordings (preliminary results)
AWI245-04	SV1005	Yes 08.01.2019	12.2 (25)	SV: 09:28:32 UTC: 09:19:53 +260.8	649	end: battery low	Monotonous and pulsed noise of varying intensity and frequency range (<1 kHz)
AWI249-02	SV1061	Yes 20.01.2019	46.4 (47)	SV: 08:13:19 UTC: +08:13:31 -6	7	stopped early: watchdog	--
AWI209-02	SV1008	No 22.01.2019	nn	not available	4	stopped early: watchdog	--
AWI208-02	SV1009	No 23.01.2019	nn	SV: 20:34:34 UTC: 20:28:21 <b>+186</b> <sup>1)</sup>	470	end: battery low	No
AWI250-01	SV1031	No 25.01.2019	nn	SV: 20:02:59 UTC: 19:57:55 <b>+50</b> <sup>1)</sup>	281	end: battery low	No.
AWI250-02	SV1003	Yes 25.01.2019	12.8 (25)	SV: 13:00:40 UTC: 12:56:36 +121.6	663	end: battery low	No
AWI207-10	SV1029	Yes 29.01.2020	9.5 (25)	SV: 16:33:39 UTC: 16:26:05 +226	660	end: battery low	monotonous and pulsed lines <400 Hz until April 2017, sporadically appearing thereafter
AWI261-01	SV1011	Yes 31.01.2021	25 (25)	SV: 10:24:01 UTC: 10:24:14 -6	1	stopped early: watchdog	--
AWI251-02	SV1013	No 01.02.2019	nn	not available	93	stopped early, cause unknown	<sup>2)</sup>
	AU0231	No 01.02.2019	nn	not available	373	end: battery low	<sup>2)</sup>

1) Values given for real-time-clock, otherwise for precision clock. 2) analysis pending. SV1053 (burned out) was the only instrument equipped with a CSAC clock. SV1031 uses old firmware without the no option available.

### Preliminary scientific results

Visual and aural inspection of single files (i.e., 10-minute wav files) was conducted using Raven Lite 2.0 in order to provide information on the acoustic presence of different marine mammals. Due to time constraints, data was screened every 15th day only. Recordings of AWI 207-10 SV1029 were only superficially screened, choosing a 30-day resolution and the acoustic data of AWI 251-2 SV1031 and AWI 251-2 AU0231 were not analyzed. For each recorder, acoustic signals of marine mammal species were depicted in preliminary biodiversity maps (Fig. 3.23) obtaining a first overview of species distribution.

#### *Pinnipeds*

All SonoVaults recorded vocalizations of leopard seals (*Hydrurga leptonyx*). Crabeater seals (*Lobodon carcinophaga*) were acoustically present in the data of all recorders except for AWI 229-13 SV1053. However, data from this acoustic device was available from 25 December 2016 to 30 January 2017 and from 18 May to 4 June 2018 only, and hence the acoustic absence of crabeater seals likely results from the short recording time covered. Calls of Weddell seals (*Leptonychotes weddellii*) were not detected in the data of acoustic devices deployed along the Greenwich meridian but were found in the records of all other recorders. Similarly, Ross seals (*Ommatophoca rossii*) were acoustically absent at mooring positions along the Greenwich meridian but their vocalizations were detected in the data of six recorders deployed in the Weddell Sea (AWI-2445 SV1057, AWI-245-4 SV1005, AWI 208-8 SV1009, AWI 250-1 SV1031, AWI 250-2 SV1003, and AWI 207-10 SV1029).

#### *Cetaceans*

Single vocalizations and/or the choruses of Antarctic blue whales (*Balaenoptera musculus intermedia*) and fin whales (*B. physalus*) as well as vocalizations of Humpback whales (*Megaptera novaeangliae*) were present at all recording positions. Vocalizations of Antarctic minke whales (*B. bonaerensis*) were found in the acoustic data of all recorders except for AWI 229-13 SV\_1053. As mentioned before this device provided data for a comparatively short amount of time, i.e. less than two months, which might most likely explain the acoustic absence of (seasonally vociferous) Antarctic minke whales in the data.

Killer whales (*Orcinus orca*) were acoustically present at four mooring positions (AWI 227-14 SV1004, AWI 244-5 SV1057, AWI 245-4 SV1005, and AWI 207-10 SV1029). Clicks of sperm whales (*Physeter macrocephalus*) were not found in the records, as well as any clicks of the two true Antarctic toothed whale species, which however vocalize well above 3.5 kHz (Steiner et. al., 1979, Backus & Schevill, 1966), i.e. higher than the frequency ranges recorded by the SonoVaults.

#### *Other sound sources*

Signals of air guns were found on 30 December 2016 (AWI 227-14 SV1004) and on 1 March 2018 (AWI 208-8 SV1009 and AWI 250-2 SV1003). Broadband sounds, presumably originating from distant ships, were occasionally detected (e.g. AWI 227-14 SV1004, 30 December 2016 and AWI 250-1 SV1031, 1 April 2013), though wind and tidal induced noise may not be excluded as alternative explanation.

We like to emphasize that these results are based on a first very coarse screening of the passive acoustic data and that it cannot be excluded that the maps presented here do not reflect the full local marine mammal biodiversity.

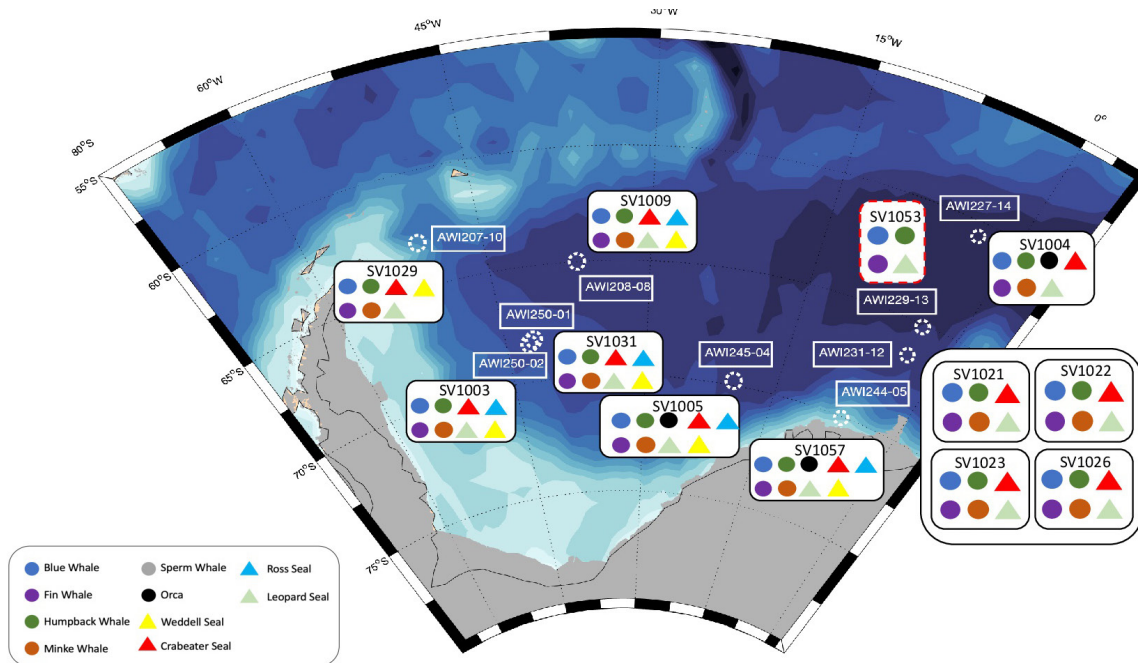


Fig. 3.23: Preliminary results on acoustic presence of marine mammal species in passive acoustic data recorded at 12 recorder positions throughout the Weddell Sea

### Data management

All passive acoustic data will be transferred to the AWI silo and made accessible through the PANGAEA database. P.I.: Ilse van Opzeeland.

### References

- Steiner WW, Hain JH, Winn HE, Perkins PJ (1979) Vocalizations and feeding behavior of the killer whale (*Orcinus orca*). *Journal of Mammalogy*, 60:823-827.
- Backus R, Schevill W (1966) Physeter clicks. In: Norris KS (ed) *Whales, dolphins and porpoises*. University of California Press.

### 3.3 Transport variations of the Antarctic Circumpolar Current

Olaf Boebel<sup>1</sup>, Rainer Graupner<sup>1</sup>, Carina Engicht<sup>1</sup>,  
Gerd Rohard<sup>1</sup>  
not on board: Sabrina Speich<sup>4</sup>, Thierry Terre<sup>5</sup>

<sup>1</sup>AWI  
<sup>2</sup>IfM-GEOMAR  
<sup>3</sup>HAFRO  
<sup>4</sup>ENS  
<sup>5</sup>LOPS

**Grant No: AWI\_PS103\_02**

#### Objectives

Pressure Inverted Echo Sounders (PIES) deliver bottom pressure, bottom temperature and travel times of sound signals from the bottom to the sea-surface, effectively providing a measure of average temperature of the water column and sea surface height (SSH). These data are used to evaluate variations of both barotropic and baroclinic geostrophic transport within the Agulhas Retroflexion. The PIES are placed along the GoodHope Section (Fig. 3.24) to the Southwest of South Africa, which in large parts coincides with ground track # 133 of the Jason (previously TOPEX/Poseidon) satellite mission to allow direct comparison with altimetry SSH. PIES-to-PIES distances are chosen to resolve the major oceanic fronts of this region (Fahrbach, 2011; Boebel, 2015).

#### Work at sea

During PS117, five out of six PIES were successfully recovered on behalf of our French colleagues (Tab. 3.20).

PIES were acoustically released by a mobile Teledyne UDB9000 unit connected to a hydrophone lowered over the side of the vessel to about 20 m. Release commands were repeated 10 times with nominally 1 minutes spacing to ensure that the PIES acoustic listening unit is not blocked during its own measurement schedule, and to re-trigger release execution after possible resets. After a set of 3 release commands each, the transponder was hoisted by 5 m to reduce the risk of surface reflections of the acoustic command to interfere with the acoustic signal proper. During this process, the ship was positioned such that the PIES logged position was at about 300 m from the bow at 2 'o clock (i.e. starboard forward) while the depth sounder and the bow thrusters were switched off. Due to the high underwater noise level of *Polarstern*, acknowledge pings of the PIES were never detected.

PIES were expected to (and did) surface at 7 min release time + 0.8 m/s\*water depth + 10 min (if released at last release command) + 15 min (you never know time). One PIES (#51 at position PIES-4) failed to surface in spite of having repeatedly sent release commands (2 sets of 10 commands, 2,5 hours apart). This recovery effort differed slightly in that

- prior to sending the PIES release commands an acoustic modem – used in connection with operation of the Ultra Clean CTD - was operated in parallel and
- that the PIES bottom location was on port-forward, rather starboard-forward.

However, we do not think these differences might have caused the failed release attempt.

Tab. 3.20: Summary of deployment and recovery information regarding the French GoodHope PIES as recovered during PS117

PIES SN DCS SN Posidonia SN	Deployment					Recovery				
	Expedition Mooring ID Station book	Date time	Position Depth	Deployment CTD	Expedition Mooring ID Station book	Release date Release time OFF time	Position (ship@ release) water depth (EK60)	Time offset date	Recovery CTD	
PIES #049	SANAP3	06.12.2014	36°13.213' S	not known	PS117	16.12.2018	36°13.283' S	on 24.12.2018	PS117_1-1	
no DCS	PIES 2	10:17	13°18.101' E		PIES 2 PS117_1-3	18:15 20:20	13° 18.341' E	10:20:00 GPS		
no ET861	not known		4832 m				4824 m	10:17:37 PIES		
PIES #048	Agulhas 2015	25.07.2015	37°24.458' S	not known	PS117	17.12.2018	37°24.350' S	on 24.12.2018	PS117_2-1	
no DCS	PIES 3	20:17	12°31.123' E		PIES 3 PS117_2-3	06:24	12° 31.405' E	09:20:00 GPS		
no ET861	not known		5070 m			08:38	5054 m	09:17:19 PIES		
PIES #051	SANAP3	07.12.2014	38° 36.099' S	not known	PS117	17.12.2018	38°36.091' S		PS117_3-1	
no DCS	PIES 4	07:54	11° 45.765' E		PIES 4 PS117_3-3	19:04	11° 45.568' E			
no ET861	not known		5120 m				5105 m			
PIES #052	SANAP3	07.12.2014	39° 58.567' S	not known	PS117	18.12.2018	39° 58.433' S	on 24.12.2018	PS117_4-1	
no DCS	PIES 5	19:56	10° 47.668' E		PIES 5 PS117_4-3	11:26	10° 47.554' E	10:30:00 GPS		
no ET861	not known		4775 m			13:31	4766 m	10:28:36 PIES		
PIES #050	Agulhas 2015	27.07.2015	41° 20.898' S	not known	PS117	19.12.2018	41° 20.790' S	on 24.12.2018	PS117_5-1	
no DCS	PIES 6	11:22	09° 53.275' E		PIES 6 PS117_5-2	00:00	09° 53.385' E	09:49:00 GPS		
no ET861	not known		4680 m			02:00	4677	09:47:01 PIES		
PIES #054	Agulhas 2015	28.07.2014	42° 41.647' S	not known	PS117	19.12.2018	42° 41.721' S	on 24.12.2018	PS117_6-3	
no DCS	PIES 7	18:19	08° 44.241' E		PIES 7 PS117_6-1	11:15	08° 44.374' E	10:06:00 GPS		
no ET861	not known		4970 m			13:15	4904	10:02:13 PIES		

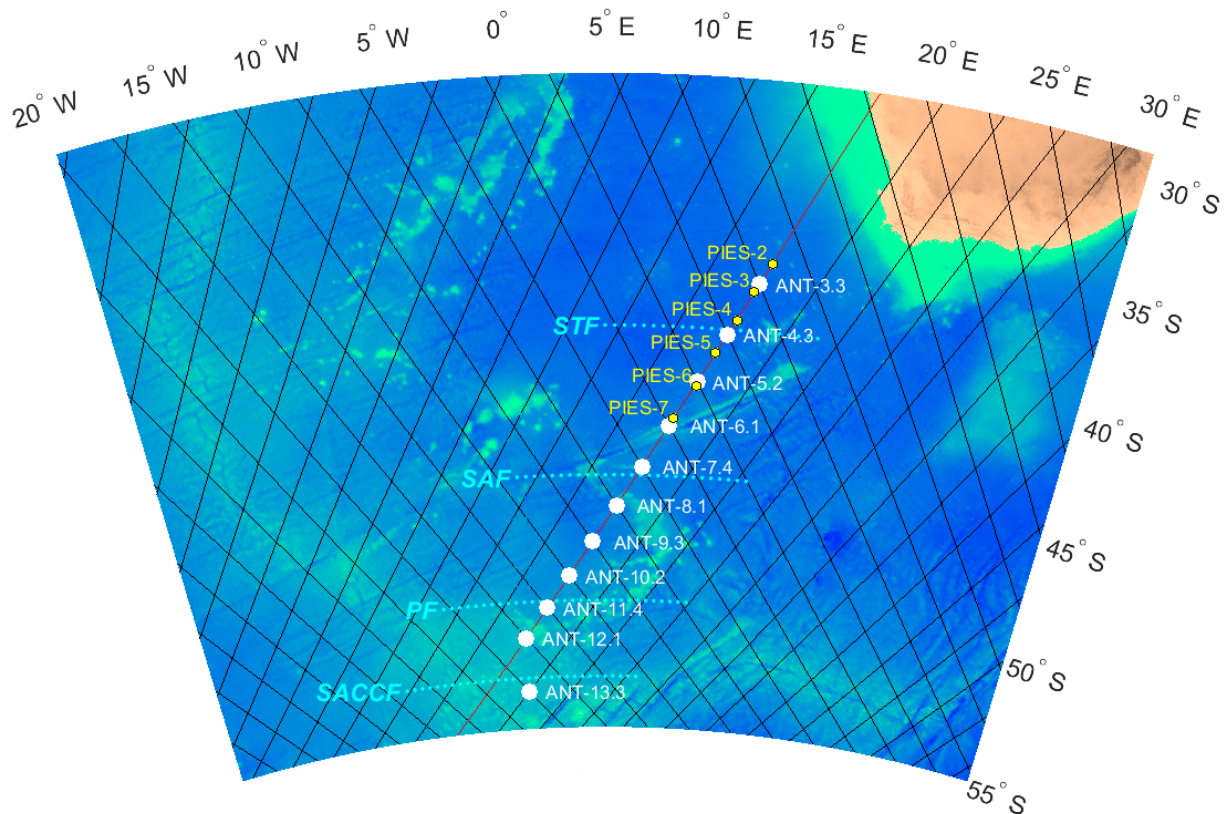


Fig. 3.24: Location of PIES composing the GoodHope array (white dots) including Jason satellite ground tracks (black lines, track 133 marked red) and climatologic locations of major ocean fronts (cyan dots).

#### Preliminary results

The PIES were opened after recovery and their memory cards were removed for the data to be downloaded and saved to local computers. Communication was established via the internal interface and time stamps were read against shiptime (GPS) (*cf.* Tab. 3.20). PIES data was forwarded by email to Sabrina Speich and Thierry Terre and instruments packed for shipment to Bremerhaven.

#### Data management

Metadata and data on the recovered instruments will be published through the SAMOC international initiative data base ([https://www.aoml.noaa.gov/phod/SAMOC\\_international/samoc\\_data.php](https://www.aoml.noaa.gov/phod/SAMOC_international/samoc_data.php)).

#### References

- Fahrbach E (2011) The Expedition of the Research Vessel "Polarstern" to the Antarctic in 2010/11 (ANT-XXVII/2), *Berichte zur Polar- und Meeresforschung* (Reports on Polar and Marine Research), Bremerhaven, Alfred Wegener Institute for Polar and Marine Research, 634, 242 p. hdl:[10013/epic.38039](https://nbn-resolving.org/urn:nbn:de:hbz:5:1-63420-p0380-3).
- Boebel O (2015) The Expedition PS89 of the Research Vessel Polarstern to the Weddell Sea in 2014/2015, *Berichte zur Polar- und Meeresforschung = Reports on polar and marine research*, Bremerhaven, Alfred Wegener Institute for Polar and Marine Research, 689, 151 p. hdl:[10013/epic.45857](https://nbn-resolving.org/urn:nbn:de:hbz:5:1-68915-p0151-7).

## 4. IRON (FE) LIMITATION AND VIRUSES, PHYTOPLANKTON CAUGHT BETWEEN A ROCK AND A HARD PLACE (FEPHYRUS)

Rob Middag<sup>1</sup>, Erin Bertrand<sup>2</sup>, Indah Ardiningsih<sup>1</sup>,  
Charlotte Eich<sup>1</sup>, Mathijs van Manen<sup>1</sup>, Sven Ober<sup>1</sup>,  
Sharyn Ossebaar<sup>1</sup>, Sven Pont<sup>1</sup>, Hung-An Tian<sup>1</sup>,  
Not on board: Loes Gerringa<sup>1</sup>, Corina Brussaard<sup>1</sup>

<sup>1</sup>NIOZ

<sup>2</sup>Dalhousie University

**Grant No: AWI\_PS117\_02**

### **Outline and objectives**

The production of oceanic phytoplankton that form the base of the marine food web depends on the availability of sunlight and nutrients, typically nitrogen and phosphorus (and silicate for diatoms). The Southern Ocean, however, is an important high nutrient low chlorophyll (HNLC) area (Bruland et al., 2014; Moore et al., 2013), where iron (Fe) affects the amount of atmospheric CO<sub>2</sub> sequestered in deep ocean waters and ocean sediments via the biological pump (De La Rocha, 2007), with far reaching implications for global climate and the local ecosystem (Arrigo et al., 2008; Boyd and Ellwood, 2010; Moore et al., 2013). Yet, it is becoming increasingly clear that the situation is more complex, and controlled by factors beyond just the scarcity of Fe. New insights highlight the importance of other trace-metals (Morel et al., 2014), co-limitation by two or more nutrients (Arrigo, 2005; Middag et al., 2013; Middag et al., 2011; Saito et al., 2008; Bertrand et al 2007) and variability in nutrient requirements between species and environmental conditions (Arrigo and van Dijken, 2003; Klunder et al., 2014; Moore et al., 2013). Notably for Fe, its solubility and probably also its availability depends strongly on the Fe-binding dissolved organic ligands (Boye et al., 2005; Croot et al., 2004; Hassler et al., 2011; Maldonado et al., 2005; Thuróczy et al., 2010, 2011, 2012). Microbial community composition as well as microbial and viral interactions impact the production and cycling of metals and metal-binding ligands (Bonnain et al., 2016; Slagter et al., 2016).

Viruses are found in high numbers in the world's oceans, including polar seas (Evans and Brussaard, 2012; Marchant et al., 2000). They infect mostly the numerically dominant microorganisms (bacteria and phytoplankton). Viral activity results in lysis of the host cells, thereby converting particulate organic carbon into dissolved and colloidal organic carbon (Brussaard et al., 2008; Lønborg et al., 2013). Through cell lysis of the host, viruses do not only affect host community composition and the flow of energy and matter away from higher trophic levels, but also play a crucial role in nutrient cycling in general (Gobler et al., 1997; Wilhelm and Suttle, 1999). Viral activity seems to play a key role in recycling organically complexed Fe (Mioni et al., 2005; Poorvin et al., 2004; Poorvin et al., 2011). Virally-induced mortality rates of phytoplankton can be measured in the field concomitantly with grazing rates, allowing optimal interpretation of the absolute and relative importance of viral lysis (Mojica et al., 2016). In a recent study, viral lysis rates of different phytoplankton groups have been found to be equally sensitive to viral infection and cell lysis as to grazing (Mojica et al., 2016). Viral lysis of Antarctic microbes contributes to the dissolved organic matter pool (Brum et al., 2016; Evans and Brussaard, 2012), thereby serving a key role in the production of ligands. However, the

role of viral lysis in driving Fe bioavailability remains poorly constrained, and the impact of global change on these processes remains difficult to predict.

The Antarctic undergoes rapid changes in physiochemical variables due to global climate change, including warming and altered Fe input (Alderkamp et al., 2012; De Jong et al., 2015; Gerringa et al., 2012; Joughin et al., 2014; Rignot et al., 2014). This will reflect in a changing phytoplankton community as not all phytoplankton species are equally sensitive to change or able to withstand changing conditions (Alderkamp et al., 2012; Arrigo, 2005; Arrigo et al., 2012; Mills et al., 2012). Additionally, the metal requirements change depending on the environmental conditions. For example, a reduction in Fe demand at higher temperatures (Sunda and Huntsman, 2011) could be explained by higher specific activity of major Fe-containing enzymes at elevated temperatures (John et al., 2002). If the response to Fe addition is not independent of temperature this could have significant implications for future projections of primary productivity in the face of global change, as current modelling assumes changes in Fe and temperature independently, not interactively, alter phytoplankton growth (Laufkötter et al., 2015).

Currently, much is still unknown about the sources of Fe and other bio-active metals to the Antarctic ecosystem. Antarctic glaciers and ice sheets are a relatively unquantified source of Fe and other metals that can fuel phytoplankton blooms (De Jong et al., 2015; Gerringa et al., 2012; Wadham et al., 2013). These glaciers and ice sheets are rapidly melting (Joughin et al., 2014; Rignot et al., 2014), potentially increasing this source (Alderkamp et al., 2012). Furthermore, little is known about the spatial extent of Fe fertilisation via Antarctic ice or the delivery of other metals from this source as the largest fraction of metals is delivered in the particulate phase and will quickly settle to the seafloor unless it can be solubilised and stabilised by organic ligands (Buck and Bruland, 2007). Moreover, other sources such as upwelling and the continental margin cannot be ignored either (De Jong et al., 2015; Gerringa et al., 2015; Middag et al., 2013; Middag et al., 2012). After entry and solubilisation into the ocean, the fate of Fe depends on the presence of ligands and the cycling through the microbial community. We are only just starting to understand how the cycling of Fe is affected by microbial actions, and in turn affects phytoplankton growth. A closer look at sources of Fe, Fe-binding ligands and the interaction with the microbial community under changing conditions is critical.

In awareness of the importance of (i) Fe as limiting nutrient for primary production in the Southern Ocean, (ii) ligands for increased availability of Fe for phytoplankton, and (iii) viral lysis as source of ligands, during this expedition we take a thus far rare synergetic approach by combining different disciplines to correlate composition, activity and losses of the phytoplankton community with Fe and ligand concentrations along a natural Fe gradient from the open Weddell Sea to the Antarctic Peninsula. Moreover, shipboard bio-assays are used to manipulate the conditions under which the microbial community grows and the natural iron gradient in the Weddell Sea will be contrasted with the transect from the Lazarev Sea to the Antarctic continent where we previously did not observe an Fe gradient.

Our proposed study addresses four key questions:

- (i) What is the relative contribution of the different sources of iron and the bio-essential metals along a transect from the Weddell Sea and Lazarev Sea to the Antarctic Peninsula and Antarctic continent?
- (ii) Is viral lysis affected by the natural iron concentrations along gradients of iron and does viral lysis affect the ligand production and nature of organic ligands?
- (iii) What is the effect of increasing temperature on metal quotas for phytoplankton, viral lysis and ligand production?

(iv) How do expression patterns of iron-requiring proteins and iron acquisition proteins change across the transect/ across trace metal gradients?

In addition to the station sampling, we performed multiple 'bioassay' experiments with temperature-controlled incubators. Our main experiments examined the combined influence of iron limitation and temperature on microbial community composition, physiology and activity or combined influence of manganese and iron on community activity.

#### 4.1 Titan, CTD sampling system for trace metals

Titan is the NIOZ facility for obtaining CTD data as well as samples for trace element analyses without contaminating the samples. A new sampler system "TITAN" was developed at NIOZ in 2005 allowing efficient sampling of seawater under ultraclean conditions (de Baar et al., 2008). It consists of a rectangular shaped all titanium frame which is fitted with a CTD system in a titanium housing and 24 Pristine samplers (Rijkenberg et al., 2015). After recovery, the complete TITAN frame is immediately placed inside a clean-air laboratory unit for sub-sampling and remains there until its next deployment.

##### Work at sea

From the start, unexpected problems were encountered with the Titan system. Testing in the container, the pressure-sensor produced a pressure of 8 dbar instead of the typical deck pressure reading of "zero". Test with the deck-unit SBE-11 gave a much better value: -0.3 dbar.

We prepared the system and programmed the SBE17 for the first cast. During this first cast the fluorometer flooded. This fluorometer, a Cyclops-7 from Turner Designs was installed the previous year for an expedition on the *Araon* where the maximum working depth was 1,000 m. However, it appears the depth range for this sensor was most likely only 600 m rather than the assumed 6,000 m. The short caused by the seawater prevented sample acquisition and all the bottles came up open. A shortcut should normally be a small problem. A fuse in the SBE17 was blown but apparently not fast enough, because after replacing the fuse not all of the functionality returned. This is a strange situation, because a shortcut may never cause such damage in one of the central units. We had no spare for this SBE17, but we could borrow a unit from NOC, Southampton, UK and this unit could be flown in at polar-station *Neumayer III*. In the meantime, we tried to repair the SBE17.

We consulted Seabird who came with the advice to use individual commands instead of using the wizard functionality in the software. This helped a lot. After a while we found out the command Bottom Bottle Closure Enabled did not work anymore and we could not produce ROS files so we had to produce bottle-files manually. Actually 95 % of the functionality was back and we could close bottles. Producing bottle-files manually was time consuming, but we could carry out the sampling program and have CTD-files.

After a few casts a new problem popped up. After programming the SBE17, we waited to switch on the CTD with the plunger till just before deployment. A few deck-measurements are OK, but sometimes it took 30 minutes before the frame could be deployed. The CTD started, but during the downcast it started with logging only nonsense. It logged, in raw format, only FFFFFFFF etc. Each cast the CTD started to measure correctly after a while being at e.g. 600 to 2,600 m depth. The problem with the FFFFFF-recordings returned when the frame was on deck again just before we switched off the CTD (but not always). The work-around we found was a short cast in the container (say 10 seconds of data). We could check the deck-pressure

and after this was more or less OK we started the CTD in the container just before launching the CTD. This “technique” was inspired by the observation that the problem never showed up when starting the CTD in the container. For unknown reasons the described problem never showed up again.

We have mounted an acoustic modem from Develogic as a replacement-communication-channel on the frame in order to be able to read out several sensors at low speed. The altimeter was especially important because we wanted to acquire samples close to the seafloor. This did not work as hoped. In the beginning of the expedition we could communicate with the frame down to 600 m (and the contact returned during the upcast at 250 m), but deeper than that the contact was lost, potentially due to background noise from the ship. We decided to leave the acoustic modem in the frame, because it logged all the CTD data in the background and that was useful because we were having troubles with the other logger, the SBE17. After some time, we could not communicate with the Develogic modem anymore under water, why is unclear. Batteries were not down. We had replaced the batteries shortly before this and the communication during the cast after was as described above. Moreover, testing in the container went flawlessly. Maybe a sound source of the ship was switched on jeopardizing our contact, but we could not find anything.

A way of localising the Titan system was realized with an IXSEA acoustic release with a pressure-sensor. We brought specially made brackets from NIOZ so we could mount the release properly. Communication was done via the Posidonia acoustic system mounted underneath *Polarstern*. This worked surprisingly well. Near the seafloor sometimes the contact was not optimal, but it was good enough.

The electronics of the winch worked quite well in the beginning of the expedition, although we had doubts about the measurement of the cable paid out. It measured 1 to 2 % more than it actually realized. On one occasion this measurement system stopped working anymore due to a defective sensor. The crew repaired this, but from that moment there were small remaining problems. On one occasion, the winch-driver thought, based on the read-out, that the frame was at 60 m depth, but all of a sudden the frame came through the surface. An emergency-stop saved the frame from loss. To prevent this from reoccurring, we placed warning tapes at the rope at 100 m (general early warning), 45 m and 20 m (stops needed for closing more than 1 one bottle. This low-tech solution worked perfectly until the end of the expedition.

A comparison with the CTD from AWI showed a dramatic difference in salinity, as did the comparison between the up and down cast from the Titan system. Temperature was good so the conductivity-sensor was suspect. We realized that it was also possible that the acoustic equipment was causing trouble. We could imagine a grounding-problem, for example. To test, we disconnected the modem, carried out a deep cast and did the salinity-comparison again, but there was no improvement. The Develogic-equipment was not causing the observed trouble.

Based on the experience with the pressure-sensor, the conductivity-sensor, the start-up problems and the disappointing functionality of the Develogic modem we decided to exchange the SBE9+ (modified for use of the acoustic modem), the SBE4 conductivity sensor and the interconnecting cable between SBE4 and SBE9+. This had positive results. After the first cast with the new set it appeared to be possible to produce .ROS files and therefore real bottle-files. We can conclude that the problem with the .ROS files was located in the SBE9+ and not as we expected in the SBE17. Whether the current pulse of the shortcut caused this problem or that something during the modification of the SBE9+ just prior to the expedition went wrong we don't know. After the expedition we will send both units to Seabird GmbH for analysis.

Having 'real' bottle-files available we discovered a new problem: below the pressure that enables an upcast (BUP-command) the SBE17 does not detect the difference between up- and downcast. As soon as a programmed pressure was reached the SBE17 closed a bottle. That means that the SBE17 started with closing bottles during the downcast. We set the BUP-pressure always quit high so we had to reject only a few deeper bottles. These rejections were carried out after confirmation by nutrient analyses.

The problem with the pressure sensor did not show up again after exchanging the SBE9+. Just before and just after a cast the pressure measured on deck was around zero, with the usual spread of around 1 to 2 dbar.

During the visit at *Neumayer III* we got the spare SBE17 from NOC. After exchanging the unit and testing in the container with the pressure-generator we discovered a new problem. The Bottom Bottle Closure Enabled command did not work on the NOC-unit too. At first this was a complete mystery. The only cause we could think of was that the programming-software on the dedicated UCC-laptop was corrupt and then only for this command. We had a second laptop with this software installed and we repeated the test programming the SBE17 with the second laptop. This test worked out as hoped, confirming the fact that the programming software on the UCC-laptop was corrupt. Very strange, because this laptop worked very well during the expedition on board RV Aaron last winter and has not been used since. The installation-files were still on the computer and we re-installed the programming-software. Everything worked perfectly now and the Bottom Bottle Closure Enabled command worked as expected and gave us some more control over the closure of the deepest bottle.

After the Neumayer visit, we had to wait for a deep station for the check of the conductivity-sensor. For a first check, we mounted a second TC-set in the frame, temporary sacrificing the duct of the DO-sensor. An AWI-cast to the bottom and an UCC cast to 2000 m on the same position confirmed that the new combination SBE9+ and SBE4 was working well. Difference in salinity was on average 0.0019 and is acceptable.

From the deepest bottle of the UCC, 2 salinity-samples were drawn. The difference between the salinity of the bottles and the salinity of the primary TC-sensor-set was in the order of 0.001. The difference between the primary and the secondary sensor-set was about 0.006. That is more than expected but good enough to use it to check the performance of the primary sensor-set.

All of a sudden the FFFF-problem that we had before re-appeared again, but now in a way that learned us something. The CTD started with FFFFFFFF, than it worked a few moments normally, after that FFFF again and after a few seconds the CTD worked normally again until we stopped it with the plunger. This looks like a problem in the Reed-relais in the plunger. It switches the CTD on and off by itself probably due the vibrations during horizontal transport. The orientation the SBE17 (horizontal) make this switch vulnerable for vibrations.

After a while the same problems as we had with our own SBE17, not closing bottles or closing bottles during the downcast, popped up with the NOC unit. What happened was totally unclear. Re-installing the programming software, that helped us with our own unit did not solve the problem and simulated casts in the container with a pressure generator were successful, unlike actual deployments. Using the second computer did not help either. We found a work around by disabling the Bottom Bottle Closure Command, using Pressure To Enable Upcast and setting the Closure Pressure of the deepest bottle just a little shallower. This way we could get a bottle closed reasonably close to the seafloor at most casts, but this was depending on our ability to estimate the actual depth using the echo sounder.

### Preliminary Results

On board, the CTD-data was preliminary processed. Due to the encountered technical problems this was not easy. The start-up problems of the CTD (FFFFF at the start of the file which has to be removed by hand with a special ASCII-editor) and the production of “pseudo-bottle files” was very time-consuming. From one file (station 16) only the downcast could be repaired. The file was too corrupt to pass all the stages of the Seabird data-processing-protocol. Later another attempt will be carried out. The data-processing-protocol consists of, beside conversion to engineering-units, a correction for the thermal mass of the C-sensor, standard low-pass filtering, loop-correction and a correction for timing due to the delays in the duct-system. This protocol is clearly described in the SBE-data-processing manual. After exchanging the SBE9+ we were able to produce “real” bottle-files instead of “pseudo”-bottle-files.

The data consists of all measured parameters (pressure, temperature, conductivity, dissolved oxygen, fluoresce and PAR) in engineering units and the most usual derived parameters as depth, salinity, density, sigma-theta and potential temperature. An example is presented in the following graph (Fig. 4.1).

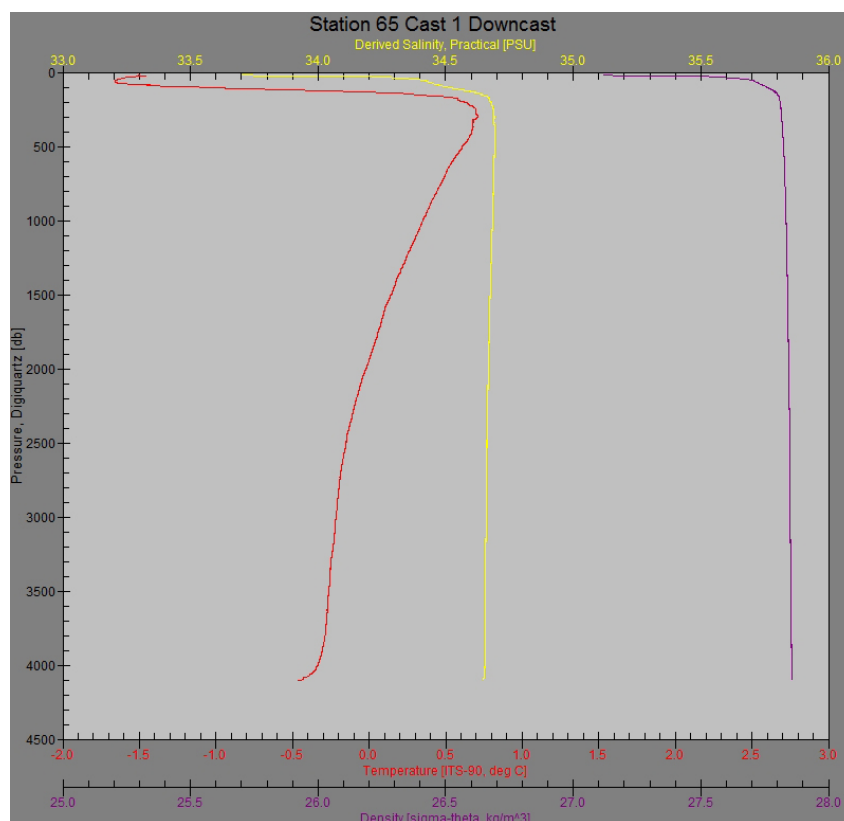


Fig. 4.1: CTD data at station 56 cast 1

### Data management

All the CTD-data, “raw” and (preliminary) processed will be placed on the ships-network. At NIOZ all the technical problems will be discussed with Seabird in order to judge the data-quality. After that the data will be processed until the status “Final” has been reached. The data is then available for the different databases as PANGAEA, GEOTRACES and NIOZ

## 4.2 Nutrients

At all AWI CTD and trace metal stations and during four bio-assays, samples were collected for shipboard macronutrient determination. The macronutrient measurements were made simultaneously on four channels for Phosphate Silicate, Nitrite, and Nitrate with Nitrite together, on a continuous gas-segmented flow TRAACS 800 Auto-Analyzer produced by Technicon (now known as SEAL Analytical). All measurements were calibrated with standards diluted in low nutrient seawater (LNSW) in the salinity range of the stations of the Southern Ocean waters at approximately 35 ‰ to ensure that analysis remained within the same ionic strength.

### Work at sea

Sample water was obtained from the Niskin bottles of the AWI CTD and from the Ultra-Clean 'Titan' CTD (UCC) from all depths (Tab. 4.1). All samples were collected in high-density polyethylene syringes (Terumo®) with a three way valve directly after the oxygen and TCO<sub>2</sub> sampling if sampled. Samples from the four bioassays were collected in 125 ml polypropylene bottles, drawn into a 20 ml syringe and filtered over a 0.2 µm Acrodisc® filter. In the lab container, the nutrient samples were transferred into 5 ml polyethylene vials (ponyvials) after rinsing three times with the sample before being capped and stored in the refrigerator at 4 °C when needed. All analyses were generally made within 4-5 hours of sampling and very occasionally up to a maximum of 15 hours later. Calibration standards were diluted from stock solutions of the different nutrients in 0.2 µm filtered low nutrient seawater (LNSW) and were freshly prepared every day. The LNSW is surface seawater depleted of most nutrients; it is also used as baseline water for the analysis between the samples. Each run of the system had a correlation coefficient of at least 0.9999 for 10 calibration points, but typically 1.0000 for linear chemistry was achieved. The samples were measured from the lowest to the highest concentration in order to keep carry-over effects as small as possible, i.e. from surface to deep waters. Prior to analysis, all samples and standards were brought to lab temperature of 21-21.5°C in about two hours in a dark draw. The caps were then removed and the ponyvials covered with parafilm against evaporation and placed in the sampler. Concentrations were recorded in µmol per liter (µmol/L) at this temperature. During every run a daily freshly diluted mixed nutrient standard, containing silicate, phosphate and nitrate (a so-called nutrient cocktail), was measured in quadruplicate. Additionally, a natural sterilized Reference Material Nutrient Sample (CRM) from Kanzo, Japan, containing known concentrations of silicate, phosphate, nitrate and nitrite in Pacific Ocean water, was analyzed in triplicate in every run, apart from the first 7 analytical runs of the expedition. The cocktail and the CRM were both used to monitor the performance of the analyzer. From every station the deepest sample bottle was sub-sampled for nutrients in duplicate, the duplicate sample-vials were all stored dark at 4 °C, and measured again in the next run with the upcoming stations, this being for statistical purposes. In total 1933 samples were analyzed for phosphate, silicate, nitrate and nitrite, of which 1487 at CTD/UCC stations. Furthermore, 396 samples were analyzed in support of the biological work of Bertrand et al (see section 4.1.4.) and 39 ice core samples were analysed for the ice work of Castellani et al..

**Tab. 4.1:** All stations and bioassays analysed for nutrients

Station No. - Cast No.	Type	No. Samples	Project
1-1	CTD	24	AWI-OZE
2-1	CTD	24	AWI-OZE
4-1	CTD	24	AWI-OZE
5-1	CTD	24	AWI-OZE
6-3	CTD	24	AWI-OZE
7-1	CTD	24	AWI-OZE

#### 4.2 Nutrients

Station No. - Cast No.	Type	No. Samples	Project
13-2	CTD	24	AWI-OZE
14-1	CTD	24	AWI-OZE
14-4	UCC	24	FEPHYRUS
15-1	CTD	24	AWI-OZE
16-1	UCC	24	FEPHYRUS
17-1	UCC	3	FEPHYRUS BA1 T=0
18-2	CTD	24	AWI-OZE
18-3	UCC	23	FEPHYRUS
19-1	CTD	24	AWI-OZE
19-3	CTD	1	COMBIBAC
20-1	UCC	24	FEPHYRUS
21-1	CTD	24	AWI-OZE
22-1	CTD	24	AWI-OZE
22-4	UCC	24	FEPHYRUS
25-1	UCC	21	FEPHYRUS
26-1	CTD	24	AWI-OZE
27-1	UCC	24	FEPHYRUS
28-1	CTD	24	AWI-OZE
29-1	CTD	24	AWI-OZE
30-1	CTD	13	AWI-OZE
30-2	UCC	24	FEPHYRUS
31-1	CTD	24	AWI-OZE
33-6	CTD	24	AWI-OZE
34-2	CTD	24	AWI-OZE
34-3	UCC	22	FEPHYRUS
35-6	CTD	24	AWI-OZE
36-1	UCC	4	FEPHYRUS BA2 T=0
38-1	UCC	24	FEPHYRUS
41-1	CTD	24	AWI-OZE
41-4	UCC	14	FEPHYRUS
41-6	CTD	14	AWI-OZE
41-8	UCC	14	FEPHYRUS
41-9	CTD	14	AWI-OZE
41-10	UCC	16	FEPHYRUS
41-12	CTD	14	AWI-OZE
41-13	UCC	17	FEPHYRUS
53-2	UCC	4	FEPHYRUS BA3 T=0
53-4	CTD	24	AWI-OZE
54-3	CTD	24	AWI-OZE
56-1	UCC	24	FEPHYRUS
56-2	CTD	24	AWI-OZE
57-6	CTD	24	AWI-OZE
61-1	UCC	20	FEPHYRUS

**4. Iron Limitation and Viruses, Phytoplankton Caught between a Rock and a Hard Place**

Station No. - Cast No.	Type	No. Samples	Project
62-1	CTD	24	AWI-OZE
63-1	CTD	24	AWI-OZE
64-4	CTD	24	AWI-OZE
65-1	UCC	21	FEPHYRUS
66-1	CTD	23	AWI-OZE
66-4	UCC	4	FEPHYRUS BA4 T=0
67-1	UCC	21	FEPHYRUS
68-2	CTD	24	AWI-OZE
69-1	CTD	21	AWI-OZE
70-1	UCC	20	FEPHYRUS
71-1	CTD	19	AWI-OZE
72-3	CTD	22	AWI-OZE
73-1	UCC	20	FEPHYRUS
74-1	CTD	17	AWI-OZE
75-1	UCC	21	FEPHYRUS
76-1	CTD	16	AWI-OZE
81-2	CTD	12	AWI-OZE
82-1	UCC	20	FEPHYRUS
83-1	CTD	13	AWI-OZE
85-1	UCC	21	FEPHYRUS
90-1	CTD	14	AWI-OZE
91-1	UCC	20	FEPHYRUS
92-1	CTD	12	AWI-OZE
93-1	UCC	19	FEPHYRUS
94-1	CTD	10	AWI-OZE
95-1	UCC	19	FEPHYRUS
99-3	CTD	11	AWI-OZE
BIOASSAY1	T=2	12	FEPHYRUS
BIOASSAY1	T=4	12	FEPHYRUS
BIOASSAY1	T=6	12	FEPHYRUS
BIOASSAY1	T=8	12	FEPHYRUS
BIOASSAY2	T=2	12	FEPHYRUS
BIOASSAY2	T=4	12	FEPHYRUS
BIOASSAY2	T=6	12	FEPHYRUS
BIOASSAY2	T=8	12	FEPHYRUS
BIOASSAY3	T=2	12	FEPHYRUS
BIOASSAY3	T=4	12	FEPHYRUS
BIOASSAY3	T=6	12	FEPHYRUS
BIOASSAY4	T=2	12	FEPHYRUS
BIOASSAY4	T=4	12	FEPHYRUS
BIOASSAY4	T=6	12	FEPHYRUS
Fe GRAD	T=2	39	FEPHYRUS

## 4.2 Nutrients

Station No. - Cast No.	Type	No. Samples	Project
Fe GRAD	T=4	39	FEPHYRUS
Fe GRAD	T=6	39	FEPHYRUS
Fe GRAD	T=8	39	FEPHYRUS
Fe GRAD Peninsula	T=Final	72	FEPHYRUS
ICE CORES		39	SIPES 2

### *Analytical Methods*

The following is a brief overview of the colorimetric methods used on the TrAAcs auto-analyzer:

Ortho-Phosphate ( $\text{PO}_4$ ) reacts with ammonium molybdate at pH 1.0 and potassium antimonyl tartrate is used as a catalyst. The yellow phosphate-molybdenum complex is reduced by ascorbic acid and forms a blue reduced molybdophosphate-complex which is measured at 880 nm (Murphy & Riley, 1962).

Silicate (Si) reacts with ammonium molybdate to a yellow complex and after reduction with ascorbic acid, the obtained blue silica-molybdenum complex is measured at 820 nm. Oxalic acid is added to prevent formation of the blue phosphate-molybdenum complex (Strickland & Parsons, 1968).

Nitrate plus Nitrite ( $\text{NO}_3 + \text{NO}_2$ ) is mixed with an imidazol buffer at pH 7.5 and reduced by a copperized cadmium column to Nitrite. The Nitrite is diazotated with sulphonylamide and naphthylethylene-diamine to a pink colored complex and measured at 550 nm. Nitrate is calculated by subtracting the Nitrite value measured on the Nitrite channel from the ' $\text{NO}_3 + \text{NO}_2$ ' value. (Grasshoff et al., 1983).

Nitrite ( $\text{NO}_2$ ) is diazotated with sulphonylamide and naphthylethylene-diamine to form a pink colored complex and measured at 550nm. (Grasshoff et al., 1983).

### *Calibration and Standards*

Nutrient primary stock standards were prepared at the NIOZ as follows:

Ortho-Phosphate ( $\text{PO}_4$ ): by weighing Potassium dihydrogen phosphate in a calibrated volumetric PP flask to make 1 mM  $\text{PO}_4$  stock solution.

Silicate: by weighing  $\text{Na}_2\text{SiF}_6$  in a calibrated volumetric PP flask to 19.84 mM Si stock solution.

Nitrate ( $\text{NO}_3$ ): by weighing Potassium nitrate in a calibrated volumetric PP flask set to make a 10mM  $\text{NO}_3$  stock solution.

Nitrite ( $\text{NO}_2$ ): by weighing Sodium nitrite in a calibrated volumetric PP flask set to make a 0.5mM  $\text{NO}_2$  stock solution.

All standards were stored at room temperature in a 100 % humidified box. The calibration standards were prepared daily by diluting the separate stock standards, using three electronic pipettes, into four 100 ml PP volumetric flasks (calibrated at the NIOZ) filled with diluted LNSW. The blank values of the diluted LNSW were measured onboard and added to the calibration values to get the absolute nutrient values.

### **Preliminary results**

The following figures (Fig. 4.2, Fig. 4.3 and Fig. 4.4) are some of the nutrient data from the zero meridian transect ( $0^\circ 0' \text{ E}$ ) from the AWI CTD stations giving an example of the nutrient data in this southern region.

#### 4. Iron Limitation and Viruses, Phytoplankton Caught between a Rock and a Hard Place

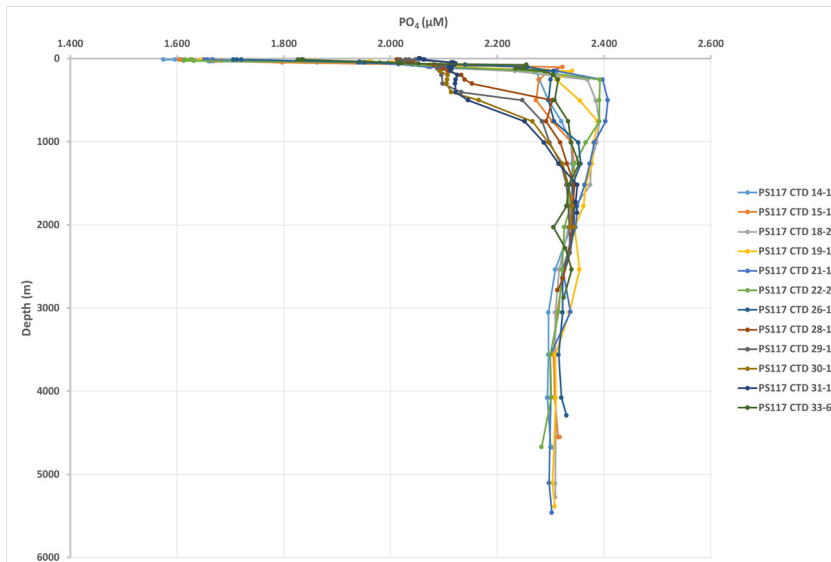


Fig. 4.2: Dissolved  $PO_4$  ( $\mu M$ ) data from the zero meridian transect

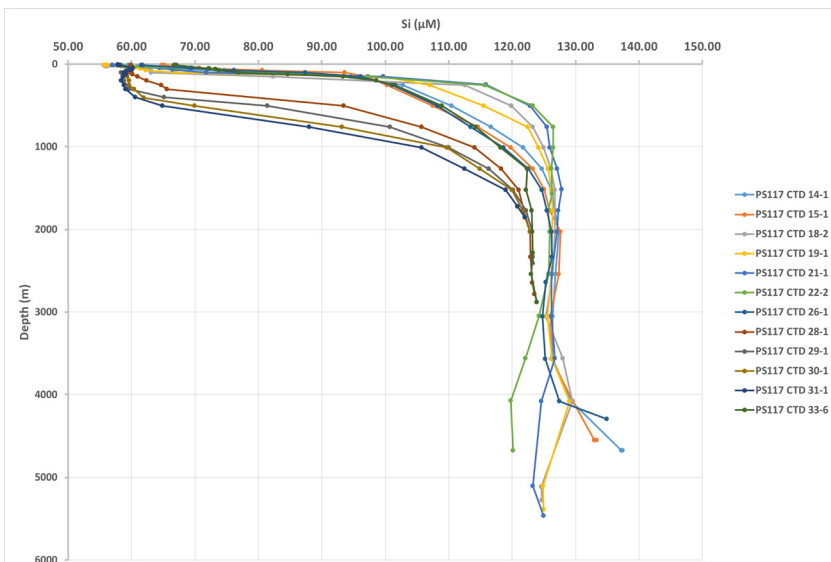


Fig. 4.3: Dissolved  $PO_4$  ( $\mu M$ ) data from the zero meridian transect

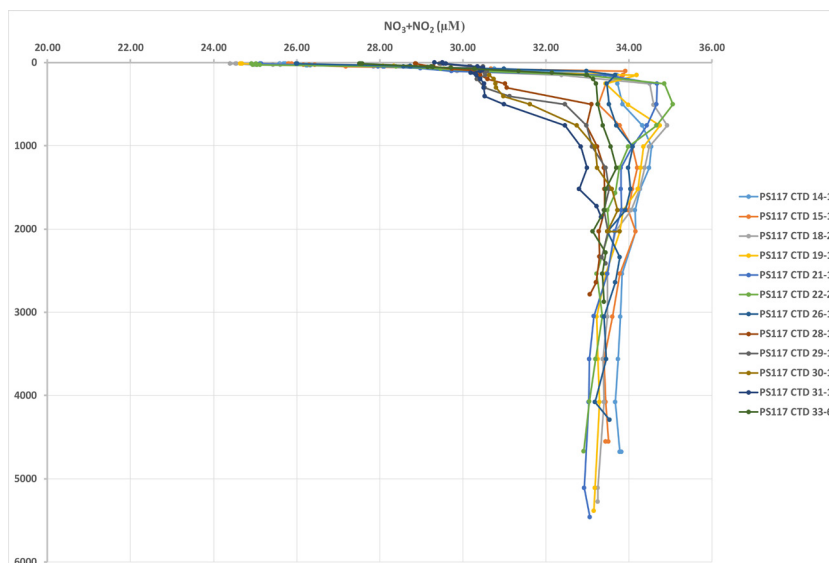


Fig. 4.4: Dissolved  $Si$  ( $\mu M$ ) data from the zero meridian transect

**Data management**

Our standards are continuously being monitored by participating in inter-calibration exercises organised by external organisations such as ICES and Quasimeme and since 2006, the inter-comparison exercise organised by MRI, Japan.

To gain some accuracy, the NIOZ made a ‘Cocktail’ standard which contains PO<sub>4</sub>, NO<sub>3</sub> and Si to monitor the performance of the analyzer throughout the expedition. The following values were obtained from the cocktail which was diluted 100 times in a calibrated PP volumetric flask, being measured in quadruplicate in every analytical run (Tab. 4.2).

**Tab. 4.2:** Cocktail characteristics

	Average value	±STDEV	N	Dilution Factor
Cocktail-1018				
PO4	2.395 µM	0.014	256	100
Si	128.37 µM	0.662	256	100
NO3+NO2	34.59 µM	0.231	256	100

The cocktail measurements showed that there were no trends observed, thus concluding that the calibration standards were stable during the expedition.

Note added post expedition (13 March 2019): After the PS117 cruise, it was decided to correct all of the nutrient data according to the NIOZ internal lab standard (ANT Cocktail 1018) that was analyzed in every analysis while onboard and therefore improve the data comparability between all the analyses/runs. The data was unable to be corrected while onboard as the internal lab standard was a new batch and its value was unknown as it hadn't previously been measured. The value that has now been assigned to the internal lab standard is the average value of all the measurements that were analyzed on board PS117 for PO<sub>4</sub>, Si and NO<sub>3</sub>. The changes in the PO<sub>4</sub>, Si and NO<sub>3</sub> data are typically very minor, however, for the best and most comparable data, these corrections are desirable.

*Mean Detection Limits*

The method detection limit was calculated during the expedition using the standard deviation of ten samples containing 2 % of the highest standard used for the calibration curve and multiplied with the student's value for n=10, thus being 2.82.(M.D.L = Standard Deviation of 10 samples x 2.82) (Tab. 4.3).

**Tab. 4.3:** Detection limits

		µM/L	Used measuring ranges µM/L	
PO4		0.005		3.505
Si		0.009		158.80
NO3+NO2	0.007		45.505	
NO2		0.002		0.500

#### 4. Iron Limitation and Viruses, Phytoplankton Caught between a Rock and a Hard Place

##### Precision at different concentration levels

Standards of three different concentrations were each measured ten times to calculate the precision of a specific concentration level. Concentration level in  $\mu\text{M/l}$  with the respective standard deviation of that concentration (Tab. 4.4).

**Tab. 4.4:** Precision

	Conc. $\mu\text{M/L}$	$\pm\text{STDEV}$	Conc. $\mu\text{M/L}$	$\pm\text{STDEV}$	Conc. $\mu\text{M/L}$	$\pm\text{STDEV}$
PO4	0.75	0.011	1.5	0.009	2.5	0.007
Si	30	0.037	60	0.057	120	0.307
NO3	7.5	0.013	15	0.022	30	0.041
NO2	0.1	0.003	0.2	0.003	0.35	0.003

##### Obtained CRM values

The average value (n=196) of measurements of CRM "CA" at 21.5°C are given in Tab. 4.5.

**Tab. 4.5:** CRM "CA" at 21.5°C

	$\mu\text{M/L}$	$\pm\text{STDEV}$	converted to $\mu\text{M/kg}$	assigned KANSO in $\mu\text{M/kg}$ :
CA				
PO4	1.458	$\pm 0.008$	1.424	1.407
Si	36.899	$\pm 0.172$	26.038	36.58
NO3	20.148	$\pm 0.072$	19.678	19.66
NO2	0.076	$\pm 0.002$	0.074	0.063

The average value (n=68) of measurements of CRM "CC" at 21.5°C are given in Tab. 4.6.

**Tab. 4.6:** CRM "CC" at 21.5°C

	$\mu\text{M/L}$	$\pm\text{STDEV}$	converted to $\mu\text{M/kg}$	assigned KANSO in $\mu\text{M/kg}$ :
CC				
PO4	2.154	$\pm 0.010$	2.104	2.080
Si	86.60	$\pm 0.367$	86.58	86.16
NO3	31.77	$\pm 0.125$	31.03	30.88
NO2	0.134	$\pm 0.002$	0.131	0.116

The CRM values obtained are in equitable agreement with the assigned values, therefore no post expedition adjustments are needed.

After finalization of the data processing, the data will be submitted to data centers, as has been done with all data of previous expeditions with FS *Polarstern*. All raw data will be stored on the NIOZ-server for secured back-up and is available to collaborators upon completion. After suitable quality control, the nutrient data and metadata will be submitted to the National Polar Data Centre (<http://www.npdc.nl/>) which is linked to other international databases.

### 4.3 Trace metal sampling and analysis

At all 23 trace metal stations and during four bio-assays, samples were collected for shipboard dissolved iron determination, total dissolvable metals (unfiltered water) and dissolved metals (0.2 µm filtered). At 23 stations samples for particulate metals and particulate carbon and nitrogen were collected at a maximum of 12 depths. Additionally, samples were collected for Particulate organic carbon (POC) and nitrogen (PON), iron binding ligands, ligand characterisation and particulate metals at most stations (Tab. 4.7).

**Tab. 4.7:** Locations and maximum depths for the 23 stations sampled with the Ultra Clean CTD

Station	Longitude	Latitude	Day	Month	Year	Max Depth [m]
14	00 00.00 E	66 30.00 S	26	12	2018	500
16	00 00.00 E	66 00.00 S	27	12	2018	3500
18	00 00.84 E	64 00.49 S	28	12	2018	5150
20	00 00.0 E	62 00.00 S	30	12	2018	5150
22	00 06.43 E	59 03.03 S	31	12	2018	4600
25	00 00.00 E	68 00.00 S	2	1	2019	4500
27	00 09.06 E	69 05.82 S	3	1	2019	3400
30	00 09.00 E	69 22.00 S	4	1	2019	2050
34	00 09.06 W	69 05.82 S	6	1	2019	5000
38	10 51.49 W	70 10.65 S	10	1	2019	2100
41	08 49.44 E	70 31.20 S	11	1	2019	175
56	36 25.32 W	65 37.23 S	23	1	2019	2100
61	45 50.73 W	64 24.59 S	26	1	2019	2800
65	47 57.91 W	64 08.05 S	27	1	2019	3400
67	48 51.07 W	63 59.24 S	28	1	2019	3400
70	49 51.47 W	63 48.96 S	29	1	2019	2900
73	51 04.31 W	63 36.98 S	30	1	2019	2300
75	51 30.08 W	63 32.37 S	30	1	2019	1855
82	52 09.33 W	63 25.70 S	31	1	2019	805
85	51 44.03 W	63 29.83 S	31	1	2019	1410
91	52 51.31 W	63 20.078 S	31	1	2019	419
93	53 24.32 W	63 15.34 S	31	1	2019	375
95	54 31.48 W	63 05.27 S	2	1	2019	460

#### Work at sea and preliminary results or work to be done in the home lab

##### *Dissolved and total dissolvable metals*

For dissolved metals, samples were filtered over a 0.2 µm PES Acropak filter under 0.5 bar inline filtered nitrogen pressure directly from the Pristine polypropylene samples. Samples for total dissolvable metals were collected unfiltered. Sample were acidified to 0.024 M HCl with Seastar Baseline acid. Samples will be transported back to the shore based laboratory for Multi-Element (ME) determination that will give the concentrations of Cd, Co, Cu, Fe, Mn, Ni, Zn, Ti, Y, La, Pb and Ga. This will be done using a SeaFAST system and a High Resolution Sector Field Inductively Coupled Plasma Mass Spectrometer (HR-ICP-MS). The seaFAST

pico system is an ultra-clean, in-line, automated, low-pressure ion chromatography system that utilises a three-step process in order to pre-concentrate an acidified seawater sample. The seaFAST system takes up a 20 ml volume of acidified seawater (0.024 M HCl) into a sample loop using a vacuum and subsequently transports the sample over a chelating resin (Nobias PA1) using a syringe pump. Directly before the sample is passed over the resin, it is mixed with an ammonium acetate buffer (~pH 6.2), to raise the pH of the acidified seawater sample to 5.8. At this pH, the trace metals of interest in the sample complex with the resin and are quantitatively removed from the seawater and its matrix. The second step in the pre-concentration is the resin wash with 'ultra pure' milliQ water. This second rinse aims to remove any loosely bound major constituent ions from the resin, such as Na<sup>+</sup>, Cl<sup>-</sup> and Ca<sup>2+</sup> and to flush the small amount of seawater present after pre-concentration out of the column. The third and final step in the pre-concentration of a sample is the elution of the trace metals from the resin. This is achieved by passing 0.5 ml of eluent acid (~1.7M HNO<sub>3</sub>), using a syringe pump, over the resin to elute the trace metals from the resin, resulting in a pre-concentration factor of 40. The eluate is deposited into a destination vial using N<sub>2</sub> gas as a carrier gas. Subsequently samples will be analysed on the Element 2 HR-ICP-MS at NIOZ.

##### *Dissolved Fe*

Dissolved iron (DFe) concentrations of 23 stations with a maximum of 20 depths were mostly measured directly on board by an automated Flow Injection Analysis (FIA) after a modified method of De Jong et al. (1998).

Filtered (0.2 µm) and acidified (pH 1.8, 1/L 12M Baseline grade Seastar HCl) seawater was concentrated on a column containing aminodiacetic acid (IDA). This material binds only transition metals and not the interfering salts. After washing the column with ultrapure water, the column is eluted with diluted hydrochloric acid. After mixing with luminol, peroxide and ammonium, the oxidation of luminol with peroxide is catalyzed by iron and a blue light is produced and detected with a photon counter. The amount of iron is calculated using a standard calibration line, where a known amount of iron is added to low iron containing seawater. Using this calibration line a number of counts per nM iron is obtained. Samples were analyzed in triplicate and average DFe concentrations and standard deviation are given.

Concentrations of DFe measured during PS117 ranged from 0.06 nM at the surface up to > 0.6 nM in the deep. The consistency of the FIA system over the course of the day was verified using a drift standard. Drift has been observed and seemed to be variable from day to day. The same drift standards measured day to day during this expedition are within 3 % deviation. A certified SAFe standard (Johnson et al., 2007) for the long term consistency and absolute accuracy was measured on a regular basis. The SAFe D1 standard of our measurement was  $0.65 \pm 0.01$  nM, consistent with the community consensus value of  $0.67 \pm 0.04$  nM (Johnson et al., 2007)

In the figure below (Fig. 4.5) three depth profiles of station 18 (open ocean), 27 (near sea ice) and 38 (closed to ice shelf) are depicted.

##### *Metal isotopes*

Due to the isotopic signatures caused by fractionation in different Fe sources, Fe isotopes have been used as a promising tool for identifying Fe sources and quantifying these sources during recent years (Conway et al., 2014). For this expedition, Fe isotopes were sampled to identify the dissolved Fe sources and quantify their contribution to the dissolved Fe pool in the Weddell Sea and nearby Southern Ocean. Besides, Zn and Cd isotopes will also be measured to investigate their sources and cyclings in this area. Metal isotopes samples were sampled

### 4.3 Trace metal sampling and analysis

at all stations and all depths. Due to anticipated low Fe concentration in surface water, 4 L filtered (0.2  $\mu\text{m}$ ) sea water was sampled for surface water (mostly shallower than 100 m), whereas 1 L filtered sea water was sampled for the remaining, deeper depths. These samples were acidified to pH  $\sim 1.8$  using ultrapure HCl (12M, Baseline grade Seastar HCl) on the ship after sampling and will be taken back to our shore based laboratory for further metal isotope analysis. In total, there were 389 Fe isotopes samples collected from 23 stations (12-20 for each station) during this expedition.

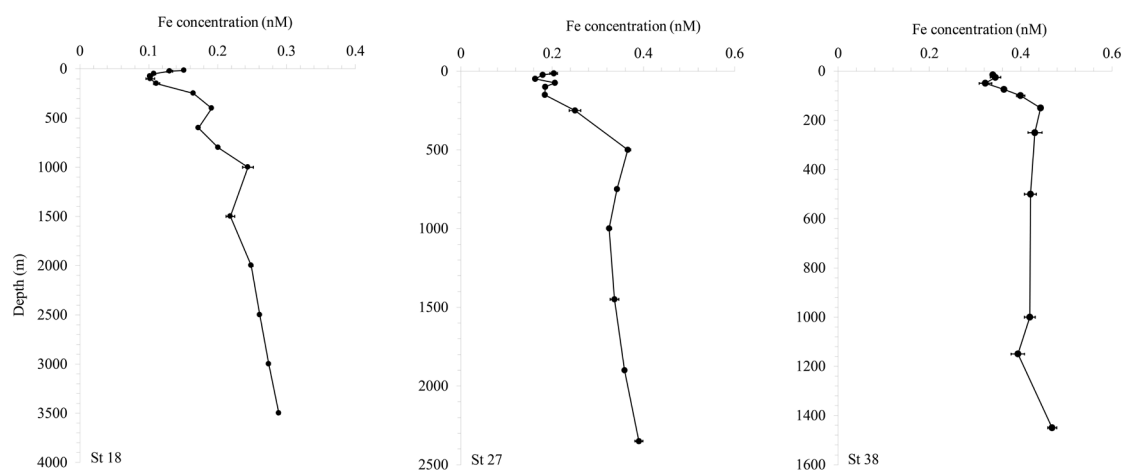


Fig. 4.5: Three depth profiles (station 18, 27 and 38) of dissolved iron. Error bars are presenting  $\pm 1$  standard deviation.

#### Iron binding ligands quantification

In the marine system, it is known that organic iron-binding ligands are essential for buffering Fe against hydrolysis and further precipitation (Liu & Millero, 2002). As reported, the majority (more than 99 %) of the dissolved iron in seawater is strongly bound to organic ligands (Boye et al., 2001; Gledhill & Buck, 2012; Thuróczy et al., 2011, 2012). However, despite their importance, limited information is available on the composition and characteristics of these compounds (Boiteau & Repeta, 2015), particularly in the Southern Ocean.

All samples for iron-binding ligands (FeL) quantification (0.2  $\mu\text{m}$  filtered) were taken from the Ultra Clean sampling system (UCC). At a total of 23 stations (Tab. 4.8) were sampled with a maximum of 12 depths per station. The FeL samples were also taken at the beginning (T0, 3 samples) and the end (TF, 12 samples) of four bio-assays experiments.

During expedition ANTXXIV/3 (PS71) in 2008, Thuróczy et al., (2011) analysed Fe-binding organic ligands in the same region. During the present expedition we used another method and applied different techniques to distinguish different fractions of the Fe binding ligand pool. The current method detects all known ligand groups, including humics. We separately determined the humic Fe-binding dissolved organic ligands (Sukekava et al., 2018). Moreover, we took samples for the analysis of strong Fe-binding ligands, the siderophores; these samples will be analysed at the home laboratory (NIOZ, the Netherlands; see van Manen in this expedition report). All samples for iron-binding ligand (FeL) quantification (0.2  $\mu\text{m}$  filtered) were taken from the Ultra Clean sampling system (UCC).

At a total of 20 stations (Tab. 4.8) were sampled with a maximum of 12 depths per station. The FeL samples were also taken at the beginning (T0, 3 samples) and the end (TF, 12 samples) of four bio-assays experiments (see section 4.1.4).

The Fe-binding ligand concentrations and conditional stability constants, were determined by competitive ligand exchange - cathodic stripping voltammetry (CLE-CSV) with Salicylaldehyde (SA) as competing ligands (Abualhaija et al., 2014; Buck et al., 2015). Samples that could not be analysed on board were immediately stored at -20°C and will be taken to NIOZ for analysis.

The voltammetric instruments for FeL quantification consisted of a BioAnalytical System (BASi) controlled growth mercury electrode coupled with an Epsilon  $\epsilon 2$  (BASi) electrochemical analyzer. This voltammetric system was controlled by computer using ECDsoft as an interface software.

For the Fe-binding ligand determination, sub-sampled aliquots of 10 mL were distributed to Teflon vials (Nalgene). Vials were rinsed with MQ and at least twice conditioned prior to use with known Fe(III) and SA concentrations added into buffered seawater. The Teflon vials were marked and always used for the same added Fe(III) concentration and these vials were only rinsed with MQ in between samples in order to keep them conditioned. For the measurement, SA was added into the final concentration of 5  $\mu\text{M}$  and buffered to pH 8.28 with 0.1 M borate buffer. Then, the working Fe(III) standard solution was added into final concentrations 0 (twice, without Fe addition); 0.5; 1; 1.5; 2; 3; 4; 5; 6; 8; 10 nM of Fe. The Fe(III) additions were allowed to equilibrate for at least 8 hours before the measurement (Abualhaija et al, 2014). For each measurement, two scans were obtained with 90 seconds deposition time. Samples were analysed in the sequence from the low to the high Fe(III) additions without rinsing the cell in between.

The data obtained by CLE-CSV needs to be interpreted for the total iron-binding ligands concentration, [Lt] and the conditional stability constant (denoted as  $\log K_{\text{FeLFe(III)}}$  values). The data was plotted using the Langmuir isotherm assuming one-ligand using non-linear regression with the freely available software R as described by Gerringa et al. (2014). The total iron-binding ligand concentrations at station 27 ranged from 1.100.17 to 4.930.33 nM Eq Fe and the logarithm of the conditional stability constant ranged from Log 21.400.15 to 22.170.11 (Fig 4.6).

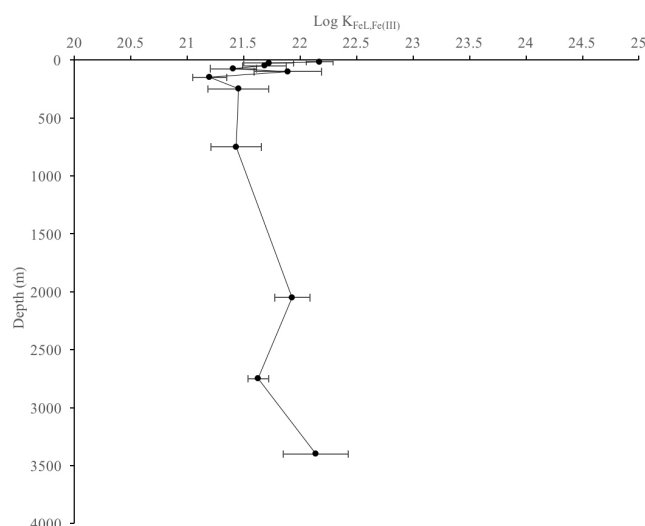


Fig. 4.6: The depth profile of the conditional stability constant ( $\log K_{\text{FeLFe(III)}}$ ) derived from the total iron-binding ligand concentrations at station 27

#### Humic substances

The rapid development of analytical methods enables us to identify many different organic substances to bind iron, making up the pool of iron-binding ligands (Bundy et al., 2015). Humic substances (HS) are part of the dissolved organic matter (DOM) in seawater with a terrestrial origin and/or a degradation product of DOM (Abualhaija et al., 2015; Laglera & van den Berg, 2009). These substances are important contributors to the iron-binding ligand pool in estuarine

### 4.3 Trace metal sampling and analysis

---

area (Laglera and van den Berg, 2009). Nevertheless, not much is currently known about its contribution to the iron-binding ligand pool in the Antarctic Ocean.

All samples for humic substances determination were taken together with the FeL samples. Sample analysis was conducted on board, and samples that could not be analysed during the expedition were stored at -20°C and will be taken to NIOZ for analysis.

Iron binding humic substances were measured through cathodic stripping voltammetry (CSV) as described by (Sukekava, 2018). Samples were buffered by BrO<sub>3</sub>/POPSO buffer. A Suwannee River Fulvic Acid (SRFA) Standard (2S101F, International Humic Substances Society, IHSS) was used to make an internal calibration to quantify the presence of humic substances by a series of standard additions in a range of 0.2 to 0.8 mg/L. The SRFA standard solution was saturated with iron after determining the binding capacity of the SRFA in Milli-Q in the home lab. The voltammetric setup consists of a Metrohm 663 VA stand, control hardware (Metrohm Autolab II and IME 663) and a consumer laptop PC running Metrohm Autolabs Nova 1. The VA stand is equipped with a Teflon measuring cell containing a Hg drop multimode electrode (Metrohm); a reference electrode (double-junction, Ag/AgCl, 3 M KCl, Metrohm), an auxiliary electrode (glassy carbon, Metrohm) and a Teflon stirrer. The system was connected to an N<sub>2</sub> line for purging and Hg drop formation pressure.

#### *Iron binding ligand characterization*

In times of iron-stress, some micro-organisms (mainly bacteria) can synthesise organic ligands called siderophores which act as strong iron-binding ligands. To identify and characterize these ligands, we took samples at 20 stations (max 12 depths; Tab. 4.8) and at the end of three bioassays (12 samples each). For this analysis, a maximum of four litre of seawater was collected (0.2 µm filtered). Immediately after sampling, siderophores were extracted using a SPE-cartridge with an average flow-rate of 6ml/min. After extraction, samples were stored in plastic bags at -20°C for later analysis at NIOZ, using High-Performance Liquid Chromatography–Inductively Coupled Plasma–Mass Spectrometry (Boiteau et al, 2013). With the use of this technique, siderophores can be detected and quantified.

#### *Particulate organic carbon (POC) and nitrogen (PON)*

For POC and PON sampling, 5L unfiltered sea water was collected from 12 depths of 20 stations (Tab. 4.8). These samples were stored in dark bottles and further filtered by glass microfiber filters (GF/F, 0.7 µm). The filters were wrapped in aluminum foil and stored in -20 °C. In addition to normal cast samplings, POC and PON samples were also collected from bioassay experiments. 1L unfiltered water were sampled from bio-assay and filtered by 0.3 µm GF/F filters. The procedure was the same as above. The C/N analysis will be conducted in the shore-based laboratory

#### *Particulate metals*

For particulate metals sampling, a maximum of six liter of unfiltered seawater was collected from 12 depths of 21 stations (Tab. 4.8) The samples were filtered on a PES filter (Supor, 0.4 µm). After filtration, the samples were stored in an acid rinsed eppendorf tube and stored at -20 °C. Beside the trace metal stations, PM samples were also collected at the end of the bioassays (see section 4.1.4). PM analysis will be performed at the home institute.

**Tab. 4.8:** Overview of samples taken from the trace metal stations; X denotes samples taken for given parameter. DFe: dissolved iron; DM: dissolved metals; TM: unfiltered sample for

#### 4. Iron Limitation and Viruses, Phytoplankton Caught between a Rock and a Hard Place

total dissolvable metals; Iso; metal isotopes; Lib: library back up sample; C/N: POC and PON; PM: particulate metals; FeL: iron binding ligand quantification; Lig Char: Iron binding ligands characterization.

Station	DFe	DM	Tm	Iso	Lib	C/N	PM	FeL	Lig. Char
14	X	X	X	X	X	X	X	X	X
16	X	X	X	X	X	X	X	X	X
18	X	X	X	X	X	X	X	X	X
20	X	X	X	X	X	X	X	X	X
22	X	X	X	X	X	X	X	X	X
25	X	X	X	X	X	X	X	X	X
27	X	X	X	X	X	X	X	X	X
31	X	X	X	X	X	X	X	X	X
34	X	X	X	X	X	X	X	X	X
38	X	X	X	X	X	X	X	X	X
41.4	X	X	X	X	X	X	X	X	X
41.8	X	X	X	X	X	X	X	X	X
41.10	X	X	X	X	X	X	X	X	X
41.14	X	X	X	X	X	X	X	X	X
56	X	X	X	X	X	X	X		
61	X	X	X	X	X	X	X	X	X
65	X	X	X	X	X				
67	X	X	X	X	X	X	X	X	X
70	X	X	X	X	X	X	X	X	X
73	X	X	X	X	X	X	X	X	X
75	X	X	X	X	X	X	X	X	X
82		X	X	X	X	X	X	X	X
85		X	X	X	X	X	X	X	X
91		X	X	X	X	X			
93		X	X	X	X	X	X	X	X
95		X	X	X	X	X	X	X	X

#### Data management

All raw data will be stored on the NIOZ-server for secured back-up and is available to collaborators upon completion of analysis. After suitable quality control, the metal data will be submitted in the final project year to the GEOTRACES International Data Management Centre ([www.bodc.ac.uk/geotraces/](http://www.bodc.ac.uk/geotraces/)) and the National Polar Data Centre (<http://www.npdc.nl/>) which is linked to other international databases. Two years after submission, data will become publicly available ([www.bodc.ac.uk/geotraces/data/policy](http://www.bodc.ac.uk/geotraces/data/policy)) and will also be incorporated in the next Data Product.

#### 4.4 Trace metal biogeochemistry and proteomics

We aimed to examine the relationship between trace metals and microbial community

### 4.3 Trace metal sampling and analysis

physiology and activity. To assess physiological status of the microbial communities, we will use quantitative proteomics and mass spectrometry to identify biomarkers of nutrient stress and other processes. For example, the expression of the iron-free protein flavodoxin, as opposed to the iron-containing ferredoxin, is indicative of iron stress in some phytoplankton (LaRoche et al., 1996) and the expression of CBA1 (cobalamin acquisition protein) is indicative of vitamin B12 stress in some phytoplankton (Bertrand et al 2012).

#### Work at sea and work to be done in the home lab

During this expedition, we collected size-fractionated samples (0.2  $\mu\text{m}$ , 3.0  $\mu\text{m}$ , and 12.0  $\mu\text{m}$  pore size) on polycarbonate filters at multiple depths from 29 different stations, for a total of 333 filters (Tab. 4.9). Samples were collected with the trace-metal clean CTD 'Titan', and immediately filtered via peristaltic pump for 2 hours, working at 4°C, then frozen and stored at -80°C. Volumes collected per depth were 3-15 L. The different size fractions were collected to harvest distinct microbial community components; the largest size fraction (>12.0  $\mu\text{m}$ ) was used to target *Phaeocystis antarctica* colonies and large diatoms, the intermediate size fraction was used to target smaller diatoms and other phytoplankton species, and the smallest size fraction (<3.0  $\mu\text{m}$  and >0.2  $\mu\text{m}$ ) was designated for smaller phytoplankton such as *Micromonas* and bacteria.

**Tab. 4.9:** Date and location for all protein samples taken from UCC CTD casts

Date	Station (UCC)	Protein sample depths
26-Dec-18	14	4
28-Dec-18	16	4
28-Dec-18	17	1
29-Dec-18	18	4
30-Dec-18	20	4
31-Dec-18	22	4
3-Jan-19	27	4
4-Jan-19	30	4
7-Jan-19	34	4
9-Jan-19	36	1
10-Jan-19	38	4
11-Jan-19	41-4	5
12-Jan-19	41-8	5
12-Jan-19	41-10	4
12-Jan-19	41-14	4
20-Jan-19	53-2	1
23-Jan-19	56-1	4
27-Jan-19	61-1	4
28-Jan-19	65-1	4
28-Jan-19	66-1	1
28-Jan-19	67-1	4
29-Jan-19	70-1	4
29-Jan-19	73-1	4
30-Jan-19	75-1	4

Date	Station (UCC)	Protein sample depths
30-Jan-19	82-1	5
31-Jan-19	85-1	5
31-Jan-19	91-1	5
31-Jan-19	93-1	5
1-Feb-19	95-1	5

In addition to the station sampling, we performed multiple ‘bioassay’ experiments with temperature-controlled incubators (Tab. 4.10). Our main experiments examined the combined influence of iron limitation and temperature on microbial community composition, physiology and activity or combined influence of manganese and iron on these parameters. We examined microbial community changes, nutrient uptake, and elemental stoichiometry in these bioassays. We also conducted smaller experiments to examine potential colimitation of iron, manganese, and vitamin B12 and to further examine the relationship between temperature, iron and net phytoplankton growth rate. The main analyses on these smaller experiments included macronutrient drawdown, chlorophyll production, and cell counts. In total, 320 different protein samples were acquired from these bioassays and smaller experiments.

**Tab. 4.10:** Bioassay Descriptions

Initiation Date	Station (UCC)	Bioassay Variables	Bioassay length [days]
28. Dec 18	17	Temperature, Fe	8
9 Jan 19	36	Temperature, Fe	8
20 Jan 19	53	Mn, Fe	6
28 Jan 19	66	Temperature, Fe	6

Once the protein samples arrive at Dalhousie University, we will use a combination of exploratory, global proteomic and targeted proteomic approaches to quantify nutrient limitation biomarkers and markers of other processes (e.g. Wu et al in revision, Bertrand et al., 2012, 2015). The Bertrand Lab’s Thermo TSQ Quantiva, a triple quadrupole instrument, will be used for targeted analyses while an Orbitrap Velos Pro at Dalhousie University’s CORE facility will be used for untargeted assessments of protein expression. In both cases, proteins are extracted, digested into peptides, separated into less complex fractions by liquid chromatography and then interfaced into the mass spectrometer. Importantly, these proteomic data are coupled with trace metal and metal-binding ligand sampling, facilitating future analysis of micronutrient impacts on plankton community metabolism.

#### Data management

All raw data will be stored on the Dalhousie server for secured back-up and is available to collaborators upon completion of analysis. After suitable quality control, the protein data and metadata will be submitted the ProteomeXchange proteomics data repository which is linked to other international databases and also submitted to the Ocean Protein Portal, which is currently in development and will be housed with the US BCO-DMO.

## 4.5 Viral and microbial ecology

Microorganisms (prokaryotes, archaea and eukaryotic phytoplankton) make up most of the ocean's living biomass and are essential for the cycling of biogeochemical elements. Moreover, phytoplankton are responsible for about half of the Earth's oxygen production and form the base of most of the pelagic food chains in the seas. Phytoplankton production is regulated by physicochemical variables such as light, temperature and nutrients. In the HNLC (high nutrients, low chlorophyll) regions of the Southern Ocean, Chlorophyll a concentrations are relatively low as compared to the concentrations of macronutrients (nitrogen, phosphorus and silicate) largely due to iron deficiency. At the same time, standing stock is controlled by predation, sedimentation and viral lysis. Viral lysis rates of Antarctic phytoplankton are currently still largely unknown, despite major difference in energy and matter transfer between grazing and viral lysis. The main focus of our sampling was to determine viral lysis rates of the microbial community and study the community composition of potential microbial host and viruses, along a natural iron gradient as well as during bioassay experiments (described in Tab. 4.10).

### Work at sea and preliminary results or work to be done in the home lab

Samples (Tab. 4.11) were collected mostly using the Titan sampling system. We sampled for microbial abundances and community composition, viral lysis rates of microbial hosts, viral production rates, bacterial grazing rates and metagenomic analysis of microbial host community as well as the pelagic virus community. Microbial abundances were sampled from six depths, surface mixed layer, Chlorophyll maximum (Chl max), and 50, 75, 100, 250 m (150 for casts <200 m). Phytoplankton abundance samples were fixed using formaldehyde buffered with hexamine (18 %/10 % v/w). Bacterial and viral abundance samples were fixed in glutaraldehyde (25 % EM-grade). All fixed samples were flash frozen in liquid nitrogen and stored at -80°C until analysis in the home lab (NIOZ). Filtrations for pigment analysis (HPLC) from specific depths (related to our viral lysis assays) were conducted for 2 fractions (total and <20 µm) and stored at -80°C after liquid nitrogen flash freezing. Samples for qualitative microscopic analysis of larger-sized phytoplankton (and zooplankton) were collected in 100 mL brown glass bottles and fixed with LUGOL solution). Fv/Fm was measured within 4 hours of sampling using PAM fluorometry (preliminary results see Tab. 4.12).

**Tab. 4.11:** Overview of variables sampled: Abun: abundance, FLB: bacterial grazing rates. VP: viral production, LH: Viral lysis rates, FeCl<sub>3</sub>: iron chloride precipitation method for filtration of viral DNA

Station PS117_	Abun.	HPLC	Lugol	Fv/Fm	FLB	VP	LH	Sterivex/ Anotop	FeCl3
13	X		X	X	X	X		X	
14	X	x	X	X	X	X	X	X	X
16	X	x	X	X					
17	X	X	X	X	X	X	X	X	X
18	X	X	X	X					
20	X	X	X	X	X	X	X	X	X
22	X	X	X	X	X	X	X	X	X
27	X	X	X	X	X	X	X	X	X
30	X	X	X	X	X	X		X	
34	X	X	X	X	X	X	X	X	X
36	X	X	X	X	X	X	X	X	X
38	X	X	X	X	X	X		X	

4. Iron Limitation and Viruses, Phytoplankton Caught between a Rock and a Hard Place

Station PS117_	Abun.	HPLC	Lugol	Fv/Fm	FLB	VP	LH	Sterivex/ Anotop	FeCl3
41_4	X	X	X	X		X			
41_8	X	X	X	X		X			
41_10	X	X	X	X	X	X	X	X	X
41_14	X	X	X	X		X			
53	X	X	X	X	X	X	X	X	X
56	X	X	X	X	X	X	X	X	X
61	X	X	X	X	X	X	X	X	X
65	X	X	X	X		X		X	
67	X	X	X	X		X	X	X	X
70	X	X	X	X		X		X	
73	X	X	X	X				X	
75	X	X	X	X	X	X	X	X	X
82	X	X	X	X		X	X	X	X
85	X	X	X	X				X	
91	X	X	X	X	X	X	X	X	X
93	X	X	X	X				X	
95	X	X	X	X	X	X	X	X	

Tab. 4.12: Preliminary results of Fv/Fm data measured on board

Station PS117_	Date	Time	1:F	1:Fm'	Fv/Fm
13	22.12.2018	09:56:37	258	255	0.055
14	27.12.2018	05:50:28	469	693	0.322333
16	28.12.2018	06:58:55	351	592	0.395333
18	29.12.2018	06:10:27	378	543	0.315333
20	30.12.2018	11:37:16	825	1127	0.268667
22	31.12.2018	21:09:10	382	487	0.224667
27	03.01.2019	18:36:07	307	469	0.299333
30	04.01.2019	0.58441	231	256	0.096667
34	07.01.2019	0.496493	206	289	0.284
38	10.01.2019	05:17:08	730	1108	0.304667
41_4	11.01.2019	21:28:08	238	293	0.14
41_8	12.01.2019	04:56:26	281	333	0.141667
41_10	12.01.2019	12:12:42	317	324	0.025
41_13	12.01.2019	15:30:02	290	311	0.056667
53	20.01.2019	15:40:18	132	227	0.4715
56	23.01.2019	10:40:19	365	1014	0.589
61	27.01.2019	05:50:40	0	406	0.8105

#### 4.5 Viral and microbial ecology

Samples for metagenomic analysis of prokaryotic and eukaryotic microbial community were collected using 0.2  $\mu\text{m}$  pore-size Sterivex filters. The filtrate was used to collect viruses using 0.02  $\mu\text{m}$  Anotop filters. Viruses were furthermore concentrated using the  $\text{FeCl}_3$  precipitation method.

Viral lysis and microzooplankton grazing rates of phytoplankton were determined simultaneously using the modified dilution method (herein referred to as LH method, Fig. 4.7), in combination with flow cytometry. Either the Chl max or otherwise the mixed layer was sampled for this assay. Samples were processed at low temperature ( $<1^\circ\text{C}$ ) and protected from light by working in dimmed light. The principle of the LH assay is that the removal of predators (grazers and viruses) by dilution allows algal cells to increase in standing stock over time (24h incubation time). Plotting the resulting apparent growth rates against the dilution factor, the slope of the linear regression represents the loss rate. Depending on the type of diluent (either grazer-free or grazer & virus-free) the exponential microzooplankton grazing rate and the viral lysis rate can be obtained. Grazer-free diluent was prepared using 0.45  $\mu\text{m}$  gravity filtration and the virus-free diluent by 30 kDa tangential flow filtration. Whole water samples were gently mixed with diluent to obtain 4 dilutions, in triplicate 1L PC-bottles (Fig. 4.7). The filled bottles (without air bubble) were incubated on a slow turning wheel at *in-situ* temperature and light conditions. Samples for phytoplankton abundances (fixed) were taken at the start and after 24h incubation.

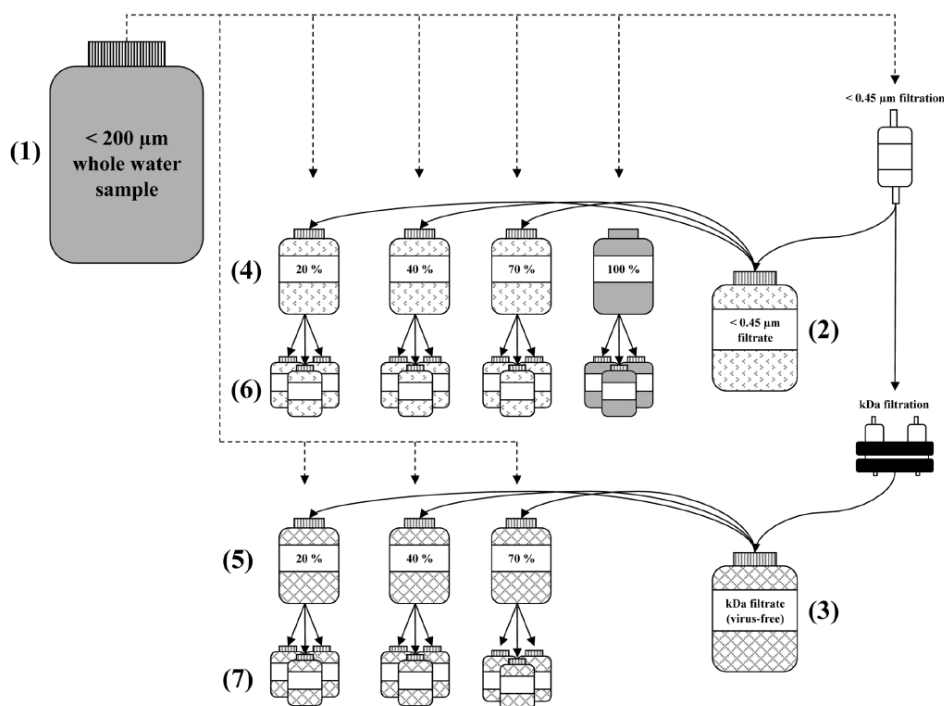


Fig. 4.7: Modified dilution assay experimental design. Mesoplankton-free whole water (1) is combined with either  $<0.45\text{-}\mu\text{m}$  filtrate (2) or 30 kDa filtrate (3) in the correct proportions to create the parallel  $t_0$  dilution series:  $<0.45\text{-}\mu\text{m}$  series, with reduced grazing mortality (4) 30 kDa series, with reduced grazing and viral mortality (5). Replicate sample bottles from the  $<0.45\text{-}\mu\text{m}$  and kDa dilution series are then created (6 and 7) and incubated under experimental conditions. (Kimmance and Brussaard, 2010).

We also determined viral lysis rates of the bacterial hosts using the virus production (VP) method. This method is based on the increase of newly released bacteriophage over time. For this, the standing stock in the whole water sample is reduced by washing while the natural bacterial community stays present. From the bacteriophage production rate, the specific lysis rate of the bacterial hosts is calculated. Additionally, the percentage of lysogen bearing bacteria hosts is determined by addition of Mitomycin C (initiate the lytic phase of any prophage). Filtrations and incubations were performed under temperature-controlled conditions. Subsamples for viruses were taken at regular time intervals and fixed with glutaraldehyde (0.5% final conc) after which the samples were flash frozen in liquid nitrogen and stored at -80°C. Samples will be analysed in the home lab (NIOZ).

Besides sampling natural waters, we participated in the bioassays (Tab. 4.10), for which we sampled microbial abundances and Fv/Fm on a bi-daily basis, and HPLC and viral lysis rates at the beginning and the end of a bioassay.

#### Data management

All raw data will be stored on the NIOZ-server for secured back-up and is available to collaborators upon completion of analysis and publication. After a quality check, data and metadata will be uploaded to the National Polar Data Centre (<http://www.npdc.nl/>) which is linked to other international databases.

#### References

- Abualhaija M M, Whitby H, & van den Berg C M G (2015) Competition between copper and iron for humic ligands in estuarine waters. *Marine Chemistry*, 172, 46-56.
- Abualhaija M M, & van den Berg C M G (2014) Chemical speciation of iron in seawater using catalytic cathodic stripping voltammetry with ligand competition against salicylaldehyde. *Marine Chemistry*, 164, 60-74.
- Alderkamp A-C, Mills M M, van Dijken GL, Laan P, Thuróczy C-E, Gerringa L J A, de Baar H J W, Payne CD, Visser R J W, Buma A G J & Arrigo K R (2012) Iron from melting glaciers fuels phytoplankton blooms in the Amundsen Sea (Southern Ocean): Phytoplankton characteristics and productivity. *Deep-Sea Research Part II-Topical Studies in Oceanography*, 71-76, 32-48.
- Arrigo KR (2005) Marine microorganisms and global nutrient cycles. *Nature*, 437, 349-355.
- Arrigo KR, Lowry KE & van Dijken GL (2012) Annual changes in sea ice and phytoplankton in polynyas of the Amundsen Sea, Antarctica. *Deep-Sea Research Part II-Topical Studies in Oceanography*, 71-76, 5-15.
- Arrigo K R, van Dijken G & Long M (2008) Coastal Southern Ocean: A strong anthropogenic CO<sub>2</sub> sink. *Geophysical Research Letters*, 35.
- Arrigo K R & van Dijken G L (2003) Phytoplankton dynamics within 37 Antarctic coastal polynya systems. *Journal of Geophysical Research-Oceans*, 108.
- Bertrand E M, Allen A E, Dupont CL, Norden-Kirchmar T, Bai J, Valas R E & Saito MA (2012) Influence of cobalamin starvation on diatom molecular physiology and the identification of a novel cobalamin acquisition protein. *PNAS* 109(26) E1762-E1771, [doi: 10.1073/pnas.1201731109](https://doi.org/10.1073/pnas.1201731109).
- Bertrand E M, McCrow J P, Moustafa A, Zheng H, McQuaid J, Delmont T O, Post A F, Sipler R, Spackeen J, Xu K, Bronk D A, Hutchins D A & Allen A E (2015). Phytoplankton-bacterial interactions mediate micronutrient colimitation at the coastal Antarctic sea ice edge. *PNAS* 112 (32) 9938–9943.
- Boiteau R M, & Repeta, D J (2015). An extended siderophore suite from *Synechococcus* sp. PCC 7002 revealed by LC-ICPMS-ESIMS *Metallomics*, 7(5), 877-884.

#### 4.5 Viral and microbial ecology

---

- Bonnain C, Breitbart M & Buck K N (2016) The Ferrojan Horse Hypothesis: Iron-Virus Interactions in the Ocean. *Frontiers in Marine Science*, 3.
- Boyd P W & Ellwood M J (2010) The biogeochemical cycle of iron in the ocean. *Nature Geoscience*, 3, 675-682.
- Boye M, van den Berg C M G, de Jong J T M, Leach H, Croot P & de Baar H J W (2001) Organic complexation of iron in the Southern Ocean. *Deep-Sea Research Part I-Oceanographic Research Papers*, 48(6), 1477-1497
- Boye M, Nishioka J, Croot P L, Laan P, Timmermans KR & de Baar HJW (2005) Major deviations of iron complexation during 22 days of a mesoscale iron enrichment in the open Southern Ocean. *Marine Chemistry*, 96, 257-271.
- Bruland K W, Middag R & Lohan M C (Eds.) (2014) *Controls of Trace Metals in Seawater. Treatise on Geochemistry 2nd edition*, 8, 19-55 pp.
- Brum J R, Hurwitz BL, Schofield O, Ducklow H W & Sullivan M B (2016) Seasonal time bombs: dominant temperate viruses affect Southern Ocean microbial dynamics. *ISME j*, 10, 437-49.
- Brussaard C P D, Wilhelm S W, Thingstad F, Weinbauer M G, Bratbak G, Heldal M, Kimmance S A, Middelboe M, Nagasaki K, Paul J H, Schroeder D C, Suttle C A, Vaque D & Wommack KE (2008) Global-scale processes with a nanoscale drive: the role of marine viruses. *ISME J*, 2, 575-578.
- Buck K N & Bruland KW (2007) The physicochemical speciation of dissolved iron in the Bering Sea, Alaska. *Limnology and Oceanography*, 52, 1800-1808.
- Buck K N, Sohst B, & Sedwick P N (2015) The organic complexation of dissolved iron along the U.S GEOTRACES (GA03) North Atlantic Section. *Deep Sea Research Part II: Topical Studies in Oceanography*, 116, 152-165.
- Bundy R M, Abdulla H A N, Hatcher P G, Biller D V, Buck K N & Barbeau K A (2015) Iron-binding ligands and humic substances in the San Francisco Bay estuary and estuarine-influenced shelf regions of coastal California. *Marine Chemistry*, 173, 183-194.
- Conway T M & John S G (2014) Quantification of dissolved iron sources to the North Atlantic Ocean. *Nature* 511:212–215.
- Croot P L, Andersson K, Öztürk M & Turner D R (2004) The distribution and speciation of iron along 6°E in the Southern Ocean. *Deep Sea Research Part II: Topical Studies in Oceanography*, 51, 2857-2879.
- Croot P L & Johansson M (2000). Determination of Iron Speciation by Cathodic Stripping Voltammetry in Seawater Using the Competing Ligand 2-(2-Thiazolylazo)-p-cresol (TAC). *Electroanalysis*, 12(8), 565-576.
- De Jong JTM, Den Das J, Bathmann U, Stoll MHC, Kattner G, Nolting RF & De Baar HJW (1998) Dissolved iron at subnanomolar levels in the Southern Ocean as determined by ship-board analysis. *Analytica Chimica Acta* 377, 113–124.
- De Jong J T M, Stammerjohn SE, Ackley SF, Tison JL, Mattielli N & Schoemann V (2015) Sources and fluxes of dissolved iron in the Bellingshausen Sea (West Antarctica): The importance of sea ice, icebergs and the continental margin. *Marine Chemistry*, 177, Part 3, 518-535.
- De La Rocha CL (2007) 6.04 - The Biological Pump. In: H.D. Holland and KK Turekian (Editors), *Treatise on Geochemistry*. Pergamon, Oxford, pp. 1-29.
- Evans C & Brussaard C P (2012) Regional variation in lytic and lysogenic viral infection in the Southern Ocean and its contribution to biogeochemical cycling. *Appl Environ Microbiol*, 78, 6741-8.

#### 4. Iron Limitation and Viruses, Phytoplankton Caught between a Rock and a Hard Place

---

- Gerringa L J A, Alderkamp A-C, Laan P, Thuróczy C-E, De Baar H J W, Mills M M, van Dijken G L, van Haren H & Arrigo KR (2012) Iron from melting glaciers fuels the phytoplankton blooms in Amundsen Sea (Southern Ocean): Iron biogeochemistry. *Deep-Sea Research Part II-Topical Studies in Oceanography*, 71-76, 16-31.
- Gerringa L J A, Laan P, van Dijken GL, van Haren H, De Baar HJW, Arrigo KR & Alderkamp AC (2015) Sources of iron in the Ross Sea Polynya in early summer. *Marine Chemistry*, 177, Part 3, 447-459.
- Gerringa L, Rijkenberg M, Thuróczy C-E & Maas L (2014). A critical look at the calculation of the binding characteristics and concentration of iron complexing ligands in seawater with suggested improvements (Vol. 11).
- Gledhill M, & Buck K N (2012) The organic complexation of iron in the marine environment: A review. *Frontiers in Microbiology*, 3(FEB)
- Gledhill M & van den Berg CMG (1994) Determination of complexation of iron(III) with natural organic complexing ligands in seawater using cathodic stripping voltammetry. *Mar. Chem.* 47, 41–54.
- Gobler C J, Hutchins DA, Fisher NS, Coper EM & Sañudo-Wilhelmy SA (1997) Release and bioavailability of C, N, P Se, and Fe following viral lysis of a marine chrysophyte. *Limnology and Oceanography*, 42, 1492-1504.
- Grasshof K (1969) *Advances in Automated Analysis*. Technicon International Congress, Volume II, pp 147-150.
- Grasshoff K et al, *Methods of seawater analysis*. Verlag Chemie GmbH, Weinheim, 1983 419 pp.
- Hassler CS, Schoemann V, Nichols CM, Butler ECV, Boyd PW (2011) Saccharides enhance iron bioavailability to Southern Ocean phytoplankton. *Proceedings of the National Academy of Sciences*, 108, 1076-1081.
- John AB, Diana EV, Paul JH (2002) Effects of temperature on growth rate, cell composition and nitrogen metabolism in the marine diatom *Thalassiosira pseudonana* (Bacillariophyceae). *Marine Ecology Progress Series*, 225, 139-146.
- Johnson KS, Boyle E, Bruland K, Measures C, Moffett J, Aquilarislas A, Barbeau K, Cai Y, Chase Z, Cullen J, Doi T, Elrod V, Fitzwater S, Gordon M, King A, Laan P, Laglera-Baquer L, Landing W, Lohan M, Mendez J, Milne A, Obata H, Osslander L, Plant J, Sarthou G, Sedwick P, Smith GJ, Sohst B, Tanner S, Van Den Berg S & Wu J (2007) Developing standards for dissolved iron in seawater. *Eos Transactions of the AGU* 88 (11), 131.
- Joughin I, Smith BE & Medley B (2014) Marine Ice Sheet Collapse Potentially Under Way for the Thwaites Glacier Basin, West Antarctica. *Science*, 344, 735-738.
- Kimmance, S and Brussaard, C (2010) Estimation of viral-induced phytoplankton mortality using the modified dilution method. *Manual of Aquatic Viral Ecology*, 65-73.
- Klunder M B, Laan P, De Baar HJW, Middag R, Neven I & Van Ooijen J (2014) Dissolved Fe across the Weddell Sea and Drake Passage: impact of DFe on nutrient uptake. *Biogeosciences*, 11, 651-669.
- Laglera L M & van den Berg, C M G (2009). Evidence for geochemical control of iron by humic substances in seawater. *Limnology and Oceanography*, 54(2), 610-619.
- Laufkötter C, Vogt M, Gruber N, Aita-Noguchi M, Aumont O, Bopp L, Buitenhuis E, Doney SC, Dunne J, Hashioka T, Hauck J, Hirata T, John J, Le Quéré C, Lima ID, Nakano H, Seferian R, Totterdell I, Vichi M & Völker C (2015) Drivers and uncertainties of future global marine primary production in marine ecosystem models. *Biogeosciences*, 12, 6955-6984.
- Liu X, & Millero F J (2002) The solubility of iron in seawater. *Marine Chemistry*, 77(1), 43-54.

#### 4.5 Viral and microbial ecology

---

- Lønborg C, Middelboe M, Brussaard C P D (2013) Viral lysis of *Micromonas pusilla*: impacts on dissolved organic matter production and composition. *Biogeochemistry*, 116, 231-240.
- Maldonado M T, Strzepek R F, Sander S & Boyd P W (2005) Acquisition of iron bound to strong organic complexes, with different Fe binding groups and photochemical reactivities, by plankton communities in Fe-limited subantarctic waters. *Global Biogeochemical Cycles*, 19.
- Marchant H, Davidson A, Wright S & Glazebrook J (2000) The distribution and abundance of viruses in the Southern Ocean during spring. *Antarctic Science*, 12, 414-417.
- Middag R, de Baar H J W, Klunder M B & Laan P (2013) Fluxes of dissolved aluminum and manganese to the Weddell Sea and indications for manganese co-limitation. *Limnology and Oceanography*, 58, 287-300.
- Middag R, de Baar H J W, Laan P, Cai P H & van Ooijen JC (2011) Dissolved manganese in the Atlantic sector of the Southern Ocean. *Deep-Sea Research Part II-Topical Studies in Oceanography*, 58, 2661-2677.
- Middag R, de Baar H J W, Laan P & Huhn O (2012) The effects of continental margins and water mass circulation on the distribution of dissolved aluminum and manganese in Drake Passage. *Journal of Geophysical Research-Oceans*, 117.
- Mills MM, Alderkamp A-C, Thuróczy C-E, van Dijken GL, Laan P, de Baar HJW & Arrigo KR (2012) Phytoplankton biomass and pigment responses to Fe amendments in the Pine Island and Amundsen polynyas. *Deep-Sea Research Part II-Topical Studies in Oceanography*, 71-76, 61-76.
- Mioni CE, Poorvin L & Wilhelm SW (2005) Virus and siderophore-mediated transfer of available Fe between heterotrophic bacteria: characterization using an Fe-specific bioreporter. *Aquatic Microbial Ecology*, 41, 233-245.
- Mojica KDA, Huisman J, Wilhelm SW & Brussaard CPD (2016) Latitudinal variation in virus-induced mortality of phytoplankton across the North Atlantic Ocean. *ISME J*, 10, 500-513.
- Moore CM, Mills MM, Arrigo KR, Berman-Frank I, Bopp L, Boyd PW, Galbraith ED, Geider RJ, Guieu C, Jaccard SL, Jickells TD, La Roche J, Lenton TM, Mahowald NM, Maranon E, Marinov I, Moore JK, Nakatsuka T, Oschlies A, Saito MA, Thingstad TF, Tsuda A, Ulloa O (2013) Processes and patterns of oceanic nutrient limitation. *Nature Geoscience*, 6, 701-710.
- Morel FMM, Milligan AJ & Saito MA (2014) 8.5 - Marine Bioinorganic Chemistry: The Role of Trace Metals in the Oceanic Cycles of Major Nutrients. In: H.D. Holland and KK Turekian (Editors), *Treatise on Geochemistry (Second Edition)*. Elsevier, Oxford, pp. 123-150.
- Murphy J & Riley JP (1962) A modified single solution method for the determination of phosphate in natural waters. *Analytica chim. Acta*, 27, p31-36.
- Poorvin L, Rinta-Kanto JM, Hutchins DA & Wilhelm SW (2004) Viral release of iron and its bioavailability to marine plankton. *Limnology and Oceanography*, 49, 1734-1741.
- Poorvin L, Sander SG, Velasquez I, Ibsanmi E, LeClerc GR & Wilhelm SW (2011) A comparison of Fe bioavailability and binding of a catecholate siderophore with virus-mediated lysates from the marine bacterium *Vibrio alginolyticus* PWH3a. *Journal of Experimental Marine Biology and Ecology*, 399, 43-47.
- Rignot E, Mougnot J, Morlighem M, Seroussi H & Scheuchl B (2014) Widespread, rapid grounding line retreat of Pine Island, Thwaites, Smith, and Kohler glaciers, West Antarctica, from 1992 to 2011. *Geophysical Research Letters*, n/a-n/a.
- Saito MA, Goepfert TJ & Ritt JT (2008) Some thoughts on the concept of colimitation: Three definitions and the importance of bioavailability. *Limnology and Oceanography*, 53, 276-290.
- Slagter HA, Gerringa LJA & Brussaard CPD (2016) Phytoplankton Virus Production Negatively Affected by Iron Limitation. *Frontiers in Marine Science*, 3.

#### 4. Iron Limitation and Viruses, Phytoplankton Caught between a Rock and a Hard Place

---

- Strickland JDH & Parsons TR (1968), A practical handbook of seawater analysis. First edition, Fisheries Research Board of Canada, Bulletin. No 167, p.65.
- Sukekava C, Downes J, Slagter H A, Gerringa L J A, & Laglera, L M (2018). Determination of the contribution of humic substances to iron complexation in seawater by catalytic cathodic stripping voltammetry. *Talanta*, 189, 359-364.
- Sunda WG & Huntsman SA (2011) Interactive effects of light and temperature on iron limitation in a marine diatom: Implications for marine productivity and carbon cycling. *Limnology and Oceanography*, 56, 1475-1488.
- Thuróczy CE, Gerringa LJA, Klunder MB, Middag R, Laan P, Timmermans KR, de Baar HJW (2010) Speciation of Fe in the Eastern North Atlantic Ocean. *Deep-Sea Research Part I-Oceanographic Research Papers*, 57, 1444-1453.
- Thuróczy C-E, Alderkamp A-C Laan P, Gerringa LJA, de Baar H.JW & Arrigo KR (2012) Key role of organic complexation of iron in sustaining phytoplankton blooms in the Pine Island and Amundsen Polynyas (Southern Ocean). *Deep-Sea Research Part II-Topical Studies in Oceanography*, 71-76, 49-60.
- Thuróczy C-E, Gerringa L J A, Klunder M, Laan P & de Baar H J W (2011) Observation of consistent trends in the organic complexation of dissolved iron in the Atlantic sector of the Southern Ocean. *Deep-Sea Research Part II-Topical Studies in Oceanography*, 58, 2695-2706.
- Wadham J L, De'ath R, Monteiro F M, Tranter M, Ridgwell A, Raiswell R & Tulaczyk S (2013) The potential role of the Antarctic Ice Sheet in global biogeochemical cycles. *Earth and Environmental Science Transactions of the Royal Society of Edinburgh*, 104, 55-67.
- Wilhelm S W & Suttle C A (1999) Viruses and Nutrient Cycles in the Sea: Viruses play critical roles in the structure and function of aquatic food webs. *BioScience*, 49, 781-788.
- Wu M, McCain J S, Rowland E, Middag R, Sandgren M, Allen A E & Bertrand E M (In revision) Proteomic signatures of manganese and iron deprivation in *Phaeocystis antarctica*: implications for phytoplankton growth in the Southern Ocean. *Nature Communications*.

## 5. PICCOLO AND SOCCOM FLOATS

Elise S. Droste<sup>1</sup>, Paul Chamberlain<sup>2</sup>, Sunke  
M. Trace-Kleeberg<sup>4</sup>,  
Not on board: Dorothee C. E. Bakker<sup>1</sup>,  
Giorgio Dall'Olmo<sup>5</sup>, Mario Hoppema<sup>3</sup>, Lynne  
D. Talley<sup>2</sup>, Karen J. Heywood<sup>1</sup>

<sup>1</sup> U East Anglia  
<sup>2</sup> Scripps  
<sup>3</sup> AWI  
<sup>4</sup> U Southampton  
<sup>5</sup> MBA

**Grant-No. AWI\_PS117\_03**

### Objectives (PICCOLO)

The PICCOLO (Processes Influencing Carbon Cycling: Observations of the Lower Limb of the Antarctic Overturning) project (2017-2022) is part of the RoSES (Role of the Southern Ocean in the Earth System) research programme, funded by the UK's Natural Environment Research Council (NERC). RoSES is closely linked with the NERC-funded ORCHESTRA (Ocean Regulation of Climate by Heat and Carbon Sequestration and Transports) programme (2016-2020). PICCOLO aims to gain a mechanistic understanding of the CO<sub>2</sub> uptake and sequestration in the lower limb of the Southern Ocean overturning circulations. Year-round sampling in this region poses enormous practical challenges, which has the risk of biasing our understanding of crucial processes that drive the carbon uptake.

The work done during the PS117 expedition contributes to the PICCOLO project with the following objectives:

- Deploying the PICCOLO floats in the central Weddell Sea in the vicinity of Maud Rise. The aim of the PICCOLO float deployments in the central Weddell Sea is to quantify seasonal physical and biogeochemical processes affecting the carbon cycle in Warm Deep Water. This water upwells in the Weddell Gyre and is modified by its circuitous route towards the dense water formation regions. The float deployments contribute to the PICCOLO overall objective to define, quantify and provide a mechanistic understanding of the key processes controlling the rate of Southern Ocean carbon uptake. Specifically, PICCOLO will follow the processes affecting the carbon transported within a water mass as it upwells in the Weddell Gyre through to sinking to the deep ocean.
- Extending the unique AWI-led record of deep ocean carbonate chemistry along the Greenwich Meridian and the Kapp Norvegia to Joinville Island section (Bakker et al., 2008; Van Heuven et al., 2011; Hoppema et al., 2015). The repeat sections have been sampled for carbonate and relevant additional parameters by AWI since 1992 (ANT-X/4). Along with previous data from the 1970s and 1980s, this section constitutes one of the longest time series of repeat hydrography in the Southern Ocean. The data will be submitted to the Global Ocean Data Analysis Project ([GLODAP](#)) (Olsen et al., 2016).

The float deployments are a part of a collaboration between the UK PICCOLO Research Program (NE/P021395/1), the US SOCCOM Program (NSF Award PLR-1425989), AWI scientists, the UK MetOffice (UKMO), and ENVEast Doctoral training partnership (NE/L002582/1). Special acknowledgement goes to Brian King (National Oceanography Centre (NOC), Southampton, UK), John Hankins (NOC, UK), and Jon Turton (UKMO) for their help with the UK floats before and after deployment, and to Greg Brasseur (University of Washington, USA) for the testing of the SOCCOM floats.

### Objectives (SOCCOM)

SOCCOM is a large-scale biogeochemical Argo deployment programme. Much of our knowledge of Southern Ocean biogeochemistry is seasonally biased to summer because that is primarily when research ships operate and observations are taken. SOCCOM will increase the number of biogeochemical measurements made monthly in the Southern Ocean by an order of magnitude, and, because of the persistence of the Argo platform, will sample year-round. To date, SOCCOM deployed floats have made over 3.5 million biogeochemical measurements, many in seasons and places chronically undersampled. Float deployment locations during PS117 have been chosen to observe distinct frontal boundaries in the Antarctic Circumpolar Current as well as distinct water masses in the Weddell Sea.

### Work at sea

#### 5.1 PICCOLO and SOCCOM floats

During the expedition, three standard Core Argo floats and two Navis SeaBird biogeochemical floats from the UK MetOffice had been deployed under PICCOLO (in the remainder of the text, these will be referred to as “PICCOLO floats”). SOCCOM deployed two Navis SeaBird biogeochemical floats and 5 Teledyne Webb Apex biogeochemical floats (from here on referred to as “SOCCOM floats”). See Tab. 5.1 for details on deployments. All floats were equipped with an ice-avoidance algorithm (Klatt et al., 2007).

Sensors on the BGC PICCOLO floats include temperature and salinity (SBE41cp); fluorescence, backscatter, and FDOM (MCOMS), dissolved oxygen (SBE63), and optics (OCR 504 Radiometer).

All SOCCOM floats are equipped with sensors to measure pH, fluorescence, backscatter, temperature, salinity, nitrate, and dissolved oxygen. The exact models of the sensor suite on each SOCCOM float is variable and can be found in the metadata of each individual float data file. Johnson et al. (2016) provides details on the performance characteristics of these sensors.

**Tab. 5.1:** Deployment date and location of PICCOLO and SOCCOM floats

Programme	Type	Float Number	Deployment Date	Deployment Location
PICCOLO	Core	8061	27 Dec 2018	67° 30.0' S 000° 5.7' E
PICCOLO	Core	8059	27 Dec 2018	66° 29.8' S 000° 1.0' E
PICCOLO	Core	8058	28 Dec 2018	65° 60.0' S 000° 0.9' E
PICCOLO	Navis	F0659	29 Dec 2018	63° 58.7' S 000° 2.6' W
PICCOLO	Navis	F0661	29 Dec 2018	63° 3.7' S 0° 3.7' E
SOCCOM	Navis	886	22 Dec 2018	51° 00.2' S 003° 55.2' E

## 5.2 Sampling and float deployment locations

Programme	Type	Float Number	Deployment Date	Deployment Location
SOCCOM	Navis	689	31 Dec 2018	59° 05.0' S 000° 05.4' E
SOCCOM	Apex	12886	6 Jan 2019	69° 01.7' S 006° 57.2' W
SOCCOM	Apex	11090	7 Jan 2019	65° 59.3' S 012° 17.4' W
SOCCOM	Apex	12749	21 Jan 2019	66° 35.9' S 027° 05.6' W
SOCCOM	Apex	12739	23 Jan 2019	65° 44.2' S 036° 49.2' W
SOCCOM	Apex	12688	27 Jan 2019	64° 11.3' S 047° 30.2' W

### 5.2 Sampling and float deployment locations

Floats have been deployed at previously-planned CTD stations across the Antarctic Circumpolar Current and the Weddell Gyre, on the Greenwich meridian section and the Fahrbach section from Kapp Norvegia to Joinville Island (Fig. 5.1). Floats have been deployed in waters at >2000 m depth, in ice free conditions to ensure successful satellite communication upon re-surfacing after deployment. The PICCOLO Core Argo floats were tested by John Hankins at the National Oceanography Centre in Southampton, UK, and have remained in pressure-activation mode until deployment. The PICCOLO BGC Argo floats were also tested by Elise Droste and Giorgio Dall'Olmo at the NOC and again at Cape Town prior to the ship's departure, after which they were left in pressure-activation mode until deployment. The SOCCOM BGC floats were tested at the University of Washington in Seattle, WA, and again at Cape Town by Greg Brusseau, after which they were left in pressure-activation mode until deployment.

The sensors on the floats require calibration samples. These have been taken from the AWI CTD rosette at the deployment stations. At PICCOLO BGC float deployment stations, calibration samples have been taken for dissolved oxygen, pigments (HPLC – High performance liquid chromatography), POC (particulate organic carbon), and salinity. At SOCCOM BGC float deployment stations, calibration samples have been taken for pH, salinity, dissolved oxygen, pigments, and POC. The Core Argo floats do not need calibration samples. Only salinity and dissolved oxygen samples have been analysed on board. The rest will be analysed at Scripps Institution of Oceanography, University of East Anglia, or Alfred-Wegener Institute (see below for specifications). Samples were taken from AWI CTD Niskin bottles in the following sequence: oxygen, DIC/TA, pH/TA, nutrients (by FePhyrus team), HPLC/POC, salinity

#### 5.2.1 DIC/TA samples

In accordance with the aim to extend the AWI-led record of carbonate chemistry along the vertical water column in the Weddell Sea, dissolved inorganic carbon (DIC) and total alkalinity (TA) samples were taken at all sampled depths, which was typically between 19-21 samples. A duplicate sample was taken at every sampled CTD station. Samples are collected in 250 mL and 500 mL glass bottles and subsequently poisoned with 100 L and 200 L of 50 % saturated mercuric chloride solution, respectively, following the protocol by Dickson et al. (2007). Prior to poisoning, a 1 % headspace was created to accommodate thermal expansion during storage. Analysis will be done at AWI. In addition to the BGC float deployment stations, DIC/TA samples were taken at most AWI CTD stations along the Greenwich meridian transect, Weddell Sea stations, and the transect from Kapp Norvegia to Joinville Island. A number of UCC stations were also sampled for DIC/TA.

### 5.2.2 pH/TA samples

pH/TA samples were only required at SOCCOM BGC float deployment stations in order to calibrate the pH sensors that is mounted on them. At these stations, the samples have been taken at all sampled depths, which is typically between 19-21 samples. Samples are collected in 500 mL glass bottles and subsequently poisoned with 240 L of 50 % saturated mercuric chloride solution, following the SOCCOM protocol. The analysis will be done by the Dickson Laboratory at Scripps Institution of Oceanography.

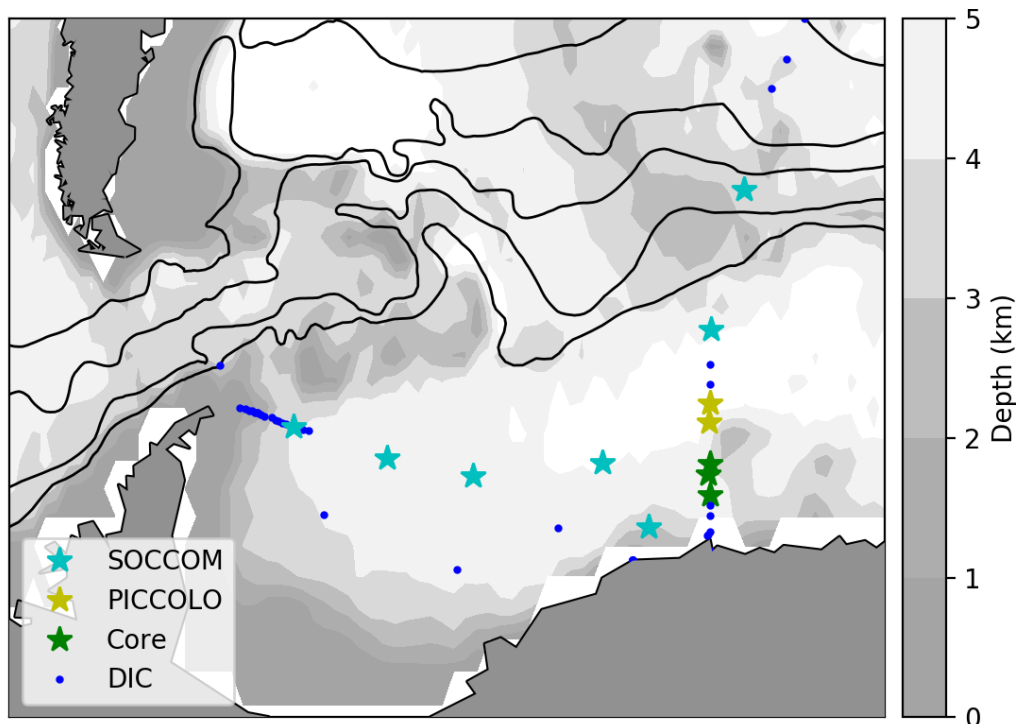


Fig. 5.1: Locations for SOCCOM BGC floats, PICCOLO BGC floats, PICCOLO Core Argo floats, and CTDs at which DIC samples were collected. Oxygen samples were collected and analysed at all stations where DIC was samples, unless the ocean depth was < 500 m. Solid black lines indicate frontal boundaries (Orsi et al. 1995).

### 5.2.3 HPLC/POC

HPLC and POC samples were collected at the chlorophyll maximum and at the surface depth (usually between 5 and 20 m) at PICCOLO and SOCCOM BGC float deployment stations only for calibration purposes, following SOCCOM sampling protocol. A duplicate sample was almost always taken at the surface depth. Occasionally, when the water volume on the AWI CTD was limited, the surface sample for HPLC/POC would be collected using a plastic bucket from the side of the ship (SOCCOM floats 689, 11090, 12749, 12739 and PICCOLO floats). Samples were filtered on a filtration rig provided by the Plymouth Marine Laboratory (PML). HPLC and POC filters (including a wet and dry blank for each, per station) were carefully folded in half, placed inside aluminium foil envelopes, and stored in liquid nitrogen

### 5.2.4 Salinity

Salinity samples were taken at all BGC float deployment stations. The salinity samples will be used in the calibration procedures of the float. Salinity was measured using the onboard AWI Optimare salinometer.

### 5.2.5 Dissolved oxygen samples

Samples for determining oxygen concentration were taken from both the AWI CTD/RO and the NIOZ Ultra Clean CTD (UCC) with the aim to calibrate the dissolved oxygen sensors mounted on these CTD rosettes. Typically, 5-6 depths were sampled with one duplicate. Between 11 and 12 depths were sampled at BGC float deployment stations. In total 314 samples were taken from 41 CTD stations, with 42 double samples to estimate the quality of sampling and titration procedures. Four samples were flagged as bad data due to errors in the pickling process or failing the titration. These are not taken into account for analysis. At station 056 (cast 2) there was a problem with the oxygen sensor. The three sensors on pump 2 were then changed and so from station 058 (cast 1) a new file for sensor calibration was started.

The concentration of dissolved oxygen in seawater was determined by Winkler titration (Carpenter, 1965) to calibrate the oxygen sensor on the AWI CTD (or UCC). This method is based on a set of redox reactions that fix the oxygen and discolour the sample and the titer (thiosulfate,  $\text{Na}_2\text{S}_2\text{O}_3$ ) required to make the sample optically clear. Titration of the samples was done using the automated Dissolved Oxygen Analyser Metrohm 765 Dosimat (Fa. SIS Kiel, S/N:8046). The dosimat was connected via serial link to a laptop running Dissolved Oxygen Analyser (DOA) software (Version 4.0.12.0 by SiS Sensoren Instrumente Systeme GmbH). The quality of the titer was checked before samples were titrated. This was done by titration with 3-5 standard solutions (potassium iodate,  $\text{KIO}_3$ ). The normality of the titer varied between 0.0476 and 0.05N. The DOA software requires temperature and salinity as input for the calculation. Temperature of the sample was measured with a FLUKE 50D K/J thermometer just before fixing the oxygen. Salinity values were retrieved from the CTD bottle file.

The reagents used for pickling are a Manganese (II) Chloride solution ( $\text{MnCl}_2 \cdot 4\text{H}_2\text{O}$ ), prepared by dissolving 600 g of  $\text{MnCl}_2$  in 1,000 ml distilled water and the alkaline solution NaOH/NaI, that was prepared by dissolving 320 g NaOH and 600 g NaI in 2,000 ml distilled water. Sulfuric acid ( $\text{H}_2\text{SO}_4$ ) 50 % (manufacturer Bernd Kraft, Duisburg, Germany) was added to the samples and sodium thiosulfate ( $\text{Na}_2\text{S}_2\text{O}_3$ ) with a concentration of 0.01N from readymade vials (manufacturer Merck KGaA, Darmstadt, Germany) was used as a titer. Potassium iodate solution ( $\text{KIO}_3$ ) from readymade vials (Merck KGaA, Darmstadt, Germany) was used as a standard.

## Preliminary (expected) results

### 5.3 Preliminary data for dissolved oxygen

The value measured from the oxygen titration is used to calibrate the CTD oxygen sensor. The concentration difference between CTD oxygen sensor and oxygen titration for all stations is shown in Fig. 5.2. The range of oxygen concentration difference for the AWI CTD with sensor 1 decreased after station 22. This could be due to increased familiarity with the method and so more accurate measurements. Sensor 1 on the AWI CTD tended to underestimate the amount of dissolved oxygen in the water compared to the titrated values (Fig. 5.2a). After the oxygen sensor on the AWI CTD was replaced, the *in-situ* measurements were slightly larger than those measured by the Winkler method (Fig. 5.2b). There is good agreement between the sensor and titrated oxygen values for the NIOZ UCC until station 027. After a change of instruments errors arose in the measured oxygen values.

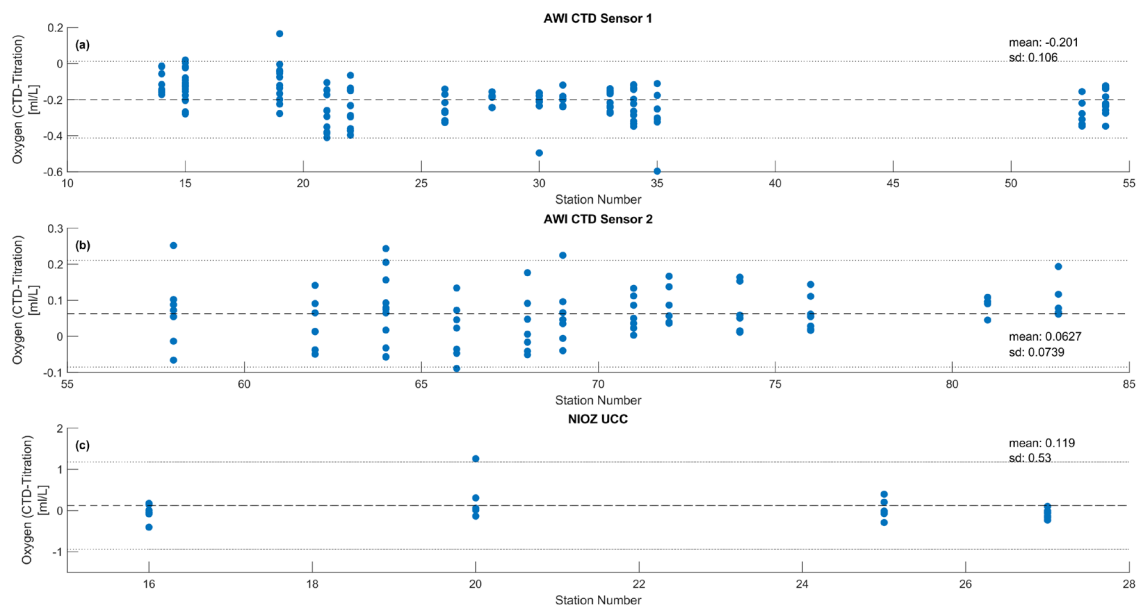


Fig. 5.2: Difference between the CTD oxygen sensor and the oxygen concentration determined from the samples by Winkler titration. (a) AWI CTD with sensor 1 (b) AWI CTD after the sensor was replaced (c) NIOZ Ultra Clean CTD (UCC). Annotated are the mean (dashed lines) and two times the standard deviation (dotted lines).

Histograms of oxygen difference show a roughly gaussian distribution for the AWI CTD (Fig. 5.3a and b). The distribution of the NIOZ UCC, on the other hand, is skewed. This suggests that there are errors in the sensor measurements.

Comparing oxygen concentration difference to depth, temperature and salinity (Fig. 5.4) shows that the AWI sensor 2 has a strong pressure dependence. The other sensors for the other parameters do not show an obvious pressure dependence.

## 5.4 Preliminary data of PICCOLO floats

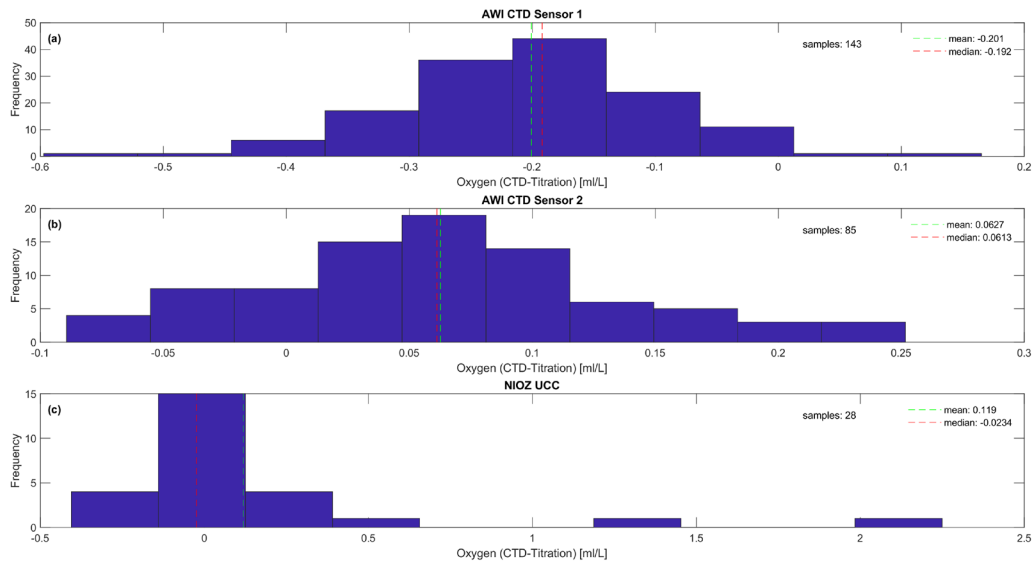


Fig. 5.3: Histogram of difference between the CTD oxygen sensor and the oxygen concentration determined from the samples by Winkler titration. (a) AWI CTD with sensor 1 (b) AWI CTD after the sensor was replaced (c) NIOZ Ultra Clean CTD (UCC). Annotated are the mean (dashed green lines) and median (dashed red lines).

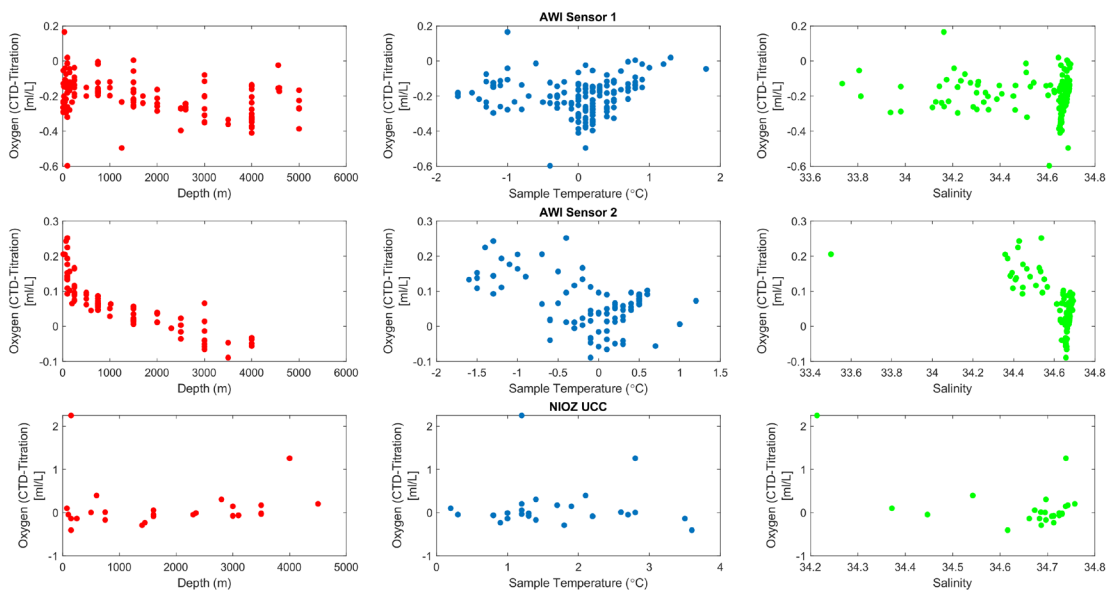


Fig. 5.4: Oxygen concentration difference (CTD optode – titration) compared to depth (red), temperature (blue) and salinity (green) for AWI CTD sensor 1 (top row), AWI CTD sensor 2 (middle row) and NIOZ UCC (bottom row).

Discrepancies in bottle volume were noticed on the 29.01.19 at 18:30 UTC. The volumes stored in the database were corrected (Tab. 5.2).

**Tab. 5.2:** Old and correct volumes of bottles used to collect and analyse oxygen samples

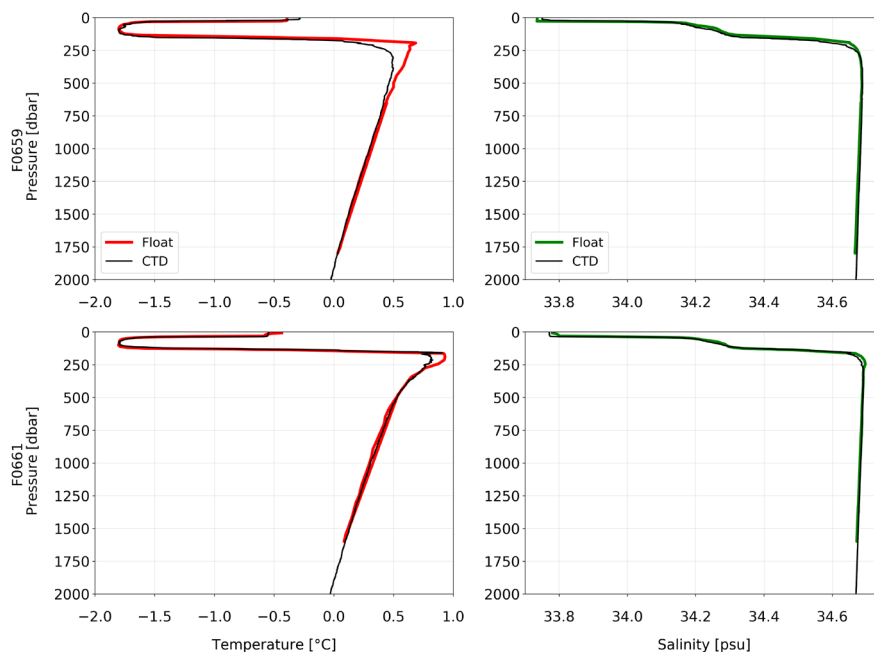
Bottle ID	Old Volume [mL]	Correct Volume [mL]	Samples
75	116.48	115.29	9
76	117.64	115.26	5
83	116.56	115.50	3
85	116.73	115.16	6

#### 5.4 Preliminary data of PICCOLO floats

We here show the first cycle of both PICCOLO BGC floats and compare their measured temperature and salinity profiles with those of the CTD that was cast at the deployment station (Fig. 5.5). The SBE41cp sensor on the floats seem to overestimate the temperature maximum. We also show the temperature and salinity profiles of the first number of cycles of both floats (Fig. 5.6).

Unfortunately, one of the PICCOLO BGC floats (F0661) lost communication with its CTD (SBE41) between its third and fourth cycle. This problem continued to occur in subsequent cycles. SeaBird Scientific has been notified and are looking into the problem. At the time of writing this report, we are changing a number of parameters in the mission configuration file, which will be uploaded by the float the next time it re-surfaces. This will hopefully be able to give us some more insight into the issues that the sensor is experiencing.

*Fig. 5.5: Temperature (left, red) and salinity (right, green) profiles of the PICCOLO BGC float F0659*



*(top) and F0661 (bottom) during their first cycle, in comparison to the respective profiles by the AWI CTD at the deployment station (black).*

## 5.4 Preliminary data of PICCOLO floats

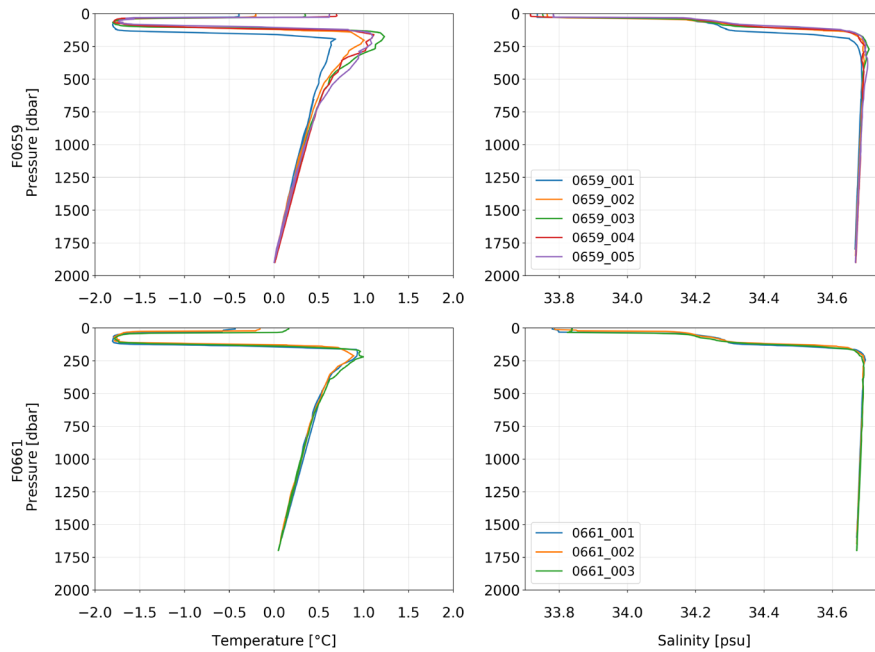
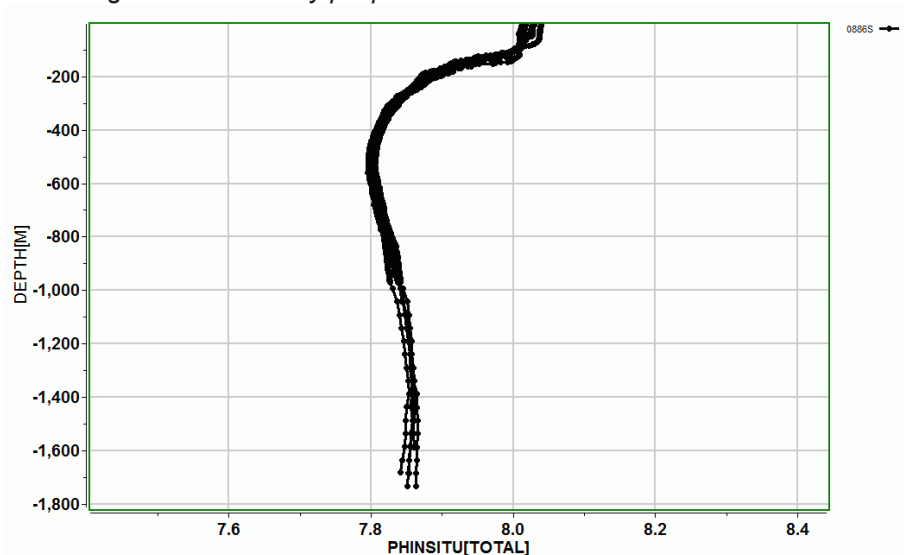


Fig. 5.6: Temperature (left, red) and salinity (right, green) profiles of the PICCOLO BGC float F0659 (top) and F0661 (bottom) for all profiles to date.

## 5.5 Preliminary data of SOCCOM floats

Initial profiles indicate that the pH sensor on SOCCOM float 689 is not functioning. All other sensors on all other floats are recording values within normal operating limits. An example of these data can be seen in the preliminary pH profiles from float 0886 (Fig. 5.7)

Fig. 5.7: Preliminary pH profiles from SOCCOM BGC float 0886



## Data Management

Data obtained by the PICCOLO floats will be made publicly available through the Argo program and will therefore comply with the Argo data management and access regulations (<http://biogeochemical-argo.org/data-management.php>, <http://biogeochemicalargo.org/data-access.php>). Raw data can be retrieved from the Global Data Centre IFREMER (<ftp://ftp.ifremer.fr/ifremer/argo>), but will still need to go through the data quality control and formatting procedures by the British Oceanographic Data Centre (BODC). SOCCOM collected data as well as shipboard calibrations are made publicly available in near real time through the SOCCOM data portal (<https://socom.princeton.edu/content/data-access>).

## References

- Bakker D C E, Hoppema M, Schröder M, Geibert W & De Baar, H J (2008) A rapid transition from ice covered CO<sub>2</sub>-rich waters to a biologically mediated CO<sub>2</sub> sink in the eastern Weddell Gyre. *Biogeosciences Discussions*, 5(2), 1205-1235.
- Carpenter J H (1965) The Chesapeake Bay Institute technique for the Winkler dissolved oxygen method. *Limnol. Oceanogr.* 10, 141-143.
- Dickson A G, Sabine C L & Christian J R (2007) Guide to best practices for ocean CO<sub>2</sub> measurements. North Pacific Marine Science Organization.
- Hoppema M, Bakker K, van Heuven S M, van Ooijen J C & de Baar H J (2015) Distributions, trends and inter-annual variability of nutrients along a repeat section through the Weddell Sea (1996–2011). *Marine chemistry*, 177, 545-553.
- Johnson K S, Plant J N, Coletti L J, Jannasch H W, Sakamoto C M, Riser S C ... & Talley L D (2017) Biogeochemical sensor performance in the SOCCOM profiling float array. *Journal of Geophysical Research: Oceans*, 122(8), 6416-6436.
- Klatt O, Boebel O, & Fahrbach E (2007) A profiling float's sense of ice. *Journal of Atmospheric and Oceanic Technology*, 24(7), 1301-1308.
- Olsen A, Key R M, van Heuven S, Lauvset S K, Velo A, Lin X ... & Jutterström S (2016) The Global Ocean Data Analysis Project version 2 (GLODAPv2)—an internally consistent data product for the world ocean. *Earth System Science Data (Online)*, 8(2).
- Orsi A H, Whitworth III T & Nowlin Jr W D (1995) On the meridional extent and fronts of the Antarctic Circumpolar Current, *Deep-Sea Research I*, 42, 641-673.
- van Heuven S M, Hoppema M, Huhn O, Slagter, H A & de Baar H J (2011) Direct observation of increasing CO<sub>2</sub> in the Weddell Gyre along the Prime Meridian during 1973–2008. *Deep Sea Research Part II: Topical Studies in Oceanography*, 58(25-26), 2613-2635.

## 6. OCCURRENCE OF MICROPLASTICS IN THE ANTARCTIC SEAS

Patricia Burkhardt-Holm<sup>1</sup>, Clara  
Leistenschneider<sup>1</sup>, Helmut Segner<sup>2</sup>  
Not on board: Linda Amaral-Zettler<sup>3</sup>,  
G. Gerdtts<sup>4</sup>

<sup>1</sup> MGU  
<sup>2</sup> U Bern  
<sup>3</sup> NIOZ  
<sup>4</sup> AWI Helgoland

**Grant-No. AWI\_PS117\_04**

### Objectives

We aim to advance our knowledge and understanding of the sources of microplastics (MP) in the remote Antarctic marine ecosystem. By applying material flow analysis and integrating the results into an ocean circulation model, we will evaluate the evidence that MP can cross the Antarctic Circumpolar Current (ACC) into the Southern Ocean around Antarctica.

A successful outcome will include achieving the following goals:

- Providing baseline information on concentrations, composition and distribution of MP in surface and sub-surface waters, as well as from ice cores from the Southern Ocean,
- Evaluate the sources of MP in the Southern Ocean, by: (1) comparing MPs in the more anthropogenically impacted Scotia Sea (SS) and Western Antarctic Peninsula (WAP) versus relatively pristine Weddell Sea (WS) and (2) modeling MP transport within and to/from Antarctica.

These comparisons will be based on characterization of MP properties, such as particle morphology, polymer composition, extent of degradation, and (b) examination of the microbial communities of the MP (Plastisphere).

### Work at sea

The upper 18 cm of surface water were sampled for MP with a Manta Trawl (floating neuston net towed to on-board crane for trawling;  $n = 24$ , Fig. 6.1 and Tab. 6.1). Sub-surface water was sampled by filtering pumped seawater from beneath the vessel at approximately 11.2 m depth ( $n = 85$ , Fig. 6.2 and Tab. 6.2). When possible, samples were scanned visually for MP on board using a dissection microscope. Suspicious particles were analyzed using Fourier Transform Infrared Spectrometry (FT-IR) to confirm that particles are synthetic polymers and to evaluate the polymer composition. Surface water samples with high densities of biological material were stored frozen at  $-20^{\circ}\text{C}$  and will be analyzed at the home laboratory at University of Basel subsequently to a purification treatment. Sub-surface water samples with particle sizes smaller  $300\ \mu\text{m}$  will be analyzed at the laboratories of AWI Helgoland in cooperation with Gunnar Gerdtts (AWI) applying Focal Plane Array (FPA) – based FT-IR (Löder et al., 2015) MP collected will be analyzed for polymer type, particle morphology and size.



Fig. 6.1: Manta Trawl (MT) deployed in the Southern Ocean. Between the yellow bridle of the MT and the steel rope of the on-board crane an 8 kg steel weight is attached to stabilise the trawl.



Fig. 6.2: Wooden protection covering geological sieves to allow for undisturbed sampling. Samples are taken from the on-board seawater intake system connected to the protected sieve stack with a water meter and a silicone hose.

### *Suspended surface solids sampled by Manta Trawl*

24 trawls were performed during PS117 (Fig. 6.3 and Tab. 6.1). Except for one trawl which was aborted due to ice accumulation in the mesh after 20 minutes (MT 7; PS117\_32-2), all trawls were completed successfully with a sampling time of 30 minutes. The Manta Trawl (MT) (aperture: 60 cm x 18 cm) is equipped with a mechanical flowmeter and a 300  $\mu$ m mesh with a removable cod end. The MT (total weight  $\approx$  15 kg) was deployed by an on-board crane adding an 8 kg steel weight to the end of the cranes steel rope connected with the rope of the MT to improve stability against dynamic forces such as wind and waves (Fig. 6.1). The on-board

crane was extended to its maximum and the steel rope of the crane was released long enough to allow for a flat sampling angle ( $\leq 30^\circ$ ). Thus, during sampling the MT was approximately 20 m behind the crane and 5 m away from the side the hull (depending on wind, current and vessel course) at starboard side. The tows were performed at a vessel speed of 2 knots during a target trawling duration of 30 minutes. This resulted in an average ( $\pm$  SD) of approximately  $203 \pm 60 \text{ m}^3$  of filtered seawater per successful sample and a total of  $4690,03 \text{ m}^3$ .

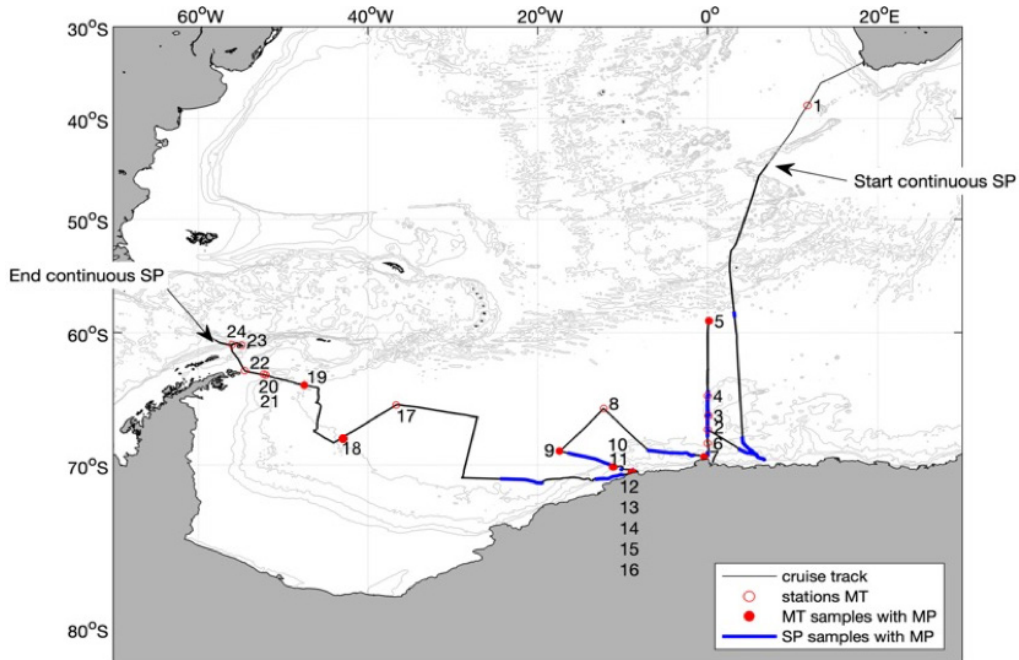


Fig. 6.3: Sampling locations. The black line represents the Polarstern track on expedition PS117. Red dots represent the sites where the MT was deployed to sample surface water for MP. Filled red dots indicate that MP was found in the sample. Continuous sampling with the seawater pump (SP) started at latitude  $-44.667677$  and longitude  $7.0855$  (and was stopped at latitude  $-60.666318$  and longitude  $57.906921$ ). Blue lines represent SP transects in which MP was found.

After every tow the MT was hauled from the water and the mesh's outside was rinsed down with the seawater hose so that particles attached to the mesh were rinsed down into the removable cod end. Subsequently the cod end was removed, transferred to a rinsed glass jar immediately and sealed with a metal lid to prevent air bore contamination of the sample. After inspecting the sample visually for MP suitable for Plastisphere analysis (inhabiting microbial community characterizations) in the laboratory the content of the cod end was rinsed with milli-Q into a pre-rinsed glass beaker and filtrated to decrease the volume of the Sample ( $70 \mu\text{m}$  or  $250 \mu\text{m}$  filters cut to size from PTFE-gauze). For visual inspection samples were transferred to a Bogorov counting chamber and screened using a stereomicroscope (Olympus SZ61) equipped with a camera (Olympus SC50) and connected to the imaging software CellSens (Version 2.1; 6 samples will need purification treatment at the home laboratory prior to visual inspection due to the high abundance of biological residue). Samples, with very low concentrations of biological residues were inspected for MP directly on  $70 \mu\text{m}$  PTFE filters. In total 11 surface water samples were analyzed on board.

Putative anthropogenic particles were sorted and analyzed for polymer composition using FT-IR spectroscopy (Agilent 4500 Portable FTIR with MicroLab PC software). Recorded spectra

will be compared against a larger reference spectra library (KnowItAll IR Spectral Library) in our home laboratory at the University of Basel to confirm the results.

Samples for microbial DNA-analysis were subdivided into three pieces. One piece was fixed in 2 mL PureGene lysis buffer, another sub-sample for microscopy via FISH and CLASI-FISH was fixed in paraformaldehyde (for less than 24 hours) then transferred to 50 % ethanol in PBS for storage at  $-20^{\circ}\text{C}$ . The third piece was used to identify polymer composition using FT-IR. For the comparison of free-living microbial communities with those on MP, 2 L of seawater were drawn with a steel bucket during MT trawling and subsequently filtered through a  $0.2\ \mu\text{m}$  Sterivex™ cartridge filter (Millipore). Cartridges were subsequently run dry and flooded with 2 ml of PureGene lysis buffer. Four items were saved for this purpose, one from MT1 and three from a RMT (PS117\_52-1; one cable binder, a piece of black tape and a rope). However, two of the items (the particle from MT1 and rope found in the RMT sample) were not identified to be synthetic polymers.

### *Sub-surface suspended solids sampled by on-board sea water pump*

To address the MP load in the sub-surface water layer, 85 samples were taken from the pumped seawater intake in the on-board wet lab. A Klaus Union Sealex Centrifugal Pump (Bochum, Germany) delivered seawater from approx. 11.2 m depth to the laboratory via stainless steel pipes (first described by Lusher et al., 2014). The first sub-surface sample (SP1 and 2) was taken parallel to the first MT using a stack of three geological sieves and a lower mesh boundary of  $20\ \mu\text{m}$  (combined with a  $100\ \mu\text{m}$  and a  $300\ \mu\text{m}$  sieve) according to the protocol of T. Mani (University of Basel) from PS111. Afterwards the protocol was modified, and samples were taken continuously along the cruise track starting at latitude  $-44,66768$  and longitude  $7,0858$  (Fig. 6.3; 2019-12-18, 09:46 (UTC)). The lower mesh size was increased to  $100\ \mu\text{m}$  combined with a  $300\ \mu\text{m}$  sieve to prevent clogging and an overflow of the samples. Every 12 or 24 hours both size fractions were transferred to pre-rinsed glass jars individually, using milli-Q and a PTFE-Squirt bottle as rinsing agent (during that procedure sampling was interrupted for 5 minutes in average). To investigate MP that might be released during ballast water exchange to the environment, one sub-surface water sample (SP8; lower mesh size  $20\ \mu\text{m}$ ) was taken parallel to the exchange of approximately  $250\ \text{m}^3$  of ballast water.

Samples were sealed with metal lids, and stored in v:v 50:50 suspended sample:EtOH at  $+4^{\circ}\text{C}$ . While samples of the  $>300\ \mu\text{m}$  fraction were transferred to cellulose filters (pore size  $12\text{-}25\ \mu\text{m}$ ) for visual inspection (56 samples analyzed on board), samples of the smaller  $100\ \mu\text{m}\text{-}300\ \mu\text{m}$  fraction will be analyzed at the laboratories of AWI in Helgoland.

During sampling sieves were protected from airborne contamination by a dimension-tailored solid wooden construction (Fig. 6.2, adapted from Kanhai et al., 2016). The sampling effort resulted in a total of 85 samples per size fraction. A mean ( $\pm$  SD) water flow duration of  $12.8 \pm 4.7$  hours at  $0.09 \pm 0.02\ \text{L s}^{-1}$  resulted in an average of  $3.8 \pm 1.4\ \text{m}^3$  filtered seawater per sample. In total  $322.3\ \text{m}^3$  of subsurface water were filtered. A similar volume to an average MT sample ( $203 \pm 6\ \text{m}^3$ ) was yielded after SP55 with a total of  $205,5\ \text{m}^3$  of filtered seawater.

### *Ice Cores for MP studies*

During PS117 five sea ice cores were taken by the SIPES2 group for MP analyses (see table 7.1 SIPES). Ice cores were stored in plastic bags at  $-20^{\circ}\text{C}$  and will be processed and analyzed according to Peeken et al. (2018) in cooperation with Ilka Peeken (AWI) and Gunnar Gerdtz (AWI).

Tab. 6.1: Summary of Manta Trawl samples for microplastics on PS117

Sample ID	Station Name	Date	Coordinates Start	Coordinates End	Area [m <sup>2</sup> ]	Filtered Vol. [m <sup>3</sup> ]
Manta Trawl (MT) 1	PS117_3-4	2018-12-17	-38,605676; 11,765578	-38,614186; 11,786013	1420,02	255,60
MT 2	PS117_14-3	2018-12-26	-67,500007; 0,014731	-67,499536; 0,088869	1405,8	253,04
MT 3	PS117_15-7	2018-12-27	-66,50279; 0,09293	-66,497953; 0,14088	190,06	1055,90
MT 4	PS117_17-2	2018-12-28	-65,001679; 0,013812	-65,005529; 0,073552	962,1	173,178
MT 5	PS117_22-3	2018-12-31	-59,035363; 0,1622	-59,047307; 0,130238	1193,4	214,81
MT 6	PS117_26-3	2019-01-03	-68,500118; 0,009492	-68,49669; 0,063063	562,32	101,22
MT 7 <sup>a</sup>	PS117_32-2	2019-01-04	-69,430119; -0,401573	-69,431673; -0,431255	657	118,26
MT 8	PS117_34-6	2019-01-19	-65,969758; -12,232134	-65,982962; -12,272461	2262,42	407,24
MT 9	PS117_35-1	2019-01-08	-69,054347; -17,474316	-69,05798; -17,428181	876,78	157,82
MT 10	PS117_36-2	2019-01-09	-70,150757; -11,083026	-70,15648; -11,15486	894,06	160,93
MT 11	PS117_38-2	2019-01-19	-70,151107; -11,201088	-70,161906; -11,207465	1106,64	199,19
MT 12	PS117_41-5	2019-01-11	-70,513894; -8,803236	-70,533164; -8,795118	1236,42	222,56
MT 13	PS117_41-7	2019-01-11	-70,507945; -8,81752	-70,523945; -8,798333	1238,22	222,88
MT 14	PS117_41-11	2019-01-12	-70,507945; -8,81752	-70,523229; -8,826951	1241,28	223,43
MT15	PS117_41-14	2019-01-12	-70,515384; -8,781321	-70,526729; -8,82164	1252,62	225,47
MT16	PS117_48-3	2019-01-19	-70,509151; -8,991134	-70,513422; -8,931363	1266,48	227,96
MT17	PS117_56-7	2019-01-23	-65,697443; -36,687479	-65,708079; -36,724115	781,74	140,71
MT18	PS117_57-5	2019-01-24	-70,507945; -8,81752	-70,523229; -8,826951	1171,26	210,83
MT19	PS117_64-3	2019-01-27	-64,196628; -47,505391	-64,213986; -47,492906	721,08	129,79
MT20	PS117_81-3	2019-01-30	-63,341187; -52,303992	-63,34944; -52,292096	1069,56	192,52
MT21	PS117_83-1	2019-01-31	-63,426911; -52,041347	-63,442039; -52,052781	1199,52	215,91

## 6. Occurrence of Microplastics in the Antarctic Seas

Sample ID	Station Name	Date	Coordinates Start	Coordinates End	Area [m <sup>2</sup> ]	Filtered Vol. [m <sup>3</sup> ]
MT22	PS117_95-2	2019-02-01	-63,080642; -54,49727	-63,066914; -54,512013	1156,5	208,17
MT23	PS117_99-4	2019-02-01	-61,012926; -56,015099	-61,019839; -56,046805	1312,02	236,16
MT24	PS117_100-2	2019-02-02	-61,054374; -54,867545	-61,059536; -54,906191	1068,48	192,33

<sup>a)</sup>Aborted after 20 min. due to ice accumulation in MantaTrawl.

**Tab. 6.2:** Summary seawater pump samples for microplastics on PS117

Sample ID	Coordinates Start	Coordinates End	Filtered Vol. [L]	Mesh Size [µm]
Seawater Pump (SP) 1	-38,61351; 11,791623	-38,60131; 11,754382	178	20
SP 2	-43,30161; 8,233274	-43,45973; 8,101273	152,5	20
SP 3	-44,66768; 7,0858	-48,20596; 5,093206	526	20
SP 4	-48,24225; 5,078457	-52,20356; 3,403959	1674	100
SP 5	-52,23723; 3,388744	-54,59126; 2,590244	6435	100
SP 6	-54,67503; 2,601824	-57,33656; 2,979147	3594	100
SP 7	-57,38811; 2,987054	-58,02244; 3,080343	3812	100
SP 8	-58,26027; 3,115871	-58,76528 3,192664	830,5	100
SP 9	-58,83714; 3,203444	-62,21459; 3,564964	773,5	20
SP 10	-62,23731; 3,566866	-65,00854; 3,812596	4875	100
SP 11	-65,05664; 3,817129	-67,96025; 4,104577	3452,5	100
SP 12	-67,99669; 4,106763	-69,54479; 6,388922	3797	100
SP 13	-69,54668; 6,438313	-68,85369; 3,620448	3651,5	100
SP 14	-68,82288; 3,52709	-67,49855; -0,000018	3606	100
SP 15	-67,49857; -0,000079	-66,51486; -0,169729	4243	100
SP 16	-66,51512; -0,17006	-66,52085; -0,091653	3721,5	100

Sample ID	Coordinates Start	Coordinates End	Filtered Vol. [L]	Mesh Size [µm]
SP 17	-66,011767; -0,004262	-64,535269; 0,033176	95	100
SP 18	-63,00069; 0,001347	-60,99677; -0,009448	2231	100
SP 19	-60,99656; -0,009755	-59,08385; 0,100012	3168	100
SP 20	-59,08404; 0,098945	-63,59823; -0,0129	8122	100
SP 21	-63,6129; -0,011185	-65,98879; -0,00766	7530,5	100
SP 22	-66,00824; -0,007549	-67,99976; -0,00104	7690,5	100
SP 23	-67,99974; -0,001088	-68,971; 0,15246	6059	100
SP 24	-68,97837; 0,159809	-69,16674; 0,006688	3919,5	100
SP 25	-69,17175; 0,006624	-69,36571; -0,158526	3592,5	100
SP 26	-69,36592; -0,159442	-69,30268; -1,579487	3844,5	100
SP 27	-69,30372; -1,584887	-69,00693; -6,99193	804,5	100
SP 28	-69,00763; -6,993489	-69,01373; -7,003758	6786	100
SP 29	-69,01482; -6,99408	-67,85038; -9,059098	4007	100
SP 30	-65,96891; -12,22967	-67,84162; -9,074264	4000	100
SP 31	-65,96856; -12,22128	-65,96875; -12,23105	3758,5	100
SP 32	-65,96854; -12,23059	-67,68612; -15,01383	3960	100
SP 33	-67,69748; -15,0326	-69,05671; -17,43267	3814,5	100
SP 34	-69,0567; -17,43072	-69,16548; -16,55439	3639	100
SP 35	-69,17287; -16,50136	-70,16063; -11,24673	2556	100
SP 36	-70,1624; -11,27275	-70,17646; -11,00258	3244	100
SP 37	-70,17653; -11,0027	-70,29848; -10,03482	4170	100
SP 38	-70,29852; -10,03535	-70,30832; -10,19833	3752	100
SP 39	-70,30847; -10,1898	-70,35264; -8,999914	3907	100
SP 40	-70,35257; -9,000182	-70,51579; -8,789991	3272	100

## 6. Occurrence of Microplastics in the Antarctic Seas

Sample ID	Coordinates Start	Coordinates End	Filtered Vol. [L]	Mesh Size [ $\mu\text{m}$ ]
SP 41	-70,52239; -8,768191	-70,5228; -8,774486	4377	100
SP 42	-70,52285; -8,772641	-70,44725; -8,484728	3607,5	100
SP 43	-70,44849; -8,482395	-70,50389; -8,191863	3801,5	100
SP 44	-70,50389; -8,191864	-70,50398; -8,190612	4454	100
SP 45	-70,50398; -8,190612	-70,50402; -8,190597	3501	100
SP 46	-70,50402; -8,190598	-70,50403; -8,190532	3579	100
SP 47	-70,50403; -8,190526	-70,50402; -8,190645	3868	100
SP 48	-70,50403; -8,190642	-70,50403; -8,190578	4336	100
SP 49	-70,50403; -8,190528	-70,32506; -8,766672	2501	100
SP 50	-70,32477; -8,772601	-70,50554; -8,937188	3800,5	100
SP 51	-70,50551; -8,937024	-70,50394; -8,190229	4338,5	100
SP 52	-70,50396; -8,190245	-70,67946; -9,910464	4230,5	100
SP 53	-70,68892; -9,925345	-70,98264; -13,28406	4182,5	100
SP 54	-70,9831; -13,28891	-70,87252; -15,46381	4040	100
SP 55	-70,87133; -15,48842	-71,23834; -19,64886	3570	100
SP 56	-71,23863; -19,64943	-70,96427; -24,44725	3874	100
SP 57	-70,96371; -24,4805	-70,8779; -28,99613	3556	100
SP 58	-70,87927; -28,98561	-70,05584; -28,55931	3971,5	100
SP 59	-70,04611; -28,55484	-67,62811; -27,52557	3480,5	100
SP 60	-67,62002; -27,52231	-66,6024; -27,0629	3732	100
SP 61	-66,60231; -27,06345	-66,16765; -31,35781	3940	100
SP 62	-66,16579; -31,37127	-65,84219; -34,43346	3657,5	100
SP 63	-65,84169; -34,44335	-65,69301; -36,67069	3843	100
SP 64	-65,69295; -36,66994	-66,44405; -38,62307	3732	100

Sample ID	Coordinates Start	Coordinates End	Filtered Vol. [L]	Mesh Size [ $\mu\text{m}$ ]
SP 65	-66,45808; -38,65897	-68,44515; -44,00705	3419	100
SP 66	-68,45057; -44,02344	-68,46515; -44,01802	3196,5	100
SP 67	-68,46513; -44,018	-67,6676; -46,32515	4490,5	100
SP 68	-67,66745; -46,32557	-67,46764; -46,03488	3639	100
SP 69	-67,46148; -46,02367	-65,50127; -46,0873	3845	100
SP 70	-65,50324; -46,0884	-64,41016; -45,84601	3827	100
SP 71	-64,41036; -45,8456	-64,25409; -47,01163	3891	100
SP 72	-64,25425; -47,01232	-64,18999; -47,50533	3638	100
SP 73	-64,18744; -47,5002	-64,06783; -48,39712	3866	100
SP 74	-64,06782; -48,40614	-63,86032; -49,56743	3894	100
SP 75	-63,85696; -49,58072	-63,73037; -50,37285	3561	100
SP 76	-63,72553; -50,40282	-63,62129; -51,07727	3868,5	100
SP 77	-63,62113; -51,07739	-63,48794; -51,74998	3970,5	100
SP 78	-63,48625; -51,77032	-63,4271; -52,15777	3846	100
SP 79	-63,4265; -52,15767	-63,44849; -51,99276	3753	100
SP 80	-63,44818; -51,99344	-63,22453; -53,65026	3581,5	100
SP 81	-63,21963; -53,68283	-61,36304; -56,07638	3653,5	100
SP 82	-61,35035; -56,078	-60,89787; -55,51887	4235	100
SP 83	-60,89323; -55,49793	-60,89323; -55,49793	3472	100
SP 84	-60,91735; -55,60286	-60,85542; -57,50484	3830	100
SP 85	-60.855628; -57.504516	-60.666318; -57.906921	4015	100

### Preliminary and expected results

All samples taken during PS117 will undergo further visual inspection, chemical and spectroscopic analysis and evaluation in the home laboratory. Thus, we present here only preliminary results.

15 out of 24 surface water samples collected with the manta trawl were screened for MP on board. All samples yielded fragments of anthropogenic origin with concentrations between 0.004 and 0.13 fragments  $m^{-3}$ . Fibers were also found in all MT samples with concentrations between 0.04 and 0.25 fibers  $m^{-3}$  (Fig. 6.4). With up to 0.12 fragments  $m^{-3}$  most of the particles were identified as ship paint by FT-IR spectroscopy and comparison to spectra of reference samples taken from ship paint of RV *Polarstern*. These ship paint particles were found in all analyzed surface water samples except for MT 14. Mostly blue, orange, white and green paint fragments were found (Fig. 6.5). While blue fragments might originate from the hull of RV *Polarstern* and the railing, orange particles might derive from the on-board cranes, green particles from the steel frames of the wooden floor of the working deck and the stairs and the floors on the different decks. White ship paint might derive from the railing and from the walls and doors of the vessel. While paint fragments of all colors might be blown or washed from the vessel into the water, blue paint fragments might also be released from the vessels hull due to mechanical abrasion from the water.

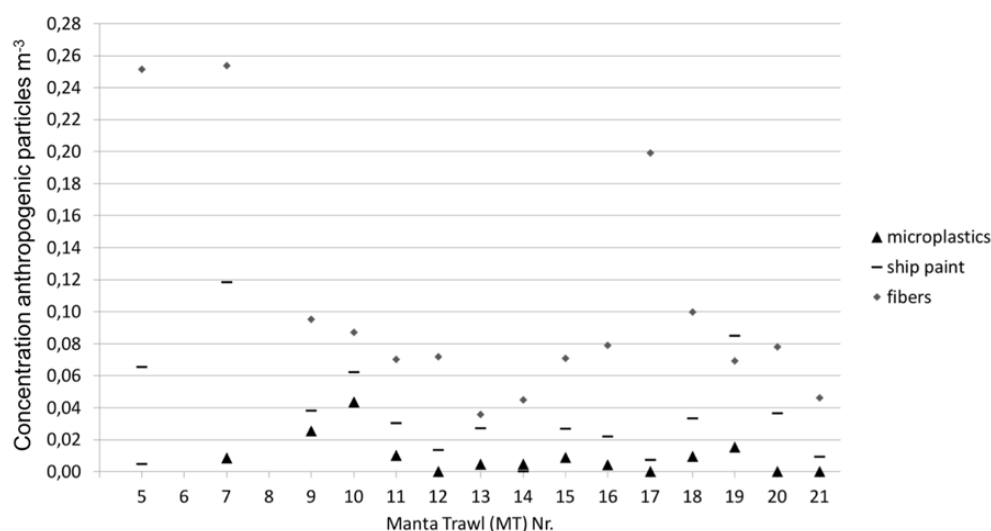


Fig. 6.4: Preliminary frequency distribution of anthropogenic particles  $m^{-3}$  in 15 surface water samples (MT) analysed on board. Samples taken during PS117 will undergo further visual inspection, spectroscopic analysis and evaluation in the home laboratory (University of Basel).

MP were found in 11 out of 15 analyzed MT samples with concentrations between 0 and 0,025 MP  $m^{-3}$ . The most abundant polymer type with five fragments was chlorobutyl (three fragments in MT10 and two in MT13; Fig. 6.6A), a copolymer made of chlorinated isobutylene and isoprene. Due to its low gas and moisture permeability it is mainly used for air hoses, seals, tire innerliners and membranes (Polymer Properties Database, 2018). Four particles of nylon and polyester were found, respectively and neoprene was found two times in our samples.

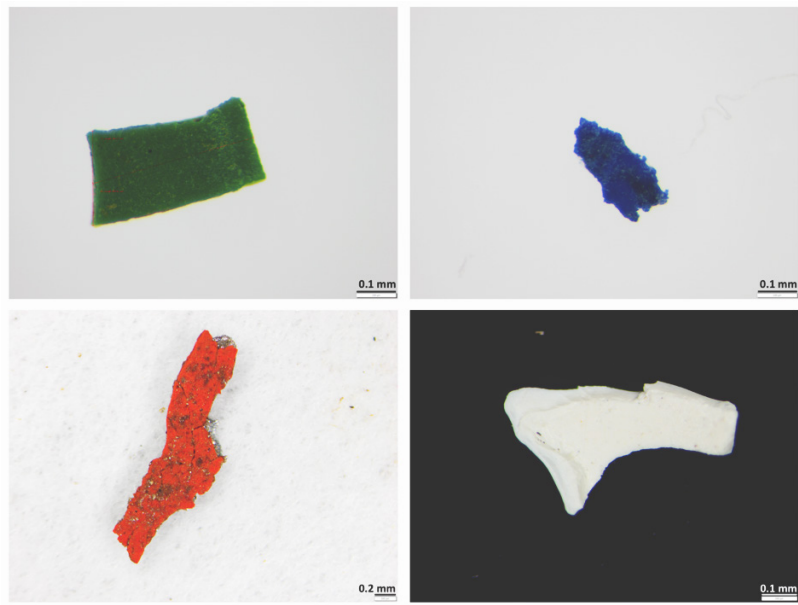


Fig. 6.5: Anthropogenic fragments identified as ship paint from MT 16 (green), MT 18 (blue), MT 7 (red/orange) and MT 10 (white) respectively.



Fig. 6.6: Chlorobutyl fragment from MT 13 (A), polyester fragment from SP 8 (B) and neoprene fragment from SP 12 (C)

The 56 sub-surface samples analyzed on board (size fraction  $>300 \mu\text{m}$ ) yielded a total volume of  $219.5 \text{ m}^3$  filtered seawater and an average volume of  $3.7 \text{ m}^3$  per sample. In contrast to the MT samples no ship paint was found in the samples taken with the seawater pump. Even though ship paint fragments might sink to deeper waters (paint fragments found in our MT samples did always sink to the bottom of the sampling jars having a higher density than water) freshly released fragments might be retained in the water surface layer due to current and bow wave induced turbulences. Further, it might be possible that vessel-released particles are transported away from the hull by the bow wave.

MP were found in 12 sub-surface water samples with concentrations between 0 and  $1.24 \text{ MP m}^{-3}$ . This excludes the sample taken parallel to the ballast water exchange. Here four polyester fragments were found, yielding a concentration of  $4.82 \text{ particles m}^{-3}$  (SWP8; Fig. 6.6B). Neoprene was the most abundant polymer ( $n=5$ ; Fig. 6.5C) followed by polyester ( $n=4$ ) and chlorobutyl ( $n=3$ ). Concentrations of fibers varied between 0 and  $3.73 \text{ fibers m}^{-3}$ .

Fibers can easily be introduced from clothing and other textiles while processing and analyzing the sample. However, the fact that in 13 inspected sub-surface samples no fibers were found might support the efficiency of our measures to avoid airborne contamination and give a hint that fibers are present in sub-surface waters of the Southern Ocean.

In contrast to plastic studies in other parts of the world's oceans where mainly polyethylene and polypropylene fragments were found (Hidalgo-Ruz et al., 2012) plastic fragments found in our samples are mainly used in isolation panels, tubing and hoses, instrument housings and cable sheathings (Polymer Properties Database, 2018).

### *Outlook*

Especially in a pristine environment like the Southern Ocean vessel-induced contamination might alter the results of microplastic studies. Thus, samplings would ideally be conducted independently from the vessel. At good weather conditions for example sampling with the MT from a small motorboat out of the reach from vessel-induced contamination might result in more undisturbed samples. Further, sediment samples, ingested microplastics by biota such as zooplankton and pelagic fish and ice cores might provide compartments that are relatively undisturbed by vessel-related activity and should be investigated with more effort in the future, not the less to investigate the uptake and impact of MP on Antarctic biota and possible sinks of MP in the Southern Ocean.

### **Data management**

Microplastic samples will either be destroyed by analysis or those not analysed will be stored at the home laboratory at University of Basel. All sequence data will be deposited in EBI's European Nucleotide Archive and will conform to the minimum information standards recommended by the Genomics Standards Consortium (<http://gensc.org/projects/mixs-gscproject/>). Metadata and results will be stored at data servers of the University of Basel. After a thorough quality control, processing and publication in a peer reviewed journal, the processed data will be stored in the PANGAEA data base.

### **References**

- Hidalgo-Ruz V, Gutow L, Thompson RC & Thiel M (2012) Microplastics in the marine environment: A review of the methods used for identification and quantification. *Environ. Sci. Technol.*, 46, 3060 – 3075.
- Kanhai LDK, Officer R, Lyashevskaya O, Thompson RC & O'Connor I (2016) Microplastic abundance, distribution and composition along a latitudinal gradient in the Atlantic Ocean. *Marine Pollution Bulletin*, 115, 307-314.
- Löder MGJ, Kuczera M, Mintenig S, Lorenz C & Gerdtz G (2015) Focal plane array detector-based micro-Fourier-transform infrared imaging for the analysis of microplastics in environmental samples. *Environ. Chem.*, 12, 563-581.
- Peeken I, Primke S, Beyer B, Gütermann G, Katlein C, Krumpfen T, Bergmann M, Hehemann L & Gerdtz G (2018) Arctic Sea ice is an important temporal sink and means of transport for microplastics. *Nature Communications*, 9:1505.
- Polymer Properties Database, polymerdatabase.com (2018): <http://polymerdatabase.com/Elastomers/Elastomers2.html>; <http://polymerdatabase.com/mainclasses.html> (Accessed: 01.02.2019).

## 7. SEA ICE PRODUCTION AND ECOLOGY STUDY (SIPES 2)

Giulia Castellani<sup>1</sup>, Klaus Meiners<sup>2</sup>, Susanne Kuehn<sup>3</sup>, Mark Milnes<sup>2</sup>, Martina Vortkamp<sup>1</sup>, André Meijboom<sup>3</sup>, Bram Feij<sup>4</sup>, Michiel van Dorssen<sup>5</sup>  
Not on board: Hauke Flores<sup>1</sup>, Anton van de Putte<sup>6</sup>, Fokje L. Schaafsma<sup>3</sup>, Jan A. van Franeker<sup>3</sup>

<sup>1</sup>AWI  
<sup>2</sup>AAD  
<sup>3</sup>WMR  
<sup>4</sup>NIOZ  
<sup>5</sup>van Dorssen Metaalbewerking  
<sup>6</sup>RBINS

**Grant-No. AWI\_PS103\_06**

### Objectives

SIPES was designed as an inter-disciplinary field study focussing on the inter-connection of sea ice physics, sea ice biology, biological oceanography and top predator ecology. Pelagic food webs in the Antarctic sea ice zone can depend significantly on carbon produced by ice-associated microalgae. Future changes in Antarctic sea ice habitats will affect sea ice primary production and habitat structure, with unknown consequences for Antarctic ecosystems. Antarctic krill (*Euphausia superba*) and other species feeding in the ice-water interface layer may play a key role in transferring carbon from sea ice into the pelagic food web, up to the trophic level of birds and mammals (Flores et al., 2012; David et al., 2016; Kohlbach et al., 2017, 2018; Meyer et al., 2017). To better understand potential impacts of changing sea ice habitats for Antarctic ecosystems, AWI's section of Polar Biological Oceanography in cooperation with Wageningen Marine Research (WMR), the Royal Belgian Institute for Natural Sciences (RBINS) and the Australian Antarctic Division (AAD) collaborate to investigate the role of sea ice in structuring Antarctic marine ecosystems. To achieve this overall objective we combined 1) quantitative sampling of the in-ice, under-ice and pelagic communities in relation to environmental parameters; 2) under-ice habitat observations using an instrumented Remotely Operated Vehicle (ROV); 3) investigations of the diet of sea ice-associated organisms; and 4) the use of molecular and isotopic biomarkers to trace sea ice-derived carbon in pelagic food webs.

In the Southern Ocean, the exploitation of marine living resources and the conservation of ecosystem health are tightly linked to each other in the management framework of the Convention for the Conservation of Antarctic Marine Living Resources (CCAMLR). Antarctic krill is important in this context, both as a major fisheries resource, and as a key carbon source for Antarctic fishes, birds, and mammals. Similar to Antarctic krill, several abundant endothermic top predators have been shown to concentrate in pack ice habitats in spite of low water column productivity (van Franeker et al., 1997). Investigations on the association of krill and other key species with under-ice habitats were complemented by systematic top predator censuses in order to develop robust statements on the impact of changing sea ice habitats on polar marine resource management and conservation objectives.

The evolutionary processes supported by gene flow and genetic selection interact with ecological processes as they overlap temporally to some extent. While gene flow has the tendency to homogenize populations, selective pressure may lead to population differentiation over evolutionary time scales. Throughout the life history of marine organisms dispersal and connectivity play crucial roles in short and long term survival, fitness and evolution. Connectivity

and dispersal are the result of interacting environmental limitations and dispersal capacity, which is influenced by physical and biological processes. The physical processes relate to hydrodynamics (barriers such as the Antarctic Polar Front (APF), transport routes (through deep-water formation) and geographical features (e.g., shallow land bridge of the Scotia Arc (Arntz et al., 2005; Ingels et al., 2006)). Biological processes include behavior, life-history traits, trophic niche, size and other basic biological characteristics. The Southern Ocean forms a unique environment to study evolutionary patterns over different time scales. During the PS117 expedition fish and amphipods samples for molecular analysis were collected. These samples will be used for Barcoding (species identification) and phylogeographic and population genetic work at RBINS.

## Work at sea

### *SUIT sampling*

A Surface and Under-Ice Trawl (SUIT: van Franeker et al., 2009) was used to sample the pelagic fauna down to 2 m under the ice and in open surface waters. The SUIT has two nets, one 0.3 mm mesh plankton net and a 7 mm mesh shrimp net. During SUIT tows, data from the physical environment were recorded using a bio-environmental sensor array. The array includes a CTD equipped with a fluorometer and an altimeter to measure the distance of the SUIT from the bottom of the ice; an ADCP to measure the water flow, and radiometers for measuring hyperspectral under-ice transmitted light. Three SUIT deployments were completed along the 0° meridian from open waters (hauls 1 and 2) into the closed pack ice (haul 3). Five SUIT hauls were carried out in the Eastern Weddell Sea, in both open water and ice covered regions. Another five SUIT hauls were carried out to sample the Western Weddell Sea. An overview of the sampling locations is given in Fig. 7.1. Macrofauna samples from the SUIT shrimp net were sorted to the lowest possible taxonomic level. The catch was entirely preserved frozen (-20°C/-80°C), in ethanol (70%/100%), or in 4% formaldehyde/seawater solution, depending on analytical objectives.

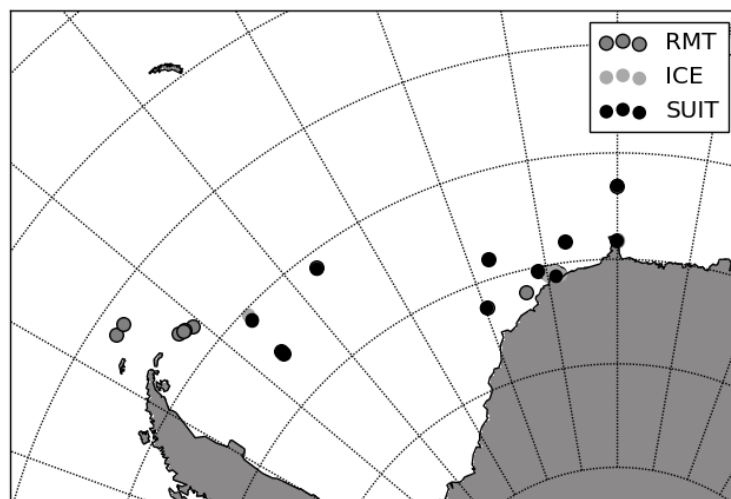


Fig. 7.1: Overview of SUIT, RMT, and ice stations sampled by SIPES-2 during PS117

### *Pelagic sampling*

A Multiple opening Rectangular Midwater Trawl (M-RMT) was used to sample the pelagic community. During deployments, sampling depth, water temperature and salinity were recorded with a CTD probe attached to the bridle of the net. The standard sampling strata were

200 -100 m, 100-50 m, and 50 m to surface. Along the zero meridian, sampling was conducted over the strata 300-100 m, 100-50 m, and 50 m to surface. We conducted 22 depth-stratified hauls with the M-RMT, each sampling 3 distinct depth layers. Three hauls were conducted between 63°S and 69°S on the 0° meridian, 10 hauls were conducted in the Eastern Weddell Sea, 7 hauls were completed in the Western Weddell Sea, and 2 close to Elephant Island (see Fig. 7.1). The catch was sorted by depth stratum and taxon, and size measurements on euphausiids and fish larvae were performed.

*Polarstern's* EK60 echosounder recorded the distribution of acoustic targets continuously during sailing. Our sampling frequencies were 38 kHz, 70 kHz, 120 kHz, and 200 kHz. During station work, the EK60 was switched off to minimize hazard risk for marine mammals approaching the ship. All EK60 data were backed up on the ship's mass storage server.

For biomarker analysis, Particulate Organic Matter (POM) was collected from filtered seawater obtained from the CTD rosette or from the UCC. Coincident deployments of the SUIT-CTD and the CTD rosette have been carried out to calibrate the SUIT-CTD.

#### *ROV deployments*

We deployed an instrumented SeaEye Falcon ROV for under-ice habitat observations during 10 stations. The ROV sensor payload consisted of an acoustic beacon for interrogation by the ship-based GAPS system to support navigation and ROV positioning, an accurate depth sensor and up-ward looking sonar to determine sea ice draft, hyperspectral irradiance and radiance sensors to measure under-ice transmitted radiation to estimate ice algal biomass (e.g., Meiners et al., 2017), an upward looking digital stills camera to quantify krill abundance at the ice-water interface, and several video-camera systems to support navigation and obtain under-ice footage. An additional surface hyperspectral irradiance sensor was installed in the ship's mast and used for data logging during all deployments. The radiometers and stills camera were triggered from the surface and sampled simultaneously. Sensor data from the ROV was transferred via a fibre-optic tether to the surface, where it was logged and time-stamped using a surface computer system. Video and image data from the upward looking cameras and the stills camera were downloaded manually from SD cards at the completion of the deployment.

#### *Sea ice work*

A total of 8 sea ice stations were sampled during PS117. Five ice stations were conducted in the Eastern Weddell Sea pack-ice zone and three stations in Western/North-Western Weddell Sea marginal ice zone (Tab. 7.1 and Fig. 7.1). On each ice station ice cores were collected for a variety of parameters and measurements including ice temperature profiles, ice bulk-salinity profiles, macronutrient concentrations (nitrate, nitrite, phosphate, silicate), ice algal pigment concentrations, POM, and gypsum concentration. On some ice stations additional cores were collected for the determination of microplastic concentrations, ice crystal structure as well as microscopic analyses. Snow thickness and ice freeboard levels were determined at all stations. We also conducted concomitant measurements of integrated ice algal biomass (using chlorophyll-*a* as biomass proxy) and under-ice transmitted irradiance and radiance spectra, in order to develop algorithms to estimate ice algal biomass from the sensor arrays mounted to the SUIT and ROV. For these measurements we deployed the radiometers with L-shaped arms beneath the ice and extracted ice cores directly above the radiometer position (e.g., Melbourne-Thomas et al., 2015). Ice cores for determination of ice bulk-salinity, macronutrient concentrations (nitrate, nitrate+nitrite, phosphate, silicate) and ice algal pigment concentrations were cut into 0.1 – 0.46 m sections (depending on total core lengths) and transported back to ship for melting at +4°C in the dark. For POM sampling, the bottom 0.2 to 0.4 m were collected in a metal barrel and then melted at +4°C in the dark. All other ice cores were stored at -20°C for transport back to AWI and analysis in the home laboratories. Samples for the determination

of ice algal pigment composition and concentrations were filtered onto GF/F filters (Whatman) and will be transported back to AWI for *in-vitro* fluorometric determination of chlorophyll-*a* and algal pigment analyses by High Performance Liquid Chromatography (HPLC).

**Tab. 7.1:** List and positions of the ice stations sampled during PS117 including the number of under-ice radiation measurements (L-arm) and other measurements. Nutr. = sampling for macronutrients, Gap layer = sampling of sea ice gap layers, Microplastics = sampling for microplastics, POM = particulate organic matter, gypsum = gypsum sampling

Station N° PS117_	Position	Date	L-arm	Nutr.	Gap-layer	Micro-plastics	POM	Gypsum
27-2 (ICE1)	69° 04.79' S 0° 00.36' W	03.01.2019	2	Yes	No	Yes	Yes	No
39-1 (ICE2)	70° 17.80' S 9° 59.94' W	10.01.2019	9	Yes	Yes	No	Yes	Yes
39-1 (ICE3)	70° 20.88' S 8° 56.68' W	11.01.2019	3	Yes	Yes	Yes	Yes	No
Heli1 (ICE4)	70° 23.66' S 8° 45.80' W	12.01.2019	2	Yes	Yes	No	No	No
Heli2 (ICE5)	70° 30.21' S 8° 11.62' W	13.01.2019	3	Yes	Yes	No	No	No
Heli3 (ICE6)	70° 30.44' S 9° 10.01' W	16.01.2019	2	Yes	No	No	No	No
Heli4 (ICE7)	70° 38.11' S 9° 54.59' W	17.01.2019	4	Yes	Yes	Yes	No	Yes
Heli5 (ICE8)	65° 12.38' S 45° 56.57' W	26.01.2019	1	No	No	Yes	No	Yes

### *Top predator censuses*

The SIPES-2 team included a top predator counting team consisting of 2 people (Susanne Kuehn and Bram Feij) making ship based counts, and a total of 3 people (Susanne Kuehn, Andre Meijboom and Bram Feij) conducting Helicopter counts. All counts include seabirds, penguins, seals, dolphins and whales. For ship-based counts a 300 m band-transect count with snapshots for birds and additional line transect count for marine mammals was used. The helicopter counts were band transects only, normally set on 250 meters bandwidth.

### **Preliminary and expected results**

#### *SUIT sampling*

**SUIT sensors data** From the 14 SUIT hauls, 6 were conducted in open water, and 8 were conducted under various types of sea ice, including different types of marginal ice zones with relatively small floes separated by brash ice. Bio-environmental profiles were obtained from each SUIT haul (see example in Fig. 7.2). The average ice coverage of the under-ice hauls was ~65 %. Preliminary mean ice draft calculated based on pressure measurements of the SUIT's CTD combined with altimeter data (see Tab. 7.2) ranged between 0.45 m in the marginal ice zone, and more than 3 m in heavy sea ice areas. The marginal ice zone in the Eastern Weddell Sea was formed by thinner floes (haul 06, 08, and 09), whereas in the

Western Weddell Sea the marginal ice zone was characterized by thicker and older floes (hauls 13 and 14). The surface layer salinity increased towards the South during the transect along the 0° meridian and then southwards in the Eastern Weddell Sea. Sea surface temperature shows a clear pattern between ice-free and ice-covered regions, the latter characterized by colder temperatures, even though always above the freezing point. Coldest temperatures were measured in the Western Weddell Sea, showing a spatial pattern but also a temporal progression moving towards the end of summer. In a first analysis of surface chlorophyll-a content, a characteristic pattern of ice-free regions compared to ice-covered regions could not be identified. Chlorophyll-a values were highly variable in the Eastern Weddell Sea, whereas they appear more uniform in the Western part, probably due to the proximity of the stations sampled in the Western Weddell Sea. More insight on the biological productivity of the system, however, can be expected as soon as spectral data from the SUIT's RAMSES sensors can be related to the chlorophyll-a content of sea ice derived from our L-arm measurements and associated ice core sampling.

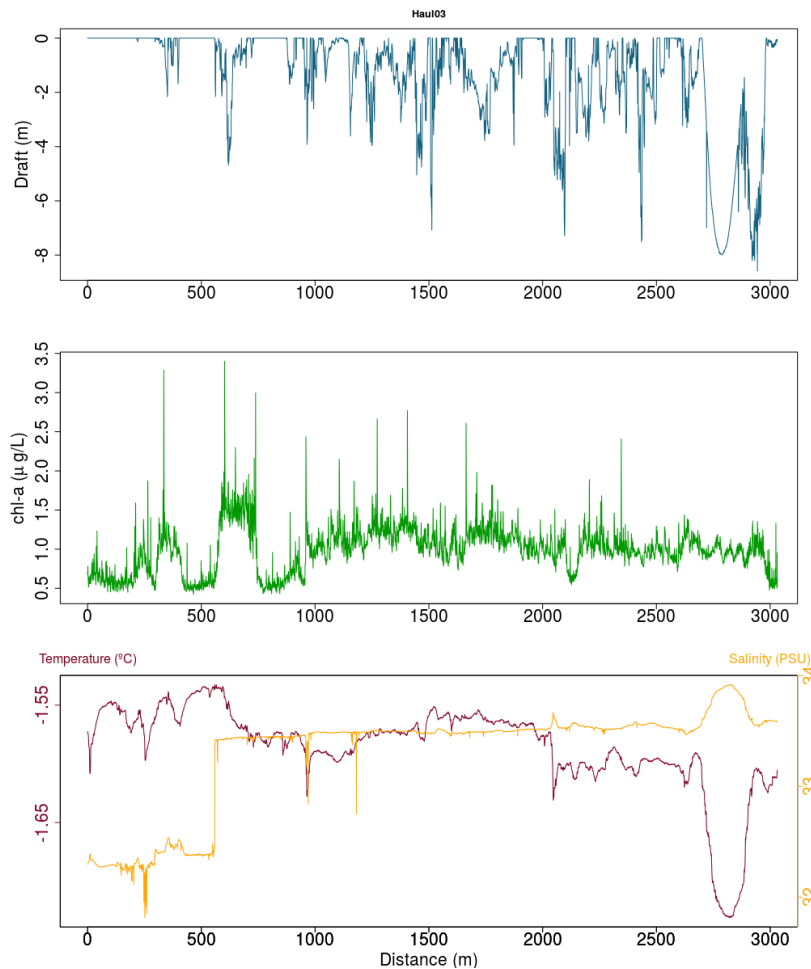


Fig. 7.2: Example of environmental data profiles obtained from the SUIT's sensors array at station 27-4

**Tab. 7.2:** Preliminary results for ice concentration (A), ice thickness ( $H_i$ ), surface temperature (T), and salinity (sal) obtained with the SUIT's sensors array

Stn PS117_	Haul	Date	°lat	°lon	A(%)	Hi(m)	Sal	T(°C)	Chl a(µg/L)
15-6	1	12.27.2018	-66.516	-0.026	0	0	32.7	-0.189	8.78
19-3	2	12.29.2018	-63.006	0.007	0	0	32.976	-0.598	0.97
27-4	3	01.03.2019	-69.078	-0.047	68	1.33	33.307	-1.586	0.99
33-2	4	01.05.2019	-69.013	-6.98	0	0	33.629	-0.359	0.54

Stn PS117_	Haul	Date	°lat	°lon	A(%)	Hi(m)	Sal	T(°C)	Chl a(µg/L)
35-5	5	01.08.2019	-69.065	-17.37	0	0	33.029	-0.046	7.96
37-1	6	01.09.2019	-70.186	-11.234	81	0.98	33.719	-1.292	2.32
48-1	7	01.16.2019	-70.532	-8.898	0	0	33.919	-0.305	0.12
51-1	8	01.18.2019	-69.062	-17.36	3	3.18	31.814	-1.592	3.33
52-1	9	01.19.2019	-71.227	-19.767	76	0.96	32.482	-1.604	7.5
56-8	10	01.23.2019	-65.714	-36.746	0	0	33.424	-1.094	1.12
58-1	11	01.25.2019	-67.663	-46.384	73	0.45	33.635	-1.803	1.37
59-2	12	01.25.2019	-67.54	-46.39	75	0.52	33.523	-1.78	1.16
60-1	13	01.26.2019	-65.5	-46.087	50	1.23	24.643	-1.396	1.25
60-3	14	01.26.2019	-65.53	-46.151	82	1.24	33.402	-1.659	1.24

**SUIT catch composition** The catch from the 7 mm mesh shrimp net was counted and sorted on board. Fig. 7.3 presents an overview of the major species encountered during the PS117 expedition. Antarctic krill *Euphausia superba* was the dominant species in most of the stations. Exceptions are station 27-4, the southernmost stations along the 0° meridian transect, dominated by the euphausiid *Thysanoessa macrura*, station 51-1 dominated by Appendicularia, and station 56-8 in open water in the Western Weddell Sea, dominated by the *Thysanoessa macrura* and characterized by a particularly low biomass and species composition (not shown here). Fig. 7.4 shows the number of individuals of *Euphausia superba* at each station, in correspondence with ice thickness. *E. superba* was abundant in the Western Weddell Sea, particularly in stations characterized by ice thickness of ~0.5 m. Those stations were carried out in the marginal ice zone, characterized by relatively small floes (~20 m diameter). *E. superba* was particularly abundant also at station 52-1 in the Eastern Weddell Sea. Also this station was carried out in the marginal ice zone characterized by small floes separated by brash ice. Station 37-1 (haul 06) is not included because during the trawl the cable broke and the SUIT net with the catch remained in water for several hours before the recovery of the net.

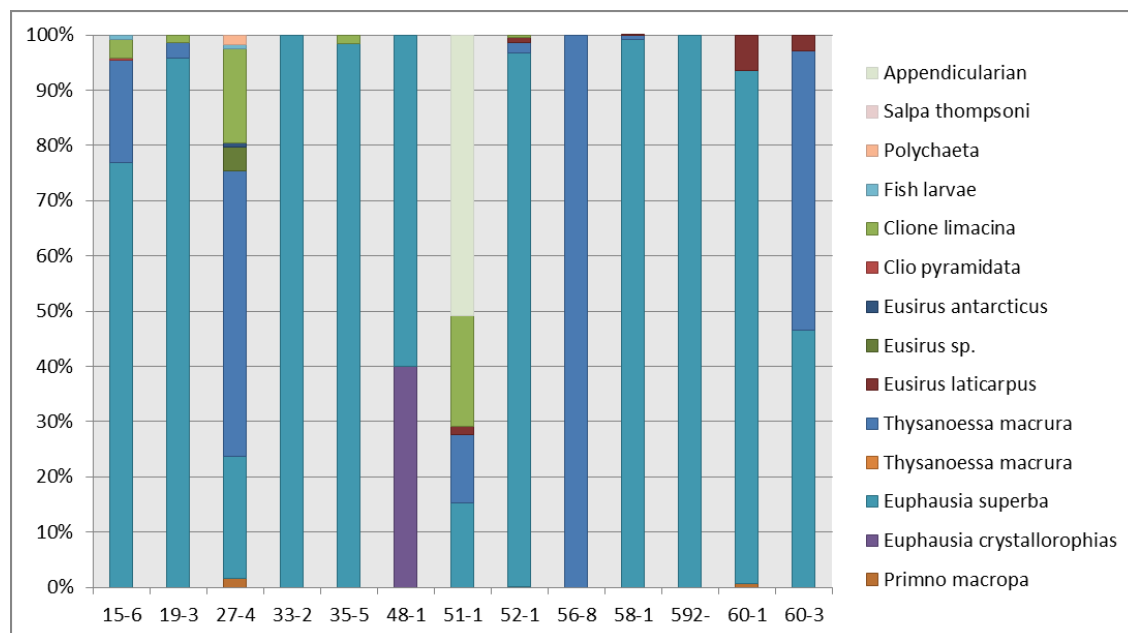


Fig. 7.3: Major taxa of the SUIT catch composition

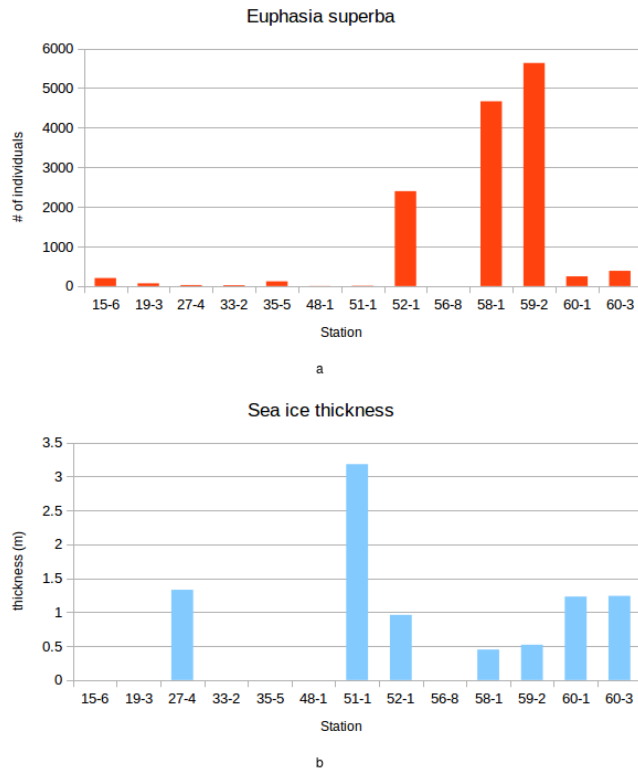


Fig. 7.4: Number of individuals of *Euphasia superba* for each station (panel a) in relation to ice thickness (panel b).

RMT sampling

RMT stations were always conducted in proximity of the SUIT stations. Extra RMT stations were conducted in the area close to Atka Bay, close to the Antarctic Peninsula and close to Elephant Island. An overview of the stations and their position is presented in Tab. 7.3. Fig. 7.5, Fig. 7.6 and Fig. 7.7 show the major taxa of the catch composition of the RMT in the

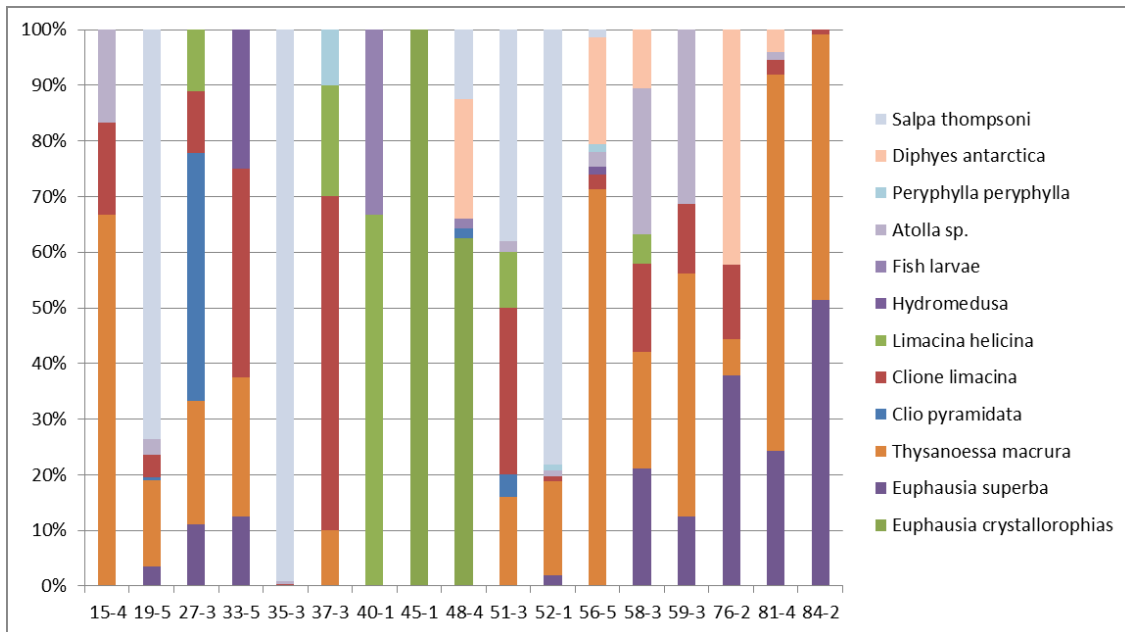


Fig. 7.5: Major taxa of the RMT catch composition at depth 200 m to 100 m

three different nets: 8-1 from 200 m depth to 100 m, 8-2 from 100 m to 50 m, and 8-3 from 50 to surface for all the stations except the two at Elephant Island (not yet analyzed). As in the SUIT net, the krill *Euphausia superba* was highly abundant in the stations carried out in the Western Weddell Sea and close to the Antarctic Peninsula. The krill was more abundant in the surface 50 m, than at depth. In deeper water the catch contained high abundances of jelly fish compared to the surface. Stations 40-1, 45-1, and 45-1 were characterized by high abundances of pteropods in all the three nets. Stations 39-3, 44-1, and 72-5 were not included in the catch analysis because a defect in the communication system with the net prevented the closing of the nets at the designated depth.

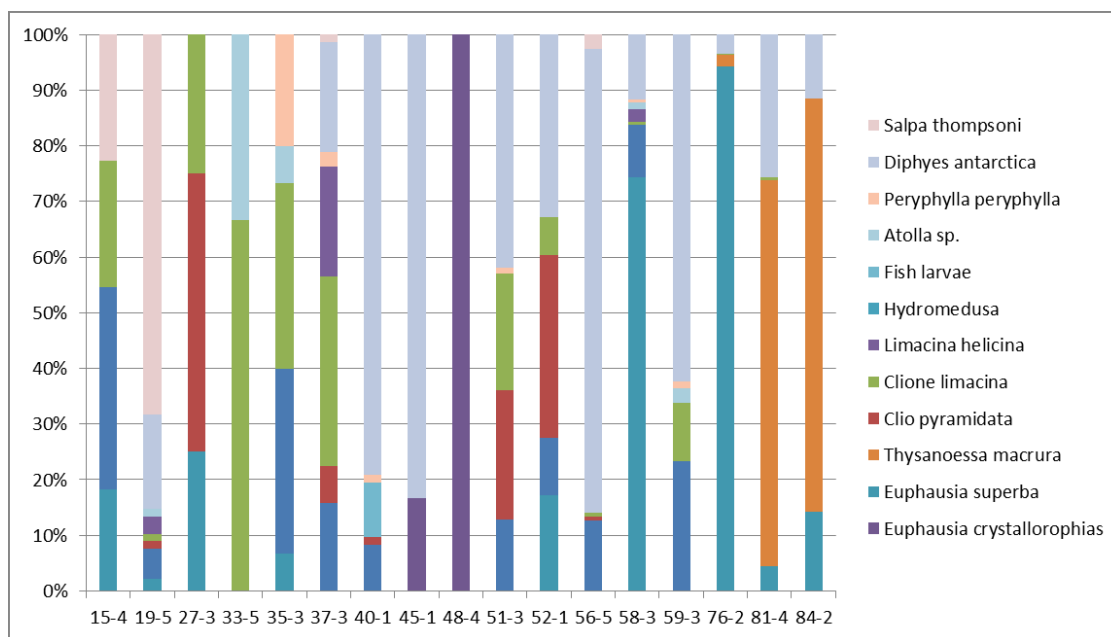


Fig. 7.6: Major taxa of the RMT catch composition at depth 100 m to 50 m

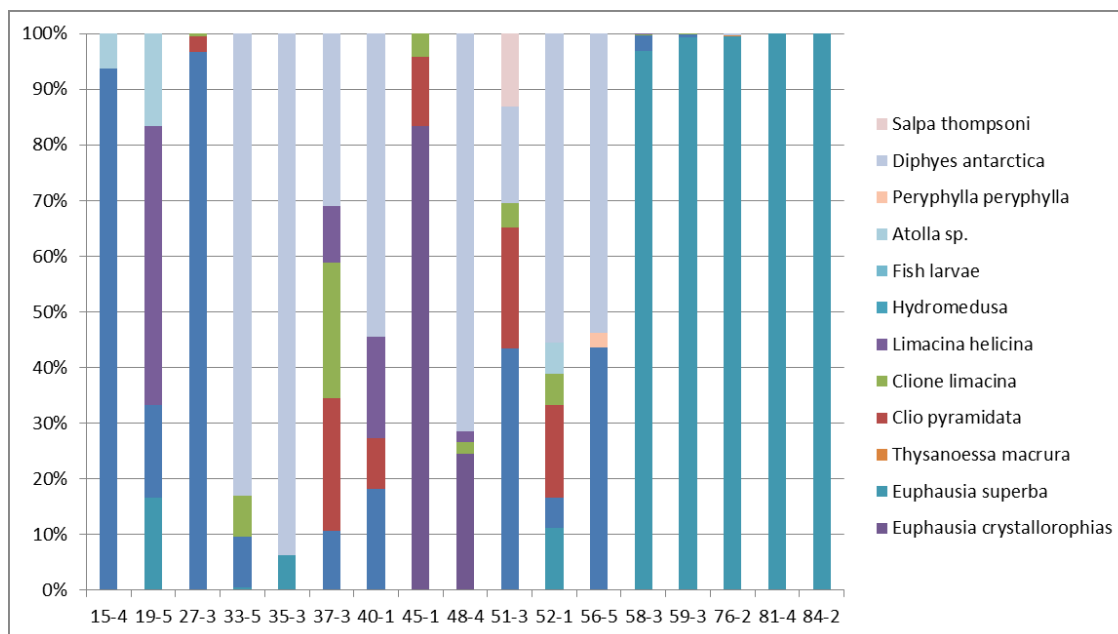


Fig. 7.7: Major taxa of the RMT catch composition at depth 50 m to surface

**Tab. 7.3:** List of RMT stations carried out during PS117, with date and position. The last column indicates the presence/absence of sea ice. The stations highlighted in light grey were conducted along the 0° meridian. The stations in white were carried out in the Eastern Weddell Sea, the stations in dark grey were conducted in the Western Weddell Sea, and the stations highlight in light yellow were conducted near Elephant Island.

Station PS117_	Haul	Date	°lat	°lon	Ice
15-4	1	12.27.2018	-66.529	-0.066	No
19-5	2	12.29.2018	-63.004	-0.005	No
27-3	3	01.03.2019	-69.085	-0.09	Yes
33-5	4	01.05.2019	-69.015	-6.996	No
35-3	5	01.08.2019	-69.055	-17.392	Yes
37-3	6	01.09.2019	-70.195	-11.232	Yes
39-3	7	01.10.2019	-70.31	-10.147	Yes
40-1	8	01.11.2019	-70.325	-8.88	No
44-1	9	01.12.2019	-70.439	-8.504	No
45-1	10	01.13.2019	-70.484	-8.327	No
48-4	11	01.16.2019	-70.511	-8.836	No
51-3	12	01.18.2019	-71.061	-13.555	Yes
52-3	13	01.19.2019	-71.239	-19.63	Yes
56-5	14	01.23.2019	-65.694	-36.661	No
58-3	15	01.25.2019	-67.666	-46.338	Yes
59-3	16	01.25.2019	-67.553	-46.345	Yes
72-5	17	01.29.2019	-63.667	-50.889	Partial
76-2	18	01.30.2019	-63.477	-51.62	Partial
81-4	19	01.30.2019	-63.341	-52.3	Partial
84-2	20	01.31.2019	-63.482	-51.839	Partial
99-5	21	02.01.2019	-61.018	-56.054	No
100-1	22	02.02.2019	-61.021	-54.816	No

### Sea ice work

The sampled ice stations comprised both first-year and multi-year sea ice and presented a high variability in the majority of site parameters. Ice thickness varied between approximately 0.8 m and >2.0 m. The snow conditions were highly variable, ranging from bare ice to more than 0.5 m snow cover. Gap layers of different thickness were observed and sampled on a number of sites (Tab. 7.1). Thick snow cover was associated with negative freeboard and surface slush layers were also observed. Ice temperatures were relatively warm (range: -0.0 to -1.9 C°, mean -1.3 C°) and the ice cover showed weak vertical temperature gradients (Fig. 7.8). Associated brine salinities (calculated according to Assur 1960) were low and ranged between 0.0 to 33.9 (Fig. 7.8). Ice bulk salinities ranged between 1.0 and 8.0. Vertical profiles are shown in Fig. 7.8. Brine volumes calculated as a function of bulk salinities and ice temperatures ranged between 6 % and >50 % with high brine volumes associated with rotten sea ice underlying gap layers. Vertical profiles for sea ice bulk-macronutrient concentrations (nitrate, silicate, phosphate) are shown in Fig. 7.9. Concentrations were relatively low with nitrate, silicate and phosphate concentrations ranging between 0.1 – 5.6  $\mu\text{mol l}^{-1}$ , 0.3 – 25.3  $\mu\text{mol l}^{-1}$  and 0.1 – 5.4  $\mu\text{mol l}^{-1}$ , respectively. Visible ice algal accumulations were observed in surface, interior and bottom layers of the ice. Pigment analyses in the home laboratories will be used to determine

chlorophyll-*a* content and pigment composition of these communities. Integrated chlorophyll-*a* concentrations will be calculated and used to establish algorithms to estimate algal biomass from under-ice spectral radiation measurements.

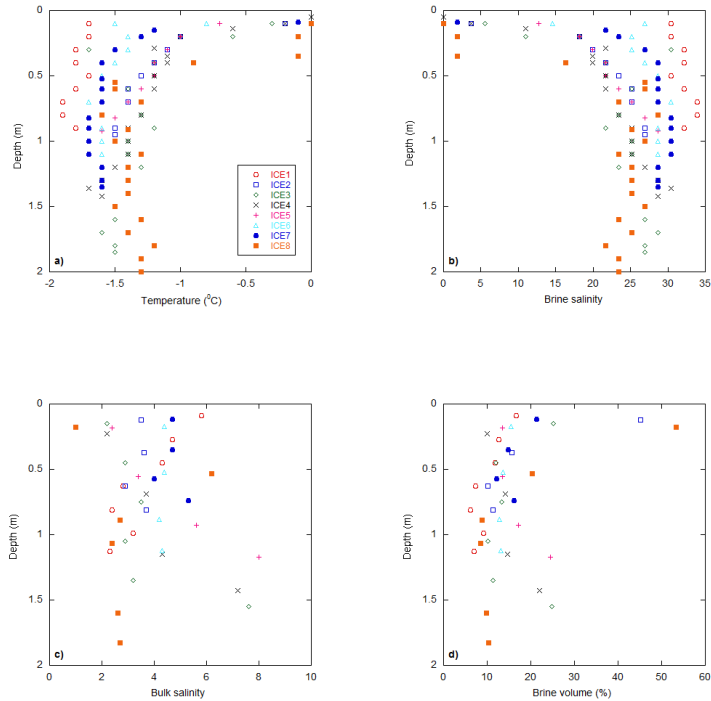


Fig. 7.8: Vertical profiles for a) ice temperature, b) brine salinity, c) ice bulk salinity and d) brine volume fraction for ice stations 1-8.

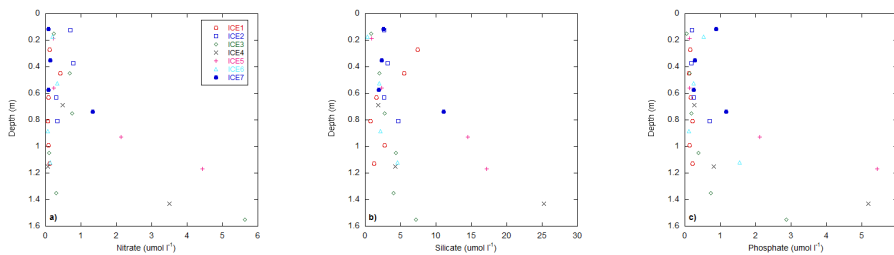


Fig. 7.9: Vertical profiles for bulk sea-ice nutrient concentrations. a) nitrate, b) silicate, c) phosphate.

### ROV work

The instrumented ROV was deployed at 10 stations and collected >12 hours of under-ice observations including >1500 simultaneously taken stills camera pictures and under-ice spectra. An example for this type of data is given in Fig. 7.10. We will use the images to determine the abundance of *Euphausia superba* at the ice-water interface and will use the spectra to estimate ice algal biomass at the same location, based on the algorithms that we will develop from the concomitant measurements of under-ice spectral radiation and ice core chlorophyll-*a* during the ice stations. On multiple stations the ROV was deployed in close

proximity to SUIT deployments and we aim to compare the data streams from the optical sensors on both platforms to derive information on the spatial variability of ice algal biomass across different length scales of the icescape.

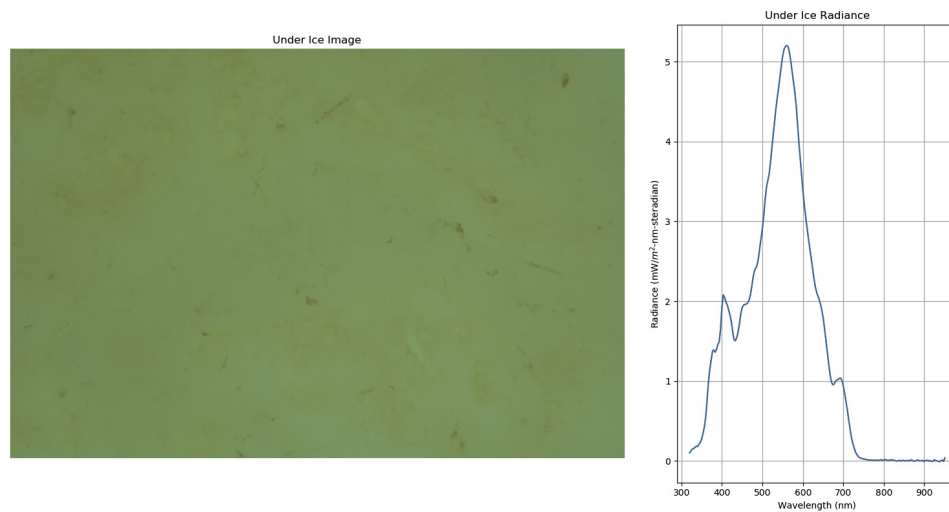


Fig. 7.10: Example for a dataset collected with the ROV. Left: Image from the up-ward looking stills camera showing krill at the ice-water interface. Right: Under-ice radiance spectra collected with an upward-looking hyperspectral radiometer from the same location.

### Top predator censuses

**Transect census** After leaving Cape Town, exercise counts were carried out and continued daylight counts started at 44°S, well north of the polar front. We met the first Chinstrap Penguins *Pygoscelis antarctica* and icebergs at 58.55°S. Due to a medevac we headed for Novolazarevskaya station with high speed and obviously no stations, which pushed counting to a higher intensity. Getting further into polar waters, the subantarctic species like Grey headed Albatross *Thalassarche chrysostoma*, Soft plumaged Petrel *Pterodroma mollis* slowly disappeared and Antarctic breeders like Snow Petrel *Pagodroma nivea*, Antarctic Petrel *Thalassoica antarctica* took their place. Humpback whales *Megaptera novaeangliae* were present and most abundant at the northern Weddell gyre area between icebergs. Fin whales were observed relative far south in the Weddell sea, possibly due to low ice concentrations. The ship-based counts continued until the continental slope of South America. See Tab. 7.4 for an overview of top predator helicopter flights and Tab. 7.5 for the species observed.

A helicopter count of the Emperor penguin *Aptenodytes forsteri* colony of Atka Bay was carried out during the Neumayer supply activities. In comparison to the ice edge area with Crabeater *Lobodon carcinophaga*, Ross *Ommatophoca rossii* and Leopard *Hydrurga leptonyx* seals, and Adelie *Pygoscelis adeliae* and Emperor penguins, Snow and Antarctic Petrels, the central ice-free Weddell Sea was found low on life. In the sea ice area in the western Weddell the numbers increased. 5 helicopter flights were carried out and showed a high abundance of seals in that area. On the closed sea ice area west of the ice edge, Weddell seals were found along the ice cracks together with high numbers of Adelie penguins. Following the marginal ice zone further to the North-west, we found Humpback whales in the more open ice and when the ice edges and open water appeared, also Fin whales *Balaenoptera physalus* and Sei whales *Balaenoptera borealis* appeared. The influence of the Antarctic peninsula got clear when Antarctic Fur seals *Arctocephalus gazella* and Brown Skua's *Catharacta (skua) lonnbergi* were counted. In the

almost ice free transect through the northern part of the Weddell sea until Drake street, high numbers of Fin whale were found together with Antarctic Fur seals, Southern fulmars and penguins, mainly Chinstrap. Due to darkness in the nights the coverage of the last part of the expedition is less dense. Between the start of the counts on 20 Dec 2018 until 2 Feb 2019 a total of 387 hours of steaming time were covered by the top predator survey.

**Tab. 7.4:** Overview Top Predator helicopter flights during PS117

Flight Number	Date	Time	Pos Start Transect (S/W)		Direction	Observer	Ice
1	14.01.2019	14:20	-70.61449	9.16091	EMP Colony	SKU	BRF/AM
2	24.01.2019	13:00	-68.48457	-44.14446	East - West	BRF	AM
3	25.01.2019	10:00	-67.61122	-46.37435	North - South	BRF	SKU
4	25.01.2019	16:00	-67.51756	-46.54162	East - West	BRF	SKU
5	26.01.2019	11:30	-65.44684	-46.09608	East - West	BRF	SKU
6	27.01.2019	15:00	-64.25059	-47.48513	North - South	BRF	AM
7	30.01.2019	14:50	-63.43766	-52.12763	North - South	BRF	SKU
8	30.01.2019	18:10	-63.39287	-52.27664	ship backtrack	BRF	SKU
9	31.01.2019	16:26	-63.39392	-52.32607	ship backtrack	BRF	SKU
10	01.02.2019	15:36	-61.02872	-56.17779	North - South	BRF	SKU

**Tab. 7.5:** Species list of seabirds and marine mammals observed during PS117

Seabirds				Marine mammals	
Emperor penguin	<i>Aptenodytes forsteri</i>	Soft-plumaged petrel	<i>Pterodroma mollis</i>	Crabeater seal	<i>Lobodon carcinophaga</i>
Chinstrap penguin	<i>Pygoscelis antarctica</i>	Atlantic petrel	<i>Pterodroma incerta</i>	Leopard seal	<i>Hydrurga leptonyx</i>
Adelie penguin	<i>Pygoscelis adeliae</i>	Grey petrel	<i>Procellaria cinerea</i>	Weddell seal	<i>Leptonychotes weddellii</i>
Wandering albatross	<i>Diomedea exulans</i>	White-chinned petrel	<i>Procellaria aequinoctialis</i>	Ross seal	<i>Ommatophoca rossii</i>
White-capped albatross	<i>Diomedea cauta</i>	Spectacled petrel	<i>Procellaria conspicillata</i>	S. Elephant seal	<i>Mirounga leonina</i>
Atl. yellow-nosed albatross	<i>Thalassarche chlororhynchos</i>	Cory's shearwater	<i>Calonectris borealis</i>	Antarctic fur seal	<i>Arctocephalus gazella</i>

Seabirds				Marine mammals	
Black-browed albatross	<i>Diomedea melanophris</i>	Sooty shearwater	<i>Puffinus griseus</i>	Cape fur seal	
Grey-headed albatross	<i>Diomedea chrysostoma</i>	Great shearwater	<i>Puffinus gravis</i>	Minke whale	<i>Balaenoptera acutorostrata</i>
Light-mantled sooty albatross	<i>Phoebetria palpebrata</i>	Subantarctic shearwater	<i>Puffinus assimilis</i>	Ant. Minke whale	<i>Balaenoptera bonaerensis</i>
Sooty albatross	<i>Phoebetria fusca</i>	Wilson's stormpetrel	<i>Oceanites oceanicus</i>	Sei whale	<i>Balaenoptera borealis</i>
Southern giant petrel	<i>Macronectes giganteus</i>	Black-bellied stormpetrel	<i>Fregetta tropica</i>	Fin whale	<i>Balaenoptera physalus</i>
Northern giant petrel	<i>Macronectes halli</i>	White/black-bellied stormpetrel	<i>Fregetta spp</i>	Blue whale	<i>Balaenoptera musculus</i>
Southern fulmar	<i>Fulmarus glacialisoides</i>	Diving petrel spec	<i>Pelecanoides sp.</i>	Humpback whale	<i>Megaptera novaeangliae</i>
Antarctic petrel	<i>Thalassoica antarctica</i>	Grey phalarope	<i>Phalaropus fulicarius</i>	Sperm whale	<i>Physeter macrocephalus</i>
Cape petrel	<i>Daption capense</i>	Kelp gull	<i>Larus dominicanus</i>	S. Bottlenose whale	<i>Hyperoodon planifrons</i>
Snow petrel	<i>Pagodroma nivea</i>	Arctic Tern	<i>Sterna paradisaea</i>	S. right whale dolphin	<i>Lissodelphis peronii</i>
Blue petrel	<i>Halobaena caerulea</i>	Antarctic tern	<i>Sterna vittata</i>	Orca	<i>Orcinus orca</i>
Antarctic prion	<i>Pachyptila desolata</i>	South polar skua	<i>Catharacta maccormicki</i>		
Prion spec.	<i>Pachyptila spp</i>	Brown skua	<i>Catharacta (skua) lonnbergi</i>		
White-headed petrel	<i>Pterodroma lessonii</i>	Long-tailed skua	<i>Stercorarius longicaudus</i>		
Great-winged petrel	<i>Pterodroma macroptera</i>	Cape gannet	<i>Sula capensis</i>		
Kerguelen petrel	<i>Pterodroma brevirostris</i>				

*CTD sampling and calibration*

An overview of the stations sampled for POM analysis and for SUIT CTD calibration is given in Tab. 7.6.

**Tab. 7.6:** List of UCC and CTD casts sampled for POM analysis and list of calibration stations for the SUIT CTD

Date	Station PS117_	Gear	°lat	°lon	Purpose
01.03.2019	27-1	UCC	-69.087	-0.008	POM
01.11.2019	41-4	UCC	-70.523	-8.769	POM
01.27.2019	64-4	CTD	-64.190	47.506	POM
01.27.2019	64-5	SUIT CTD	-64.190	47.506	cal
01.28.2019	68-4	SUIT CTD	-63.924	-49.232	cal
01.29.2019	72-3	CTD	-63.670	-50.884	POM

*Concluding remarks*

Based on the net catches, the area surveyed was characterized by highly variable zooplankton abundances. Elevated abundances of Antarctic krill were encountered in the ice-water interface layer, confirming earlier findings from the same region suggesting that Antarctic krill is often more abundant under sea ice than in the epipelagic layer. The stations in the sea ice-covered area of the Western Weddell sea showed more biomass than in the Eastern Weddell Sea. Patterns in top predator distribution resembled those of zooplankton, with elevated abundances of whales associated with relatively high under-ice krill abundances in the marginal ice zone on the northbound leg. Sea ice habitat properties evidently had a decisive impact on the distribution of animals in the investigation area. The high variability of sea ice properties found during our ice station work suggests that meters to kilometers scale measurements of sea ice properties, such as those performed with the ROV and the SUIT, can be valuable in capturing this variability at more appropriate spatial scales.

**Data management**

Almost all sample processing will be carried out in the home laboratories at AWI, WMR, AAD and RBINS. This may take up to three years depending on the parameters as well as analytical methods (chemical measurements and species identifications and quantifications). As soon as the data are available they will be accessible to other expedition participants and research partners on request. Metadata will be shared at the earliest convenience; data will be published depending on the finalization of PhD theses and publications. Metadata will be submitted to PANGAEA, the Antarctic Master Directory (including the Southern Ocean Observation System), the Antarctic Biodiversity Portal [www.Biodiversity.aq](http://www.Biodiversity.aq), and the Australian Antarctic Data Centre, and will be open for external use.

**References**

Arntz WE, Thatje S, Gerdes D, Gili J M, Gutt J, Jacob U, Montiel A, Orejas C & Teixido N (2005) The Antarctic-Magellan connection: macrobenthos ecology on the shelf and upper slope, a progress report. *Scientia Marina*, 69, 237-269.

Assur A (1960) Composition of sea ice and its tensile strength. SIPRE Research Report 44: 1-49.

- Daly K L (2004) Overwintering growth and development of larval *Euphausia superba*: an interannual comparison under varying environmental conditions west of the Antarctic Peninsula, Deep-Sea Research Part II 51, 2139–2168
- Flores H, Van Franeker J A, Siegel V, Haraldsson M, Strass V, Meesters E H W G, Bathmann U & Wolff WJ (2012) The association of Antarctic krill *Euphausia superba* with the under-ice habitat. PloS one 7, e31775.
- Flores H, Van Franeker J-A, Cisewski B, Leach H, Van de Putte AP, Meesters EHWG, Bathmann U & Wolff WJ (2011) Macrofauna under sea ice and in the open surface layer of the Lazarev Sea, Southern Ocean. Deep Sea Research Part II: Topical Studies in Oceanography 58, 1948–1961.
- Ingels J, Vanhove S, De Mesel I & Vanreusel A (2006) The biodiversity and biogeography of the free-living nematode genera *Desmodora* and *Desmodorella* (family Desmodoridae) at both sides of the Scotia Arc. Polar Biology 29, 936-949.
- van Franeker JA, Bathmann U & Mathot S. (1997) Carbon fluxes to Antarctic top predators. Deep-Sea Research II 44, 435–455.
- Franeker JA, Flores H & Van Dorssen M (2009) The Surface and Under Ice Trawl (SUIT), in: Flores, H (Ed.), Frozen Desert Alive - The Role of Sea Ice for Pelagic Macrofauna and its Predators. PhD thesis. University of Groningen, pp. 181–188.
- Marr J (1962) The natural history and geography of the Antarctic krill (*Euphausia superba* Dana). Discovery Reports 32, 37 – 444.
- Melbourne-Thomas J, Meiners KM, Mundy CJ, Schallenberg C, Tattersall KL, Dieckmann GS (2015) Algorithms to estimate Antarctic sea-ice algal biomass from under-ice irradiance spectra at regional scales. Marine Ecology Progress Series 536, 107–121.
- Meiners KM, Arndt S, Bestley S, Krumpen T, Ricker R., Milnes M ... & Proud. R (2017) Antarctic pack ice algal distribution: Floe-scale spatial variability and predictability from physical parameters. Geophysical Research Letters 44, 7382-7390.
- Melnikov IA, Spiridonov VA (1996) Antarctic krill under perennial sea ice in the western Weddell Sea Antarctic Science 8 (4), 323-329.
- Meyer B, Freier U, Grimm V, Groeneveld J, Hunt B, Kerwath S, King R., Klaas C, Pakhomov E, Meiners KM, ... & Yilmaz, NI (2017) Hide, survive and hitch a ride, a new view on the krill - sea ice relationship. Nature Ecology and Evolution 1, 1853-1861.

## 8. ALGENOM-2: MOLECULAR ECOLOGY AND EVOLUTION OF PRIMARY PRODUCERS

Sarah Lena Eggers<sup>1</sup>, Barbara Glemser<sup>1</sup>, Verena Braun<sup>1</sup>,  
Not on board: Bánk Beszteri<sup>1</sup>, Gernot Glöckner<sup>2</sup>,  
Ute Postel<sup>2</sup>, Michael Kloster<sup>1</sup>, Uwe John<sup>1</sup>, Klaus Valentin<sup>1</sup>

<sup>1</sup>AWI

<sup>2</sup>Univ.Cologne

### Grant-No. AWI\_PS117\_06

Microscopic primary producers (microalgae) form the basis of food webs and are important drivers of the biological carbon and silicate pump in the Southern Ocean like in other oceans as well. Our working group collected samples for two different research projects addressing the diversity and ecology of these microscopic organisms in the pelagic of the Southern Ocean. Sampling at PS117 is the continuation of our activities performed two years ago on PS103. The aims of these projects are the following:

#### 8.1 Microevolutionary genomics of *Fragilariopsis kerguelensis*

The aim of this project is to characterize the amount of neutral and adaptive genomic variation among populations of one of the best studied diatom species of the Southern Ocean, *Fragilariopsis kerguelensis* (O'Meara) Hustedt; and to get insights into microevolutionary dynamics and their relation to main environmental regimes (Antarctic Circumpolar Current [ACC] vs. Weddell Sea) and gradients (latitudinal gradient across the ACC and associated physico-chemical gradients). For this, we aimed at isolating clonal cultures from at least 8-10 populations along the North-South transect from the Northern edge of the Antarctic Circumpolar Current and in the Weddell Sea. These cultures will be transported to the home laboratory for population genomic and phenotypic characterization. Work based on similar sampling of the taxon revealed the presence of three distinct, previously unrecognized species; our sampling at PS117 will focus on improving our sampling of especially that newly revealed species which has the broadest biogeographic range.

*Fragilariopsis kerguelensis* (O'Meara) Hustedt is one of the ubiquitous diatom species of the Southern Ocean (Smetacek, Assmy et al., 2004) Assmy et al. 2004. It occurs at moderate to high abundances throughout the ACC as well as south of it, although at lower abundances, but practically all the way to the Antarctic ice shelf (Pinkernell & Beszteri, 2014). Although not always dominant at the surface, it is almost always present in ACC water samples and its thick frustules are among the main constituents of the siliceous ooze belt on the seafloor, due also to their good preservation (Cortese & Gersonde, 2007; Cortese & Gersonde, 2008). The species has received much attention not only for this reason but also because it has emerged as a model system for understanding the unique biological oceanographic properties of the high nutrient, low productivity open ocean water masses of the Southern Ocean, and the intriguing interactions between oceanic nutrient budgets and organismal adaptations (Assmy, Henjes et al., 2006; Cortese & Gersonde, 2007; Hoffmann, Peeken et al., 2007; Timmermans & van der Wagt, 2010; Cortese, Gersonde et al., 2012; Assmy, Smetacek et al., 2013; Fuchs, Scalco et

al., 2013; Shukla, Crosta et al., 2013). For instance, the growth of thick-shelled diatoms like *F. kerguelensis* is responsible for decoupling surface silicate from nitrate consumption in surface ACC water masses (Assmy, Smetacek et al., 2013). A full genome sequencing project has also been initiated for *F. kerguelensis* (under the lead of Prof. Thomas Mock, Univ. East Anglia, Norwich, UK and with participation of members of our team), providing novel possibilities for molecular ecological/evolutionary investigations of this diatom species.

The predominant mode of reproduction in phytoplankton organisms is vegetative division. In spite of this, the traditional paradigm (which had probably not been based on anything else besides the lack of data) that phytoplankton blooms or non-bloom populations are largely clonal has by now largely been overturned. In practically every case investigated, populations of phytoplankters have turned out to be assemblages of highly diverse clonal lineages (Rynewson & Armbrust, 2000; Rynewson & Armbrust, 2005; Rynewson, Lin et al., 2009). A single-cell genome sequencing study has recently demonstrated the coexistence of hundreds of differentiated “ecotypes” of the cyanobacterium *Prochlorococcus* within a single water sample (Kashtan, Roggensack et al., 2014). In the case of eukaryotic phytoplankton, comparative genome sequencing of the globally abundant haptophyte *Emiliania huxleyi* revealed a large variation in gene contents of individual isolates from diverse geographic origins which was hypothesized to have contributed to the ability of this species to adapt to varied environmental conditions (Read, Kegel et al., 2013; von Dassow, John et al., 2015). The emerging picture is that phytoplankton species and even individual populations are far from homogeneous, and that phytoplankton populations adapt in their genomic composition to local environmental factors. Hardly anything is known about the amount of such genomic diversity and its distribution along the genome, as well as in geographic space and in time in important phytoplankton taxa contributing substantially to biogeochemical cycles in high latitude regions. Regarding phytoplankton of the Southern Ocean, the only taxon that has been studied at some depth in this respect up to now is the Haptophyte *Phaeocystis* (Gabler-Schwarz & Medlin, 2011) for which microsatellite markers have been applied to study population diversity and differentiation revealing novel insights about genetic and functional differentiation. About the important diatom species of the region, however, no such data have been available so far.

In our ongoing project, we sampled a meridional transect through the ACC to the shelf ice edge during PS103 by isolating numerous *F. kerguelensis* clonal strains from different populations. These strains were subjected to an in-depth molecular and morphometric characterization in the meanwhile. These revealed the presence of three subpopulations with partially overlapping distributions, with the area near the Southern Boundary of the ACC appearing as a biogeographic boundary between two of these groups. Interestingly, pairs of subpopulations occurring in sympatry seem to have evolved a physiological reproductive barrier since they do not produce offspring in laboratory crosses, but the pair of allopatric subpopulations can produce offspring in the lab. This provides an exciting system in which genomic divergence with and without reproductive contact, i.e., with or without an accompanying evolution into distinct species, can be investigated in the Southern Ocean pelagic system. At the present expedition, we originally intended to continue this work in two main respects. First, by sampling a comparable meridional transect again two years later, we were interested whether the genomic divergence and biogeographic patterns observed at PS103 persist – based on the amount of genomic divergence among the subpopulations observed, we hypothesized that it would. Second, we intended to better resolve the transition in population genomic composition along the meridional environmental gradients of the ACC by sampling a tighter selection of stations especially in the region between the Subantarctic Front and the Southern Boundary of the ACC.

## 8.2 Taxonomic and gene expressional trends in protistan plankton communities along temperature gradients

Temperature is one of the major drivers of biodiversity and ecosystem functioning. We recently used large scale community transcriptome sequencing to analyze the fundamental effect of temperature on protistan plankton biodiversity and metabolic function. The study was based on five samples from three temperature regimes, polar, subpolar, and equatorial. Along this rather rough temperature gradient we saw an increase of dinoflagellates at the cost of diatoms and a decrease of transcripts related to protein biosynthesis at higher temperatures. We postulated that this might reflect a general temperature related resource allocation trend in marine protistan plankton. To test this hypothesis, to extend the geographic range sampled and to refine the picture obtained about temperature dependent shifts in transcriptional allocation to major cellular processes, we previously conducted sampling along two transects between Spitsbergen and Cape Town, covering a broad temperature range at a high resolution, and sequenced RNA samples with high coverage. The latter was made possible through a grant coined "Sea of Change", awarded to Thomas Mock, KV, and co-workers, by the Joint Genome Institute (<http://genome.jgi.doe.gov/SeaofArctiOcean/SeaofArctiOcean.info.html>). To this, a set of Southern Ocean metatranscriptomes were added from our sampling at PS103. Here again, similarly to the other project, the main intended aim for PS117 was to test the persistence of molecular taxonomic-transcriptomic patterns, and to obtain a higher resolution across the ACC.

### Work at sea

Altogether, we sampled at 27 stations (see details in Tab. 8.1) for both projects. Sampling was performed by both CTD casts with water collection at two depths, and a 20 µm mesh size phytoplankton hand net. On four occasions, weather conditions proved to be too rough for managing the hand net. Here, sampling was performed by obtaining seawater samples from the on-board seawater supply system; several liters of the seawater sample were concentrated by gravitational filtration through a 20 µm mesh size gauze.

### *Community nucleic acid sampling.*

Seawater subsamples were filtered onto 1.2 µm pore size membrane filters on an 8-channel peristaltic pump filtration system in a cold container tempered to 1-2 °C. At each station/depth, three replicate filters were collected for eukaryotic (1.2 µm pore size) DNA and RNA samples. Filters for DNA extraction were frozen after addition of 700 µL DNA extraction buffer, and samples for RNA extraction were frozen after addition of 600 µl RNA extraction buffer, in liquid nitrogen. All filters for nucleic acid extraction are stored and being transported to the home laboratory at -80 °C. The DNA samples will be used for marker gene amplification (small subunit ribosomal DNA) and sequencing for characterizing eukaryotic community composition and its changes along our route. The RNA samples will be used for preparation and sequencing of community transcriptome libraries for assessing gene expressional trends in protistan plankton along the North-to-South temperature gradient.

### *Contextual parameters*

Further seawater subsamples were filtered for measuring contextual parameters. A subsample was filtered under dimmed light onto glass fiber filter and frozen at -80 °C for HPLC based pigment analysis. A further subsample was filtered upon pre-combusted glass fiber filters for measuring particulate organic carbon. Additionally, a subsample was taken to determine biogenic silicate concentrations. Finally, quantitative subsamples from the Niskin bottles, as well as a subsample from the phytoplankton net, was fixed with formaldehyde for microscopic observation and counting of microphytoplankton.

*Cultivation*

For population genomic analyses and for experimental work, clonal cultures of the diatom *Fragilariopsis kerguelensis* were isolated from 14 populations by picking single chains and repeatedly washing them in sterile filtered F/2 phytoplankton growth medium under the inverted microscope. In living material, colonies of this species cannot be differentiated from colonies of all congeners with high certainty. Using strains isolated at PS103, we have started documenting them by a combination of different morphological and molecular approaches. This is only possible using isolated clonal strains but is essential for linking live colony morphology to valve morphology and to molecular sequence data. We have also continued these activities during PS117.

After inoculation, isolates were incubated in a laboratory container at 3-4 °C and an 18:6 hours daily light-dark cycle at total illumination intensities between 1,000-2,500 Lux. Strains were observed on a regular basis, re-isolated to clean of contaminants as necessary (and as time permitted; some strains will need to be cleaned of remaining contaminants in the home lab) and finally, transferred into 15 ml Falcon tubes for transport. The isolates are being transported back to the home laboratory at 4 °C for experimental work and in depth genomic and population genomic characterization.

**Tab. 8.1:** Summary of sampling activities of our group during PS117. CTD: both depths sampled for the full set of parameters described in the text (eukaryotic nucleic acids, microscopy, and contextual measurements). HN: hand net (\* weather conditions were too rough for HN, seawater filtration instead). Cultures: number of *Fragilariopsis* cultures isolated at the corresponding station.

Station number PS117_	Latitude	Longitude	CTD (surface, chl max.)	HN	Cultures
1	-36.13	13.18	+	+	-
2	-37.24	12.31	+	+	-
3	-38.36	11.46	-	+	-
4	-39.59	10.48	+	+	-
5	-41.30	9.53	+	+	-
6	-42.42	8.44	+	+	-
7	-44.40	7.50	+	+	47
13	-51.0	3.59	+	+	60
Novo detour	-51-56		-	+	
14	-67.30	0.00	+	+	12
15	-66.31	0.40	+	+	24
18	-64.05	0.10	+	+	24
19	-63.00	0.00	+	+	24
21	-61.00	0.00	+	+	36
22	-59.30	0.60	+	+	36
26	-68.30	0.00	+	+	24
31	-69.24	0.00	+	+	12
33	-69.00	6.59	+	+	
34	-65.58	12.15	+	+	24
35	-69.30	17.23	+	+	12
53	-70.54	28.53	+	+	-

Station number PS117_	Latitude	Longitude	CTD (surface, chl max.)	HN	Cultures
54	-66.36	27.70	+	+	-
56	-65.37	36.25	+	+	-
57	-68.29	44.60	+	+	-
63	-64.15	47.00	+	+	-
68	-63.55	49.16	+	+	-
72	-63.39	50.49	+	+	-

### Preliminary and expected results

Unforeseen developments led to PS117 skipping most of the originally planned stations in the ACC. This only allowed us to sample two locations/populations in the originally planned main focus area of our project. These samples will nevertheless be valuable for getting an insight into the persistence of taxonomic-transcriptomic-population genomic patterns first uncovered based on our PS103 sampling, but fail to provide the planned improved spatial resolution. On the other hand, compensating for this, our sampling in the Weddell Sea was performed more extensively than planned, and these samples can hopefully provide the basis for a similar initial mapping of molecular diversity patterns in this region like we could do previously using PS103 samples for the ACC. Due to the highly interesting pattern of population genomic zonation uncovered by our work with *F. kerguelensis* strains sampled during PS103, it remains a task for the future to extend those investigations and better understand the nature and origin of this zonation pattern; to which extend and in which ways differentiation of the discovered subpopulations provide them selective advantages in their native habitats; how generally such zonation patterns characterize also other pelagic taxa; and how such subdivision might affect projected responses of pelagic microscopic organisms to ongoing environmental change.

To provide environmental-oceanographic context to all above analyses, CTD data obtained by the HAFOS group during the present expedition will be used, alongside the samples collected by our group for determining concentrations of photosynthetic pigments, particulate organic carbon, inorganic nutrients and biogenic silica.

### Data management

Measurement results of contextual parameters will be deposited in PANGAEA ([www.pangaea.de](http://www.pangaea.de)). Permanent diatom slides and material will be deposited in the Hustedt Diatom Study Centre (herbarium code BRM). The main type of primary data to be obtained during the expedition is nucleotide sequence data which will be deposited in the corresponding databases of the International Nucleotide Sequence Database Cooperation (INSDC: <http://www.insdc.org/>).

### References

- Assmy P, Henjes, J, Smetacek V & Montresor M (2006) Auxospore formation by the silica-sinking, oceanic diatom *Fragilariopsis kerguelensis* (Bacillariophyceae). *Journal of Phycology*, 42, 1002-1006.
- Assmy P, Smetacek V, Montresor M, Klaas C, Henjes J, Strass VH, Arrieta JM, Bathmann U, Berg GM, Breitbarth E, Cisewski B, Friedrichs L, Fuchs N, Herndl GJ, Jansen S, Kragefsky S, Latasa, M, Peeken I, Rottgers R, Scharek R, Schuller SE, Steigenberger S, Webb A & Wolf-Gladrow D (2013) Thick-shelled, grazer-protected diatoms decouple ocean carbon and silicon cycles in the iron-limited Antarctic Circumpolar Current. *Proceedings of the National Academy of Sciences of the United States of America*, 110, 20633-20638.
- Cortese G & Gersonde R (2007) Morphometric variability in the diatom *Fragilariopsis kerguelensis*: Implications for Southern Ocean paleoceanography. *Earth and Planetary Science Letters*, 257, 526-544.

## 8.2 Taxonomic and gene expressional trends in protistan plankton communities

---

- Cortese G & Gersonde R (2008) Plio/Pleistocene changes in the main biogenic silica carrier in the Southern Ocean, Atlantic Sector. *Marine Geology*, 252, 100-110.
- Cortese G, Gersonde R, Maschner K & Medley P (2012) Glacial-interglacial size variability in the diatom *Fragilariopsis kerguelensis*: Possible iron/dust controls? *Paleoceanography*, 27.
- Fuchs N, Scalco E, Kooistra WHCF, Assmy P & Montresor M (2013) Genetic characterization and life cycle of the diatom *Fragilariopsis kerguelensis*. *European Journal of Phycology*, 48, 411-426.
- Gabler-Schwarz S & Medlin LK (2011) Microsatellite Markers for *Phaeocystis antarctica*: Assessment of Population Structure and Physiological Responses. *European Journal of Phycology*, 46, 91-91.
- Hoffmann LJ, Peeken I & Lochte K (2007) Effects of iron on the elemental stoichiometry during EIFEX and in the diatoms *Fragilariopsis kerguelensis* and *Chaetoceros dichaeta*. *Biogeosciences*, 4, 569-579.
- Kashtan N, Roggensack SE, Rodrigue S, Thompson JW, Biller SJ, Coe A, Ding HM, Marttinen P, Malmstrom RR, Stocker R, Follows MJ, Stepanauskas R & Chisholm SW (2014) Single-Cell Genomics Reveals Hundreds of Coexisting Subpopulations in Wild *Prochlorococcus*. *Science*, 344, 416-420.
- Pinkernell, S & Beszteri, B (2014) Potential effects of climate change on the distribution range of the main silicate sinker of the Southern Ocean, *Ecology and Evolution*. 4, 3147-3161.
- Read BA, Kegel J, Klute MJ, Kuo A, Lefebvre SC, Maumus F, Mayer C, Miller J, Monier A, Salamov A, Young J, Aguilar M, Claverie JM, Frickenhaus S, Gonzalez K, Herman EK, Lin YC, Napier J, Ogata H, Sarno AF, Shmutz J, Schroeder D, de Vargas C, Verret F, von Dassow P, Valentin K, Van de Peer Y, Wheeler G, Dacks JB, Delwiche CF, Dyhrman ST, Glockner G, John U, Richards T, Worden AZ, Zhang XY, Grigoriev IV, Allen AE, Bidle K, Borodovsky M, Bowler C, Brownlee C, Cock JM, Elias M, Gladyshev VN, Groth M, Guda C, Hadaegh A, Iglesias-Rodriguez MD, Jenkins J, Jones BM, Lawson T, Leese F, Lindquist E, Lobanov A, Lomsadze A, Malik SB, Marsh ME, Mackinder L, Mock T, Mueller-Roeber B, Pagarete A, Parker M, Probert I, Quesneville H, Raines C, Rensing SA, Riano-Pachon DM, Richier S, Rokitta S, Shiraiwa Y, Soanes DM, van der Giezen M, Wahlund TM, Williams B, Wilson W, Wolfe G, Wurch LL & Annotation EH (2013) Pan genome of the phytoplankton *Emiliania* underpins its global distribution. *Nature*, 499, 209-213.
- Rynearson TA & Armbrust EV (2000) DNA fingerprinting reveals extensive genetic diversity in a field population of the centric diatom *Ditylum brightwellii*. *Limnology and Oceanography*, 45, 1329-1340.
- Rynearson TA & Armbrust EV (2005) Maintenance of clonal diversity during a spring bloom of the centric diatom *Ditylum brightwellii*. *Molecular Ecology*, 14, 1631-1640.
- Rynearson TA, Lin EO & Armbrust EV (2009) Metapopulation Structure in the Planktonic Diatom *Ditylum brightwellii* (Bacillariophyceae). *Protist*, 160, 111-121.
- Shukla SK, Crosta X, Cortese G & Nayak GN (2013) Climate mediated size variability of diatom *Fragilariopsis kerguelensis* in the Southern Ocean. *Quaternary Science Reviews*, 69, 49-58.
- Smetacek V, Assmy P & Henjes, J (2004) The role of grazing in structuring Southern Ocean pelagic ecosystems and biogeochemical cycles. *Antarctic Science*, 16, 541-558.
- Timmermans KR & van der Wagt B (2010) Variability in Cell Size, Nutrient Depletion, and Growth Rates of the Southern Ocean Diatom *Fragilariopsis kerguelensis* (Bacillariophyceae) after Prolonged Iron Limitation. *Journal of Phycology*, 46, 497-506.
- von Dassow P, John, U, Ogata H, Probert I, Bendif E, Kegel JU, Audic, S, Wincker P, Da Silva C, Claverie JM, Doney S, Glover DM, Flores, DM, Herrera Y, Lescot M, Garet-Delmas MJ & de Vargas C (2015) Life-cycle modification in open oceans accounts for genome variability in a cosmopolitan phytoplankton. *ISME Journal*, 9, 1365-1377.

## 9. COMBINED EFFECTS OF TEMPERATURE AND ORGANIC MATTER AVAILABILITY ON DEGRADATION ACTIVITY BY ANTARCTIC BACTERIOPLANKTON

Birthe Zäncker<sup>1</sup>, Isabel Diercks<sup>2</sup>  
Not on board: Judith Piontek<sup>2</sup>

<sup>1</sup>MBA  
<sup>2</sup>IOW

Grant-No. AWI\_PS117\_07

### Objectives

Global warming poses new threats to marine ecosystems since rising seawater temperature potentially induces cascading effects in biogeochemical cycles and food webs. In Antarctic marine systems, low seawater temperature, and the low availability of labile organic matter are major environmental constraints on bacterial growth and degradation activity. However, temperature and the availability of resources for heterotrophic bacteria undergo considerable change induced by climate warming combined with subsequent ice melt and changes in primary productivity. Changes in temperature and resource availability can induce shifts in the structure and composition of bacterioplankton communities but there is a limited understanding of how changes in community composition affect community metabolism and functioning.

The relevance of low temperatures for bacterial growth in the polar oceans is still under debate (Kirchman and Moran, 2009). Recent studies suggest that the influence of temperature on bacterial communities strongly varies in time and space. Strong temperature effects can be observed when substrates are in excess due to phytoplankton blooming (Ducklow et al., 2002), whereas nutrient-limitation has a high potential to render temperature unimportant in promoting microbial growth (Moran et al., 2010; Calvo-Diaz et al., 2014). Phytoplankton exudates can coagulate and form polysaccharide-rich gel-like particles, called transparent exopolymer particles (TEP), which can be found ubiquitously throughout marine and freshwater environments (Alldredge et al., 1993; Passow, 2002) it has been shown that these gel-particles are not only ubiquitous and abundant, but also play a significant role in the biogeochemical cycling of elements and the structuring of food webs. TEP may be quantified either microscopically or colorimetrically. Although data based on measurements using one or other of these methods are not directly comparable, the results are consistent. TEP abundances in fresh and marine waters are in the same range as those of phytoplankton, with peak values occurring during phytoplankton blooms. TEP are very sticky particles that exhibit the characteristics of gels, and consist predominantly of acidic polysaccharides. In marine systems the majority of TEP are formed abiotically from dissolved precursors, which are released by phytoplankton that are either actively growing or are senescent. TEP are also generated during the sloughing of cell surface mucus and the disintegration of colonial matrices. The impact of exopolymers in the creation of microhabitats and in the cycling of trace compounds varies with the state in which the polymers occur, either as particles or as solute slimes. As particles, TEP provide surfaces for the colonization by bacteria and transfer by adsorption, trace solute substances into the particulate pool. As dissolved polymers they are mixed with the water and can neither be filtered nor aggregated. Because of their high abundances, large size and high stickiness,

TEP enhance or even facilitate the aggregation of solid, non-sticky particles. They have been found to form the matrices of all marine aggregates investigated to date. By aggregating solid particles, TEP promote the sedimentation of particles, and, because their carbon content is high, their direct contribution to fluxes of carbon into deep water is significant. The direct sedimentation of TEP may represent a mechanism for the selective sequestration of carbon in deep water, because the C:N ratios of TEP lie well above the Redfield ratio. The turnover time of TEP as a result of bacterial degradation appears to range from hours to months, depending on the chemical composition and age of TEP. TEP may also be utilized not only by filter feeders (some protozoans and appendicularian. TEP can act as microbial hotspots, providing a surface and potential substrate for microbes such as bacteria and fungi (Engel et al., 2004; Taylor & Cunliffe, 2016; Cunliffe et al., 2017).

The overarching goals of this project are (1) to assess bacterioplankton communities and their activities at low temperatures in the surface layer of the Weddell Sea, and (2) to explore the synergistic potential of temperature and the availability of labile organic matter in the regulation of heterotrophic bacterial degradation activity. Field sampling combined with on-board incubation experiments were conducted in order to investigate microbial community composition, bacterial productivity and remineralization activity, and its dependence on temperature and substrate supply.

### **Work at sea**

The working program in the Weddell Sea consisted of two work packages (*WP*) consisting of field studies (*WP 1*) and on-board experiments (*WP 2*).

#### **9.1 WP 1: Field studies**

23 stations located along the Greenwich (0°-) meridian and in the Weddell Sea were sampled. Sampling along north-south and east-west transects allowed for analysis of a variety of gradients in phytoplankton production and ice coverage and their impact on microbial activities throughout the water column. Stations were sampled each with seven depths from the surface to 250 m and at 750 m and 3,500 m depth.

At each depth, samples for DNA extraction to analyse the microbial community structure, enzyme rates to investigate the heterotrophic bacterial activity, and <sup>3</sup>H-labelled leucine incorporation to characterize the bacterial biomass production were taken. In addition, the organic matter was sampled, including gelatinous particles and the microbial communities attached to them, dissolved organic carbon (DOC), dissolved amino acid (DAA) and dissolved carbohydrate (DCHO) concentrations. Samples for microscopic analyses of the microbial community using fluorescent methods were taken along with phytoplankton and bacterial abundance samples. Chlorophyll *a* samples were taken at the uppermost five depths to calibrate the fluorometer of the CTD. At certain stations, cryopreserved samples for fungi cultivation and phospholipid fatty acid (PLFA) analysis were taken (Tab. 9.1). Samples were taken back frozen for further analysis at IOW and MBA.

In collaboration with SIPES-2, bottoms of ice cores were received from Giulia Castellani and Klaus Meiners. Samples were thawed at 4°C and subsequently filtered for DNA analysis of fungal community composition and for fungi cultivation in the home lab at MBA.

Tab. 9.1: Sampled CTD stations and depths during PS117 including parameters that will be analysed from each sample

#	Station	Latitude	Longitude	Sampled depth [m]	Extra-cellular enzyme activities	Gel particles	DOC, DAA, DCHO	Microbial abundance	Bacterial biomass production	Microbial community composition	Fungi cultivation	PLFA chl a	fluorescent microscopy
1	PS117_2	37° 30.623' S	12° 27.759' E	15, 50, 75, 250, 750, 3500		x				x			x
2	PS117_6	42° 42.657' S	8° 43.338' E	15, 55, 75, 250, 750, 3500		x				x			x
3	PS117_7	44° 40.013' S	7° 05.133' E	15, 55, 75, 250, 750, 3500		x				x			x
4	PS117_13	57° 00.015' S	3° 55.612' E	15, 30, 75, 250, 750, 3500		x				x			x
5	PS117_14	67° 28.912' S	0° 00.131' W	15, 35, 50, 75, 250, 750, 3500	x	x	x	x	x	x		x	x
6	PS117_15	66° 30.873' S	0° 10.214' W	15, 25, 50, 75, 250, 750, 3500	x	x	x	x	x	x	x	x	x
7	PS117_19	63° 00.000' S	0° 00.053' E	15, 39, 50, 75, 250, 750, 3500	x	x	x	x	x	x		x	x
8	PS117_21	60° 59.855' S	0° 00.000' W	15, 48, 75, 250, 750, 3500		x				x			x
9	PS117_26	68° 30.032' S	0° 00.063' E	15, 45, 75, 250, 750, 3500		x				x			x

#	Station	Latitude	Longitude	Sampled depth [m]	Extra-cellular enzyme activities	Gel particles	DOC, DAA, DCHO	Microbial abundance	Bacterial biomass production	Microbial community composition	Fungi cultivation	PLFA	chl a	fluorescent microscopy
10	PS117_31	69° 23.890' S	0° 18.560' E	15, 50, 75, 250, 750, 3500		x				x				x
11	PS117_33	69° 01.405' S	6° 58.698' W	15, 52, 75, 125, 250, 750, 2250	x	x	x	x	x	x			x	x
12	PS117_34	65° 58.306' S	12° 13.095' W	10, 22, 50, 75, 250, 750, 3500	x	x	x	x	x	x			x	x
13	PS117_35	69° 05.043' S	17° 12.432' W	15, 35, 50, 75, 250, 750, 3500	x	x	x	x	x	x			x	x
14	PS117_41	70° 32.140' S	8° 52.250' W	20, 50, 75, 150	x	x	x	x	x	x			x	x
15	PS117_53	70° 54.045' S	28° 50.801' W	20, 45, 60, 75, 250, 750, 3500	x	x	x	x	x	x			x	x
16	PS117_54	66° 35.652' S	27° 10.080' W	15, 45, 60, 75, 250, 750, 3500	x	x	x	x	x	x			x	x
17	PS117_56	65° 41.660' S	36° 40.654' W	15, 50, 75, 250, 750, 3500	x	x	x	x	x	x			x	x
18	PS117_57	68° 27.900' S	44° 01.009' W	15, 60, 75, 250, 750, 3500	x	x	x	x	x	x			x	x
19	PS117_63	64° 15.265' S	47° 01.707' W	15, 50, 75, 250, 750, 3500	x	x	x	x	x	x			x	x

9. Combined Effects of Temperature and Organic Matter Availability on Degradation Activity

#	Station	Latitude	Longitude	Sampled depth [m]	Extracellular enzyme activities	Gel particles	DOC, DAA, DCHO	Microbial abundance	Bacterial biomass production	Microbial community composition	Fungi cultivation	PLFA	chl a	fluorescent microscopy
20	PS117_66	64° 04.180' S	48° 23.172' W	15, 50, 75, 90, 250, 750, 3500	x	x	x	x	x	x	x	x	x	x
21	PS117_76	63° 28.642' S	51° 37.176' W	15, 50, 75, 250, 750, 0 1500	x	x	x	x	x	x			x	x
22	PS117_92	63° 18.324' S	53° 05.691' W	15, 50, 75, 250		x				x			X	x
23	PS117_94	63° 13.295' S	53° 42.475' W	15, 50, 75, 250	x	x	x	x	x	x			x	x
ice_1	ICE3	70° 20.880' S	8° 11.620' W			x				x	x			
ice_2	ICE6	70° 30.440' S	9° 54.590' W			x				x	x			
ice_3	ICE7	70° 38.110' S	9° 54.590' W			x				x	x			
ice_4	ICE8	65° 12.380' S	45° 56.570' W			x				x	x			

## 9.2 WP 2: On-board experiments on temperature effects and organic matter availability on bacterial communities

At three stations (Fig. 9.1), samples were taken to start onboard incubation experiments at varying depths just below the deep chlorophyll maximum. The incubations were used to test the response of Antarctic bacterial communities to temperature at varying organic matter availability. Treatments were incubated in triplicates to ensure statistical relevance. Bacterial adaptation to *in-situ* temperature and elevated temperature (0°C and 4°C) in dependence of organic matter availability (seawater without and with additional carbon sources) was tested (Fig. 9.2). Two organic matter sources were added to the different incubation treatments: glucose to provide a readily usable carbon source for bacteria, and laminarin, which needs to be treated with extracellular enzymes before it can be ingested by bacteria. Laminarin is considered to be one of the most abundant types of carbohydrate in the marine environment since it is a major storage glucan of bloom-forming phytoplankton (Painter, 1983). The bacterial community was monitored every day by taking samples for bacterial abundance and fluorescent *in-situ* hybridization. Every other day, respiration, extracellular enzyme activity and bacterial biomass production were measured. Additional samples for DNA analysis, DAA, DCHO and DOC as well as nutrients and chlorophyll a concentrations were taken at the beginning and the end of the experiment. Incubations were conducted for five days in the dark to avoid organic matter production by phytoplankton.

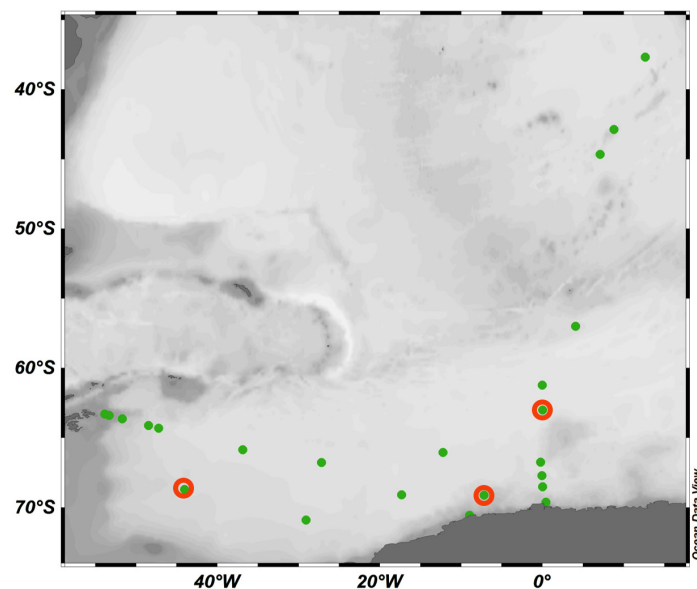


Fig. 9.1: Sampled CTD stations (green dots) and positions of selected stations where incubations were started (red empty circles)

A second set of incubations was used to analyse the interactions of bacteria with gel-like particles, namely the polysaccharide-rich transparent exopolymer particles (TEP) (Passow, 2002) it has been shown that these gel-particles are not only ubiquitous and abundant, but also play a significant role in the biogeochemical cycling of elements and the structuring of food webs. TEP may be quantified either microscopically or colorimetrically. Although data based on measurements using one or other of these methods are not directly comparable, the results are consistent. TEP abundances in fresh and marine waters are in the same range as those of phytoplankton, with peak values occurring during phytoplankton blooms. TEP are very sticky particles that exhibit the characteristics of gels, and consist predominantly of

acidic polysaccharides. In marine systems the majority of TEP are formed abiotically from dissolved precursors, which are released by phytoplankton that are either actively growing or are senescent. TEP are also generated during the sloughing of cell surface mucus and the disintegration of colonial matrices. The impact of exopolymers in the creation of microhabitats and in the cycling of trace compounds varies with the state in which the polymers occur, either as particles or as solute slimes. As particles, TEP provide surfaces for the colonization by bacteria and transfer by adsorption, trace solute substances into the particulate pool. As dissolved polymers they are mixed with the water and can neither be filtered nor aggregated. Because of their high abundances, large size and high stickiness, TEP enhance or even facilitate the aggregation of solid, non-sticky particles. They have been found to form the matrices of all marine aggregates investigated to date. By aggregating solid particles, TEP promote the sedimentation of particles, and, because their carbon content is high, their direct contribution to fluxes of carbon into deep water is significant. The direct sedimentation of TEP may represent a mechanism for the selective sequestration of carbon in deep water, because the C:N ratios of TEP lie well above the Redfield ratio. The turnover time of TEP as a result of bacterial degradation appears to range from hours to months, depending on the chemical composition and age of TEP. TEP may also be utilized not only by filter feeders (some protozoans and appendicularian. Seawater was filtered through 0.2  $\mu\text{m}$  to remove all organisms and particulate organic matter and subsequently bubbled for 2 h to produce new TEP. Two replicates were incubated with the original community diluted 1:10 in the newly produced TEP suspension, two replicates were incubated as controls without any addition (Fig. 9.3). Over a course of five days, the recolonization of TEP by bacteria and fungi was monitored by taking daily samples for TEP quantification and sequencing of TEP. At the beginning and end of the experiment, nutrient and DNA samples were taken as well to characterize the start and end conditions of the incubations.

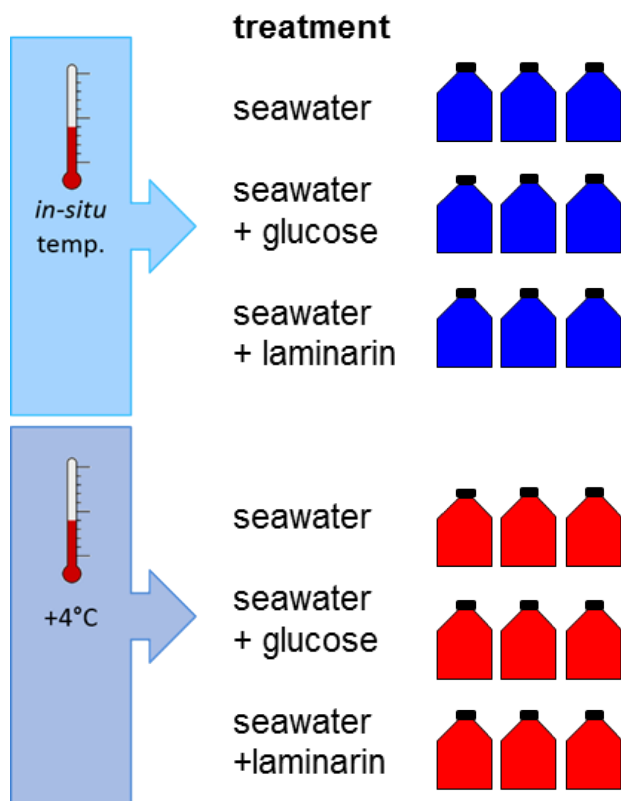
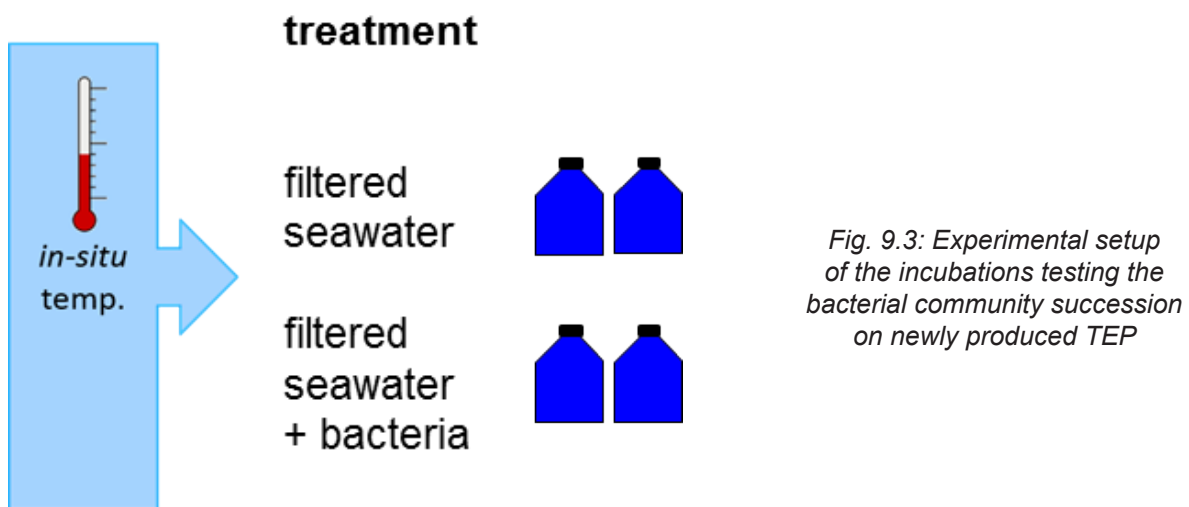


Fig. 9.2: Experimental setup of the incubations testing the combined effects of temperature and organic matter availability on the Antarctic bacterial community

Results of *WP 1* will be used to elucidate the *in situ* response of bacterial activity to changes in temperature and organic matter concentrations. Combined with results from previous expeditions (PS103, PS111), the data set will give insight into bacterial responses over different years and sea ice conditions. In addition, the fungal community in the water column and its importance in the degradation of organic matter such as gel-like particles will be characterized and compared to the importance of the bacterial community. In order to properly estimate the carbon sequestration in the Southern Ocean under elevated CO<sub>2</sub> concentrations in the atmosphere, it is vital to understand the role of all players of organic matter degradation in the water column.



The first set of incubations of *WP 2* will further corroborate the bacterial response to temperature changes under defined organic matter availabilities. The second set of incubations of *WP 2* will give insight into the functional groups of bacterial TEP colonizers.

### Preliminary and expected results

Extracellular enzyme activity was measured onboard and the data will be analysed at IOW in Rostock.

Samples for DCHO, DAA, DOC, bacterial cell abundances, gel-like particles, microbial community composition, PLFA and fungi cultivation were preserved and stored at RT, +4°C, -20°C and -80°C according to established protocols and will be analyzed in the home laboratories at IOW in Rostock and MBA in Plymouth (UK).

### Data management

Sample analysis will be conducted within one and a half years after the expedition. Subsequently, the data will be published in international peer-reviewed journals. Data will be made publically available via PANGAEA after publication.

**References**

- Allredge AL, Passow U & Logan BE (1993) The abundance and significance of a class of large , transparent organic particles in the ocean. *Deep Res I*, 40, 1131–40.
- Calvo-Diaz A, Franco-Vidal L & Moran X (2014) Annual cycles of bacterioplankton biomass and production suggest a general switch between temperature and resource control in temperate coastal ecosystems. *J Plankton Res*, 36, 859–65.
- Cunliffe M, Hollingsworth A, Bain C, Sharma V & Taylor JD (2017) Algal polysaccharide utilisation by saprotrophic planktonic marine fungi. *Fungal Ecol*, 30, 135–8.
- Ducklow HW, Kirchman DL & Anderson TR (2002) The magnitude of spring bacterial production in the North Atlantic Ocean. *Limnol Ocean*, 47, 1684–93.
- Engel A, Thoms S, Riebesell U, Rochelle-Newall E & Zondervan I (2004). Polysaccharide aggregation as a potential sink of marine dissolved organic carbon. *Nature*, 428, 929–32.
- Kirchman DL & Moran X. Microbial growth in the polar oceans - role of temperature and potential impact of climate change (2009) *Nat Rev Microbiol*, 7:451–9.
- Moran X, Calvo-Diaz A & Ducklow HW (2010) Total and phytoplankton mediated bottom-up control of bacterioplankton change with temperature in NE Atlantic shelf waters. *Aquat Microb Ecol* 58, 229–39.
- Painter TJ (1983) Algal polysaccharides. *The Polysaccharides*. Academic Press, New York, 195–285.
- Passow U (2002) Transparent Exopolymer Particles in Aquatic Environments. *Prog Oceanogr*, 55, 287–333.
- Taylor JD & Cunliffe M (2016) Coastal bacterioplankton community response to diatom-derived polysaccharide microgels. *Environ Microbiol Rep*, 9, 151–157.

## 10. MOLECULAR ECOLOGY, PHYSIOLOGY AND LIFE HISTORY TOOLS TO MONITOR ANTARCTIC TOOTHFISH (*DISSOSTICHUS MAWSONI*) POPULATIONS IN THE WEDDELL SEA

Chiara Papetti<sup>1</sup> (not on board), Emilio Riginella<sup>2</sup>, Nils Koschnick<sup>3</sup>, Mario La Mesa<sup>4</sup> (not on board), Jilda A Caccavo<sup>1</sup> (not on board), Lorenzo Zane<sup>1</sup> (not on board), Magnus Lucassen<sup>3</sup> (not on board) Stefan Hain<sup>3</sup> (not on board), Vladimir Laptikhovsky<sup>5</sup>, Rebecca Gorniak<sup>3</sup>

<sup>1</sup>UNIPD  
<sup>2</sup>SZN  
<sup>3</sup>AWI  
<sup>4</sup>ISMAR-CNR  
<sup>5</sup>CEFAS

### Grant No AWI\_PS117\_08 & AWI\_PS117\_09

#### Objectives

The Antarctic toothfish *Dissostichus mawsoni* is a mesopredator in the Antarctic marine food web. It feeds mainly on the silverfish *Pleuragramma antarctica* (and thereby is a trophic competitor of penguins for it) and is the prey of larger predators (e.g. seals, killer whales). The toothfish has a commercial value worth between 20 and 100 dollars per kg and is therefore the target of an economically relevant fishery in the Southern Ocean (Hanchet et al., 2015). Current Antarctic fisheries management by the Commission for the Conservation of Antarctic Marine Living Resources (CCAMLR, [www.ccamlr.org](http://www.ccamlr.org)) largely depends on mathematical/statistical models to determine stock sizes and catch rates, but these models frequently fail in the absence of adequate and accurate biological and physical data.

After 20 years of the fishery experiencing very high yields, still little is known about the biology of toothfish, and this lack of knowledge impinges on the sound management of the species. The hundreds of Agassiz and bottom trawl samples taken by AWI in the Weddell Sea over the last 35 years yielded less than 40 specimens.

The standard way of catching Antarctic toothfish applied by the commercially operated fishing vessels makes use of horizontal longlines, often several kilometres long with thousands of baited hooks. However, it is very difficult to deploy such longlines from a normal scientific research vessel such as *Polarstern*. Therefore, the project did pilot a novel, targeted approach by catching a limited amount (max. 5 tonnes) of toothfish with vertical longlines. Vertical longlines have been used occasionally to catch Antarctic toothfish in experimental settings (Kokorin & Serbin, 2009), through sea ice (Parker et al., 2013; Parker et al., 2016) and for special research surveys (Parker et al., 2015). Piloting the use of vertical longlines from *Polarstern* combines the long-term experience gained by AWI in deploying oceanographic moorings in the Weddell Sea with the fisheries expert guidance kindly provided by CCAMLR partners from UK and New Zealand.

Fishery is not the only factor potentially affecting the abundance and health of toothfish populations. Climate change – water temperature rise, ocean acidification, changes of sea ice coverage and further oceanographic parameters – have the potential to affect the entire Antarctic ecosystem, altering food and light availability and causing physiological stress. Thereby, these factors may act synergistically on population dynamics and structure especially on species already facing fishery pressure.

Although currently only the Western Antarctic is facing dramatic climate change, recent results from IPCC-scenario simulations reveal a pronounced sensitivity of the south-eastern Weddell Sea to projected environmental changes. Hellmer et al. (2012) predict a 0.5-0.7° C increase in the temperature of bottom water masses, which occur in the potential habitat of adult Antarctic toothfish on the continental slope in depths between 550 m - 2,100 m. Inflow of melting water and “warm” bottom water reaching the shelf will cause basal melting of the shelf ice (e.g. the Ronne-Filchner ice shelf), which may induce large-scale shifts in water masses and temperature distribution, including increased PCO<sub>2</sub>. Although these shifts in temperature are quite small, they may have significant influence on animal performance of highly cold-adapted, stenothermic species like *D. mawsoni* and thus consequences for species abundance and distribution. The cold-adapted toothfish, exposed already to fishery pressure, may thus require additional management and conservation measures to minimize the effects of environmental changes and human impact (Griffiths et al., 2017).

There are proposed measures to protect, conserve and limit the fishery of this species. The fishery of *D. mawsoni* in the Ross Sea has been partially closed since 1st December 2017 when the (largest in the world) Marine Protected Area (MPA) took effect. A proposal for an MPA in the Weddell Sea has been prepared by Germany and proposed by the EU under the CCAMLR.

To be able to apply sound management to the Antarctic toothfish resources in the Weddell Sea, to monitor MPA effectiveness stock trends, the main objectives of the research are:

- to investigate the population connectivity and demography via life history data, ecological and genetic information. This implies the collection of samples from muscle or fin, photos for morphology description, otoliths for age determination and microchemistry analysis, gonads for sexual maturity and fecundity assessment. These samples will contribute to provide data for testing and further developing the *D. mawsoni* population hypotheses for CCAMLR statistical area 48, which were established at the CCAMLR expert workshop held in Berlin in February 2018;
- to study specific adaptations that may hinder the toothfish survival under warming conditions. This implies the collection of samples of all body tissues deep frozen and tissues fixed in formalin;
- the health of the population/stock (the “hologenome” from toothfish). This implies the collection of faeces and different tracts of gastrointestinal apparatus (i.e., midgut and hindgut) and sites within gut locations (i.e., content and wall), buccal swabs. This design will allow us to determine if distinct bacterial taxa are enriched in the different gut locations (i.e., midgut and hindgut), if microbial communities in the gut content (lumen) differ from those associated directly with the gut wall (mucosa), and how the relationship between communities within the content and wall changes along the gut;
- to demonstrate that important and targeted investigations on *D. mawsoni* (e.g. tagging, sampling of toothfish tissues, especially for genetics and genomics) can successfully be carried out via vertical longlines deployed by research vessels such as *Polarstern*;
- to gain data and information for a better understanding of the population structure and dynamics of *D. mawsoni* as a key species in the Weddell Sea ecosystem and to improve knowledge about its life cycle and its role in the wider ecosystem and food chains.

### Work at sea

The biological sampling of Antarctic toothfish was undertaken with 8 vertical longlines / moorings (Fig. 10.1) to be deployed in 3 clusters at 800 m, 1,000 m and 1,200 m water depths at different geographical locations along the route of PS117. Preferred sampling areas would

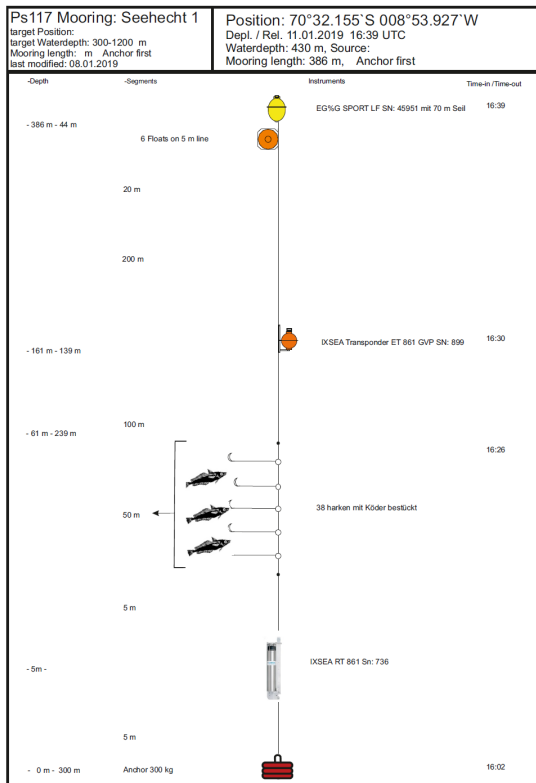


Fig. 10.1: Scheme of the vertical longline

be the eastern Weddell Sea (e.g. around Maud Rise or near the German *Neumayer Station III*) and on the continental slope around the tip of the Antarctic Peninsula. The exact locations depended on sea ice cover and time available. The vertical longlines were deployed via the mid-ship sliding beam when *Polarstern* was stationary. This means that the line has entered the water vertically in approx. 1 m distance from the ships side. During deployment and recovery of the gear only few baited hooks were exposed at a time, thereby avoiding any incidental bird catch / mortality. Due to the expected heavy sea ice conditions, the vertical longlines ended around 100 m below the sea surface to avoid being dragged by ice flows. Soaking time was between 22 and 88 hours. The deployment and hydroacoustic release of the vertical longlines was monitored by the acoustic positioning system Posidonia. After sufficient soaking time, a pop-up buoy was released by hydroacoustic signal to the IXSEA Transponder ET 861 and surfaced to allow the line to be hauled on board. In case of failure of the longline, the bottom transponder (IXSEA RT 861) was released leaving the main bottom weight (single railway carriage wheel) on the sea floor.

Medium- and small-sized fish (including possibly juvenile Antarctic toothfish) was expected to be caught using baited traps (Fig. 10.2) applied to a newly developed lander system (M. Lucassen, unpublished, AWI). This trap was deployed twice during the expedition in conjunction with the vertical longline deployment. After the catch, live fish were placed into the aquaria systems, kept alive and controlled regularly. The fish-food was weighed prior to fish feeding.

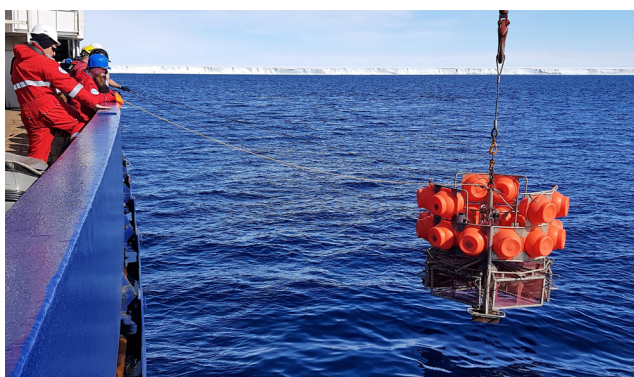


Fig. 10.2: Fishing trap

Captured fishes were sampled the following way:

1. After identification for each specimen a set of standard measurements and biological parameters (total length, total weight, gutted weight, gonad weight, sex and stage of maturity) were recorded and entered in a database. Sampling entailed dissection of a small amount of lateral muscle tissue and/or fin clips, under clean conditions,

and storage of tissue samples in 2 ml of 99 % absolute ethanol (at 4°C). A replicated sample of these tissues and additional organs (spleen, blood, brain, liver, heart) of interest were preserved at -80°C. Otoliths and gonads were collected in parallel and stored dry or in Dietrich solution (and formalin for mature female), respectively.

2. For gene expression profiling and genome sequencing, all available tissues together with blood and serum from undamaged fish were dissected directly after short recovery from the haul. Depending on available specimens, short-term exposures to elevated temperatures or specific diets might be conducted. At the end, these fish were sacrificed and sampled. Tissue samples were excised, flash frozen in liquid nitrogen and stored at -80°C or fixed in formalin until in Bremerhaven (Germany). These samples will also serve for the long-term molecular genetics and physiological sample archive of the AWI working group of Dr. Lucassen, for which sampling started in 2003 for the eastern Weddell Sea and the Antarctic Peninsula. This will allow in the long-term for the detection of spatio-temporal biodiversity and population shifts and comparison among Antarctic regions.
3. All other captured fish were dissected to separate the entire gut contents, which were stored at -80°C until further processing. No fish with punctured intestinal tracts were considered. From each fish, the intestinal tract was further dissected using a sterile scalpel to separate the midgut (immediately after the stomach) and the hindgut (immediately before the anus) sections. For each of these two sections, the gut content was squeezed out and the gut wall separated. Gut wall samples were washed twice with sterile artificial seawater to remove any remaining gut content. All samples were frozen at -80°C.
4. All toothfish specimens not needed for this research were expected to be tagged with standard CCAMLR t-bar tags in accordance with the CCAMLR tagging procedures / guidelines and released after collection of weight and length data in order to understand the longer-term links with other potential parts of this population. Biological samples of specimens from other (by-catch) species caught on the sampling gear were retained to understand species composition and life histories of those species in the areas sampled.

### Preliminary and expected results

A total of 8 longlines and 2 fish traps were deployed during the expedition.

1. In the easternmost part of the Weddell Sea, no toothfish was captured even after 88 hours of vertical long line soaking at the depth of ~ 1,000 m off *Neumayer Station III*. Only one grenadier *Macrourus caml* was captured there (PS117; Station 47-1). No fish at all was caught by the longline set at ~ 400 m.
2. Six other lines were deployed and hauled in the western part of the Weddell Sea, close to the tip of Antarctic Peninsula, at depths of ~800, ~1,000 and ~1,200 m (PS117; Stations 86-1, 87-1, 88-1, 101-1, 102-1 and 103-1). They resulted in capture of 6 grenadiers of three species (*M.caml*, *M.whitsoni* and *M.carinatus*) and two icefishes *Chionobathyscus dewitti*. No toothfish was captured.
3. Two fishes, *Cryodraco antarcticus* and *Trematomus hansonii* were captured on 16 January (PS117; Station 48-2) by use of the fish trap in the eastern Weddell Sea and used to study daily food requirements of the Antarctic fish until 1 February. The two fishes were kept in two separate tanks at temperature varying from 0.8 to 1.9°C. Fishes were fed by squid *Loligo vulgaris ad libitum*. Food was weighed and put into the

tanks every morning. Uneaten squid was removed from tank also every morning and reweighed. During 17 days of the experiment *C. antarcticus* refused food, whereas *T. hansonii* consumed the squid 4 times. A total weight of eaten food was 46.1 g, which is 12.8 % of *T. hansonii* body mass and 0.75 % of body mass per day. When these two animals were sacrificed, on 1 February, they still had some undigested squid in their stomach although feeding was suspended on 25 January. These data will expand our scarce knowledge of the Antarctic fish diet requirements.

4. The fish trap deployed in station 89-1 was not successfully recovered (PS117; Station 89-1) probably because of a failure of the transponder. Of the eight deployed longlines, two were recovered using release of the bottom transponder, as the upper transponder did not respond in one case to hydro-acoustic signal, and in another case the rope released by the upper transponder became entangled with buoys and did not reach the surface.

All fishes were sampled in agreement with aforementioned eco-physiological scientific protocols.

### Data management

All data will be published in internationally recognised, peer-reviewed scientific journals and *Polarstern* and the Alfred Wegener Institute Helmholtz Centre for Polar and Marine Research will be properly acknowledged. The molecular data will be submitted to the respective database (NCBI, EMBL), all other data will be stored in PANGAEA. Samples may become available for other scientists on request.

### References

- CCAMLR (2018) Report of the workshop for the development of a *Dissostichus mawsonii* population hypothesis for Area 48, 8 pp. Available at <https://www.ccamlr.org/en/toothfish-life-history-workshop>.
- Griffiths HJ, Meijers AJS, Bracegirdle TJ (2017) More losers than winners in a century of future Southern Ocean seafloor warming. *Nature Climate Change*, 7, 749-754.
- Hanchet S, Dunn A, Parker S, Horn P, Stevens D, Mormede S (2015) The Antarctic toothfish (*Dissostichus mawsonii*): biology, ecology, and life history in the Ross Sea region. *Hydrobiologia*, 761, 397-414.
- Hellmer HH, Kauker F, Timmermann R, Determann J, Rae J (2012) Twenty-first-century warming of a large Antarctic ice-shelf cavity by a redirected coastal current. *Nature*, 485, 225-228.
- Hanchet SM, Dunn A, Parker SJ, Horn P, Stevens D, Mormede S (2015) The Antarctic toothfish (*Dissostichus mawsonii*): biology, ecology, and life history in the Ross Sea region. *Hydrobiologia*, 761 (1): 397–414. doi:10.1007/s10750-015-2435-6.
- Kokorin NV, Serbin VV (2009) First experimental settings of deepwater vertical longlines in the Antarctic toothfish fishery *Dissostichus mawsonii* Norman, 1937 (Perciformes, Nototheniidae) in the Amundsen Sea. Document WG-FSA-09/08. CCAMLR, Hobart, Australia. 13 p.
- Parker SJ, Hanchet SM, Mormede S, Dunn A, Sarralde R (2013) Results of a CCAMLR sponsored research survey to monitor abundance of pre-recruit Antarctic toothfish in the southern Ross Sea, February 2013. Document WG-SAM-13/32. CCAMLR, Hobart, Australia. 31 p.
- Parker SJ, Hanchet SM, S. Mormede S (2015) A proposal for a standardised survey for Antarctic toothfish in McMurdo Sound. Document WG-FSA-15/33. CCAMLR, Hobart, Australia. 7 p.
- Parker SJ, Mormede S, DeVries A, Hanchet SM, Eisert R (2016) Have toothfish returned to McMurdo Sound, Antarctica? *Antarctic Science*, 28 (1): 29–34. doi: 10.1017/S0954102015000450 dissection and sampling procedure.

## 11. YOPP AWIMET-PS: THE “YEAR OF POLAR PREDICTION” (YOPP): ADDITIONAL RADIOSOUNDINGS DURING THE SPECIAL OBSERVING PERIOD

Darragh Kenny<sup>1</sup>, Markus Rex<sup>1</sup>  
Not on board: Holger Schmithüsen<sup>1</sup>

<sup>1</sup>AWI

**Grant-No. AWI\_PS117\_10**

### Objectives

The „Year of Polar Prediction“ (YOPP) is one of the key elements of the Polar Prediction Project (PPP, [www.polarprediction.net](http://www.polarprediction.net)). Its mission is:

Enable a significant improvement in environmental prediction capabilities for the polar regions and beyond, by coordinating a period of intensive observing, modelling, verification, user-engagement and education activities.

Within YOPP there are three “Special Observing Periods” (SOPs) defined:

- SOP-NH1: 1 Feb. 2018 – 31 Mar. 2018 in the Arctic
- SOP-NH2: 1 Jul. 2018 – 30 Sep. 2018 in the Arctic
- SOP-SH: 16 Nov 2018 – 15 Feb 2019 in the Antarctic

To contribute to the special observing efforts of YOPP the radiosounding activity on board *Polarstern* is increased to 4 soundings per day. This follows the internationally compiled science plan of PPP<sup>1</sup> and the recommendations in the implementation plan<sup>2</sup> of the project.

### Work at sea

Whenever *Polarstern* is south of 60°S, the routinely launched daily radiosounding is extended by another 3 soundings per day. Together, the soundings cover all synoptic main hours, namely 00, 06, 12 and 18 UTC.

### Data management

Data management is identical to the routinely performed radiosoundings. Data on board will be made available through the DWD staff to any interested scientist. Data will be published on Pangaea after the expedition. Any scientific publication shall use the data from PANGAEA.

### Expected results

Radiosonde measurements are known to be one of the highest impact global observation systems for operational weather prediction analysis (“analysis” is the best guess of the status of the atmosphere at a certain point in time). Temporarily intensified soundings, together with modelling studies, are capable to quantify the impact on operational analysis products. During YOPP it is expected that the impact of polar radiosounding activities on weather prediction capabilities can be estimated. This will give important reasoning for the optimisation of the polar meteorological observation network, which is one distinct goal of YOPP.

### References

World Weather Research Programme (2013) WWRP Polar Prediction Project Science Plan. WWRP/PPP No. 1. World Meteorological Organization, Geneva<sup>1</sup>.

World Weather Research Programme (2016) WWRP Polar Prediction Project Implementation Plan for the Year of Polar Prediction (YOPP), Version 2.0. WWRP/PPP No. 4. World Meteorological Organization, Geneva. <sup>2</sup>

---

<sup>1</sup> [http://www.polarprediction.net/fileadmin/user\\_upload/www.polarprediction.net/Home/Documents/Final\\_WWRP\\_PPP\\_Science\\_Plan.pdf](http://www.polarprediction.net/fileadmin/user_upload/www.polarprediction.net/Home/Documents/Final_WWRP_PPP_Science_Plan.pdf)

<sup>2</sup> [http://www.polarprediction.net/fileadmin/user\\_upload/www.polarprediction.net/Home/YOPP/YOPP\\_Documents/FINAL\\_WWRP\\_PPP\\_YOPP\\_Plan\\_28\\_July\\_2016\\_web-1.pdf](http://www.polarprediction.net/fileadmin/user_upload/www.polarprediction.net/Home/YOPP/YOPP_Documents/FINAL_WWRP_PPP_YOPP_Plan_28_July_2016_web-1.pdf)

## **ABBILDUNGSINDEX / INDEX OF FIGURES**

## ABBILDUNGSVERZEICHNIS / INDEX OF FIGURES

Abb. 1.1: Fahrtverlauf der Antarktis Expedition PS117. Beginn der Reise war am 15 Dezember 2018 in Kapstadt, Südafrika, Ende am 7 Februar 2019 in Punta Arenas, Chile.S: <a href="https://doi.pangaea.de/10.1594/PANGAEA.899721">https://doi.pangaea.de/10.1594/PANGAEA.899721</a> .	6
Fig. 1.1: Track of expedition PS117 to the Antarctic, starting in Cape Town on 15 December 2018, ending in Punta Arenas, Chile, on 7 February 2019. See also <a href="https://doi.pangaea.de/10.1594/PANGAEA.899721">https://doi.pangaea.de/10.1594/PANGAEA.899721</a> .	6
Fig. 2.1: Distribution of wind force during PS117	12
Fig. 2.2: Distribution of wind directions during PS117	12
Fig. 2.3: Distribution of wave heights during PS117	12
Fig. 2.4: Distribution of cloud coverage during PS117.	13
Fig. 2.5: Weather enroute PS117	13
Fig. 2.6: Distribution of wave heights during PS117	14
Fig. 3.1: Map of mooring locations occupied since 2016/17 or earlier. The lower panel is an enlargement of the black box in the top panel. Green dots indicate moorings recovered and blue dots moorings exchanged during this expedition PS117. The current number "n" of the mooring ID "AWIxxx-n" is the number of the deployed mooring. If the mooring was not exchanged, "n" represents the number of the recovered mooring.	18
Fig. 3.2: Top: Map of locations of CTD stations. Labels indicate station and cast numbers as given in the station list. Bottom: Enlarged map of the CTD section at the tip of the Antarctic Peninsula; see box in map above.	29
Fig. 3.3: Greenwich Meridian CTD section during PS117. Nominal station spacing is 60 nm, though some stations had to be skipped due to operational circumstances.	31
Fig. 3.4: Temperature (top) and salinity (bottom) records from past and current CTD casts at 61°S, 0°E.	32
Fig. 3.5: Section of potential temperature at the tip of the Antarctic Peninsula	32
Fig. 3.6: Sections of a) potential temperature, b) zonal velocities measured by the VMADCP, and c) zonal velocities measured by the LADCP at the Antarctic shelf near the Greenwich meridian. The local ice conditions prohibited occupying stations further up the shelf. Note that all stations are located on the upstream (eastern) side of the local shelf tongue.	37
Fig. 3.7: Sections of a) potential temperature (top), b) meridional velocities measured by the VMADCP (middle), and c) meridional velocities measured by the LADCP at the Antarctic Peninsula (bottom).	37
Fig. 3.8: Tidal ellipses and scaled vectors showing modelled flow directions during AWI-CTD station 1 (just before low tide), 6 (just before high tide), 9 (just after low tide) and 12 (as high tide) as obtained from the Padman et al. (2002) tidal modell.	38
Fig. 3.9: Top to bottom: Modelled tidal height (black curve) and phases of rising tide (white) and ebbing tide (cyan); Vessel mounted ADCP zonal velocity profiles during periods while on station; ditto for meridonal velocity; Potential temperature profiles, interpolated.	39

Fig. 3.10: Top: Potential temperature profiles while on station during tidal experiment, interpolated in time; bottom: salinity while on station during tidal experiment, interpolated in time	39
Fig. 3.11: HAFOS sound source array as installed up to Polarstern expedition PS117. White stars with concentric circles: Sources (re)deployed on PS103 with 200 nm range. All sound sources, but the 2 southernmost ones, were recovered during PS117. Top-left to the marked position: Serial number of sound source, mooring number, sound source position number and sweep time (GPS).	41
Fig. 3.12: Spectrogram as recorded by icListen 1414 during first gauging of Develogic sound source D0018. Recognizable is the initial RAFOS sweep, the 5 frequency up-sweeps and the final RAFOS sweep.	45
Fig. 3.13: Resonance curves of develogic RAFOS source D0018 before (left) and after (right) cutting.	46
Fig. 3.14: Left: Resonance curve of develogic RAFOS source D0017 as recorded by icListen 1415 during 1st gauging. Right: Resonance curve of develogic RAFOS source D0043 as recorded by icListen 1415 (during 2nd gauging).	46
Fig. 3.15: Deviation in salinity between OPS measurements and in-situ CTD measurements versus time (top) and versus pressure (bottom) for the primary and secondary sensor. The pressure effect is slightly more pronounced for the secondary sensor and in addition the drift is notable while the drift is almost zero for the primary sensor.	47
Fig. 3.16: Positions of ARVOR float deployments. The WMO number of the floats is indicated at each deployment position. Grey solid lines represent the isobaths -4000, -3000, -2000, and -1000. The map on the top right corner indicates the area of deployment.	50
Fig. 3.17: Feeder attached to front of Fiona (two black “antlers”) with recovery rope (red) attached to shackle (not visible) in center of feeder. In the background the mobile GAPS antenna suspended over the side of the ship.	53
Fig. 3.18: Sketch of ship-side (deck-side) setup of mobile GAPS antenna and ROV Fiona deployment. Red: 20-t boom (Großer Schiebebalken) and 5-to boom (Kleiner Schiebebalken). Green: ROV Fiona with tether and tether reel. Black: ROV surface power supply (SPS) and integrated navigation console (INC).	55
Fig. 3.19: Flow chart of navigational information	56
Fig. 3.20: Map showing the 14 locations of acoustic recorders recovered during PS117.	64
Fig. 3.21: Recording days of passive acoustic recorders retrieved during PS117. Note that AWI250-01 stems from a different deployment period (2012-2014) than all other recorders (2016-2018).	67
Fig. 3.22: Deployment positions of acoustic recorders moored during PS117	69
Fig. 3.23: Preliminary results on acoustic presence of marine mammal species in passive acoustic data recorded at 12 recorder positions throughout the Weddell Sea	77
Fig. 3.24: Location of PIES composing the GoodHope array (white dots) including Jason satellite ground tracks (black lines, track 133 marked red) and climatologic locations of major ocean fronts (cyan dots).	80

Fig. 4.1:	CTD data at station 56 cast 1	86
Fig. 4.2:	Dissolved PO <sub>4</sub> (µM) data from the zero meridian transect	91
Fig. 4.3:	Dissolved PO <sub>4</sub> (µM) data from the zero meridian transect	91
Fig. 4.4:	Dissolved Si (µM) data from the zero meridian transect	91
Fig. 4.5:	Three depth profiles (station 18, 27 and 38) of dissolved iron. Error bars are presenting ± 1 standard deviation.	96
Fig. 4.6:	The depth profile of the conditional stability constant (log ) derived from the total iron-binding ligand concentrations at station 27	97
Fig. 4.7:	Modified dilution assay experimental design. Mesoplankton-free whole water (1) is combined with either <0.45-µm filtrate (2) or 30 kDa filtrate (3) in the correct proportions to create the parallel t0 dilution series: <0.45µm series, with reduced grazing mortality (4)30 kDa series, with reduced grazing and viral mortality (5). Replicate sample bottles from the <0.45-µm and kDa dilution series are then created (6 and 7) and incubated under experimental conditions. (Kimmance and Brussaard, 2010).	104
Fig. 5.1:	Locations for SOCCOM BGC floats, PICCOLO BGC floats, PICCOLO Core Argo floats, and CTDs at which DIC samples were collected. Oxygen samples were collected and analysed at all stations where DIC was samples, unless the ocean depth was < 500 m. Solid black lines indicate frontal boundaries (Orsi et al. 1995 ).	113
Fig. 5.2:	Difference between the CTD oxygen sensor and the oxygen concentration determined from the samples by Winkler titration. (a) AWI CTD with sensor 1 (b) AWI CTD after the sensor was replaced (c) NIOZ Ultra Clean CTD (UCC). Annotated are the mean (dashed lines) and two times the standard deviation (dotted lines)	115
Fig. 5.3:	Histogram of difference between the CTD oxygen sensor and the oxygen concentration determined from the samples by Winkler titration. (a) AWI CTD with sensor 1 (b) AWI CTD after the sensor was replaced (c) NIOZ Ultra Clean CTD (UCC). Annotated are the mean (dashed green lines) and median (dashed red lines).	116
Fig. 5.4:	Oxygen concentration difference (CTD optode – titration) compared to depth (red), temperature (blue) and salinity (green) for AWI CTD sensor 1 (top row), AWI CTD sensor 2 (middle row) and NIOZ UCC (bottom row).	116
Fig. 5.5:	Temperature (left, red) and salinity (right, green) profiles of the PICCOLO BGC float F0659 (top) and F0661 (bottom) during their first cycle, in comparison to the respective profiles by the AWI CTD at the deployment station (black).	117
Fig. 5.6:	Temperature (left, red) and salinity (right, green) profiles of the PICCOLO BGC float F0659 (top) and F0661 (bottom) for all profiles to date.	118
Fig. 5.7:	Preliminary pH profiles from SOCCOM BGC float 0886	118
Fig. 6.1:	Manta Trawl (MT) deployed in the Southern Ocean. Between the yellow brindle of the MT and the steel rope of the on-board crane an 8 kg steel weight is attached to stabilise the trawl.	121
Fig. 6.2:	Wooden protection covering geological sieves to allow for undisturbed sampling. Samples are taken from the on-board seawater intake system connected to the protected sieve stack with a water meter and a silicone hose.	121

Fig. 6.3:	Sampling locations. The black line represents the Polarstern track on expedition PS117. Red dots represent the sites where the MT was deployed to sample surface water for MP. Filled red dots indicate that MP was found in the sample. Continuous sampling with the seawater pump (SP) started at latitude -44.667677 and longitude 7.0855 (and was stopped at latitude -60.666318 and longitude 57.906921). Blue lines represent SP transects in which MP was found.	122
Fig. 6.4:	Preliminary frequency distribution of anthropogenic particles $m^{-3}$ in 15 surface water samples (MT) analysed on board. Samples taken during PS117 will undergo further visual inspection, spectroscopic analysis and evaluation in the home laboratory (University of Basel).	129
Fig. 6.5:	Anthropogenic fragments identified as ship paint from MT 16 (green), MT 18 (blue), MT 7 (red/orange) and MT 10 (white) respectively.	130
Fig. 6.6:	Chlorobutyl fragment from MT 13 (A), polyester fragment from SP 8 (B) and neoprene fragment from SP 12 (C)	130
Fig. 7.1:	Overview of SUIT, RMT, and ice stations sampled by SIPES-2 during PS117	133
Fig. 7.2:	Example of environmental data profiles obtained from the SUIT's sensors array at station 27-4	136
Fig. 7.3:	Major taxa of the SUIT catch composition	137
Fig. 7.4:	Number of individuals of <i>Euphasia superba</i> for each station (panel a) in relation to ice thickness (panel b).	138
Fig. 7.5:	Major taxa of the RMT catch composition at depth 200 m to 100 m	138
Fig. 7.6:	Major taxa of the RMT catch composition at depth 100 m to 50 m	139
Fig. 7.7:	Major taxa of the RMT catch composition at depth 50 m to surface	139
Fig. 7.8:	Vertical profiles for a) ice temperature, b) brine salinity, c) ice bulk salinity and d) brine volume fraction for ice stations 1-8.	141
Fig. 7.9:	Vertical profiles for bulk sea-ice nutrient concentrations. a) nitrate, b) silicate, c) phosphate.	141
Fig. 7.10:	Example for a dataset collected with the ROV. Left: Image from the up-ward looking stills camera showing krill at the ice-water interface. Right: Under-ice radiance spectra collected with an upward-looking hyperspectral radiometer from the same location.	142
Fig. 9.1:	Sampled CTD stations (green dots) and positions of selected stations where incubations were started (red empty circles)	158
Fig. 9.2:	Experimental setup of the incubations testing the combined effects of temperature and organic matter availability on the Antarctic bacterial community	159
Fig. 9.3:	Experimental setup of the incubations testing the bacterial community succession on newly produced TEP	160
Fig. 10.1:	Scheme of the vertical longline	164
Fig. 10.2:	Fishing trap	164

## **TABELLENVERZEICHNIS / INDEX OF TABLES**

## TABELLENINDEX / INDEX OF TABLES

Tab. 1.1: Verteilung der Stationszeiten nach Gerät	5
Tab. 3.1: Mooring recoveries during PS117. <sup>1)</sup> indicates PIES landers, <sup>2)</sup> indicates the PIES landers that did not surface, <sup>3)</sup> indicates recovery of a mooring deployed during ANT-XXIX/2 (PS81 2012/13); all other moorings were deployed during PS103 (2016/17). "CTD Stat.Nr." is the station number of the CTD cast carried out at the mooring location.	17
Tab. 3.2: Mooring deployments during PS117. <sup>1)</sup> denotes a mooring not deployed due to bad weather conditions.	17
Tab. 3.3: Instrumentation of deployed oceanographic moorings	19
Tab. 3.4: Moorings recovered during PS117. Date and time of the recovery represent date and time of the first release command.	21
Tab. 3.5: Comparison for Seabird sensors SBE37 moored during PS117. Columns CTD and PRES indicate the corresponding station number and the CTD pressure during the 5 minute stop. $X_{corr} = X_{reading} + dX$ , with $X$ = temperature (t), conductivity(c) or pressure (p).	25
Tab. 3.6: Offsets for Seabird sensors SBE37 and SBE39 recovered during PS117. Their temperature and conductivity data was adjusted based on a linear interpolation between prior (dt1, dc1) and post recovery (dt2, dc2 dp2) offsets. For pressure the post recovery offset was applied as a constant offset. $X_{corr} = X_{reading} + dX$ , with $X$ = temperature (t), conductivity(c) or pressure (p).	26
Tab. 3.7: CTD-Sensor configuration and the related station numbers	28
Tab. 3.8: List of CTD profiles taken during PS117	29
Tab. 3.9: Configuration file of the Master LADCP	34
Tab. 3.10: Configuration file of the Slave LADCP	35
Tab. 3.11: List of common problems with corresponding station numbers	35
Tab. 3.12: Recovery of sound sources during PS117	40
Tab. 3.13: Recovery of sound sources during PS117	42
Tab. 3.14: Salinity samples from the water sampler and measured with the OPS	48

Tab. 3.15: ARVOR float deployments. Float profiles can be downloaded on <a href="https://www.jcommops.org/board/wa/Platform?ref=xxxxxxx">https://www.jcommops.org/board/wa/Platform?ref=xxxxxxx</a> with xxxxxxx standing for the wmo number. *featuring Ice Sensing Algorith (ISA).	51
Tab. 3.16: Overview of SonoVault and AURAL recorders recovered during PS117	65
Tab. 3.17: Overview of the recording periods and SD-card status of all recorders that were recovered during PS117.	68
Tab. 3.18: Overview of acoustic recorders deployed during PS117	70
Tab. 3.19: Overview of results of preliminary technical and data quality evaluation of recorders recovered during PS117	74
Tab. 3.20: Summary of deployment and recovery information regarding the French GoodHope PIES as recovered during PS117	79
Tab. 4.1: All stations and bioassays analysed for nutrients	87
Tab. 4.2: Cocktail characteristics	92
Tab. 4.3: Detection limits	92
Tab. 4.4: Precision	93
Tab. 4.5: CRM "CA" at 21.5°C	93
Tab. 4.6: CRM "CC" at 21.5°C	93
Tab. 4.7: Locations and maximum depths for the 23 stations sampled with the Ultra Clean CTD	94
Tab. 4.8: Overview of samples taken from the trace metal stations; X denotes samples taken for given parameter. DFe: dissolved iron; DM: dissolved metals; TM: unfiltered sample for total dissolvable metals; Iso; metal isotopes; Lib: library back up sample; C/N: POC and PON; PM: particulate metals; FeL: iron binding ligand quantification; Lig Char: Iron binding ligands characterization.	98
Tab. 4.9: Date and location for all protein samples taken from UCC CTD casts	100
Tab. 4.10: Bioassay Descriptions	101
Tab. 4.11: Overview of variables sampled: Abun: abundance, FLB: bacterial grazing rates. VP: viral production, LH: Viral lysis rates, FeCl <sub>3</sub> : iron chloride precipitation method for filtration of viral DNA	102
Tab. 4.12: Preliminary results of Fv/Fm data measured on board	103

Tab. 5.1: Deployment date and location of PICCOLO and SOCCOM floats	111
Tab. 5.2: Old and correct volumes of bottles used to collect and analyse oxygen samples	117
Tab. 6.2: Summary seawater pump samples for microplastics on PS117	125
Tab. 7.1: List and positions of the ice stations sampled during PS117 including the number of under-ice radiation measurements (L-arm) and other measurements. Nutr. = sampling for macronutrients, Gap layer = sampling of sea ice gap layers, Microplastics = sampling for microplastics, POM = particulate organic matter, gypsum = gypsum sampling	135
Tab. 7.2: Preliminary results for ice concentration (A), ice thickness ( $H_i$ ), surface temperature (T), and salinity (sal) obtained with the SUIT's sensors array	136
Tab. 7.3: List of RMT stations carried out during PS117, with date and position. The last column indicates the presence/absence of sea ice. The stations highlighted in light grey were conducted along the 0° meridian. The stations in white were carried out in the Eastern Weddell Sea, the stations in dark grey were conducted in the Western Weddell Sea, and the stations highlight in light yellow were conducted near Elephant Island.	140
Tab. 7.4: Overview Top Predator helicopter flights during PS117	143
Tab. 7.5: Species list of seabirds and marine mammals observed during PS117	143
Tab. 7.6: List of UCC and CTD casts sampled for POM analysis and list of calibration stations for the SUIT CTD	145
Tab. 8.1: Summary of sampling activities of our group during PS117. CTD: both depths sampled for the full set of parameters described in the text (eukaryotic nucleic acids, microscopy, and contextual measurements). HN: hand net (* weather conditions were too rough for HN, seawater filtration instead). Cultures: number of <i>Fragilariopsis</i> cultures isolated at the corresponding station.	150
Tab. 9.1: Sampled CTD stations and depths during PS117 including parameters that will be analysed from each sample	155

## **APPENDIX**

**A.1 Teilnehmende Institute / Participating Institutions**

**A.2 Fahrtteilnehmer / Cruise Participants**

**A.3 Schiffsbesatzung / Ship's Crew**

**A.4 Stationsliste / Station List**

## A.1 TEILNEHMENDE INSTITUTE / PARTICIPATING INSTITUTIONS

	Address
AAD	Australian Antarctic Division, Sea Ice Group Channel Highway 203 7050 Kingston / Australia
AWI	Alfred-Wegener-Institut Helmholtz-Zentrum für Polar- und Meeresforschung Am Handelshafen 12 27570 Bremerhaven / Germany
CAU	Christian-Albrechts-Universität zu Kiel Christian-Albrechts-Platz 4 24118 Kiel / Germany
CEFAS	CEFAS Fisheries Division Pakefield Rd. NR33 0HT Lowestoft / United Kingdom
Dalhousie University	Dalhousie University Biology, 1355 Oxford St, PO Box 15000 B3H 4R2, Halifax / Canada
DWD	Deutscher Wetterdienst Seeschiffahrtsberatung Bernhard-Nocht Strasse 76 20359 Hamburg / Germany
ENS	Ecole Normale Supérieure Department of Geosciences Laboratoire de Météorologie Dynamique UMR 8539, IPSL 24 rue Lhomond 75231 Paris Cedex 05 / France
HeliService	HeliService International GmbH Gorch-Fock-Straße 105 26721 Emden / Germany
HS Brhv	Hochschule Bremerhaven An der Karlstadt 8 27568 Bremerhaven / Germany
HUB	Humboldt-Universität zu Berlin, Institut für Biologie Unter den Linden 6 10099 Berlin / Germany

	<b>Address</b>
IOW	Universität Rostock Mathematisch-Naturwissenschaftliche Fakultät Wismarsche Str. 45 18057 Rostock / Germany
LOPS	Laboratoire d'Océanographie Physique et Spatiale UMR 6523 CNRS - IFREMER - IRD - UBO CS10070 - 29280 Plouzané / France
MBA	The Marine Biological Association Cell and Molecular Group Cunliffe lab Citadel Hill PL1 2PB Plymouth / United Kingdom
M van Dorssen Metaalbewerking	M van Dorssen Metaalbewerking Schilderend 113 1791 BE Den Burg / Netherlands
MGU	Man-Society-Environment (MGU), Dept of Environmental Sciences Vesalgasse 1 4051 Basel / Switzerland
NIOZ	Royal Netherlands Institute for Sea Research (NIOZ) Department of Ocean Systems Landsdiep 4, t'Hornjte 1797SZ, Texel / Netherlands
Reederei F. Laeisz GmbH	Reederei F. Laeisz (Bremerhaven) GmbH Bartelstr. 1 27570 Bremerhaven / Germany
RBINS	Royal Belgian Institute for Natural Sciences BEDIC, OD Nature Vautierstraat 29 1000 Brussels / Belgium
Scripps	Scripps Institution of Oceanography CASPO 9500 Gilman Drive 92093 La Jolla / United States
SZN	Stazione Zoologica Anton Dohrn Integrative Marine Ecology Villa Comunale 80121 Napoli / Italy

	<b>Address</b>
U Basel	Universität Basel Departement Umweltwissenschaften Vesalgasse 1 CH-4051 Basel / Switzerland
U Bern	Universität Bern Zentrum für Fisch- und Wildtiermedizin Länggass-Strasse 122 3012 Bern / Switzerland
UBremen	Universität Bremen Bibliothekstraße 128359 Bremen / Germany
UOL	Carl von Ossietzky Universität Oldenburg Ammerländer Heerstraße 114-118 26129 Oldenburg / Germany
U East Anglia	University of East Anglia School of Environmental Sciences Norwich Research Park NR4 7TJ, Norwich / United Kingdom
U Southampton	University of Southampton of Ocean and Earth Science, Waterfront Campus, European Way SO14 3ZH Southampton / United Kingdom
WMR	Wageningen Marine Research Ecosystems Ankerpark 27 1781AG Den Helder / Netherlands

## A.2 FAHRTTEILNEHMER / CRUISE PARTICIPANTS

Name	Vorname/ First Name	Affiliation	Beruf/ Profession	Disziplin/ Discipline
Allerholt	Jacob	HS Brhv	Student (BA)	Engineering
Ardiningsih	Indah	NIOZ	PhD student	Oceanography
Bertrand	Erin	Dalhousie University	Scientist	Biology
Boebel	Olaf	AWI	Scientist	Oceanography
Braun	Verena	AWI	Student (MA)	Glaciology
Bruns <sup>2)</sup>	Thomas	DWD	Scientist	Meteorology
Castellani	Giulia	AWI	Scientist	Physics
Chamberlain	Paul	Scripps	PhD student	Oceanography
Diercks	Isabel- Katharina	IOW	Student (MA)	Biology
Droste	Elise	U East Anglia	PhD student	Oceanography
Eggers	Sarah Lena	AWI	Technician	Biology
Eich	Charlotte	NIOZ	PhD student	Biology
Engicht	Carina	AWI	Technician	Oceanography
Enriquez	Alberto	HeliService	Technician	Aviation
Feij	Bram	NIOZ	Observer	Biology
Filun	Diego	AWI	PhD student	Biology
Gischler	Michael	HeliService	Pilot	Aviation
Glemser	Barbara	AWI	Student (MA)	Biology
Gorniak	Rebecca	AWI	Technician	Biology
Graupner	Rainer	AWI	Technician	Oceanography
Hempelt	Juliane	DWD	Technician	Meteorology
Holm-Burkhardt	Patricia	MGU	Scientist	Biology
Kendzia	Jan	HeliService	Pilot	Aviation
Kenny <sup>2)</sup>	Darragh	AWI	Student (MA)	Meteorology
Koschnick	Nils	AWI	Engineer	Biology
Krusenbaum	Moritz	CAU	Student (BA)	Oceanography
Kühn	Susanne	WMR	PhD student	Biology
Laptikhovsky	Vladimir	CEFAS	Scientist	Biology
Le Paih	Nicolas	AWI	PhD student	Oceanography
Leistenschneider	Clara	U Basel	PhD student	Biology
Meijboom	André	WMR	Scientist	Biology
Meiners	Klaus	AAD	Scientist	Biology
Meister	Marlene	HUB	Student (MA)	Biology
Middag	Rob	NIOZ	Scientist	Chemistry
Miller <sup>1)</sup>	Max	DWD	Scientist	Meteorology

<b>Name</b>	<b>Vorname/ First Name</b>	<b>Affiliation</b>	<b>Beruf/ Profession</b>	<b>Disziplin/ Discipline</b>
Milnes	Mark	AAD	Engineer	Engineering
Ober	Sven	NIOZ	Engineer	Oceanography
Ossebaar	Sharyn	NIOZ	Technician	Chemistry
Pont	Sven	NIOZ	Scientist	Biology
Probst	Lewin	AWI	Engineer	Oceanography
Rex <sup>1)</sup>	Markus	AWI	Scientist	Physics
Richter	Roland	HeliService	Engineer	Aviation
Riginella	Emilio	SZN	Scientist	Biology
Rohardt	Gerd	AWI	Scientist	Oceanography
Schaffer	Janin	AWI	Scientist	Oceanography
Segner	Helmut	U Bern	Scientist	Biology
Smolentseva	Margarita	AWI	PhD student	Physics
Spiesecke	Stefanie	AWI	Engineer	Oceanography
Tian	Hung-An	NIOZ	PhD student	Chemistry
Trace-Kleeberg	Sunke	U Southampton	Student (MA)	Oceanography
van Dorssen	Michiel	M van Dorssen Metaalbewerking	Technician	Biology
van Manen	Mathijs	NIOZ	PhD student	Chemistry
Vortkamp	Martina	AWI	Technician	Biology
Zäncker	Birthe	MBA	Scientist	Oceanography
Zwicker <sup>1)</sup>	Sarah	UOL	Student (MA)	Biology

<sup>1)</sup> towards Neumayer only

<sup>2)</sup> from Neumayer onwards only

### A.3 SCHIFFSBESATZUNG / SHIP'S CREW

	Name	Vorname	Rank
1	Langhinrichs	Moritz	Master
2	Spielke	Steffen	Chiefmate
3	Kentges	Felix	1st Mate
4	langer	Carl	2nd Mate
5	Peine	Lutz Gerhard	2nd Mate
6	Grafe	Jens	Chief
7	De Bruin	Frederik	2nd Eng.
8	Haack	Michael Detlev	2nd Eng.
9	Krinfeld	Oleksandr	2nd Eng.
10	Redmer	Jens	E-Eng.
11	Christian	Boris	ChiefELO
12	Ganter	Armin	ELO
13	Himmel	Frank	ELO
14	Hüttebräucker	Olaf	ELO
15	Nasis	Ilias	ELO
16	Rudde-Teufel	Claus Friedrich	Ships doc
17	Brück	Sebastian	Bosun
18	Reise	Lutz	Carpen.
19	Klee	Philipp	MP Rat.
20	Köpnick	Ulrich	MP Rat.
21	Möller	Falke	MP Rat.
22	Neubauer	Werner	MP Rat.
23	Schade	Tom	MP Rat.
24	Bäcker	Andreas	AB
25	Hans	Stefan	AB
26	Wende	Uwe	AB
27	Preußner	Jörg	Storek.
28	Decker	Jens	MPRat
29	Gebhardt	Norman	MPRat
30	Luckhardt	Arne	MPRat
31	Rhau	Lars-Peter	MP Rat
32	Schwarz	Uwe	MP Rat
33	Schnieder	Sven	Cook
34	Möller	Wolfgang Hans	He,,.Cooksm.
35	Sllinski	Frank	Cooksm.
36	Czyborra	Bärbel	Chief Stew.

---

	<b>Name</b>	<b>Vorname</b>	<b>Rank</b>
37	Wöckener	Martina	Nurse
38	Arendt	Rene	2nd Stew.
39	Chen	Dansheng	2nd Stew.
40	Dibenau	Torsten	2nd Stew.
41	Golla	Gerald	2nd Stew.
42	Silinski	Carmen	2nd Stew.
43	Sun	Yong Sheng	2nd Stew.
44	Kreutzmann	Lennart	Apprent.
45	Peper	Sven	Apprent.

## A.4 STATIONSLISTE / STATION LIST

Station	Date	Time	Latitude	Longitude	Depth [m]	Gear	Action	Comment
PS117_0_Underway-1	2018-12-15	16:01	-33.94138	18.25109	83	ADCP_150	profile start	
PS117_0_Underway-1	2019-02-03	19:22	-59.40752	-60.03992	2217	ADCP_150	profile end	
PS117_0_Underway-3	2018-12-15	16:13	-33.97176	18.23005	90	FBOX	profile start	
PS117_0_Underway-3	2019-02-03	19:22	-59.40773	-60.03898	2214	FBOX	profile end	
PS117_0_Underway-5	2018-12-15	16:13	-33.97240	18.22960	92	PCO2_GO	profile start	
PS117_0_Underway-5	2019-02-03	19:22	-59.40787	-60.03841	2214	PCO2_GO	profile end	
PS117_0_Underway-6	2018-12-15	16:14	-33.97322	18.22905	93	PCO2_SUB	profile start	
PS117_0_Underway-6	2018-12-20	12:30	-44.76239	6.98056	4512	PCO2_SUB	profile end	
PS117_0_Underway-8	2018-12-16	07:24	-35.52363	14.97763	4708	GRAV	profile start	
PS117_0_Underway-8	2019-02-03	19:21	-59.40808	-60.03751	2208	GRAV	profile end	
PS117_0_Underway-9	2018-12-15	16:02	-33.94276	18.25018	83	SVP	profile start	
PS117_0_Underway-9	2019-02-03	19:22	-59.40763	-60.03943	2217	SVP	profile end	
PS117_0_Underway-10	2018-12-16	13:41	-36.06308	13.69055	4843	TSG_KEEL	profile start	
PS117_0_Underway-10	2019-02-03	19:21	-59.40848	-60.03553	2212	TSG_KEEL	profile end	
PS117_0_Underway-11	2018-12-16	13:41	-36.06308	13.69055	4843	TSG_KEEL_2	profile start	
PS117_0_Underway-11	2019-02-03	19:21	-59.40829	-60.03649	2209	TSG_KEEL_2	profile end	
PS117_0_Underway-12	2018-12-15	08:00	-33.90975	18.43583	NA	WST	profile start	
PS117_0_Underway-12					NA		profile end	
PS117_0_Underway-13	2018-12-16	07:55	-35.57268	14.87194	4741	MAG	profile start	
PS117_0_Underway-13	2019-02-03	19:21	-59.40819	-60.03698	2211	MAG	profile end	
PS117_0_Underway-14	2018-12-16	10:00	-35.75713	14.44588	4827	WHW	station start	
PS117_0_Underway-14	2018-12-16	10:00	-35.75717	14.44576	4827	WHW	profile start	

A.4 Stationsliste / Station List

Station	Date	Time	Latitude	Longitude	Depth [m]	Gear	Action	Comment
PS117_0_Underway-14	2019-02-03	19:23	-59.40731	-60.04079	2220	WHW	profile end	
PS117_1-1	2018-12-16	15:47	-36.22096	13.30109	4824	CTDOZE	station start	
PS117_1-1	2018-12-16	17:40	-36.22258	13.30492	4824	CTDOZE	at depth	
PS117_1-1	2018-12-16	19:54	-36.21905	13.30482	4824	CTDOZE	station end	
PS117_1-2	2018-12-16	16:28	-36.22243	13.30345	4823	HN	station start	
PS117_1-2	2018-12-16	16:36	-36.22226	13.30433	4824	HN	station end	
PS117_1-3	2018-12-16	18:13	-36.22161	13.30557	NA	PIES	station start	
PS117_1-3	2018-12-16	20:21	-36.21991	13.31225	4824	PIES	station end	
PS117_2-1	2018-12-17	03:43	-37.40706	12.52003	5054	CTDOZE	station start	
PS117_2-1	2018-12-17	05:40	-37.40786	12.52238	5054	CTDOZE	at depth	
PS117_2-1	2018-12-17	07:58	-37.40599	12.52612	5054	CTDOZE	station end	
PS117_2-2	2018-12-17	06:04	-37.40777	12.52107	5054	HN	station start	
PS117_2-2	2018-12-17	06:10	-37.40720	12.52137	5054	HN	station end	
PS117_2-3	2018-12-17	06:19	-37.40639	12.52233	5054	PIES	station start	
PS117_2-3	2018-12-17	08:35	-37.40024	12.53827	5054	PIES	station end	
PS117_2-4	2018-12-17	07:22	-37.40762	12.52755	5054	HN	station start	
PS117_2-4	2018-12-17	07:31	-37.40703	12.52667	5054	HN	station end	
PS117_3-1	2018-12-17	16:25	-38.60264	11.76337	5105	UCCTD	station start	
PS117_3-1	2018-12-17	18:19	-38.60204	11.76266	5105	UCCTD	at depth	
PS117_3-1	2018-12-17	20:16	-38.59942	11.75566	5094	UCCTD	station end	
PS117_3-2	2018-12-17	17:28	-38.60199	11.76267	5105	HN	station start	
PS117_3-2	2018-12-17	17:34	-38.60178	11.76267	5105	HN	station end	
PS117_3-3	2018-12-17	19:04	-38.60159	11.75972	NA	PIES	station start	
PS117_3-3	2018-12-17	23:45	-38.60180	11.75394	5094	PIES	station end	
PS117_3-4	2018-12-17	21:48	-38.60454	11.76206	5105	MT	station start	
PS117_3-4	2018-12-17	22:30	-38.61533	11.78855	5096	MT	station end	
PS117_4-1	2018-12-18	08:45	-39.97547	10.79519	4765	CTDOZE	station start	
PS117_4-1	2018-12-18	10:32	-39.97528	10.79678	4765	CTDOZE	at depth	
PS117_4-1	2018-12-18	12:48	-39.97460	10.79267	4764	CTDOZE	station end	
PS117_4-2	2018-12-18	09:24	-39.97517	10.79575	4766	HN	station start	
PS117_4-2	2018-12-18	09:34	-39.97606	10.79569	4766	HN	station end	
PS117_4-3	2018-12-18	11:13	-39.97293	10.79512	NA	PIES	station start	
PS117_4-3	2018-12-18	13:27	-39.97460	10.79818	4763	PIES	station end	
PS117_5-1	2018-12-18	21:53	-41.34813	9.88886	4677	CTDOZE	station start	
PS117_5-1	2018-12-18	23:33	-41.34687	9.88952	4678	CTDOZE	at depth	
PS117_5-1	2018-12-19	01:34	-41.34684	9.88977	4677	CTDOZE	station end	
PS117_5-2	2018-12-19	00:00	-41.34647	9.88975	NA	PIES	station start	
PS117_5-2	2018-12-19	01:56	-41.35129	9.88758	4673	PIES	station end	
PS117_5-3	2018-12-19	00:56	-41.34697	9.88938	4678	HN	station start	
PS117_5-3	2018-12-19	01:04	-41.34682	9.88970	4677	HN	station end	
PS117_6-1	2018-12-19	11:08	-42.69477	8.73954	NA	PIES	station start	
PS117_6-1	2018-12-19	13:11	-42.69412	8.74289	4904	PIES	station end	
PS117_6-2	2018-12-19	11:32	-42.69470	8.74000	4904	SUIT	station start	

Station	Date	Time	Latitude	Longitude	Depth [m]	Gear	Action	Comment
PS117_6-2	2018-12-19	11:45	-42.69415	8.73470	4903	SUIT	profile start	
PS117_6-2	2018-12-19	11:56	-42.69156	8.72722	4897	SUIT	profile end	
PS117_6-2	2018-12-19	12:16	-42.69130	8.71953	4895	SUIT	station end	
PS117_6-3	2018-12-19	13:20	-42.69394	8.74391	4903	CTDOZE	station start	
PS117_6-3	2018-12-19	15:14	-42.69383	8.73775	4904	CTDOZE	at depth	
PS117_6-3	2018-12-19	17:15	-42.69338	8.73895	4904	CTDOZE	station end	
PS117_6-4	2018-12-19	15:15	-42.69382	8.73774	4904	HN	station start	
PS117_6-4	2018-12-19	15:17	-42.69378	8.73774	4904	HN	station end	
PS117_6-4	2018-12-19	15:18	-42.69376	8.73773	4904	HN	station start	
PS117_6-4	2018-12-19	15:21	-42.69370	8.73776	4904	HN	station end	
PS117_6-5	2018-12-19	17:27	-42.69313	8.73874	4903	Test	station start	
PS117_6-5	2018-12-19	17:42	-42.69291	8.73854	4903	Test	at depth	
PS117_6-5	2018-12-19	18:00	-42.69223	8.73860	4903	Test	station end	
PS117_7-1	2018-12-20	07:00	-44.66130	7.09171	4591	CTDOZE	station start	
PS117_7-1	2018-12-20	08:48	-44.66466	7.08530	4592	CTDOZE	at depth	
PS117_7-1	2018-12-20	11:11	-44.66442	7.08617	4592	CTDOZE	station end	
PS117_7-2	2018-12-20	08:04	-44.66304	7.08632	4591	HN	station start	
PS117_7-2	2018-12-20	08:09	-44.66289	7.08586	4591	HN	station end	
PS117_7-3	2018-12-20	11:20	-44.66229	7.08673	4592	HN	station start	
PS117_7-3	2018-12-20	11:24	-44.66144	7.08776	4591	HN	station end	
PS117_7-3	2018-12-20	11:24	-44.66135	7.08787	4592	HN	station start	
PS117_7-3	2018-12-20	11:25	-44.66101	7.08822	4591	HN	station end	
PS117_7-4	2018-12-20	11:30	-44.65987	7.08820	4592	FLOAT	station start	
PS117_7-4	2018-12-20	11:30	-44.65976	7.08796	4591	FLOAT	station end	
PS117_8-1	2018-12-20	21:13	-46.02559	5.94902	3119	FLOAT	station start	
PS117_8-1	2018-12-20	21:24	-46.03934	5.94424	3113	FLOAT	station end	
PS117_9-1	2018-12-21	02:48	-47.00151	5.57544	4319	FLOAT	station start	
PS117_9-1	2018-12-21	02:59	-47.01728	5.56889	4484	FLOAT	station end	
PS117_10-1	2018-12-21	08:15	-47.94244	5.20016	4208	FLOAT	station start	
PS117_10-1	2018-12-21	08:24	-47.96977	5.18917	4182	FLOAT	station end	
PS117_11-1	2018-12-21	14:00	-48.98669	4.77266	3611	FLOAT	station start	
PS117_11-1	2018-12-21	14:09	-49.00223	4.76593	3576	FLOAT	station end	
PS117_12-1	2018-12-21	19:33	-49.99549	4.35437	2927	FLOAT	station start	
PS117_12-1	2018-12-21	19:38	-50.00533	4.35054	2505	FLOAT	station end	
PS117_13-1	2018-12-22	01:23	-50.99908	3.92583	3448	HN	station start	
PS117_13-1	2018-12-22	01:27	-50.99940	3.92623	3447	HN	station end	
PS117_13-2	2018-12-22	01:36	-50.99948	3.92602	3447	CTDOZE	station start	
PS117_13-2	2018-12-22	02:26	-50.99994	3.92674	3447	CTDOZE	at depth	
PS117_13-2	2018-12-22	03:36	-51.00020	3.92693	3449	CTDOZE	station end	
PS117_13-3	2018-12-22	03:50	-51.00313	3.92297	3440	FLOAT	station start	
PS117_13-3	2018-12-22	03:54	-51.00328	3.91605	3434	FLOAT	station end	
PS117_14-1	2018-12-26	18:30	-67.49862	-0.00218	4634	CTDOZE	station start	
PS117_14-1	2018-12-26	20:32	-67.49940	-0.00067	4634	CTDOZE	at depth	

A.4 Stationsliste / Station List

Station	Date	Time	Latitude	Longitude	Depth [m]	Gear	Action	Comment
PS117_14-1	2018-12-26	22:40	-67.49930	0.00063	4633	CTDOZE	station end	
PS117_14-2	2018-12-26	19:00	-67.49783	-0.00093	4634	HN	station start	
PS117_14-2	2018-12-26	19:01	-67.49785	-0.00084	4634	HN	station end	
PS117_14-3	2018-12-26	23:00	-67.49982	0.00955	4631	MT	station start	
PS117_14-3	2018-12-26	23:36	-67.49954	0.08887	4627	MT	station end	
PS117_14-4	2018-12-26	23:47	-67.49976	0.09187	4627	UCCTD	station start	
PS117_14-4	2018-12-27	00:06	-67.49995	0.09086	NA	UCCTD	at depth	
PS117_14-4	2018-12-27	00:37	-67.50016	0.08904	4627	UCCTD	station end	
PS117_14-5	2018-12-27	00:42	-67.50014	0.09321	4627	FLOAT	station start	
PS117_14-5	2018-12-27	00:44	-67.50027	0.09785	4626	FLOAT	station end	
PS117_15-1	2018-12-27	05:52	-66.51517	-0.17104	4548	CTDOZE	station start	
PS117_15-1	2018-12-27	07:41	-66.51447	-0.16962	4517	CTDOZE	at depth	
PS117_15-1	2018-12-27	09:58	-66.51463	-0.17083	4515	CTDOZE	station end	
PS117_15-2	2018-12-27	07:14	-66.51485	-0.16926	4523	HN	station start	
PS117_15-2	2018-12-27	07:16	-66.51485	-0.16920	4522	HN	station end	
PS117_15-3	2018-12-27	10:30	-66.51528	-0.08062	4613	MOOR	station start	retrieval of AWI231-12
PS117_15-3	2018-12-27	12:58	-66.52778	-0.09393	4638	MOOR	station end	
PS117_15-4	2018-12-27	13:31	-66.52806	-0.07190	4614	M-RMT	station start	
PS117_15-4	2018-12-27	14:04	-66.52915	-0.04427	4603	M-RMT	at depth	
PS117_15-4	2018-12-27	14:05	-66.52911	-0.04203	4604	M-RMT	profile start	
PS117_15-4	2018-12-27	14:48	-66.52873	0.04253	4578	M-RMT	profile end	
PS117_15-4	2018-12-27	15:15	-66.52939	0.06574	4578	M-RMT	station end	
PS117_15-5	2018-12-27	16:02	-66.51874	-0.07545	4616	MOOR	station start	deployment of AWI231-13
PS117_15-5	2018-12-27	18:37	-66.51708	-0.07458	4612	MOOR	station end	
PS117_15-6	2018-12-27	19:00	-66.51913	-0.05093	4593	SUIT	station start	
PS117_15-6	2018-12-27	19:26	-66.51636	-0.02825	4543	SUIT	at depth	
PS117_15-6	2018-12-27	19:28	-66.51606	-0.02503	4532	SUIT	profile start	
PS117_15-6	2018-12-27	19:58	-66.51024	0.03153	4564	SUIT	profile end	
PS117_15-6	2018-12-27	20:26	-66.50718	0.06111	4534	SUIT	station end	
PS117_15-7	2018-12-27	20:47	-66.50377	0.08496	4514	MT	station start	
PS117_15-7	2018-12-27	20:53	-66.50275	0.09324	4509	MT	profile start	
PS117_15-7	2018-12-27	21:27	-66.49790	0.14148	4517	MT	station end	
PS117_15-8	2018-12-27	21:32	-66.49740	0.14704	4508	FLOAT	station start	
PS117_15-8	2018-12-27	21:34	-66.49711	0.15057	4500	FLOAT	station end	
PS117_16-1	2018-12-28	00:24	-65.99961	-0.00320	3411	UCCTD	station start	
PS117_16-1	2018-12-28	01:47	-66.00004	-0.00026	3414	UCCTD	at depth	
PS117_16-1	2018-12-28	03:05	-66.00005	-0.00040	3414	UCCTD	station end	
PS117_16-2	2018-12-28	03:13	-65.99973	0.01284	3399	FLOAT	station start	
PS117_16-2	2018-12-28	03:15	-65.99963	0.01607	3388	FLOAT	station end	
PS117_17-1	2018-12-28	08:30	-65.00127	-0.00505	3743	UCCTD	station start	
PS117_17-1	2018-12-28	08:38	-65.00067	-0.00549	3742	UCCTD	at depth	
PS117_17-1	2018-12-28	09:01	-65.00037	-0.00084	3737	UCCTD	station end	

Station	Date	Time	Latitude	Longitude	Depth [m]	Gear	Action	Comment
PS117_17-2	2018-12-28	09:03	-65.00051	0.00125	3735	MT	station start	
PS117_17-2	2018-12-28	09:15	-65.00234	0.01785	3723	MT	profile start	
PS117_17-2	2018-12-28	09:45	-65.00830	0.06656	3688	MT	profile end	
PS117_17-2	2018-12-28	09:50	-65.00468	0.07567	3677	MT	station end	
PS117_18-1	2018-12-28	15:24	-64.01112	-0.02717	189	MOOR	station start	retrieval of AWI229-13
PS117_18-1	2018-12-28	16:55	-64.00713	-0.02259	5198	MOOR	station end	
PS117_18-2	2018-12-28	17:19	-63.97244	-0.02068	5203	CTDOZE	station start	
PS117_18-2	2018-12-28	19:43	-63.96464	-0.02909	5204	CTDOZE	at depth	
PS117_18-2	2018-12-28	22:25	-63.96467	-0.03427	5205	CTDOZE	station end	
PS117_18-3	2018-12-28	18:50	-63.96861	-0.02760	5202	HN	station start	
PS117_18-3	2018-12-28	18:52	-63.96846	-0.02791	5202	HN	station end	
PS117_18-4	2018-12-28	22:38	-63.96614	-0.04197	5206	UCCTD	station start	
PS117_18-4	2018-12-29	01:22	-63.97095	-0.05445	5206	UCCTD	at depth	
PS117_18-4	2018-12-29	03:12	-63.97152	-0.05563	5206	UCCTD	station end	
PS117_18-5	2018-12-29	03:26	-63.97788	-0.04318	5204	FLOAT	station start	
PS117_18-5	2018-12-29	03:27	-63.97840	-0.04250	5203	FLOAT	station end	
PS117_19-1	2018-12-29	09:02	-62.99842	-0.00466	5309	CTDOZE	station start	
PS117_19-1	2018-12-29	10:59	-63.00009	0.00013	5307	CTDOZE	at depth	
PS117_19-1	2018-12-29	13:11	-63.00038	0.00066	5307	CTDOZE	station end	
PS117_19-2	2018-12-29	09:55	-62.99969	-0.00478	5308	HN	station start	
PS117_19-2	2018-12-29	09:58	-62.99988	-0.00402	5308	HN	station end	
PS117_19-3	2018-12-29	13:31	-63.00194	0.00116	5307	SUIT	station start	
PS117_19-3	2018-12-29	13:43	-63.00663	0.00741	5306	SUIT	profile start	
PS117_19-3	2018-12-29	14:14	-63.02504	0.03285	5305	SUIT	profile end	
PS117_19-3	2018-12-29	14:33	-63.03099	0.04148	5300	SUIT	station end	
PS117_19-4	2018-12-29	15:04	-63.00045	-0.00053	5307	CTDOZE	station start	
PS117_19-4	2018-12-29	15:11	-63.00035	-0.00138	5307	CTDOZE	at depth	
PS117_19-4	2018-12-29	15:15	-62.99988	-0.00229	5308	CTDOZE	station end	
PS117_19-5	2018-12-29	15:58	-63.00240	-0.00311	5306	M-RMT	station start	
PS117_19-5	2018-12-29	17:40	-63.01999	0.01343	5304	M-RMT	at depth	
PS117_19-5	2018-12-29	17:40	-63.02010	0.01357	5304	M-RMT	profile start	
PS117_19-5	2018-12-29	18:43	-63.05788	0.05801	5298	M-RMT	profile end	
PS117_19-5	2018-12-29	19:02	-63.05655	0.05566	5299	M-RMT	station end	
PS117_19-6	2018-12-29	19:17	-63.06146	0.06013	5297	FLOAT	station start	
PS117_19-6	2018-12-29	19:18	-63.06256	0.06134	5298	FLOAT	station end	
PS117_20-1	2018-12-30	02:59	-62.00096	0.00085	5366	UCCTD	station start	
PS117_20-1	2018-12-30	04:46	-62.00227	0.00271	5366	UCCTD	at depth	
PS117_20-1	2018-12-30	06:34	-62.00149	0.00007	5366	UCCTD	station end	
PS117_21-1	2018-12-30	11:52	-60.99742	-0.00017	5386	CTDOZE	station start	
PS117_21-1	2018-12-30	13:53	-60.99596	-0.01084	5395	CTDOZE	at depth	
PS117_21-1	2018-12-30	16:09	-60.99558	-0.00222	5394	CTDOZE	station end	
PS117_21-2	2018-12-30	12:23	-60.99589	-0.00663	5386	HN	station start	
PS117_21-2	2018-12-30	12:25	-60.99563	-0.00664	5386	HN	station end	

A.4 Stationsliste / Station List

Station	Date	Time	Latitude	Longitude	Depth [m]	Gear	Action	Comment
PS117_22-1	2018-12-31	00:38	-59.04814	0.11784	4637	MOOR	station start	retrieval of AWI-227-14
PS117_22-1	2018-12-31	02:45	-59.03811	0.09541	4637	MOOR	station end	
PS117_22-2	2018-12-31	03:05	-59.05032	0.10688	4643	CTDOZE	station start	
PS117_22-2	2018-12-31	04:53	-59.05092	0.10724	4645	CTDOZE	at depth	
PS117_22-2	2018-12-31	06:49	-59.05010	0.10723	4643	CTDOZE	station end	
PS117_22-3	2018-12-31	07:10	-59.03359	0.16545	4610	MT	station start	
PS117_22-3	2018-12-31	07:17	-59.03609	0.16060	4619	MT	at depth	
PS117_22-3	2018-12-31	07:17	-59.03615	0.16046	4620	MT	profile start	
PS117_22-3	2018-12-31	07:46	-59.04626	0.13495	4630	MT	profile end	
PS117_22-3	2018-12-31	07:51	-59.04733	0.12969	4632	MT	station end	
PS117_22-4	2018-12-31	08:00	-59.04990	0.10935	4641	MOOR	station start	deployment of AWI 227-15
PS117_22-4	2018-12-31	10:40	-59.06147	0.10250	4658	MOOR	station end	
PS117_22-5	2018-12-31	10:58	-59.08374	0.10007	NA	UCCTD	station start	
PS117_22-5	2018-12-31	12:46	-59.08398	0.09968	4679	UCCTD	at depth	
PS117_22-5	2018-12-31	14:38	-59.08419	0.10048	4679	UCCTD	station end	
PS117_22-6	2018-12-31	12:10	-59.08322	0.09979	4500	HN	station start	
PS117_22-6	2018-12-31	12:12	-59.08339	0.10014	4679	HN	station end	
PS117_22-7	2018-12-31	14:46	-59.08456	0.09612	4680	FLOAT	station start	
PS117_22-7	2018-12-31	14:46	-59.08457	0.09606	4680	FLOAT	station end	
PS117_22-8	2018-12-31	14:47	-59.08481	0.09388	4681	FLOAT	station start	
PS117_22-8	2018-12-31	14:47	-59.08481	0.09383	4681	FLOAT	station end	
PS117_22-9	2018-12-31	14:50	-59.08394	0.08986	4681	FLOAT	station start	
PS117_22-9	2018-12-31	14:50	-59.08391	0.08982	4681	FLOAT	station end	
PS117_23-1	2018-12-31	19:36	-59.97238	0.00029	5371	FLOAT	station start	
PS117_23-1	2018-12-31	19:39	-59.97463	-0.00656	5369	FLOAT	station end	
PS117_23-2	2018-12-31	19:40	-59.97493	-0.00756	5368	FLOAT	station start	
PS117_23-2	2018-12-31	19:41	-59.97529	-0.00858	5367	FLOAT	station end	
PS117_24-1	2019-01-01	16:09	-64.01224	-0.01676	NA	MOOR	station start	mooring AWI229-13
PS117_24-1	2019-01-01	18:56	-64.03372	-0.01163	5194	MOOR	station end	
PS117_24-2	2019-01-01	19:42	-64.05835	0.10063	5193	MOOR	station start	deployment of AWI-229-14
PS117_24-2	2019-01-01	23:21	-64.01349	0.00813	NA			
PS117_25-1	2019-01-02	19:55	-68.00024	-0.00033	4514	UCCTD	station start	
PS117_25-1	2019-01-02	21:38	-67.99975	-0.00119	4514	UCCTD	at depth	
PS117_25-1	2019-01-02	22:58	-68.00201	0.00434	4513	UCCTD	station end	
PS117_26-1	2019-01-03	02:15	-68.49815	-0.00226	4269	CTDOZE	station start	
PS117_26-1	2019-01-03	03:49	-68.49999	-0.00035	4265	CTDOZE	at depth	
PS117_26-1	2019-01-03	05:36	-68.50047	0.00048	4264	CTDOZE	station end	
PS117_26-2	2019-01-03	05:37	-68.50047	0.00044	4264	HN	station start	
PS117_26-2	2019-01-03	05:44	-68.50036	-0.00036	4264	HN	station end	
PS117_26-3	2019-01-03	05:45	-68.50034	-0.00030	4264	MT	station start	
PS117_26-3	2019-01-03	05:53	-68.50010	0.01216	4262	MT	at depth	

Station	Date	Time	Latitude	Longitude	Depth [m]	Gear	Action	Comment
PS117_26-3	2019-01-03	05:53	-68.50010	0.01235	4262	MT	profile start	
PS117_26-3	2019-01-03	06:21	-68.49666	0.05789	4262	MT	profile end	
PS117_26-3	2019-01-03	06:27	-68.49716	0.06398	4262	MT	station end	
PS117_27-2	2019-01-03	11:06	-69.07988	-0.00597	3273	ICE	station start	
PS117_27-2	2019-01-03	14:31	-69.09542	-0.02276	3219	ICE	station end	
PS117_27-1	2019-01-03	12:03	-69.08673	-0.00854	3257	UCCTD	station start	
PS117_27-1	2019-01-03	13:06	-69.09141	-0.01034	3244	UCCTD	at depth	
PS117_27-1	2019-01-03	14:10	-69.09469	-0.01883	3226	UCCTD	station end	
PS117_27-3	2019-01-03	15:36	-69.08383	-0.09061	3148	M-RMT	station start	
PS117_27-3	2019-01-03	16:05	-69.08567	-0.08504	3148	M-RMT	at depth	
PS117_27-3	2019-01-03	16:08	-69.08598	-0.08315	3150	M-RMT	profile start	
PS117_27-3	2019-01-03	16:22	-69.09001	-0.06369	3183	M-RMT	profile end	
PS117_27-3	2019-01-03	16:45	-69.08913	-0.05470	3201	M-RMT	station end	
PS117_27-4	2019-01-03	17:35	-69.07562	-0.05237	3221	SUIT	station start	
PS117_27-4	2019-01-03	18:14	-69.07787	-0.04587	3223	SUIT	profile start	
PS117_27-4	2019-01-03	18:43	-69.09884	-0.01291	3227	SUIT	profile end	
PS117_27-4	2019-01-03	19:18	-69.10214	-0.02380	3207	SUIT	station end	
PS117_27-5	2019-01-03	19:32	-69.10128	-0.02994	3203	ROV	station start	
PS117_27-5	2019-01-03	21:06	-69.10773	-0.06094	3140	ROV	station end	
PS117_28-1	2019-01-03	23:01	-69.22411	0.05417	2878	CTDOZE	station start	
PS117_28-1	2019-01-04	00:20	-69.22798	0.03132	2782	CTDOZE	at depth	
PS117_28-1	2019-01-04	01:41	-69.23222	0.00725	2731	CTDOZE	station end	
PS117_29-1	2019-01-04	02:55	-69.32609	0.03591	2444	CTDOZE	station start	
PS117_29-1	2019-01-04	04:05	-69.32764	0.01139	2426	CTDOZE	at depth	
PS117_29-1	2019-01-04	05:09	-69.32977	-0.01953	2392	CTDOZE	station end	
PS117_30-1	2019-01-04	05:40	-69.36078	-0.08280	2150	CTDOZE	station start	
PS117_30-1	2019-01-04	06:42	-69.36312	-0.11161	2105	CTDOZE	at depth	
PS117_30-1	2019-01-04	08:01	-69.36344	-0.13433	2082	CTDOZE	station end	
PS117_30-2	2019-01-04	08:16	-69.36349	-0.13760	2078	UCCTD	station start	
PS117_30-2	2019-01-04	09:14	-69.36500	-0.15154	2061	UCCTD	at depth	
PS117_30-2	2019-01-04	10:02	-69.36672	-0.16598	2059	UCCTD	station end	
PS117_31-1	2019-01-04	11:01	-69.39213	-0.28920	1888	CTDOZE	station start	
PS117_31-1	2019-01-04	12:07	-69.39797	-0.30970	1885	CTDOZE	at depth	
PS117_31-1	2019-01-04	13:16	-69.40205	-0.32298	1880	CTDOZE	station end	
PS117_32-1	2019-01-04	11:30	-69.39473	-0.30212	1885	HN	station start	
PS117_32-1	2019-01-04	11:39	-69.39553	-0.30227	1884	HN	station end	
PS117_32-2	2019-01-04	14:03	-69.42793	-0.37875	1876	MT	station start	
PS117_32-2	2019-01-04	14:15	-69.42944	-0.39963	1895	MT	station end	
PS117_32-2	2019-01-04	14:16	-69.43012	-0.40157	1898	MT	station start	
PS117_32-2	2019-01-04	14:44	-69.42807	-0.42745	1929	MT	station end	
PS117_33-1	2019-01-05	09:52	-69.00699	-6.99207	2944	CTDOZE	station start	
PS117_33-1	2019-01-05	10:06	-69.01087	-6.99810	2938	CTDOZE	at depth	
PS117_33-1	2019-01-05	10:16	-69.01058	-6.99975	2939	CTDOZE	station end	

A.4 Stationsliste / Station List

Station	Date	Time	Latitude	Longitude	Depth [m]	Gear	Action	Comment
PS117_33-2	2019-01-05	10:25	-69.01081	-6.99997	2940	SUIT	station start	
PS117_33-2	2019-01-05	10:47	-69.01358	-6.98231	2926	SUIT	profile start	
PS117_33-2	2019-01-05	11:16	-69.01787	-6.91219	2846	SUIT	profile end	
PS117_33-2	2019-01-05	11:35	-69.01987	-6.89576	2839	SUIT	station end	
PS117_33-3	2019-01-05	12:30	-69.00544	-7.00154	NA	MOOR	station start	retrieval of AWI244-5
PS117_33-3	2019-01-05	17:30	-68.99317	-7.09004	2989	MOOR	station end	
PS117_33-4	2019-01-05	18:33	-68.98753	-7.12598	3017	MOOR	station start	deployment of AWI244-6
PS117_33-4	2019-01-05	20:55	-69.00496	-7.03538	2974	MOOR	station end	
PS117_33-5	2019-01-05	21:15	-69.00725	-7.03772	2970	M-RMT	station start	
PS117_33-5	2019-01-05	21:58	-69.01460	-6.99603	2933	M-RMT	profile start	
PS117_33-5	2019-01-05	22:34	-69.02380	-6.92573	2867	M-RMT	profile end	
PS117_33-5	2019-01-05	23:30	-69.02523	-6.96263	2891	M-RMT	station end	
PS117_33-6	2019-01-05	23:49	-69.02613	-6.96427	2893	CTDOZE	station start	
PS117_33-6	2019-01-06	01:17	-69.02657	-6.96376	2892	CTDOZE	at depth	
PS117_33-6	2019-01-06	02:53	-69.02782	-6.96081	2887	CTDOZE	station end	
PS117_33-7	2019-01-06	02:53	-69.02790	-6.96004	2887	FLOAT	station start	
PS117_33-7	2019-01-06	03:00	-69.03080	-6.94966	2881	FLOAT	station end	
PS117_34-1	2019-01-06	21:05	-65.96844	-12.22112	5049	MOOR	station start	retrieval of AWI248-2
PS117_34-1	2019-01-06	23:44	-65.96880	-12.21560	5048	MOOR	station end	
PS117_34-2	2019-01-07	00:00	-65.97033	-12.21907	5048	CTDOZE	station start	
PS117_34-2	2019-01-07	01:47	-65.97062	-12.21959	5048	CTDOZE	at depth	
PS117_34-2	2019-01-07	04:16	-65.97041	-12.21737	5048	CTDOZE	station end	
PS117_34-3	2019-01-07	04:19	-65.97045	-12.21727	5049	UCCTD	station start	
PS117_34-3	2019-01-07	06:09	-65.97233	-12.21858	5048	UCCTD	at depth	
PS117_34-3	2019-01-07	07:37	-65.97368	-12.21691	5048	UCCTD	station end	
PS117_34-4	2019-01-07	06:16	-65.97235	-12.21829	5048	HN	station start	
PS117_34-4	2019-01-07	06:19	-65.97239	-12.21822	5048	HN	station end	
PS117_34-5	2019-01-07	07:53	-65.96856	-12.23121	5049	MOOR	station start	deployment of AWI248-3
PS117_34-5	2019-01-07	10:40	-65.96869	-12.23065	5048	MOOR	station end	
PS117_34-6	2019-01-07	10:59	-65.96867	-12.22923	5048	MT	station start	
PS117_34-6	2019-01-07	11:05	-65.97003	-12.23297	5048	MT	profile start	
PS117_34-6	2019-01-07	11:35	-65.98111	-12.26718	5045	MT	profile end	
PS117_34-6	2019-01-07	11:43	-65.98405	-12.27547	5045	MT	station end	
PS117_34-7	2019-01-07	11:50	-65.98843	-12.28882	5046	FLOAT	station start	
PS117_34-7	2019-01-07	11:53	-65.98873	-12.29609	5046	FLOAT	station end	
PS117_35-1	2019-01-08	06:42	-69.05356	-17.47753	4774	MT	station start	
PS117_35-1	2019-01-08	06:47	-69.05458	-17.47191	4774	MT	at depth	
PS117_35-1	2019-01-08	06:47	-69.05460	-17.47169	4774	MT	profile start	
PS117_35-1	2019-01-08	07:14	-69.05766	-17.43288	4774	MT	profile end	
PS117_35-1	2019-01-08	07:18	-69.05800	-17.42791	4774	MT	station end	

Station	Date	Time	Latitude	Longitude	Depth [m]	Gear	Action	Comment
PS117_35-2	2019-01-08	07:22	-69.05880	-17.41695	4774	MOOR	station start	retrieval of AWI245-4
PS117_35-2	2019-01-08	09:42	-69.05582	-17.42975	4775	MOOR	station end	
PS117_35-3	2019-01-08	09:47	-69.05595	-17.43097	4774	M-RMT	station start	
PS117_35-3	2019-01-08	10:38	-69.05533	-17.39254	4774	M-RMT	profile start	
PS117_35-3	2019-01-08	11:15	-69.05401	-17.32110	4775	M-RMT	profile end	
PS117_35-3	2019-01-08	11:47	-69.06421	-17.38306	4772	M-RMT	station end	
PS117_35-4	2019-01-08	12:03	-69.06093	-17.39020	4773	MOOR	station start	deployment of AWI-245-5
PS117_35-4	2019-01-08	14:24	-69.06066	-17.39113	4773	MOOR	station end	
PS117_35-5	2019-01-08	14:25	-69.06067	-17.39114	4772	SUIT	station start	
PS117_35-5	2019-01-08	14:52	-69.06559	-17.36818	4773	SUIT	profile start	
PS117_35-5	2019-01-08	15:22	-69.07915	-17.30927	4771	SUIT	profile end	
PS117_35-5	2019-01-08	15:41	-69.08365	-17.29198	4770	SUIT	station end	
PS117_35-6	2019-01-08	16:03	-69.07251	-17.31063	4772	CTDOZE	station start	
PS117_35-6	2019-01-08	18:04	-69.07211	-17.30857	4772	CTDOZE	at depth	
PS117_35-6	2019-01-08	20:52	-69.07268	-17.30835	4773	CTDOZE	station end	
PS117_35-7	2019-01-08	16:34	-69.07238	-17.30979	4772	HN	station start	
PS117_35-7	2019-01-08	16:36	-69.07239	-17.30952	4772	HN	station end	
PS117_36-1	2019-01-09	09:22	-70.13877	-11.01419	2201	UCCTD	station start	
PS117_36-1	2019-01-09	09:41	-70.14338	-11.01496	2183	UCCTD	at depth	
PS117_36-1	2019-01-09	09:59	-70.14716	-11.02615	2159	UCCTD	station end	
PS117_36-2	2019-01-09	10:07	-70.14934	-11.06639	2077	MT	station start	
PS117_36-2	2019-01-09	10:42	-70.15588	-11.13955	1724	MT	profile end	
PS117_36-2	2019-01-09	10:52	-70.15748	-11.18002	1709	MT	station end	
PS117_37-1	2019-01-09	11:50	-70.17206	-11.30522	1751	SUIT	station start	
PS117_37-1	2019-01-09	12:22	-70.18639	-11.23349	1647	SUIT	profile start	
PS117_37-1	2019-01-09	17:42	-70.21074	-11.25928	1699	SUIT	station end	
PS117_37-2	2019-01-09	17:55	-70.19333	-11.25782	1658	ROV	station start	
PS117_37-2	2019-01-09	20:00	-70.19829	-11.25885	1656	ROV	station end	
PS117_37-3	2019-01-09	20:29	-70.19468	-11.23996	1650	M-RMT	station start	
PS117_37-3	2019-01-09	21:25	-70.19012	-11.19837	1634	M-RMT	profile start	
PS117_37-3	2019-01-09	21:59	-70.18167	-11.13930	1664	M-RMT	profile end	
PS117_37-3	2019-01-09	22:24	-70.17897	-11.09190	1761	M-RMT	station end	
PS117_38-1	2019-01-09	22:44	-70.17563	-11.00102	2100	UCCTD	station start	
PS117_38-1	2019-01-09	23:32	-70.17513	-11.00104	2101	UCCTD	at depth	
PS117_38-1	2019-01-10	00:30	-70.17662	-10.99875	2098	UCCTD	station end	
PS117_38-2	2019-01-10	01:10	-70.15006	-11.21280	1725	MT	station start	
PS117_38-2	2019-01-10	01:57	-70.15558	-11.17307	1721	MT	station end	
PS117_39-1	2019-01-10	08:17	-70.29671	-9.99902	1850	ICE	station start	
PS117_39-1	2019-01-10	12:00	-70.29907	-10.04312	1964	ICE	station end	
PS117_39-2	2019-01-10	12:14	-70.29930	-10.04485	1968	ROV	station start	
PS117_39-2	2019-01-10	13:39	-70.29952	-10.04981	1978	ROV	station end	
PS117_39-3	2019-01-10	17:11	-70.31656	-10.16109	2083	M-RMT	station start	

A.4 Stationsliste / Station List

Station	Date	Time	Latitude	Longitude	Depth [m]	Gear	Action	Comment
PS117_39-3	2019-01-10	19:26	-70.30884	-10.16738	2115	M-RMT	station end	
PS117_39-4	2019-01-10	19:43	-70.30962	-10.17411	2085	SOSO	station start	
PS117_39-4	2019-01-10	20:41	-70.31099	-10.19095	2020	SOSO	at depth	
PS117_39-4	2019-01-10	21:27	-70.31212	-10.20429	1996	SOSO	station end	
PS117_39-5	2019-01-10	21:29	-70.31216	-10.20470	1996	SOSO	station start	
PS117_39-5	2019-01-10	22:09	-70.31311	-10.21604	1994	SOSO	at depth	
PS117_39-5	2019-01-10	22:56	-70.31426	-10.22901	1995	SOSO	station end	
PS117_40-1	2019-01-11	04:16	-70.32492	-8.86952	986	M-RMT	station start	
PS117_40-1	2019-01-11	05:11	-70.32537	-8.91015	940	M-RMT	profile start	
PS117_40-1	2019-01-11	05:45	-70.32427	-8.98114	840	M-RMT	profile end	
PS117_40-1	2019-01-11	06:07	-70.32464	-8.99277	822	M-RMT	station end	
PS117_40-2	2019-01-11	07:53	-70.34792	-8.94472	643	ICE	station start	
PS117_40-2	2019-01-11	11:54	-70.35231	-9.01180	558	ICE	station end	
PS117_40-3	2019-01-11	09:38	-70.35146	-8.97381	585	ROV	station start	
PS117_40-3	2019-01-11	11:04	-70.35261	-8.99749	567	ROV	station end	
PS117_41-1	2019-01-11	14:15	-70.52215	-8.76983	200	CTDOZE	station start	
PS117_41-1	2019-01-11	14:27	-70.52240	-8.76756	192	CTDOZE	at depth	
PS117_41-1	2019-01-11	14:39	-70.52290	-8.76660	192	CTDOZE	station end	
PS117_41-2	2019-01-11	15:02	-70.53332	-8.87446	420	TRAP	station start	
PS117_41-2	2019-01-11	15:34	-70.53568	-8.87092	406	TRAP	station end	
PS117_41-3	2019-01-11	15:57	-70.53607	-8.90123	442	MOOR	station start	deployment of Fischverankerung/ fish mooring
PS117_41-3	2019-01-11	16:42	-70.53594	-8.89839	443	MOOR	station end	
PS117_41-4	2019-01-11	17:06	-70.52262	-8.76899	202	UCCTD	station start	
PS117_41-4	2019-01-11	17:19	-70.52273	-8.76915	208	UCCTD	at depth	
PS117_41-4	2019-01-11	17:42	-70.52265	-8.76978	215	UCCTD	station end	
PS117_41-5	2019-01-11	17:54	-70.51132	-8.80228	281	MT	station start	
PS117_41-5	2019-01-11	18:00	-70.51502	-8.80294	289	MT	at depth	
PS117_41-5	2019-01-11	18:00	-70.51512	-8.80291	289	MT	profile start	
PS117_41-5	2019-01-11	18:28	-70.53088	-8.79457	303	MT	profile end	
PS117_41-5	2019-01-11	18:33	-70.53323	-8.79523	305	MT	station end	
PS117_41-6	2019-01-11	20:57	-70.52188	-8.76886	192	CTDOZE	station start	
PS117_41-6	2019-01-11	21:19	-70.52237	-8.76814	194	CTDOZE	at depth	
PS117_41-6	2019-01-11	21:43	-70.52230	-8.76790	194	CTDOZE	station end	
PS117_41-7	2019-01-11	22:00	-70.50307	-8.79818	256	MT	station start	
PS117_41-7	2019-01-11	22:40	-70.52759	-8.79407	302	MT	station end	
PS117_41-8	2019-01-11	23:57	-70.52174	-8.76858	191	UCCTD	station start	
PS117_41-8	2019-01-12	00:13	-70.52202	-8.76860	192	UCCTD	at depth	
PS117_41-8	2019-01-12	00:32	-70.52230	-8.76761	193	UCCTD	station end	
PS117_41-9	2019-01-12	04:05	-70.52074	-8.77117	200	CTDOZE	station start	
PS117_41-9	2019-01-12	04:19	-70.52027	-8.77045	193	CTDOZE	at depth	
PS117_41-9	2019-01-12	04:33	-70.52044	-8.77171	199	CTDOZE	station end	

Station	Date	Time	Latitude	Longitude	Depth [m]	Gear	Action	Comment
PS117_41-10	2019-01-12	06:53	-70.52198	-8.76827	191	UCCTD	station start	
PS117_41-10	2019-01-12	07:14	-70.52202	-8.76811	191	UCCTD	at depth	
PS117_41-10	2019-01-12	07:37	-70.52166	-8.76944	197	UCCTD	station end	
PS117_41-11	2019-01-12	07:50	-70.50309	-8.81110	323	MT	station start	
PS117_41-11	2019-01-12	08:01	-70.50857	-8.81815	362	MT	profile start	
PS117_41-11	2019-01-12	08:36	-70.52675	-8.83227	361	MT	station end	
PS117_41-12	2019-01-12	09:02	-70.52288	-8.76915	209	CTDOZE	station start	
PS117_41-12	2019-01-12	09:16	-70.52226	-8.76864	195	CTDOZE	at depth	
PS117_41-12	2019-01-12	09:39	-70.52264	-8.76729	193	CTDOZE	station end	
PS117_41-13	2019-01-12	11:57	-70.52282	-8.76818	200	UCCTD	station start	
PS117_41-13	2019-01-12	12:11	-70.52347	-8.77174	225	UCCTD	at depth	
PS117_41-13	2019-01-12	12:31	-70.52344	-8.77403	219	UCCTD	station end	
PS117_41-14	2019-01-12	12:53	-70.51425	-8.77798	189	MT	station start	
PS117_41-14	2019-01-12	12:59	-70.51648	-8.78496	246	MT	profile start	
PS117_41-14	2019-01-12	13:25	-70.52607	-8.81929	329	MT	profile end	
PS117_41-14	2019-01-12	13:28	-70.52682	-8.82198	338	MT	station end	
PS117_41-15	2019-01-12	14:37	-70.53480	-8.88659	438	MOOR	station start	
PS117_41-15	2019-01-12	15:44	-70.53417	-8.89065	438	MOOR	station end	
PS117_42-1	2019-01-12	16:59	-70.39415	-8.77887	520	ICE	station start	
PS117_42-1	2019-01-12	17:41	-70.39322	-8.78145	522	ICE	station end	
PS117_43-1	2019-01-12	18:30	-70.32743	-8.75006	1047	MOOR	station start	
PS117_43-1	2019-01-12	19:21	-70.32543	-8.76835	1048	MOOR	station end	
PS117_44-1	2019-01-12	22:09	-70.45078	-8.41635	386	M-RMT	station start	
PS117_44-1	2019-01-12	23:18	-70.44651	-8.48621	373	M-RMT	profile start	
PS117_44-1	2019-01-12	23:49	-70.46249	-8.44955	328	M-RMT	profile end	
PS117_44-1	2019-01-13	00:06	-70.46458	-8.44531	323	M-RMT	station end	
PS117_45-1	2019-01-13	01:06	-70.47979	-8.34668	276	M-RMT	station start	
PS117_45-1	2019-01-13	01:51	-70.48325	-8.30782	274	M-RMT	at depth	
PS117_45-1	2019-01-13	02:37	-70.48034	-8.26509	288	M-RMT	station end	
PS117_46-1	2019-01-13	09:50	-70.50350	-8.19362	272	ICE	station start	
PS117_46-1	2019-01-13	14:30	-70.50399	-8.19063	271	ICE	station end	
PS117_47-1	2019-01-16	07:58	-70.32828	-8.76558	1028	MOOR	station start	retrieval of Fischverankerung/fish mooring
PS117_47-1	2019-01-16	12:33	-70.32337	-8.78089	1057	MOOR	station end	
PS117_48-1	2019-01-16	15:31	-70.53550	-8.89146	440	SUIT	station start	
PS117_48-1	2019-01-16	15:43	-70.53125	-8.89885	452	SUIT	profile start	
PS117_48-1	2019-01-16	16:14	-70.51300	-8.93477	459	SUIT	profile end	
PS117_48-1	2019-01-16	16:38	-70.50099	-8.95584	448	SUIT	station end	
PS117_48-2	2019-01-16	17:04	-70.53704	-8.87424	423	TRAP	station start	
PS117_48-2	2019-01-16	19:01	-70.53518	-8.89049	439	TRAP	station end	
PS117_48-3	2019-01-16	19:23	-70.50898	-8.99915	452	MT	station start	
PS117_48-3	2019-01-16	19:30	-70.50931	-8.98865	448	MT	profile start	

A.4 Stationsliste / Station List

Station	Date	Time	Latitude	Longitude	Depth [m]	Gear	Action	Comment
PS117_48-3	2019-01-16	19:58	-70.51289	-8.93999	462	MT	profile end	
PS117_48-3	2019-01-16	20:10	-70.51697	-8.94087	452	MT	station end	
PS117_48-4	2019-01-16	20:22	-70.50433	-8.93744	452	M-RMT	station start	
PS117_48-4	2019-01-16	22:06	-70.51093	-8.83652	405	M-RMT	profile end	
PS117_48-4	2019-01-16	23:00	-70.46595	-8.73313	289	M-RMT	station end	
PS117_49-1	2019-01-17	05:16	-70.45936	-8.35030	346	ROV	station start	
PS117_49-1	2019-01-17	06:04	-70.45889	-8.35115	347	ROV	station end	
PS117_49-1	2019-01-17	06:16	-70.45866	-8.35191	348	ROV	station start	
PS117_49-1	2019-01-17	07:26	-70.45700	-8.35724	357	ROV	station end	
PS117_50-1	2019-01-17	21:10	-70.64150	-9.92838	406	ICE	station start	
PS117_50-1	2019-01-17	21:33	-70.64254	-9.93094	406	ICE	station end	
PS117_51-1	2019-01-18	11:19	-71.00324	-13.52645	2008	SUIT	station start	
PS117_51-1	2019-01-18	11:43	-71.00589	-13.50927	2035	SUIT	profile start	
PS117_51-1	2019-01-18	12:09	-71.00843	-13.47768	2174	SUIT	profile end	
PS117_51-1	2019-01-18	12:40	-71.01364	-13.48302	2190	SUIT	station end	
PS117_51-2	2019-01-18	13:10	-71.02325	-13.48569	2106	ROV	station start	
PS117_51-2	2019-01-18	14:19	-71.04372	-13.51757	2043	ROV	station end	
PS117_51-3	2019-01-18	15:07	-71.06103	-13.55616	2054	M-RMT	station start	
PS117_51-3	2019-01-18	15:29	-71.06965	-13.51033	1933	M-RMT	at depth	
PS117_51-3	2019-01-18	15:30	-71.06976	-13.50975	1932	M-RMT	profile start	
PS117_51-3	2019-01-18	16:10	-71.07571	-13.42703	1962	M-RMT	profile end	
PS117_51-3	2019-01-18	16:31	-71.08120	-13.43520	1915	M-RMT	station end	
PS117_52-1	2019-01-19	08:07	-71.21780	-19.77495	4451	SUIT	station start	
PS117_52-1	2019-01-19	08:48	-71.22762	-19.76559	4448	SUIT	profile start	
PS117_52-1	2019-01-19	10:05	-71.23742	-19.65345	4428	SUIT	station end	
PS117_52-2	2019-01-19	10:15	-71.23833	-19.64883	4428	ROV	station start	
PS117_52-2	2019-01-19	12:25	-71.24671	-19.63662	4428	ROV	station end	
PS117_52-3	2019-01-19	12:38	-71.23918	-19.63175	4380	M-RMT	station start	
PS117_52-3	2019-01-19	12:59	-71.24145	-19.58193	4432	M-RMT	profile start	
PS117_52-3	2019-01-19	13:30	-71.24000	-19.50725	4433	M-RMT	profile end	
PS117_52-3	2019-01-19	13:53	-71.24135	-19.51944	4420	M-RMT	station end	
PS117_53-1	2019-01-20	05:48	-70.89108	-28.89597	4405	MOOR	station start	retrieval of AWI249-2
PS117_53-1	2019-01-20	07:45	-70.88243	-28.93999	4413	MOOR	station end	
PS117_53-2	2019-01-20	08:22	-70.87592	-28.97265	4415	UCCTD	station start	
PS117_53-2	2019-01-20	08:45	-70.87436	-28.99232	4414	UCCTD	at depth	
PS117_53-2	2019-01-20	09:04	-70.87392	-29.00392	4416	UCCTD	station end	
PS117_53-3	2019-01-20	09:10	-70.87289	-29.01382	4414	MOOR	station start	deployment of AWI249-3
PS117_53-3	2019-01-20	12:16	-70.88817	-28.98919	4407	MOOR	station end	
PS117_53-4	2019-01-20	12:50	-70.90940	-28.81964	4396	CTDOZE	station start	
PS117_53-4	2019-01-20	12:59	-70.90847	-28.82286	4399	CTDOZE	at depth	
PS117_53-4	2019-01-20	13:01	-70.90829	-28.82369	4398	CTDOZE	station end	
PS117_53-4	2019-01-20	13:20	-70.90827	-28.84099	4401	CTDOZE	station start	

Station	Date	Time	Latitude	Longitude	Depth [m]	Gear	Action	Comment
PS117_53-4	2019-01-20	14:58	-70.90711	-28.84878	4400	CTDOZE	at depth	
PS117_53-4	2019-01-20	17:30	-70.90098	-28.84692	4399	CTDOZE	station end	
PS117_54-1	2019-01-21	14:59	-66.60839	-27.11849	4883	MOOR	station start	retrieval ofAWI 209-8
PS117_54-1	2019-01-21	17:56	-66.61623	-27.01078	4872	MOOR	station end	
PS117_54-2	2019-01-21	18:17	-66.61326	-27.06883	4871	CTDOZE	station start	
PS117_54-2	2019-01-21	20:15	-66.61219	-27.05940	4872	CTDOZE	at depth	
PS117_54-2	2019-01-21	22:45	-66.60161	-27.07236	4872	CTDOZE	station end	
PS117_54-3	2019-01-21	22:41	-66.60211	-27.06614	4875	FLOAT	station start	
PS117_54-3	2019-01-21	22:52	-66.59886	-27.09314	4875	FLOAT	deployed	
PS117_54-3	2019-01-21	22:53	-66.59884	-27.09345	4873	FLOAT	station end	
PS117_55-1	2019-01-22	17:55	-65.84271	-34.41260	4794	SOSO	station start	
PS117_55-1	2019-01-22	18:35	-65.84308	-34.41478	4794	SOSO	at depth	
PS117_55-1	2019-01-22	19:37	-65.84286	-34.41027	4795	SOSO	station end	
PS117_55-2	2019-01-22	19:37	-65.84286	-34.41028	4794	SOSO	station start	
PS117_55-2	2019-01-22	20:17	-65.84329	-34.41026	4795	SOSO	at depth	
PS117_55-2	2019-01-22	21:03	-65.84258	-34.41060	4795	SOSO	station end	
PS117_55-3	2019-01-22	21:03	-65.84256	-34.41071	4795	SOSO	station start	
PS117_55-3	2019-01-22	21:48	-65.84230	-34.41087	4795	SOSO	at depth	
PS117_55-3	2019-01-22	22:31	-65.84329	-34.42150	4794	SOSO	station end	
PS117_56-1	2019-01-23	03:28	-65.67261	-36.58836	4770	UCCTD	station start	
PS117_56-1	2019-01-23	04:21	-65.67322	-36.59030	4770	UCCTD	at depth	
PS117_56-1	2019-01-23	06:16	-65.67374	-36.59555	4771	UCCTD	station end	
PS117_56-2	2019-01-23	06:20	-65.67380	-36.59608	4771	CTDOZE	station start	
PS117_56-2	2019-01-23	07:50	-65.67437	-36.59823	4771	CTDOZE	at depth	
PS117_56-2	2019-01-23	09:23	-65.67977	-36.61667	4770	CTDOZE	station end	
PS117_56-3	2019-01-23	08:18	-65.67588	-36.59793	4771	HN	station start	
PS117_56-3	2019-01-23	08:25	-65.67646	-36.59892	4771	HN	station end	
PS117_56-4	2019-01-23	09:36	-65.69416	-36.67715	4768	MOOR	station start	retrieval of 208-8
PS117_56-4	2019-01-23	11:32	-65.69435	-36.66253	4768	MOOR	station end	
PS117_56-5	2019-01-23	11:24	-65.69452	-36.66221	4768	M-RMT	station start	
PS117_56-5	2019-01-23	12:29	-65.70899	-36.69864	4766	M-RMT	at depth	
PS117_56-5	2019-01-23	12:29	-65.70920	-36.69920	4765	M-RMT	profile start	
PS117_56-5	2019-01-23	13:07	-65.72900	-36.75620	4763	M-RMT	profile end	
PS117_56-5	2019-01-23	13:19	-65.73011	-36.75928	4762	M-RMT	station end	
PS117_56-6	2019-01-23	13:52	-65.69674	-36.68416	4766	MOOR	station start	deployment AWI 208-9
PS117_56-6	2019-01-23	16:05	-65.69632	-36.68377	4765	MOOR	station end	
PS117_56-7	2019-01-23	16:08	-65.69642	-36.68431	4766	MT	station start	
PS117_56-7	2019-01-23	16:14	-65.69812	-36.68961	4765	MT	profile start	
PS117_56-7	2019-01-23	16:42	-65.70711	-36.72031	4764	MT	profile end	
PS117_56-7	2019-01-23	16:47	-65.70829	-36.72498	4763	MT	station end	
PS117_56-8	2019-01-23	16:52	-65.70925	-36.72882	4763	SUIT	station start	

A.4 Stationsliste / Station List

Station	Date	Time	Latitude	Longitude	Depth [m]	Gear	Action	Comment
PS117_56-8	2019-01-23	17:11	-65.71391	-36.74569	4763	SUIT	profile start	
PS117_56-8	2019-01-23	17:41	-65.72643	-36.78975	4761	SUIT	profile end	
PS117_56-8	2019-01-23	18:05	-65.73271	-36.81268	4761	SUIT	station end	
PS117_56-9	2019-01-23	18:06	-65.73326	-36.81366	4761	FLOAT	station start	
PS117_56-9	2019-01-23	18:11	-65.73737	-36.82119	4761	FLOAT	station end	
PS117_57-1	2019-01-24	11:22	-68.46110	-44.13430	4141	MOOR	station start	retrieval of AWI 250-1
PS117_57-1	2019-01-24	13:31	-68.45892	-44.15107	4138	MOOR	station end	
PS117_57-2	2019-01-24	13:57	-68.48181	-44.10777	NA	MOOR	station start	retrieval of AWI 250-1
PS117_57-2	2019-01-24	17:51	-68.48093	-44.09643	4141	MOOR	station end	
PS117_57-3	2019-01-24	17:57	-68.48103	-44.09598	4141	CTDOZE	station start	
PS117_57-3	2019-01-24	18:12	-68.48128	-44.09602	4141	CTDOZE	at depth	
PS117_57-3	2019-01-24	18:17	-68.48116	-44.09625	4141	CTDOZE	station end	
PS117_57-4	2019-01-24	18:32	-68.48038	-44.09739	4141	MOOR	station start	deployment of AWI250-3
PS117_57-4	2019-01-24	20:31	-68.48150	-44.09989	4141	MOOR	station end	
PS117_57-5	2019-01-24	21:01	-68.46915	-44.00409	4151	MT	station start	
PS117_57-5	2019-01-24	21:10	-68.46662	-44.01126	4151	MT	profile start	
PS117_57-5	2019-01-24	21:40	-68.45693	-44.05369	4148	MT	profile end	
PS117_57-5	2019-01-24	21:44	-68.45521	-44.06267	4147	MT	station end	
PS117_57-6	2019-01-24	21:51	-68.46165	-44.03911	4147	CTDOZE	station start	
PS117_57-6	2019-01-24	23:13	-68.46583	-44.01685	4151	CTDOZE	at depth	
PS117_57-6	2019-01-25	00:38	-68.46559	-44.01772	4151	CTDOZE	station end	
PS117_57-7	2019-01-24	22:08	-68.46603	-44.01717	4151	HN	station start	
PS117_57-7	2019-01-24	22:17	-68.46583	-44.01723	4151	HN	station end	
PS117_58-1	2019-01-25	08:04	-67.66223	-46.40159	3844	SUIT	station start	
PS117_58-1	2019-01-25	08:29	-67.66331	-46.38240	3844	SUIT	profile start	
PS117_58-1	2019-01-25	09:26	-67.66863	-46.30833	3850	SUIT	station end	
PS117_58-2	2019-01-25	09:25	-67.66863	-46.30831	3849	ROV	station start	
PS117_58-2	2019-01-25	11:12	-67.66571	-46.33163	3850	ROV	station end	
PS117_58-3	2019-01-25	12:35	-67.66478	-46.34090	3849	M-RMT	station start	
PS117_58-3	2019-01-25	12:59	-67.67374	-46.31238	3848	M-RMT	at depth	
PS117_58-3	2019-01-25	12:59	-67.67386	-46.31204	3847	M-RMT	profile start	
PS117_58-3	2019-01-25	13:29	-67.68731	-46.27395	3845	M-RMT	profile end	
PS117_58-3	2019-01-25	13:42	-67.68872	-46.27145	3844	M-RMT	station end	
PS117_59-1	2019-01-25	15:23	-67.53254	-46.37823	3896	ROV	station start	
PS117_59-1	2019-01-25	16:47	-67.53417	-46.40367	3894	ROV	station end	
PS117_59-2	2019-01-25	16:53	-67.53425	-46.40626	3894	SUIT	station start	
PS117_59-2	2019-01-25	17:38	-67.53972	-46.38856	3892	SUIT	profile start	
PS117_59-2	2019-01-25	18:13	-67.54815	-46.32631	3898	SUIT	profile end	
PS117_59-2	2019-01-25	19:48	-67.55484	-46.33319	3895	SUIT	station end	
PS117_59-3	2019-01-25	20:17	-67.55214	-46.34683	3893	M-RMT	station start	
PS117_59-3	2019-01-25	20:54	-67.56329	-46.31810	3893	M-RMT	profile start	

Station	Date	Time	Latitude	Longitude	Depth [m]	Gear	Action	Comment
PS117_59-3	2019-01-25	21:32	-67.58340	-46.27097	3885	M-RMT	profile end	
PS117_59-3	2019-01-25	22:00	-67.58085	-46.24091	3885	M-RMT	station end	
PS117_60-1	2019-01-26	10:00	-65.49603	-46.06684	4334	SUIT	station start	
PS117_60-1	2019-01-26	10:53	-65.50054	-46.08671	4333	SUIT	profile start	
PS117_60-1	2019-01-26	11:24	-65.52226	-46.09367	4330	SUIT	profile end	
PS117_60-1	2019-01-26	12:00	-65.52348	-46.10888	4329	SUIT	station end	
PS117_60-2	2019-01-26	11:51	-65.52397	-46.10578	4330	ROV	station start	
PS117_60-2	2019-01-26	13:37	-65.51905	-46.13896	4328	ROV	station end	
PS117_60-3	2019-01-26	13:52	-65.52460	-46.14702	4326	SUIT	station start	
PS117_60-3	2019-01-26	14:03	-65.52962	-46.15168	4324	SUIT	profile start	
PS117_60-3	2019-01-26	14:33	-65.54845	-46.18631	4319	SUIT	profile end	
PS117_60-3	2019-01-26	14:52	-65.54856	-46.19221	4318	SUIT	station end	
PS117_61-1	2019-01-26	22:15	-64.40918	-45.84839	4458	UCCTD	station start	
PS117_61-1	2019-01-26	23:48	-64.40969	-45.84483	4458	UCCTD	at depth	
PS117_61-1	2019-01-27	01:29	-64.40651	-45.84403	4459	UCCTD	station end	
PS117_62-1	2019-01-27	03:15	-64.33345	-46.43955	4425	CTDOZE	station start	
PS117_62-1	2019-01-27	04:45	-64.33417	-46.44233	4425	CTDOZE	at depth	
PS117_62-1	2019-01-27	06:38	-64.33374	-46.44033	4425	CTDOZE	station end	
PS117_63-1	2019-01-27	08:28	-64.25591	-47.01158	4322	CTDOZE	station start	
PS117_63-1	2019-01-27	10:08	-64.25352	-47.01132	4320	CTDOZE	at depth	
PS117_63-1	2019-01-27	12:04	-64.25525	-47.02545	4454	CTDOZE	station end	
PS117_63-2	2019-01-27	09:35	-64.25379	-47.01218	4321	HN	station start	
PS117_63-2	2019-01-27	09:44	-64.25388	-47.01227	4321	HN	station end	
PS117_64-1	2019-01-27	13:34	-64.21850	-47.48871	NA	MOOR	station start	retrieval of AWI 257-1
PS117_64-1	2019-01-27	15:42	-64.21249	-47.47280	4219	MOOR	station end	
PS117_64-2	2019-01-27	16:04	-64.21598	-47.49020	4216	MOOR	station start	deployment of AWI257-2
PS117_64-2	2019-01-27	17:52	-64.21564	-47.48996	4215	MOOR	station end	
PS117_64-3	2019-01-27	18:02	-64.21545	-47.49162	4213	MT	station start	
PS117_64-3	2019-01-27	18:13	-64.21279	-47.49337	4208	MT	profile start	
PS117_64-3	2019-01-27	18:41	-64.19687	-47.50521	4208	MT	profile end	
PS117_64-3	2019-01-27	18:46	-64.19312	-47.50587	4208	MT	station end	
PS117_64-4	2019-01-27	18:52	-64.18803	-47.51595	4208	CTDOZE	station start	
PS117_64-4	2019-01-27	20:25	-64.18786	-47.51804	4208	CTDOZE	at depth	
PS117_64-4	2019-01-27	22:54	-64.19009	-47.50698	4209	CTDOZE	station end	
PS117_64-5	2019-01-27	22:57	-64.19005	-47.50641	4209	HCTD	station start	
PS117_64-5	2019-01-27	23:02	-64.18999	-47.50560	4209	HCTD	at depth	
PS117_64-5	2019-01-27	23:05	-64.19000	-47.50514	4209	HCTD	station end	
PS117_64-6	2019-01-27	23:06	-64.18963	-47.50433	4209	FLOAT	station start	
PS117_64-6	2019-01-27	23:08	-64.18828	-47.50246	4210	FLOAT	station end	
PS117_65-1	2019-01-28	00:39	-64.13173	-47.96784	4102	UCCTD	station start	
PS117_65-1	2019-01-28	01:55	-64.13376	-47.96983	4102	UCCTD	at depth	
PS117_65-1	2019-01-28	03:13	-64.13373	-47.97175	4101	UCCTD	station end	

A.4 Stationsliste / Station List

Station	Date	Time	Latitude	Longitude	Depth [m]	Gear	Action	Comment
PS117_66-1	2019-01-28	04:39	-64.09909	-48.36811	3926	CTDOZE	station start	
PS117_66-1	2019-01-28	06:04	-64.09516	-48.37130	3926	CTDOZE	at depth	
PS117_66-1	2019-01-28	07:45	-64.09388	-48.38920	3918	CTDOZE	station end	
PS117_66-2	2019-01-28	08:04	-64.06970	-48.38613	3927	UCCTD	station start	
PS117_66-2	2019-01-28	08:23	-64.07000	-48.38725	3927	UCCTD	at depth	
PS117_66-2	2019-01-28	08:43	-64.06981	-48.38788	3927	UCCTD	station end	
PS117_66-3	2019-01-28	08:36	-64.06956	-48.38865	3927	MOOR	station start	retrieval of AWI258-1
PS117_66-3	2019-01-28	10:28	-64.06873	-48.39070	NA	MOOR	station end	
PS117_66-4	2019-01-28	10:33	-64.06877	-48.39088	NA	UCCTD	station start	
PS117_66-4	2019-01-28	10:49	-64.06911	-48.39242	NA	UCCTD	at depth	
PS117_66-4	2019-01-28	11:08	-64.06867	-48.39381	NA	UCCTD	station end	
PS117_67-1	2019-01-28	12:33	-63.98891	-48.85227	3712	UCCTD	station start	
PS117_67-1	2019-01-28	13:55	-63.98920	-48.85041	3713	UCCTD	at depth	
PS117_67-1	2019-01-28	15:12	-63.98745	-48.84398	3714	UCCTD	station end	
PS117_68-1	2019-01-28	17:03	-63.91924	-49.27091	3450	MOOR	station start	retrieval of AWI259-1
PS117_68-1	2019-01-28	18:31	-63.91677	-49.26176	3452	MOOR	station end	
PS117_68-2	2019-01-28	18:38	-63.91736	-49.25924	3454	CTDOZE	station start	
PS117_68-2	2019-01-28	20:00	-63.91894	-49.24533	3464	CTDOZE	at depth	
PS117_68-2	2019-01-28	21:29	-63.92368	-49.23274	3474	CTDOZE	station end	
PS117_68-3	2019-01-28	19:48	-63.91895	-49.24841	3463	HN	station start	
PS117_68-3	2019-01-28	19:49	-63.91894	-49.24792	3463	HN	station end	
PS117_68-3	2019-01-28	19:51	-63.91894	-49.24761	3463	HN	station start	
PS117_68-3	2019-01-28	19:52	-63.91899	-49.24714	3463	HN	station end	
PS117_68-4	2019-01-28	21:27	-63.92348	-49.23329	3473	HCTD	station start	
PS117_68-4	2019-01-28	21:31	-63.92377	-49.23257	3474	HCTD	at depth	
PS117_68-4	2019-01-28	21:33	-63.92391	-49.23243	3474	HCTD	station end	
PS117_69-1	2019-01-28	23:29	-63.84764	-49.61953	3232	CTDOZE	station start	
PS117_69-1	2019-01-29	00:46	-63.84935	-49.61497	3237	CTDOZE	at depth	
PS117_69-1	2019-01-29	02:11	-63.85273	-49.60853	3247	CTDOZE	station end	
PS117_70-1	2019-01-29	03:21	-63.81536	-49.85443	3012	UCCTD	station start	
PS117_70-1	2019-01-29	04:17	-63.81286	-49.85512	3008	UCCTD	at depth	
PS117_70-1	2019-01-29	05:20	-63.81108	-49.84963	3007	UCCTD	station end	
PS117_71-1	2019-01-29	06:16	-63.77560	-50.02432	2856	CTDOZE	station start	
PS117_71-1	2019-01-29	07:21	-63.77736	-50.02429	2857	CTDOZE	at depth	
PS117_71-1	2019-01-29	08:30	-63.77835	-50.02383	2858	CTDOZE	station end	
PS117_71-2	2019-01-29	08:50	-63.77834	-50.09015	2817	MOOR	station start	retrieval of AWI 260-1
PS117_71-2	2019-01-29	10:18	-63.77722	-50.08211	2822	MOOR	station end	
PS117_72-1	2019-01-29	12:39	-63.65553	-50.80497	NA	MOOR	station start	retrieval of AWI207-10
PS117_72-1	2019-01-29	15:28	-63.65526	-50.81287	2553	MOOR	station end	

Station	Date	Time	Latitude	Longitude	Depth [m]	Gear	Action	Comment
PS117_72-2	2019-01-29	15:34	-63.65580	-50.81085	2554	MOOR	station start	deployment AWI2017-11 (207-11?)
PS117_72-2	2019-01-29	17:13	-63.65580	-50.81079	2554	MOOR	station end	
PS117_72-3	2019-01-29	17:35	-63.67112	-50.87856	2530	CTDOZE	station start	
PS117_72-3	2019-01-29	18:33	-63.67041	-50.87703	2530	CTDOZE	at depth	
PS117_72-3	2019-01-29	19:42	-63.66796	-50.88448	2527	CTDOZE	station end	
PS117_72-4	2019-01-29	17:56	-63.67092	-50.87790	2530	HN	station start	
PS117_72-4	2019-01-29	17:57	-63.67089	-50.87788	2530	HN	station end	
PS117_72-4	2019-01-29	17:58	-63.67086	-50.87788	2530	HN	station start	
PS117_72-4	2019-01-29	18:00	-63.67083	-50.87790	2530	HN	station end	
PS117_72-5	2019-01-29	19:46	-63.66734	-50.88482	2527	M-RMT	station start	
PS117_72-5	2019-01-29	20:18	-63.67522	-50.89221	2521	M-RMT	profile start	
PS117_72-5	2019-01-29	20:42	-63.68988	-50.89294	2518	M-RMT	profile end	
PS117_72-5	2019-01-29	21:23	-63.69207	-50.90388	2513	M-RMT	station end	
PS117_73-1	2019-01-29	22:03	-63.61852	-51.07098	2395	UCCTD	station start	
PS117_73-1	2019-01-29	23:00	-63.62189	-51.07725	2395	UCCTD	at depth	
PS117_73-1	2019-01-29	23:58	-63.61344	-51.11372	2357	UCCTD	station end	
PS117_74-1	2019-01-30	00:40	-63.58007	-51.29763	2239	CTDOZE	station start	
PS117_74-1	2019-01-30	01:38	-63.57901	-51.29412	2241	CTDOZE	at depth	
PS117_74-1	2019-01-30	02:36	-63.57977	-51.28930	2246	CTDOZE	station end	
PS117_75-1	2019-01-30	03:59	-63.52746	-51.51482	1908	UCCTD	station start	
PS117_75-1	2019-01-30	04:42	-63.52671	-51.51629	1905	UCCTD	at depth	
PS117_75-1	2019-01-30	05:33	-63.52224	-51.51528	1890	UCCTD	station end	
PS117_76-1	2019-01-30	06:02	-63.47951	-51.62221	1811	CTDOZE	station start	
PS117_76-1	2019-01-30	06:48	-63.47912	-51.62089	1814	CTDOZE	at depth	
PS117_76-1	2019-01-30	07:36	-63.47737	-51.62031	1822	CTDOZE	station end	
PS117_76-2	2019-01-30	07:38	-63.47696	-51.61997	1825	M-RMT	station start	
PS117_76-2	2019-01-30	08:10	-63.48668	-51.62417	1755	M-RMT	at depth	
PS117_76-2	2019-01-30	08:10	-63.48711	-51.62440	1752	M-RMT	profile start	
PS117_76-2	2019-01-30	08:41	-63.50838	-51.63591	1691	M-RMT	profile end	
PS117_76-2	2019-01-30	09:01	-63.51068	-51.63459	NA	M-RMT	station end	
PS117_76-3	2019-01-30	08:54	-63.51056	-51.63593	NA	MOOR	station start	retrieval of AWI 261-1
PS117_76-3	2019-01-30	11:07	-63.49917	-51.63853	1664	MOOR	station end	
PS117_77-1	2019-01-30	11:47	-63.47819	-51.87390	1193	MOOR	station start	
PS117_77-1	2019-01-30	12:40	-63.47825	-51.87300	1194	MOOR	station end	
PS117_78-1	2019-01-30	13:30	-63.45223	-52.00111	1032	MOOR	station start	
PS117_78-1	2019-01-30	14:16	-63.45295	-51.99475	1040	MOOR	station end	
PS117_79-1	2019-01-30	15:16	-63.41464	-52.21869	766	MOOR	station start	
PS117_79-1	2019-01-30	16:01	-63.41594	-52.21785	769	MOOR	station end	
PS117_80-1	2019-01-30	16:32	-63.39827	-52.33045	625	TRAP	station start	
PS117_80-1	2019-01-30	16:33	-63.39824	-52.33029	625	TRAP	station end	
PS117_81-1	2019-01-30	17:05	-63.40032	-52.28630	666	MOOR	station start	retrieval of AWI 262-1

A.4 Stationsliste / Station List

Station	Date	Time	Latitude	Longitude	Depth [m]	Gear	Action	Comment
PS117_81-1	2019-01-30	18:29	-63.39187	-52.27602	666	MOOR	station end	
PS117_81-2	2019-01-30	18:47	-63.38830	-52.27059	667	CTDOZE	station start	
PS117_81-2	2019-01-30	19:16	-63.38300	-52.26451	670	CTDOZE	at depth	
PS117_81-2	2019-01-30	19:38	-63.37779	-52.25888	666	CTDOZE	station end	
PS117_81-3	2019-01-30	20:00	-63.34166	-52.29630	589	MT	station start	
PS117_81-3	2019-01-30	20:08	-63.34148	-52.30254	584	MT	profile start	
PS117_81-3	2019-01-30	20:35	-63.34938	-52.29214	605	MT	profile end	
PS117_81-3	2019-01-30	20:39	-63.35194	-52.29249	606	MT	station end	
PS117_81-4	2019-01-30	20:47	-63.33990	-52.29968	585	M-RMT	station start	
PS117_81-4	2019-01-30	21:22	-63.35263	-52.31906	583	M-RMT	profile start	
PS117_81-4	2019-01-30	22:00	-63.37535	-52.33949	590	M-RMT	profile end	
PS117_81-4	2019-01-30	22:28	-63.38648	-52.31936	620	M-RMT	station end	
PS117_82-1	2019-01-30	23:00	-63.42483	-52.15971	839	UCCTD	station start	
PS117_82-1	2019-01-30	23:39	-63.42458	-52.15673	842	UCCTD	at depth	
PS117_82-1	2019-01-31	00:18	-63.42429	-52.13343	866	UCCTD	station end	
PS117_83-1	2019-01-31	00:36	-63.42672	-52.04151	969	MT	station start	
PS117_83-1	2019-01-31	00:43	-63.42836	-52.04220	970	MT	profile start	
PS117_83-1	2019-01-31	01:12	-63.44250	-52.05315	971	MT	station end	
PS117_83-2	2019-01-31	01:41	-63.47659	-51.99352	1063	CTDOZE	station start	
PS117_83-2	2019-01-31	02:18	-63.47255	-51.99450	1058	CTDOZE	at depth	
PS117_83-2	2019-01-31	02:48	-63.46742	-51.99310	1055	CTDOZE	station end	
PS117_84-1	2019-01-31	03:25	-63.49171	-51.87345	1205	CTDOZE	station start	
PS117_84-1	2019-01-31	04:10	-63.49242	-51.87290	1206	CTDOZE	at depth	
PS117_84-1	2019-01-31	04:34	-63.49171	-51.87084	1208	CTDOZE	station end	
PS117_84-2	2019-01-31	04:52	-63.48206	-51.83775	1247	M-RMT	station start	
PS117_84-2	2019-01-31	05:08	-63.48654	-51.85160	1231	M-RMT	at depth	
PS117_84-2	2019-01-31	05:10	-63.48859	-51.85440	1228	M-RMT	profile start	
PS117_84-2	2019-01-31	05:39	-63.50621	-51.88002	1208	M-RMT	profile end	
PS117_84-2	2019-01-31	06:01	-63.50784	-51.88408	1205	M-RMT	station end	
PS117_85-1	2019-01-31	06:46	-63.49751	-51.73875	1455	UCCTD	station start	
PS117_85-1	2019-01-31	07:32	-63.49247	-51.73484	1460	UCCTD	at depth	
PS117_85-1	2019-01-31	08:15	-63.48760	-51.73085	1468	UCCTD	station end	
PS117_86-1	2019-01-31	08:50	-63.47631	-51.87019	1197	MOOR	station start	retrieval of short term mooring Tooth Fish 3
PS117_86-1	2019-01-31	10:10	-63.48276	-51.87034	1201	MOOR	station end	
PS117_87-1	2019-01-31	10:40	-63.44952	-51.99424	1039	MOOR	station start	retrieval of TOOTHFISH-4
PS117_87-1	2019-01-31	11:43	-63.44804	-51.99309	1039	MOOR	station end	
PS117_88-1	2019-01-31	12:32	-63.41266	-52.21610	766	MOOR	station start	retrieval of TOOTHFISH-5
PS117_88-1	2019-01-31	13:55	-63.41253	-52.20890	751	MOOR	station end	
PS117_89-1	2019-01-31	14:23	-63.39468	-52.32817	604	TRAP	station start	
PS117_89-1	2019-01-31	16:34	-63.39722	-52.33362	NA	TRAP	station end	

Station	Date	Time	Latitude	Longitude	Depth [m]	Gear	Action	Comment
PS117_90-1	2019-01-31	17:36	-63.36429	-52.59727	498	CTDOZE	station start	
PS117_90-1	2019-01-31	17:55	-63.36473	-52.59842	498	CTDOZE	at depth	
PS117_90-1	2019-01-31	18:16	-63.36403	-52.60087	498	CTDOZE	station end	
PS117_91-1	2019-01-31	19:08	-63.33463	-52.85525	452	UCCTD	station start	
PS117_91-1	2019-01-31	19:27	-63.33458	-52.85645	451	UCCTD	at depth	
PS117_91-1	2019-01-31	19:57	-63.33349	-52.85668	453	UCCTD	station end	
PS117_92-1	2019-01-31	20:39	-63.30556	-53.06779	453	CTDOZE	station start	
PS117_92-1	2019-01-31	20:57	-63.30559	-53.06837	453	CTDOZE	at depth	
PS117_92-1	2019-01-31	21:19	-63.30775	-53.06959	455	CTDOZE	station end	
PS117_93-1	2019-01-31	22:21	-63.25572	-53.40539	409	UCCTD	station start	
PS117_93-1	2019-01-31	23:04	-63.25594	-53.42682	389	UCCTD	station end	
PS117_94-1	2019-01-31	23:50	-63.22010	-53.70663	306	CTDOZE	station start	
PS117_94-1	2019-02-01	00:05	-63.21981	-53.70714	306	CTDOZE	at depth	
PS117_94-1	2019-02-01	00:31	-63.22234	-53.72914	303	CTDOZE	station end	
PS117_95-1	2019-02-01	02:31	-63.08775	-54.52458	497	UCCTD	station start	
PS117_95-1	2019-02-01	02:46	-63.08526	-54.52456	501	UCCTD	at depth	
PS117_95-1	2019-02-01	03:10	-63.08503	-54.52446	502	UCCTD	station end	
PS117_95-2	2019-02-01	03:28	-63.08075	-54.49713	493	MT	station start	
PS117_95-2	2019-02-01	04:01	-63.06551	-54.51309	458	MT	station end	
PS117_96-1	2019-02-01	13:14	-61.06809	-56.12676	800	MOOR	station start	
PS117_96-1	2019-02-01	13:58	-61.06901	-56.12682	796	MOOR	station end	
PS117_97-1	2019-02-01	14:19	-61.04565	-56.15993	1028	MOOR	station start	
PS117_97-1	2019-02-01	15:09	-61.04715	-56.15611	999	MOOR	station end	
PS117_98-1	2019-02-01	15:32	-61.02823	-56.17939	1249	MOOR	station start	
PS117_98-1	2019-02-01	16:18	-61.03131	-56.17565	1202	MOOR	station end	
PS117_99-1	2019-02-01	17:14	-61.02079	-55.97495	NA	MOOR	station start	retrieval of AWI 251-2
PS117_99-1	2019-02-01	17:42	-61.02271	-55.97711	334	MOOR	station end	
PS117_99-2	2019-02-01	17:43	-61.02262	-55.97723	334	MOOR	station start	deployment of AWI 251-3
PS117_99-2	2019-02-01	18:32	-61.02297	-55.97794	335	MOOR	station end	
PS117_99-3	2019-02-01	18:48	-61.01433	-56.01250	412	CTDOZE	station start	
PS117_99-3	2019-02-01	19:10	-61.01399	-56.01208	412	CTDOZE	at depth	
PS117_99-3	2019-02-01	19:29	-61.01309	-56.01066	406	CTDOZE	station end	
PS117_99-4	2019-02-01	19:31	-61.01298	-56.01075	407	MT	station start	
PS117_99-4	2019-02-01	19:39	-61.01305	-56.01634	445	MT	profile start	
PS117_99-4	2019-02-01	20:08	-61.01978	-56.04656	590	MT	profile end	
PS117_99-4	2019-02-01	20:12	-61.02015	-56.05000	605	MT	station end	
PS117_99-5	2019-02-01	20:19	-61.01971	-56.05365	625	M-RMT	station start	
PS117_99-5	2019-02-01	20:55	-61.01412	-56.07985	741	M-RMT	at depth	
PS117_99-5	2019-02-01	20:56	-61.01402	-56.08041	743	M-RMT	profile start	
PS117_99-5	2019-02-01	21:31	-61.00475	-56.13156	1012	M-RMT	profile end	
PS117_99-5	2019-02-01	22:00	-60.99148	-56.08136	978	M-RMT	station end	
PS117_100-1	2019-02-02	06:59	-61.02006	-54.81437	562	M-RMT	station start	

Station	Date	Time	Latitude	Longitude	Depth [m]	Gear	Action	Comment
PS117_100-1	2019-02-02	07:29	-61.03101	-54.83478	504	M-RMT	at depth	
PS117_100-1	2019-02-02	07:29	-61.03117	-54.83510	501	M-RMT	profile start	
PS117_100-1	2019-02-02	08:02	-61.04980	-54.86767	284	M-RMT	profile end	
PS117_100-1	2019-02-02	08:27	-61.05327	-54.86381	250	M-RMT	station end	
PS117_100-2	2019-02-02	08:32	-61.05359	-54.86279	242	MT	station start	
PS117_100-2	2019-02-02	08:40	-61.05451	-54.86858	252	MT	profile start	
PS117_100-2	2019-02-02	09:08	-61.05954	-54.90619	210	MT	profile end	
PS117_100-2	2019-02-02	09:30	-61.06062	-54.93754	156	MT	station end	
PS117_101-1	2019-02-02	13:29	-61.07163	-56.12648	764	MOOR	station start	
PS117_101-1	2019-02-02	14:25	-61.07073	-56.12926	NA	MOOR	station end	
PS117_102-1	2019-02-02	14:42	-61.04951	-56.15450	975	MOOR	station start	AWI030
PS117_102-1	2019-02-02	15:30	-61.05033	-56.15395	NA	MOOR	station end	
PS117_103-1	2019-02-02	15:44	-61.03091	-56.17143	NA	MOOR	station start	fish mooring
PS117_103-1	2019-02-02	16:38	-61.03335	-56.17120	1171	MOOR	station end	

**Gear abbreviation Gear**

ADCP_150	ADCP 150kHz
CTDOZE	CTD AWI-OZE
FBOX	FerryBox
FLOAT	Float
GRAV	Sea Gravimeter
HCTD	Hand CTD
HN	Hand Net
ICE	Ice Station
M-RMT	Multiple Rectangular Midwater Trawl
MAG	Magnetometer
MOOR	Mooring
MT	Manta Trawl
PCO2_GO	pCO2 GO
PCO2_SUB	pCO2 Subctech
PIES	Pies
ROV	Remotely Operated Vehicle
SOSO	Sound Source
SUIT	Surface and Under Ice Trawl
SVP	Sound Velocity Profiler
TRAP	Fish Trap
TSG_KEEL	Thermosalinograph Keel
TSG_KEEL_2	Thermosalinograph Keel 2
Test	Test
UCCTD	Ultra Clean CTD
WHW	Whale Watching
WST	Weatherstation

Die **Berichte zur Polar- und Meeresforschung** (ISSN 1866-3192) werden beginnend mit dem Band 569 (2008) als Open-Access-Publikation herausgegeben. Ein Verzeichnis aller Bände einschließlich der Druckausgaben (ISSN 1618-3193, Band 377-568, von 2000 bis 2008) sowie der früheren **Berichte zur Polarforschung** (ISSN 0176-5027, Band 1-376, von 1981 bis 2000) befindet sich im electronic Publication Information Center (**ePIC**) des Alfred-Wegener-Instituts, Helmholtz-Zentrum für Polar- und Meeresforschung (AWI); see <http://epic.awi.de>. Durch Auswahl "Reports on Polar- and Marine Research" (via "browse"/"type") wird eine Liste der Publikationen, sortiert nach Bandnummer, innerhalb der absteigenden chronologischen Reihenfolge der Jahrgänge mit Verweis auf das jeweilige pdf-Symbol zum Herunterladen angezeigt.

The **Reports on Polar and Marine Research** (ISSN 1866-3192) are available as open access publications since 2008. A table of all volumes including the printed issues (ISSN 1618-3193, Vol. 377-568, from 2000 until 2008), as well as the earlier **Reports on Polar Research** (ISSN 0176-5027, Vol. 1-376, from 1981 until 2000) is provided by the electronic Publication Information Center (**ePIC**) of the Alfred Wegener Institute, Helmholtz Centre for Polar and Marine Research (AWI); see URL <http://epic.awi.de>. To generate a list of all Reports, use the URL <http://epic.awi.de> and select "browse"/ "type" to browse "Reports on Polar and Marine Research". A chronological list in declining order will be presented, and pdf-icons displayed for downloading.

#### **Zuletzt erschienene Ausgaben:**

**732 (2019)** The Expedition PS117 of the Research Vessel POLARSTERN to the Weddell Sea in 2018/2019, edited by Olaf Boebel

**731 (2019)** The Expedition PS116 of the Research Vessel POLARSTERN to the Atlantic Ocean in 2018, edited by Claudia Hanfland and Bjela König

**730 (2019)** The Expedition PS110 of the Research Vessel POLARSTERN to the Atlantic Ocean in 2017/2018, edited by Frank Niessen

**729 (2019)** The Expedition SO261 of the Research Vessel SONNE to the Atacama Trench in the Pacific Ocean in 2018, edited by Frank Wenzhöfer

**728 (2019)** The Expedition PS115/2 of the Research Vessel POLARSTERN to the Arctic Ocean in 2018, edited by Ruediger Stein

**727 (2019)** The Expedition PS115/1 of the Research Vessel POLARSTERN to the Greenland Sea and Wandel Sea in 2018, edited by Volkmar Damm

**726 (2019)** The Expedition PS108 of the Research Vessel POLARSTERN to the Fram Strait and the AWI-HAUSGARTEN in 2017, edited by Frank Wenzhöfer

**725 (2018)** Russian-German Cooperation: Expeditions to Siberia in 2017, edited by Jens Strauss, Julia Boike, Dmitry Yu. Bolshiyakov, Mikhail N. Grigoriev, Hassan El-Hajj, Anne Morgenstern, Pier Paul Overduin, Annegret Udke

**724 (2018)** The Expedition PS113 of the Research Vessel POLARSTERN to the Atlantic Ocean in 2018, edited by Volker Strass

**723 (2018)** The Expedition PS114 of the Research Vessel POLARSTERN to the Fram Strait in 2018, edited by Wilken-Jon von Appen

**722 (2018)** The Expedition PS112 of the Research Vessel POLARSTERN to the Antarctic Peninsula Region in 2018, edited by Bettina Meyer and Wiebke Weßels

#### **Recently published issues:**



**ALFRED-WEGENER-INSTITUT**  
HELMHOLTZ-ZENTRUM FÜR POLAR-  
UND MEERESFORSCHUNG

**BREMERHAVEN**

Am Handelshafen 12  
27570 Bremerhaven  
Telefon 0471 4831-0  
Telefax 0471 4831-1149  
[www.awi.de](http://www.awi.de)

